

Neutrino interactions & cross sections

Marco Martini



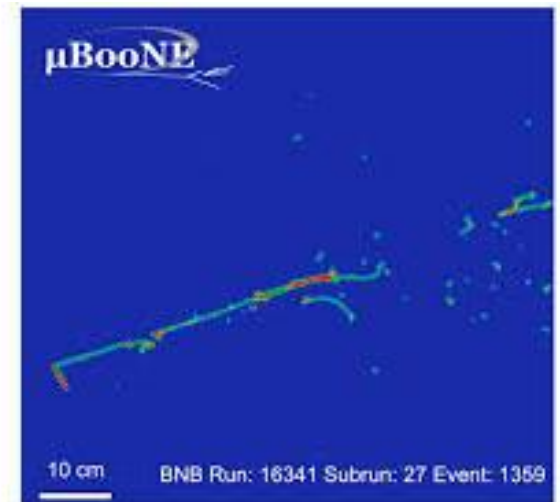
DUNE-France Analysis workshop #2
15 November 2023 IJCLAB

- Summary of my lectures at Ecole de GIF 2022

[Ecole de Gif 2022: La Physique des Neutrinos \(5-9 septembre 2022\): Sections efficaces d'interaction de neutrinos](#)



- Emphasis on recent cross sections on Argon



Some Review papers

[1305.7513.pdf \(arxiv.org\)](#)

REVIEWS OF MODERN PHYSICS, VOLUME 84, JULY–SEPTEMBER 2012

From eV to EeV: Neutrino cross sections across energy scales

J. A. Formaggio*

Laboratory for Nuclear Science Massachusetts Institute of Technology, Cambridge, Massachusetts 02139, USA

G. P. Zeller†

Fermi National Accelerator Laboratory, Batavia, Illinois 60510, USA

[1611.07770.pdf \(arxiv.org\)](#)

IOP Publishing

Journal of Physics G: Nuclear and Particle Physics

J. Phys. G: Nucl. Part. Phys. **45** (2018) 013001 (98pp)

<https://doi.org/10.1088/1361-6471/aa8bf7>

Topical Review

Neutrino–nucleus cross sections for oscillation experiments

Teppei Katori^{1,4,5} and Marco Martini^{2,3,4,5}

[2108.12212.pdf \(arxiv.org\)](#)

 **symmetry**



Review

A New Generation of Neutrino Cross Section Experiments: Challenges and Opportunities

Antonio Branca^{1,*}, Giulia Brunetti¹, Andrea Longhin^{2,3}, Marco Martini^{4,5}, Fabio Pupilli³ and Francesco Terranova¹

[1706.03621.pdf \(arxiv.org\)](#)

Progress in Particle and Nuclear Physics 100 (2018) 1–68



Contents lists available at ScienceDirect

Progress in Particle and Nuclear Physics

journal homepage: www.elsevier.com/locate/ppnp



Review

NuSTEC¹ White Paper: Status and challenges of neutrino–nucleus scattering



L. Alvarez-Ruso^a, M. Sajjad Athar^b, M.B. Barbaro^c, D. Cherdack^d, M.E. Christy^e, P. Coloma^f, T.W. Donnelly^g, S. Dytman^h, A. de Gouvêaⁱ, R.J. Hill^{j,f}, P. Huber^k, N. Jachowicz^l, T. Katori^m, A.S. Kronfeld^f, K. Mahnⁿ, M. Martini^o, J.G. Morfin^{f,*}, J. Nieves^a, G.N. Perdue^f, R. Petti^p, D.G. Richards^q, F. Sánchez^r, T. Sato^{s,t}, J.T. Sobczyk^u, G.P. Zeller^f

[2206.13792.pdf \(arxiv.org\)](#)





Progress in Particle and Nuclear
Physics

Volume 129, March 2023, 104019

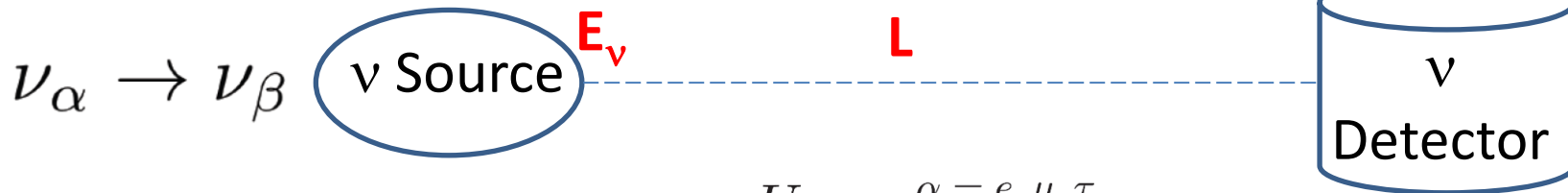


Review

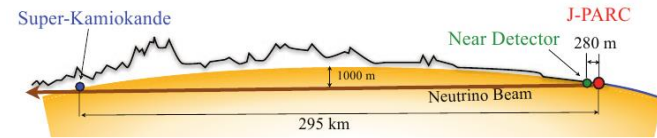
Neutrinos and their interactions with matter

M. Sajjad Athar  , A. Fatima, S.K. Singh

Neutrino oscillation experiments



$$\nu_\alpha = U_{\alpha i} \nu_i \quad \begin{matrix} \alpha = e, \mu, \tau \\ i = 1, 2, 3 \end{matrix}$$



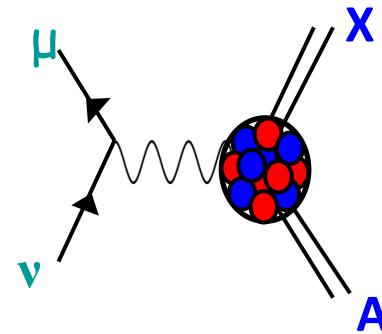
$$N_{\nu_\beta}(\overline{E_\nu}) \sim \int \Phi_{\nu_\alpha}(E_\nu) P_{\nu_\alpha \rightarrow \nu_\beta}(E_\nu, L, \{\Theta\}) \sigma_{\nu_\beta}(E_\nu) \epsilon_{\text{det.}} d(E_\nu, \overline{E_\nu}) dE_\nu$$

Number of detected events



Modern accelerator-based neutrino oscillation experiments:

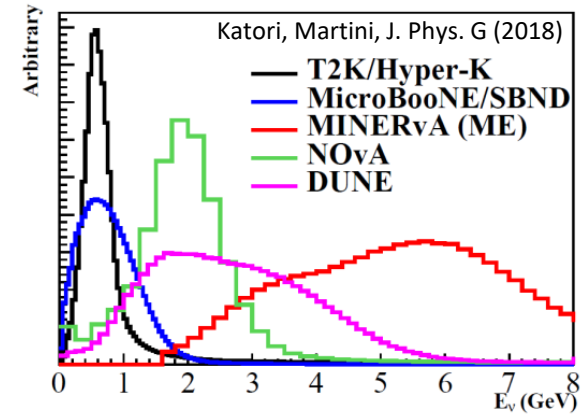
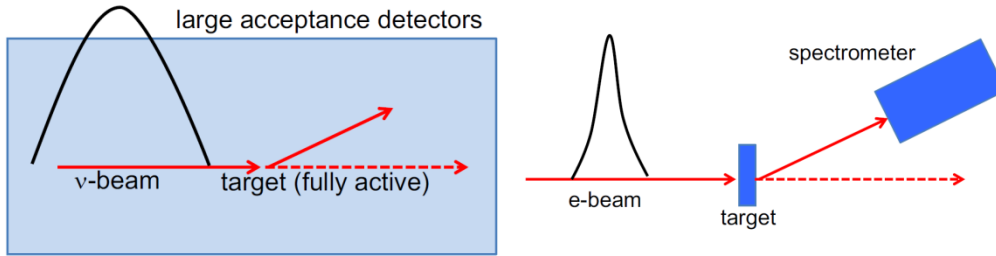
- The neutrino energy is reconstructed from the final states
- Nuclear targets (C, O, Ar, Fe...)



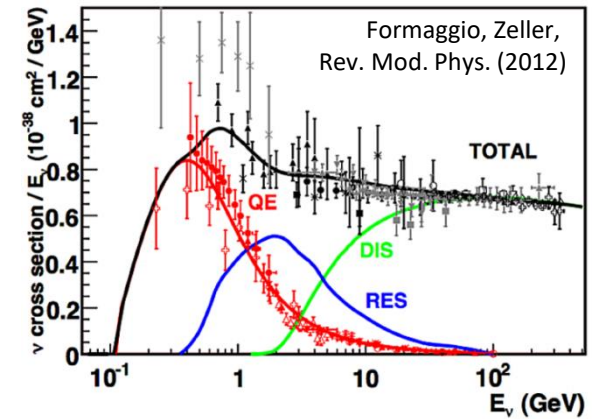
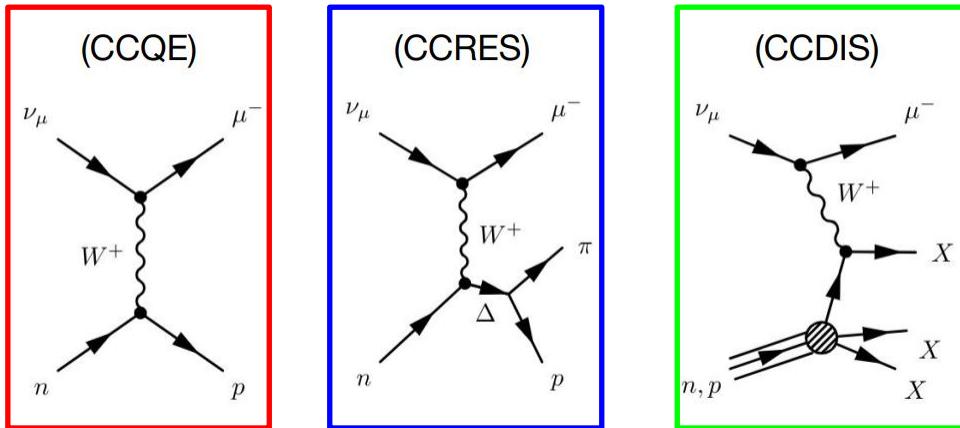
→ the knowledge of the neutrino-nucleus cross section is crucial

Some important points of the accelerator-based ν experiment

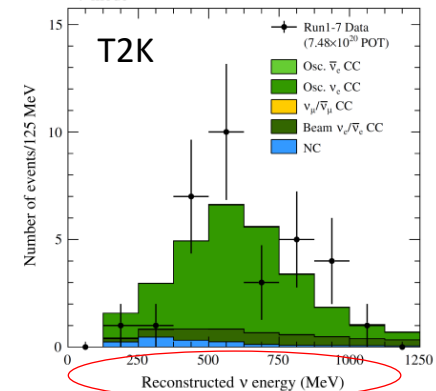
- Neutrino beams are not monochromatic (at difference with respect to electron beams)



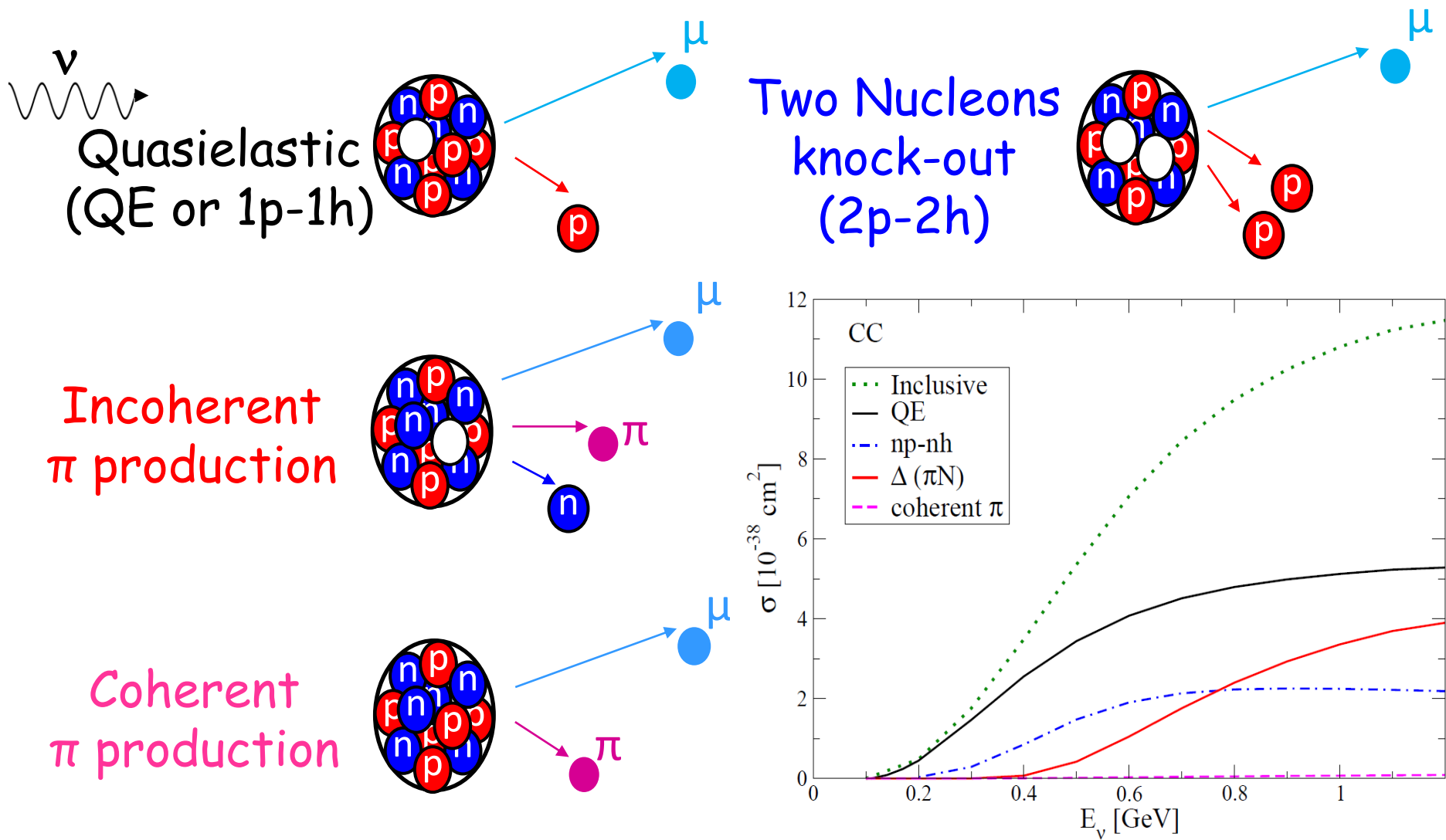
- Different reaction mechanisms contribute



- The neutrino energy is reconstructed from the final states of the reaction (often from CCQE events)

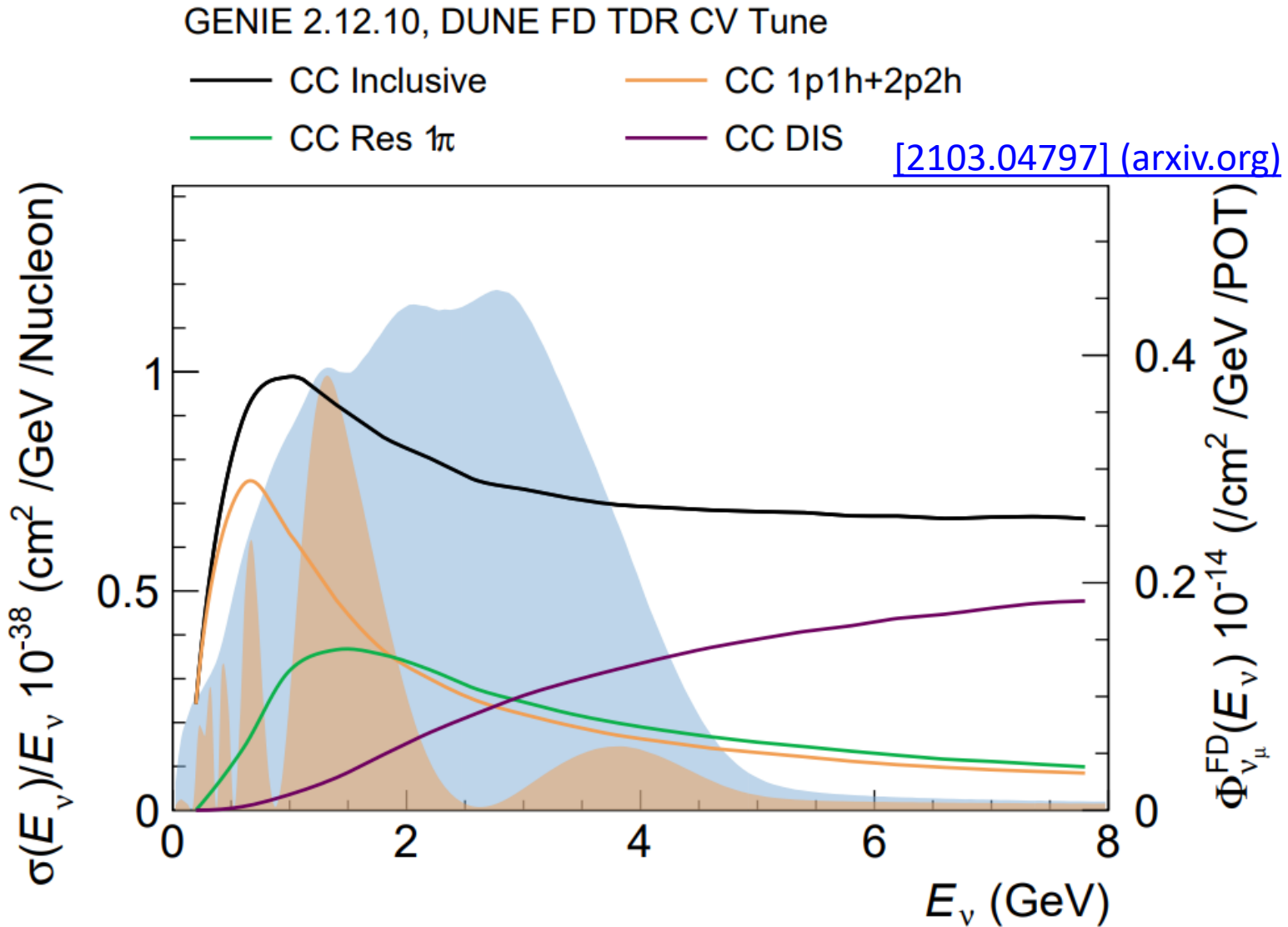


In this talk: Neutrino - nucleus interaction @ $E_\nu \sim O(1 \text{ GeV})$

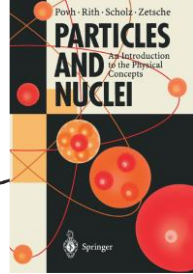


Different processes are entangled

DUNE unoscillated and oscillated ν_μ fluxes ϕ and cross sections σ in different channels

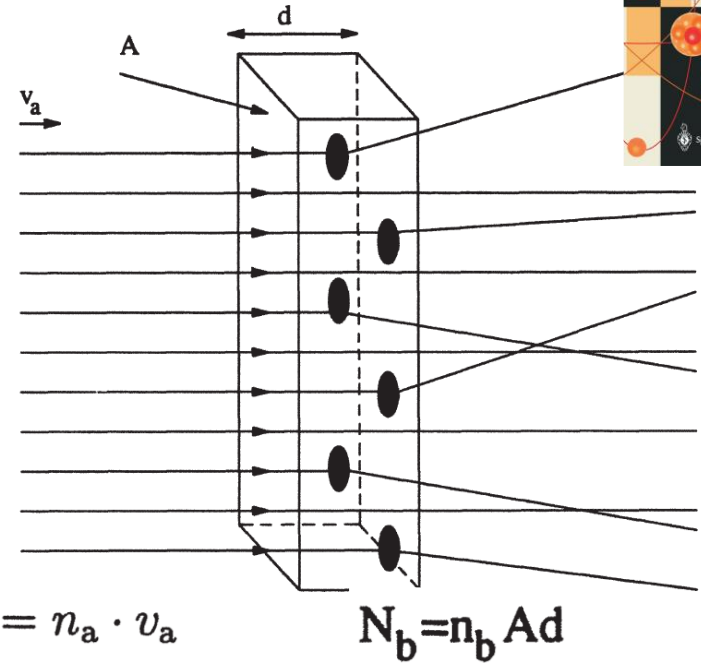


Cross Section generalities - textbook definitions



- **Definition:** The **Cross Section** is a measure for the **probability** of a process to happen
- **Dimensions:** **Area**

$$a + b \rightarrow a' + b^*$$



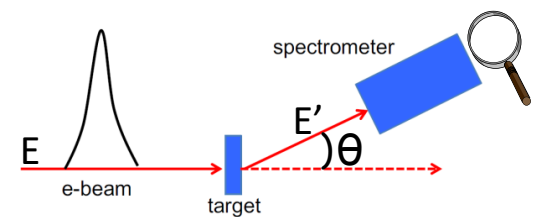
$$\sigma_b = \frac{\dot{N}}{\Phi_a \cdot N_b}$$

$$\Phi_a = \frac{\dot{N}_a}{A} = n_a \cdot v_a$$

$$N_b = n_b A d$$

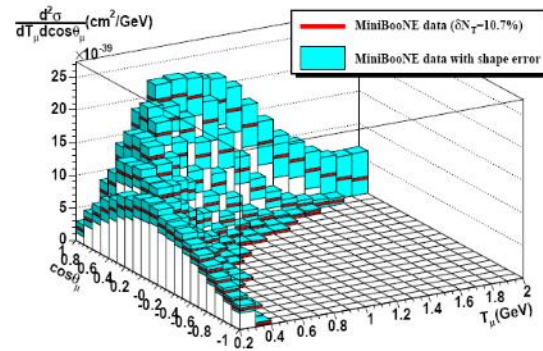
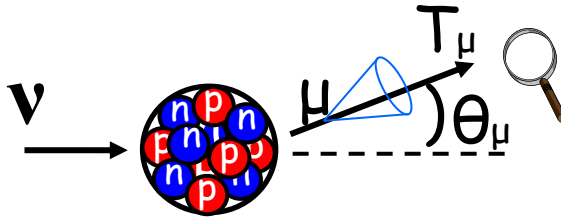
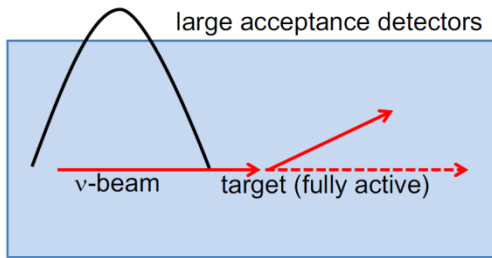
number of reactions per unit time

beam particles per unit time per unit area \times scattering centres



$$\sigma_{\text{tot}}(E) = \int_0^{E'_{\text{max}}} \int_{4\pi} \frac{d^2\sigma(E, E', \theta)}{d\Omega dE'} d\Omega dE'$$

Neutrino flux integrated double differential cross sections



Flux-integrated differential cross section is where theorists and experimentalists meet for ν interaction

Theory

$$\frac{d^2\sigma}{dT_l d\cos\theta} = \frac{1}{\int \Phi(E_\nu) dE_\nu} \int dE_\nu \left[\frac{d^2\sigma}{d\omega d\cos\theta} \right]_{\omega=E_\nu-E_l} \Phi(E_\nu)$$

Unfolding matrix to remove detector effects

Number of observed events

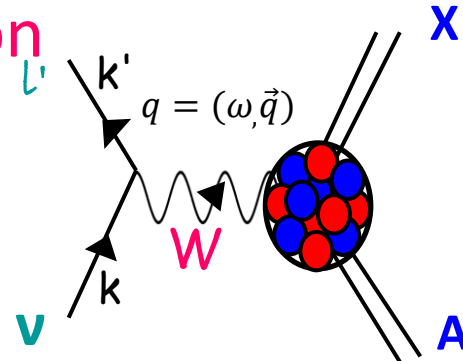
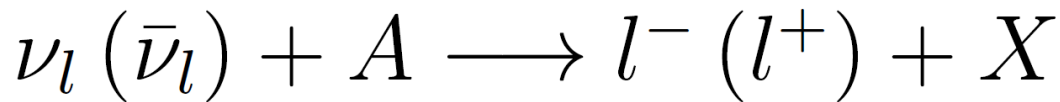
Background contribution

Experimental Definition

$$\left(\frac{d^2\sigma}{dT_l \cos\theta} \right)_i = \frac{\sum_j U_{ij} (d_j - b_j)}{\Phi \cdot T \cdot \epsilon_i \cdot (\Delta T_l, \Delta \cos\theta)_i}$$

← Total integrated flux
 ↓ Number of target nucleons in the Fiducial Volume
 ↘ Efficiency
 ↘ Bin widths

Charged current neutrino-nucleus cross section



$$\mathcal{L}_W = \frac{G_F}{\sqrt{2}} \cos \theta_C l_\mu J^\mu$$

From weak Lagrangian to cross section in terms of

Leptonic and Hadronic tensors (see for example the GIF lectures)

Lab frame

$$\frac{d^2 \sigma}{d\Omega_{k'} d\omega} = \frac{G_F^2 \cos^2 \theta_C}{4\pi^2} \frac{|\mathbf{k}'|}{|\mathbf{k}|} L_{\mu\nu} W^{\mu\nu}(\mathbf{q}, \omega)$$

$d\Omega_{k'}$ differential solid angle in the direction specified by the charged-lepton momentum \mathbf{k}'

$$k \equiv (E_\nu, \mathbf{k}) \quad k' \equiv (E_l', \mathbf{k}') \quad q = k - k' \equiv (\omega, \mathbf{q}) \quad \omega = E_\nu - E_l'$$

initial and final lepton 4-momenta

four-momentum transfer

energy transfer

$$L_{\mu\nu} = k_\mu k'_\nu + k'_\mu k_\nu - g_{\mu\nu} k \cdot k' \pm i \epsilon_{\mu\nu\kappa\lambda} k^\kappa k'^\lambda \quad W^{\mu\nu} = \sum_f \langle 0 | J^{\mu\dagger}(q) | f \rangle \langle f | J^\nu(q) | 0 \rangle \delta^{(4)}(p_0 + q - p_f)$$

Leptonic tensor

Hadronic tensor

The charged current cross section is a linear combination of five contributions

$$\frac{d^2 \sigma}{d\Omega_{k'} d\omega} = \sigma_0 [L_{00} W^{00} + L_{33} W^{33} + (L_{03} + L_{30}) W^{03} + (L_{11} + L_{22}) W^{11} \pm (L_{12} - L_{21}) W^{12}]$$

A simplified expressions particularly useful for illustration

- Final lepton mass contributions ignored ($m_l=0$)
- Obtained by keeping only the leading terms for the hadronic tensor in the development of the hadronic current in p/M_N

$$\frac{d^2\sigma}{d\cos\theta d\omega} = \frac{G_F^2 \cos^2\theta_c}{\pi} |k'| E_l' \cos^2\frac{\theta}{2} \left[\frac{(\mathbf{q}^2 - \omega^2)^2}{\mathbf{q}^4} G_E^2 R_T(\mathbf{q}, \omega) + \frac{\omega^2}{\mathbf{q}^2} G_A^2 R_{\sigma\tau(L)}(\mathbf{q}, \omega) \right] \\ + 2 \left(\tan^2\frac{\theta}{2} + \frac{\mathbf{q}^2 - \omega^2}{2\mathbf{q}^2} \right) \left(G_M^2 \frac{\mathbf{q}^2}{4M_N^2} + G_A^2 \right) R_{\sigma\tau(T)}(\mathbf{q}, \omega) \pm 2 \frac{E_\nu + E_l'}{M_N} \tan^2\frac{\theta}{2} G_A G_M R_{\sigma\tau(T)}(\mathbf{q}, \omega)$$

Explicitly appear:

1. The different **kinematic variables** (related to the leptonic tensor)
2. The nucleon Electric, Magnetic, and Axial **form factors** (\leftrightarrow nucleon properties)
3. The **nuclear response functions** (\leftrightarrow nuclear dynamics)

Nuclear response functions $R(\mathbf{q}, \omega)$:

$$R_\alpha^{PP'}(\mathbf{q}, \omega) = \sum_n \langle n | \sum_{j=1}^A O_\alpha^P(j) e^{i\mathbf{q}\cdot\mathbf{x}_j} | 0 \rangle \langle n | \sum_{k=1}^A O_\alpha^{P'}(k) e^{i\mathbf{q}\cdot\mathbf{x}_k} | 0 \rangle^* \delta(\omega - E_n + E_0),$$

Isovector R_τ

$$O_\alpha^N(j) = \tau_j^\pm$$

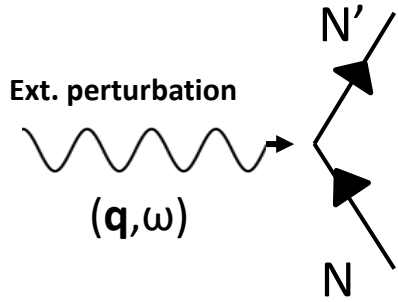
Isospin Spin-Longitudinal $R_{\sigma\tau(L)}$

$$(\boldsymbol{\sigma}_j \cdot \hat{\mathbf{q}}) \tau_j^\pm$$

Isospin Spin-Transverse $R_{\sigma\tau(T)}$

$$(\boldsymbol{\sigma}_j \times \hat{\mathbf{q}})^i \tau_j^\pm$$

Free (or bare) nuclear response function



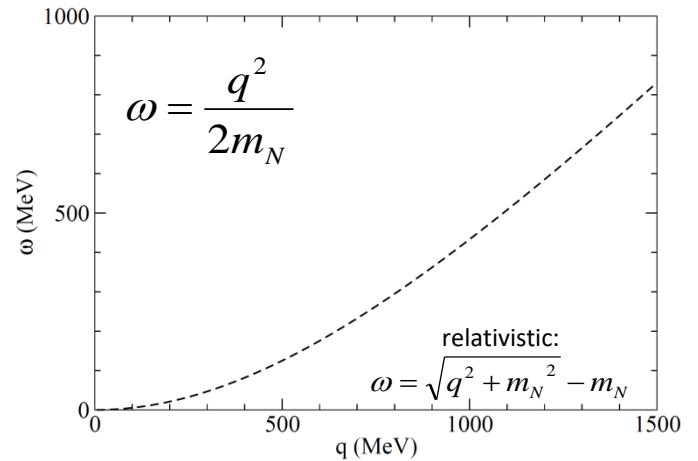
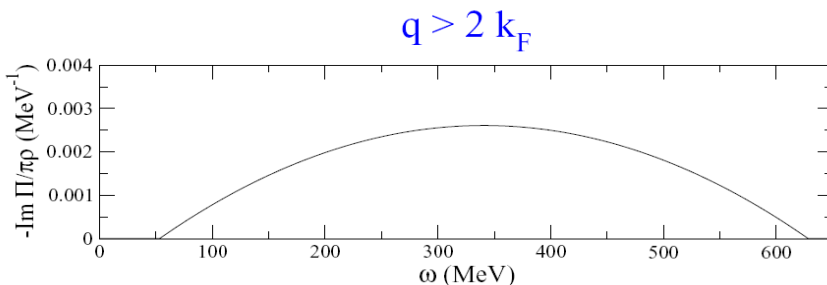
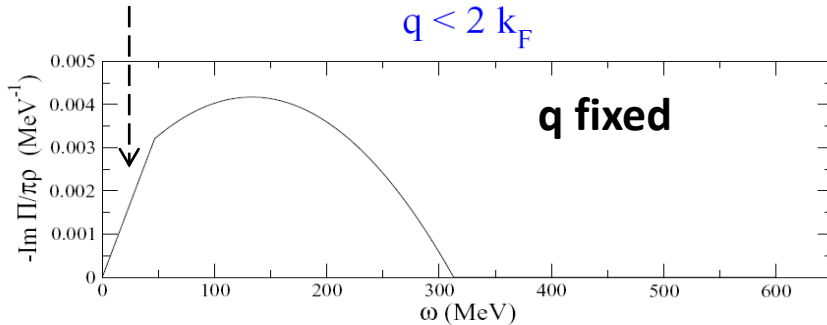
- Free nucleon at rest:
Response functions $\propto \delta(\omega - q^2/2m_N)$

- Nucleon inside the nucleus:

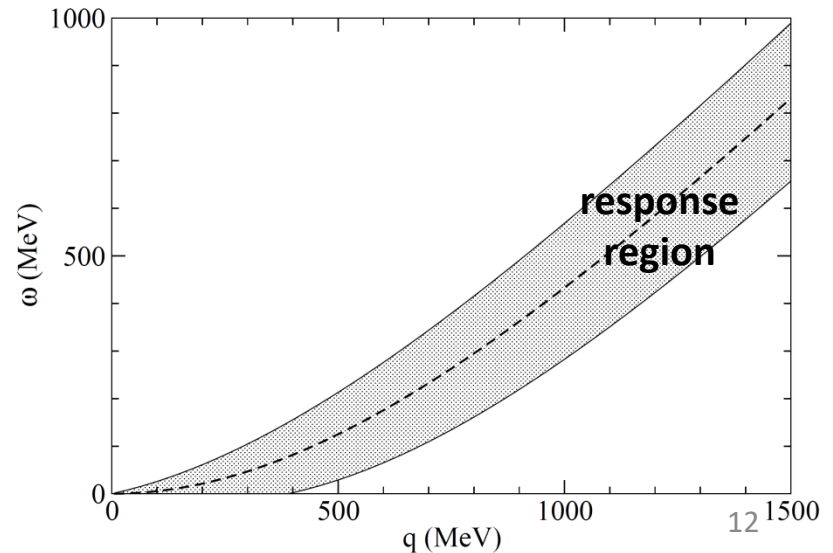
Nucleon-Nucleon interaction switched off \leftrightarrow Nucleons respond individually

Fermi Gas Quasielastic Response

- Fermi motion spreads δ distribution
- Pauli blocking cuts part of the low q and ω response

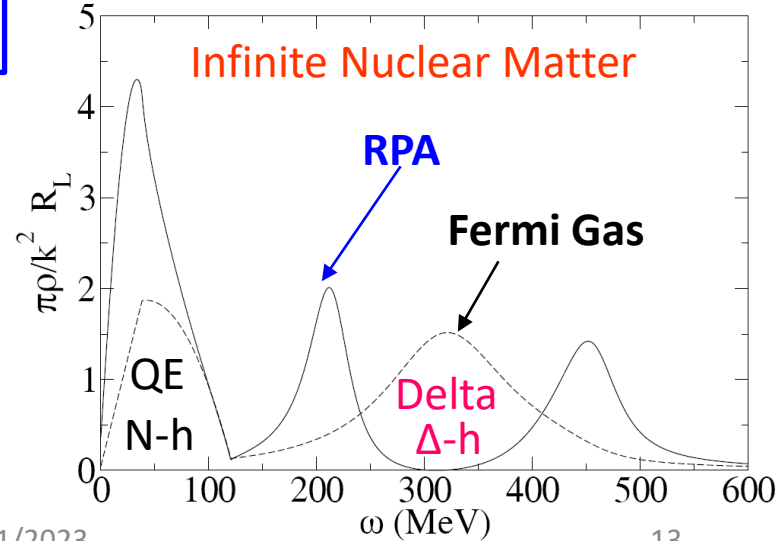
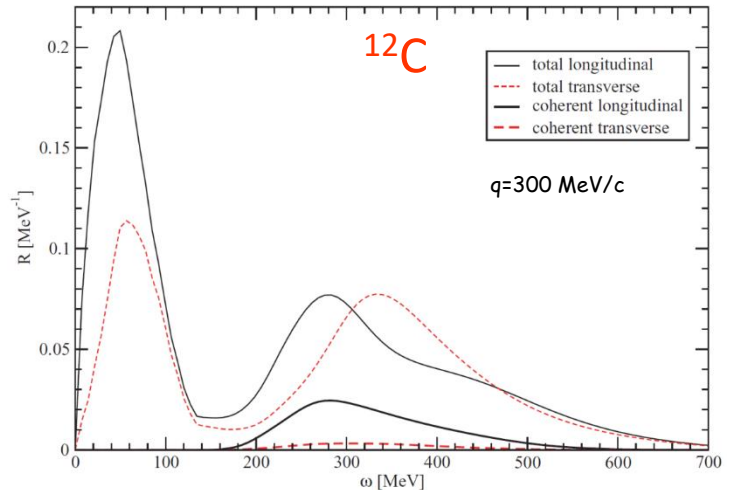
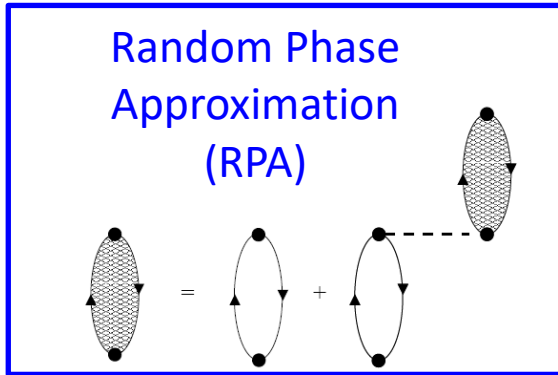
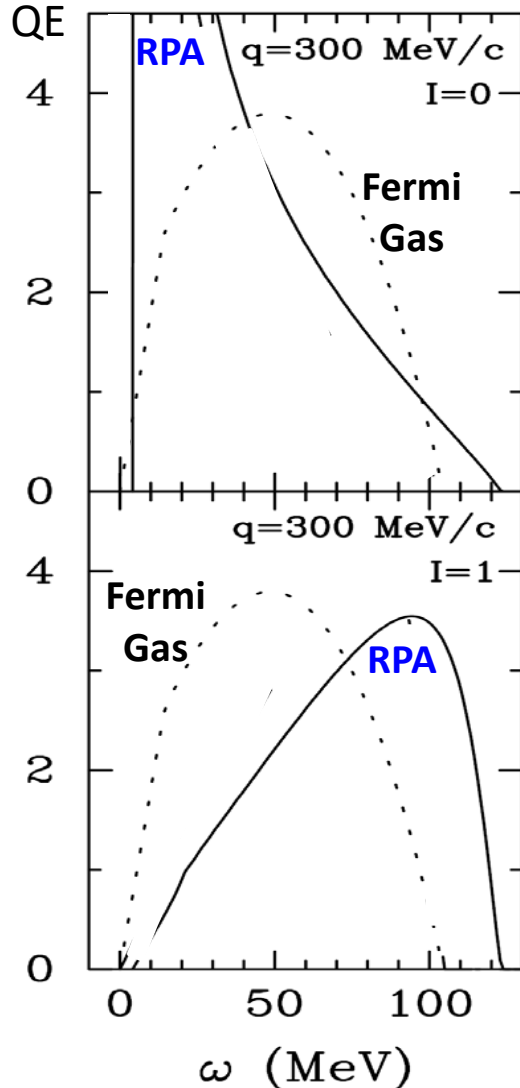


$$\frac{q^2}{2m_N} - \frac{qk_F}{m_N} \leq \omega \leq \frac{q^2}{2m_N} + \frac{qk_F}{m_N}$$



Switching on the nucleon-nucleon interaction

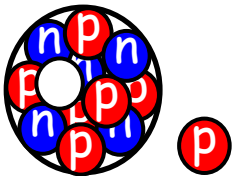
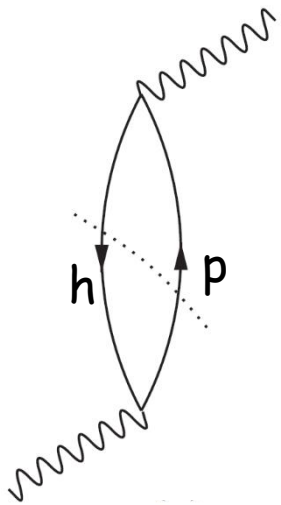
- External force acting on one nucleon is transmitted to the neighbors by the interaction – **Long Range Correlations**
- The nuclear response becomes collective
- Shift of the peak with respect to Fermi Gas, decrease, increase depending on the channels of excitation



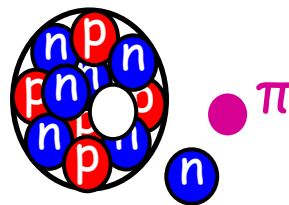
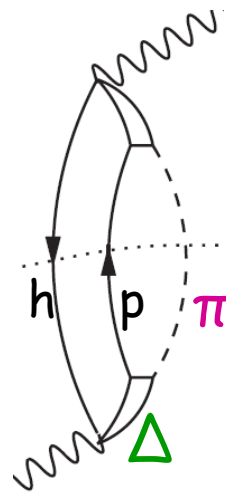
Nuclear Responses for different excitations

$$R_\alpha = \sum_{n \neq 0} |\langle n | \hat{O}_{(\alpha)} | 0 \rangle|^2 \delta[\omega - (E_n - E_0)]$$

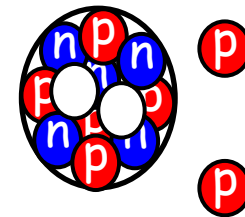
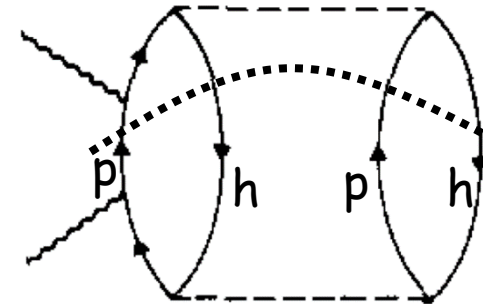
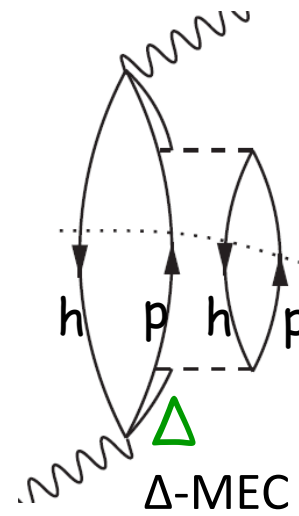
1p-1h
Quasielastic



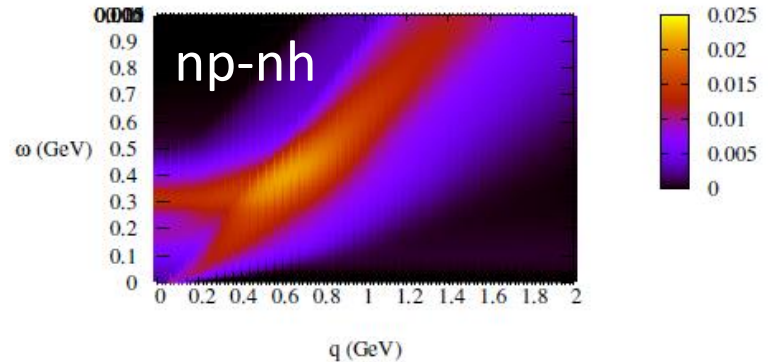
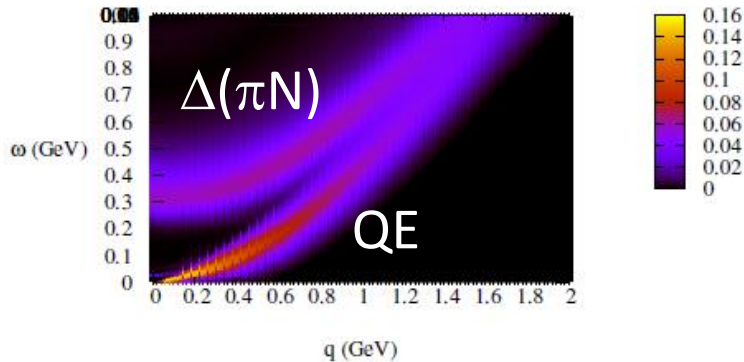
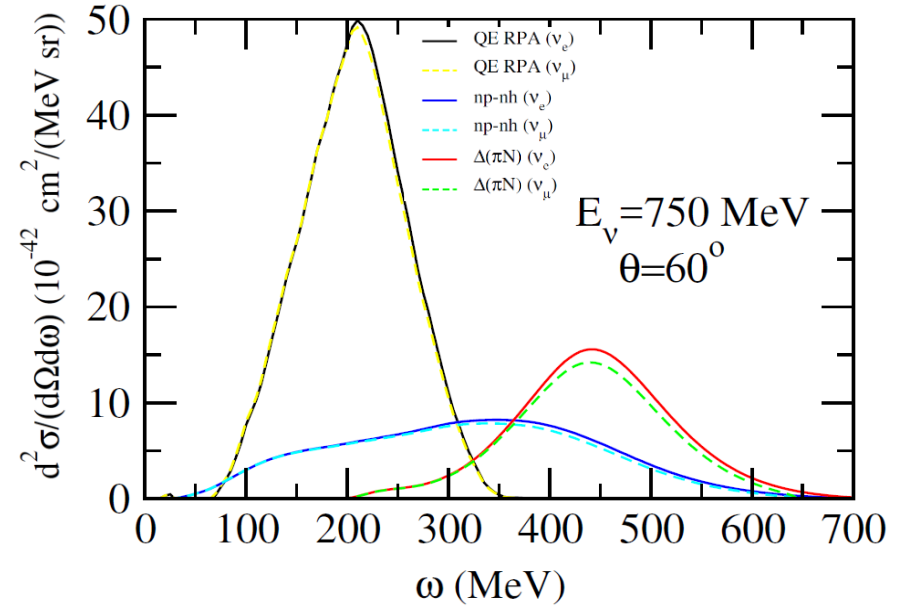
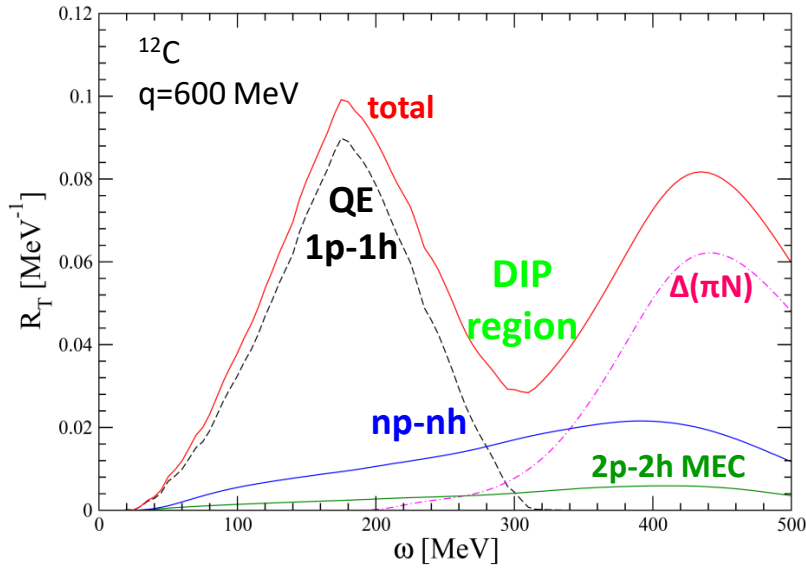
1p-1h
($\Delta \rightarrow \pi N$) 1π production



2p-2h:
two examples



Nuclear responses and neutrino cross sections at fixed kinematics



QE peak:

$$\omega = \sqrt{q^2 + M_N^2} - M_N = \frac{Q^2}{2M_N} = \frac{q^2 - \omega^2}{2M_N}$$

Δ peak:

$$\omega = \sqrt{q^2 + M_\Delta^2} - M_N = \frac{Q^2}{2M_N} + \frac{M_\Delta^2 - M_N^2}{2M_N}$$

np-nh excitations fill the DIP region

np-nh enlarges the region of response to the whole (ω, q) plane

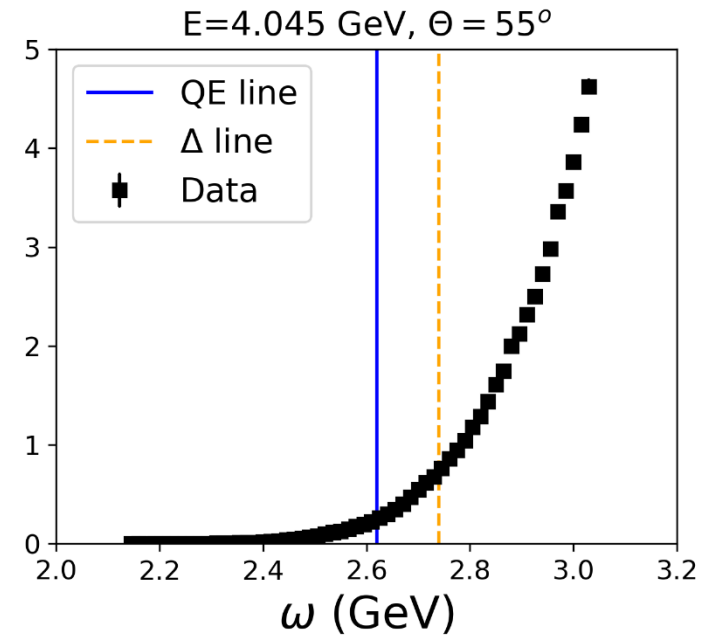
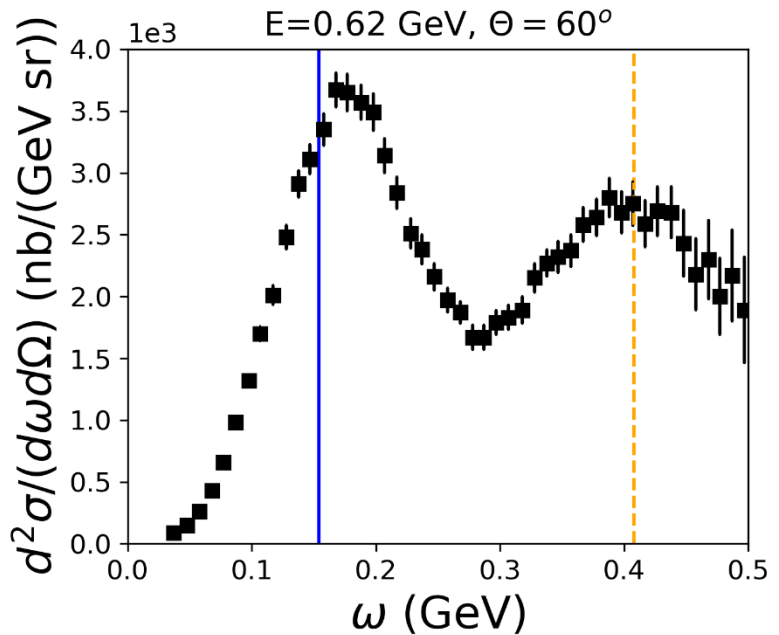
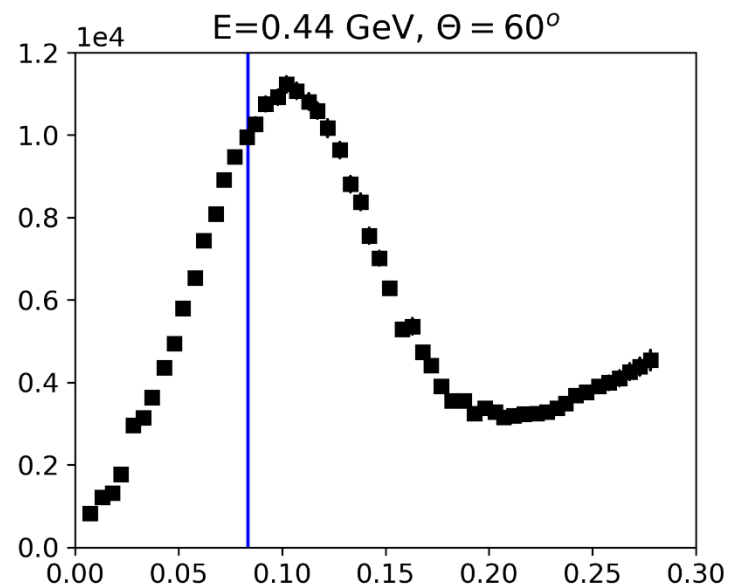
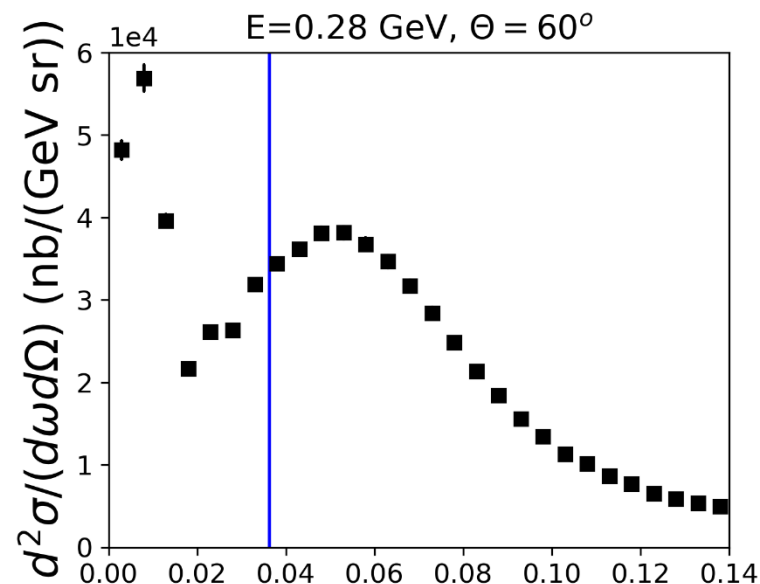
N.B. The responses can be tested in other processes (scattering of e, π ...)

Examples of electron scattering cross section on ^{12}C

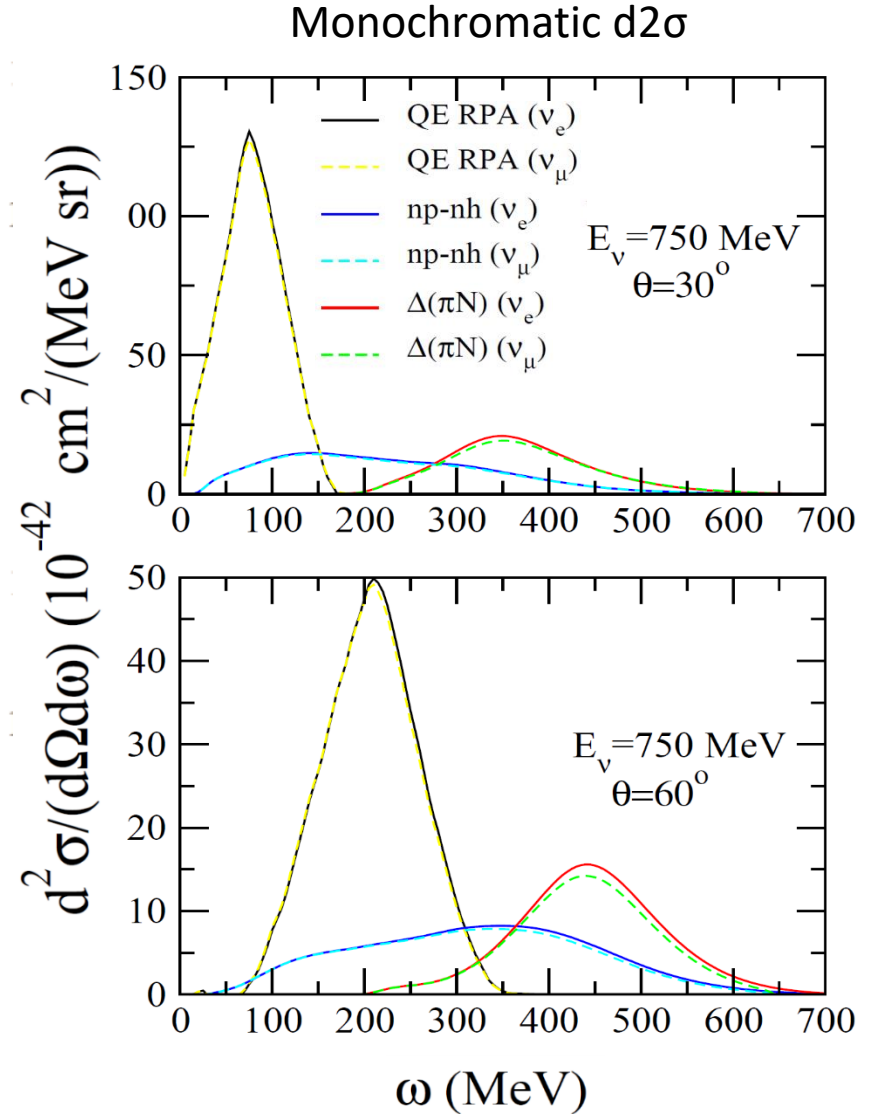
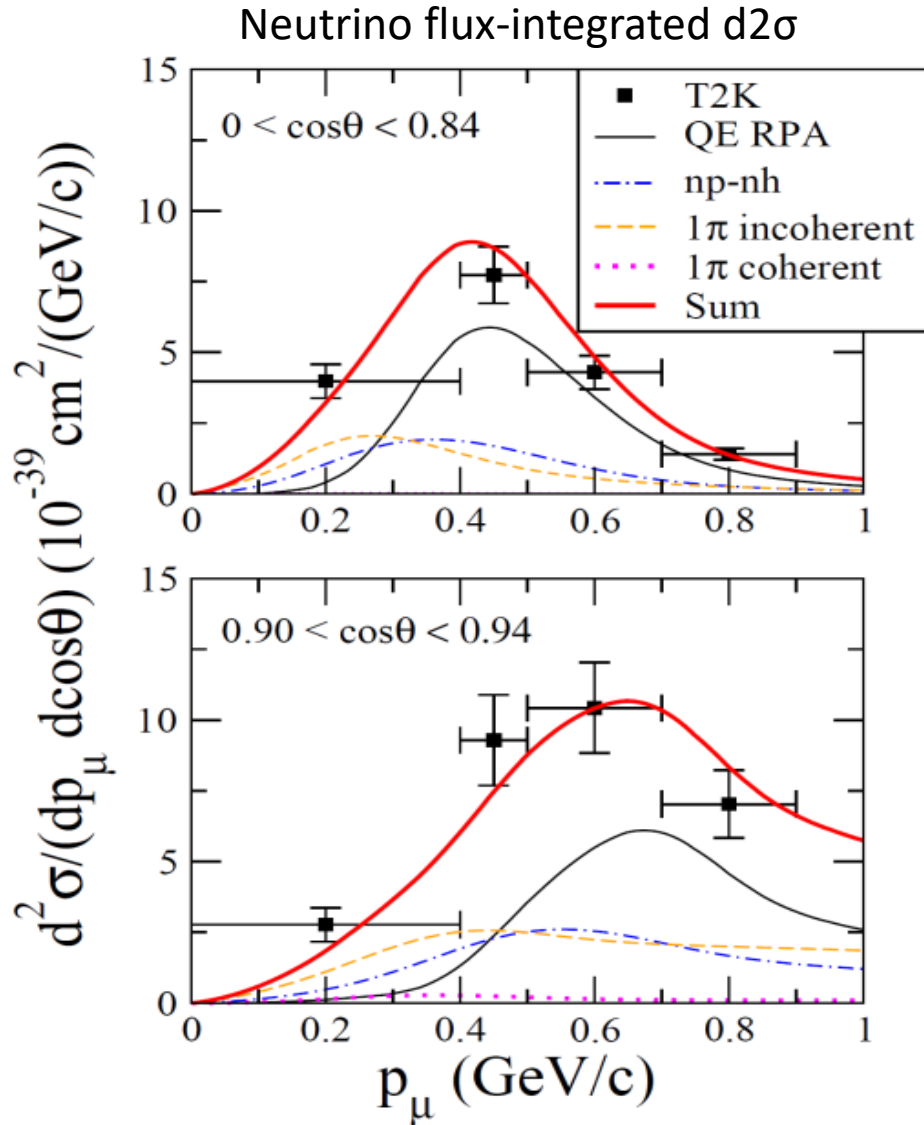
Remind: monochromatic beam

$$\omega_{QE} = \frac{E^2(1 - \cos\theta)}{M_N + E(1 - \cos\theta)}$$

$$\omega_{\Delta} = \frac{M_N \Delta M + E^2(1 - \cos\theta)}{M_N + E(1 - \cos\theta)}$$



Remark: flux-integrated .vs. monochromatic beam cross sections

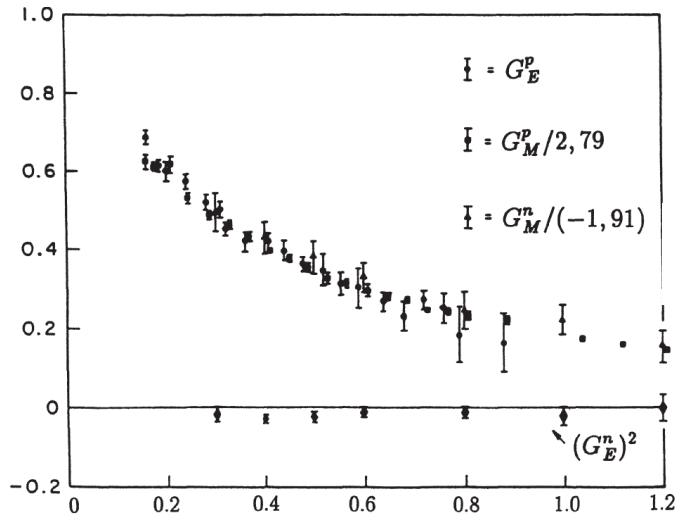


In the flux-integrated cross sections the different channels are entangled

The Form Factors

$$\frac{d^2\sigma}{d\cos\theta d\omega} = \frac{G_F^2 \cos^2\theta_c}{\pi} |\mathbf{k}'| E_l' \cos^2\frac{\theta}{2} \left[\frac{(q^2 - \omega^2)^2}{q^4} G_E^2 R_\tau + \frac{\omega^2}{q^2} G_A^2 R_{\sigma\tau(L)} + 2 \left(\tan^2\frac{\theta}{2} + \frac{q^2 - \omega^2}{2q^2} \right) \left(G_M^2 \frac{\omega^2}{q^2} + G_A^2 \right) R_{\sigma\tau(T)} \pm 2 \frac{\epsilon + \epsilon'}{M_N} \tan^2\frac{\theta}{2} G_A G_M R_{\sigma\tau(T)} \right]$$

Vector form factors



$$G_E^p(Q^2) = \frac{G_M^p(Q^2)}{2.79} = \frac{G_M^n(Q^2)}{-1.91} = G^{\text{dipole}}(Q^2)$$

$$G^{\text{dipole}}(Q^2) = \left(1 + \frac{Q^2}{0.71 (\text{GeV}/c)^2} \right)^{-2}$$

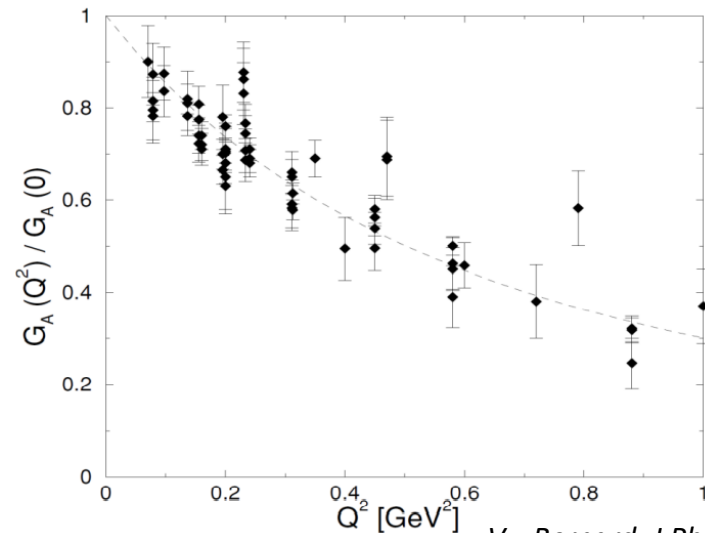
$$Q^2 = q^2 - \omega^2$$

Global dipole-like behavior

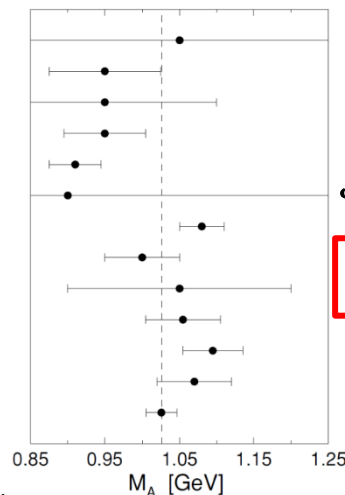
Weak **vector form factors** are well constrained by electron scattering experiments (CVC)

Q^2 evolution of the **axial form factor** is less well-known, mainly based on old bubble chamber data

Axial form factor



Argonne (1969)
Argonne (1973)
CERN (1977)
Argonne (1977)
CERN (1979)
BNL (1980)
BNL (1981)
Argonne (1982)
Fermilab (1983)
BNL (1986)
BNL (1987)
BNL (1990)
Average



$$G_A(Q^2) = g_A (1 + Q^2 / M_A^2)^{-2}$$

$$g_A = 1.26 \text{ from neutron } \beta \text{ decay}$$

$$M_A = (1.026 \pm 0.021) \text{ GeV}/c^2$$

from ν - ^2H (bubble-chamber) CCQE
and
from π electroproduction

CCQE, CCQE-like and CC0 π

MiniBooNE CC Quasielastic cross section on Carbon and the M_A puzzle

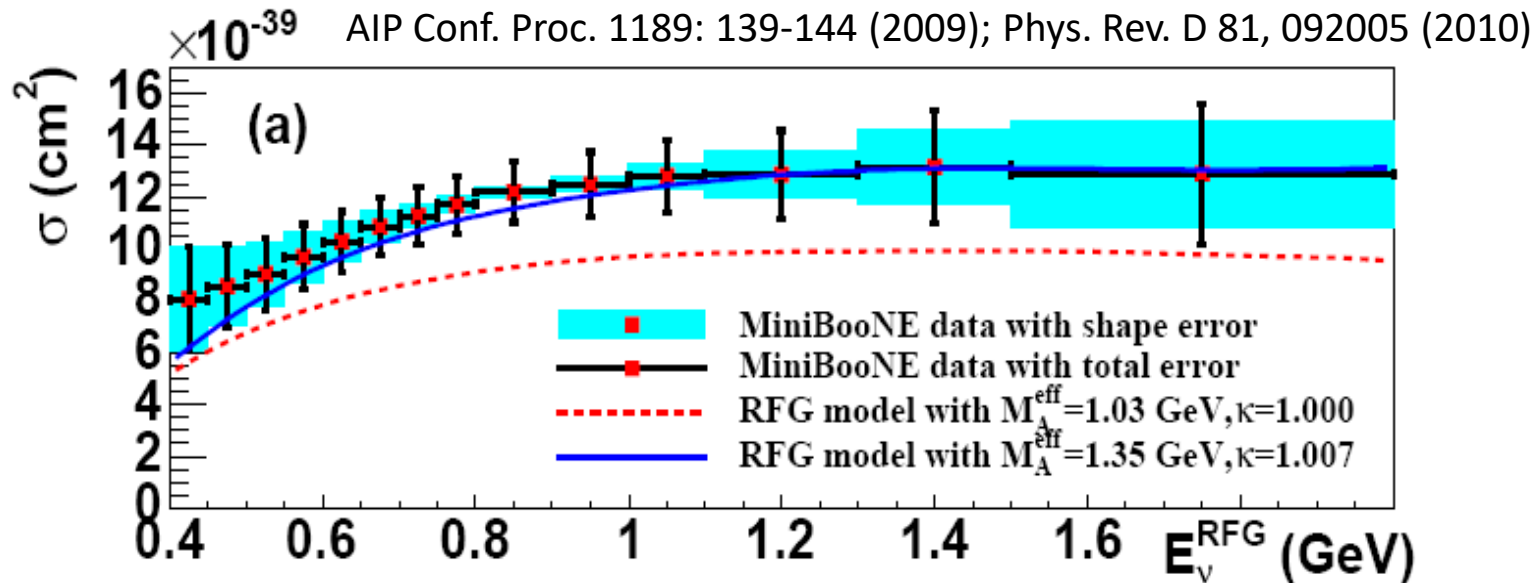
First Measurement of Muon Neutrino Charged Current Quasielastic (CCQE) Double Differential Cross Section

Cite as: AIP Conference Proceedings 1189, 139 (2009); <https://doi.org/10.1063/1.3274144>
Published Online: 02 December 2009

Tepepei Katori and MiniBooNE collaboration

PHYSICAL REVIEW D 81, 092005 (2010)

First measurement of the muon neutrino charged current quasielastic double differential cross section

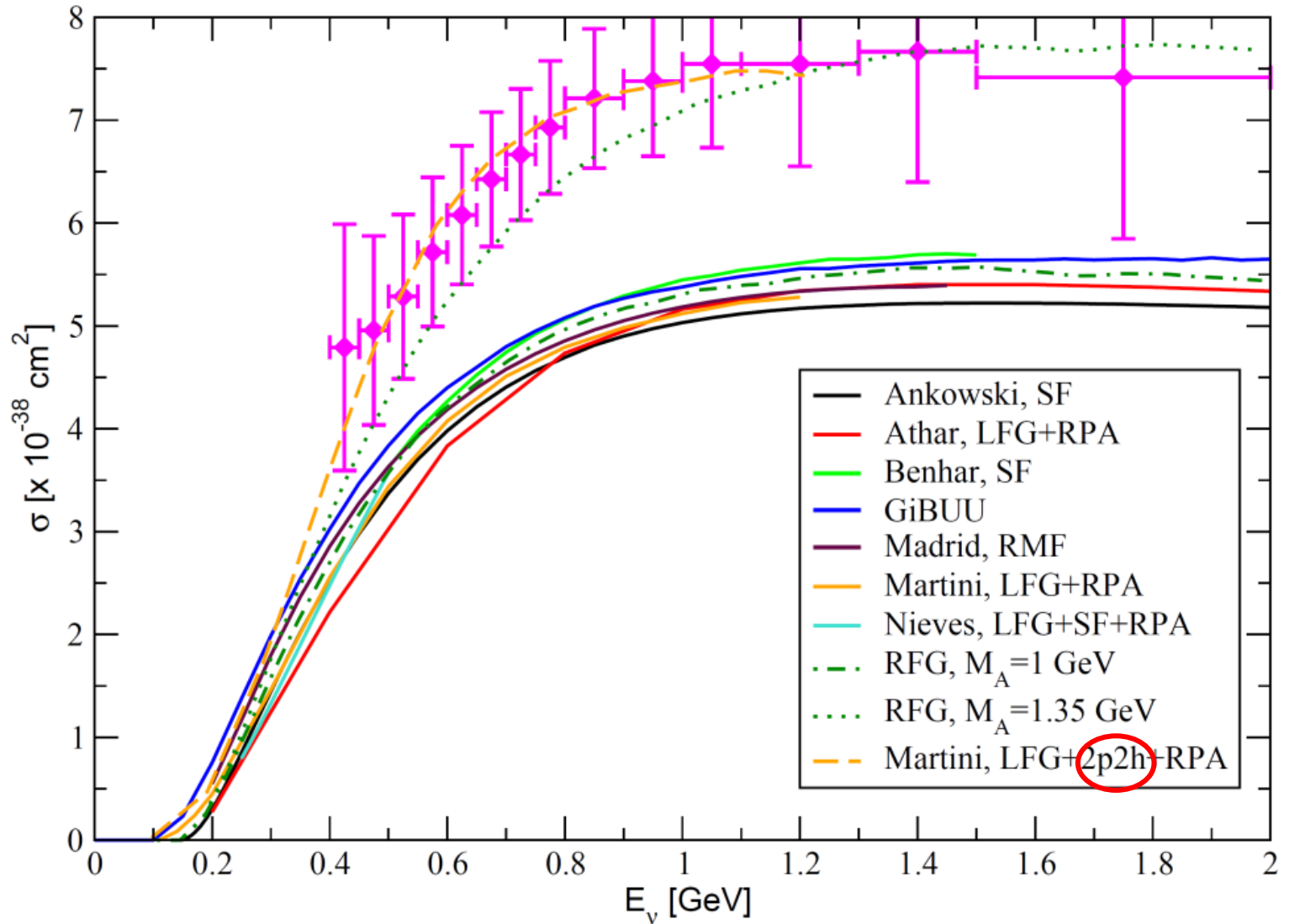


Comparison with a prediction based on Relativistic Fermi Gas (RFG) using $M_A=1.03$ GeV (standard value) reveals a discrepancy

In the Relativistic Fermi Gas (RFG) model an axial mass of **1.35 GeV** is needed to account for data **puzzle??**

Comparison of different theoretical models for Quasielastic

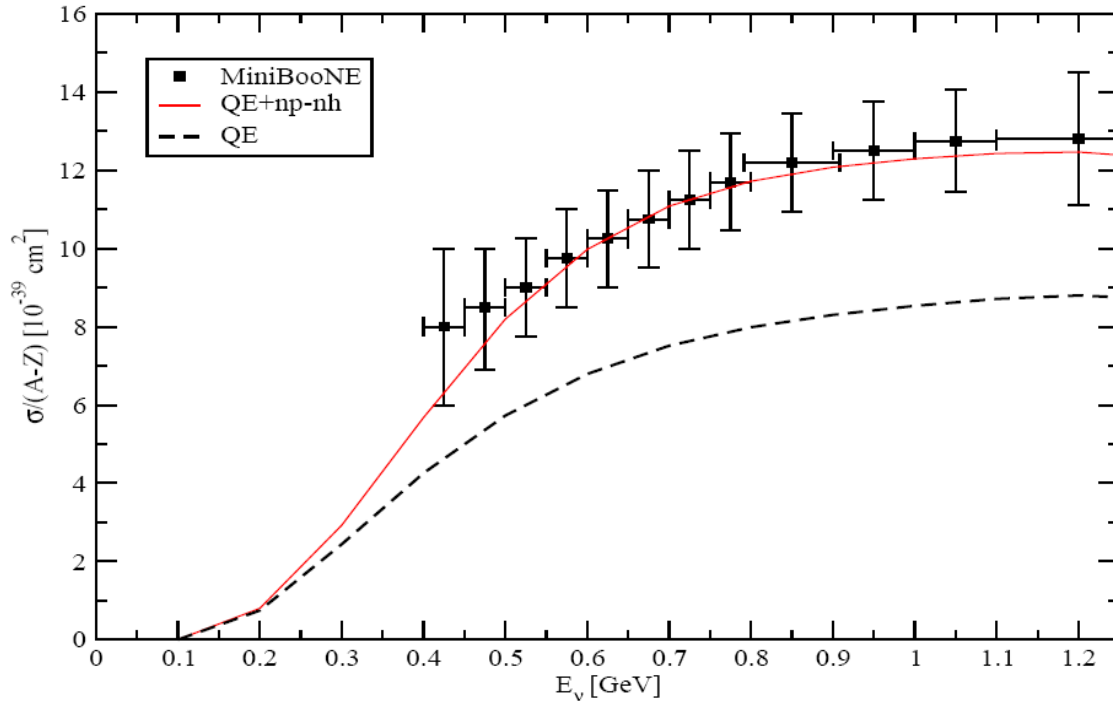
L. Alvarez-Ruso , arXiv:1012.3871 (Neutrino 2010)



puzzle??

An explanation of this puzzle

Inclusion of the multinucleon emission channel (np-nh = 2p-2h + 3p-3h)

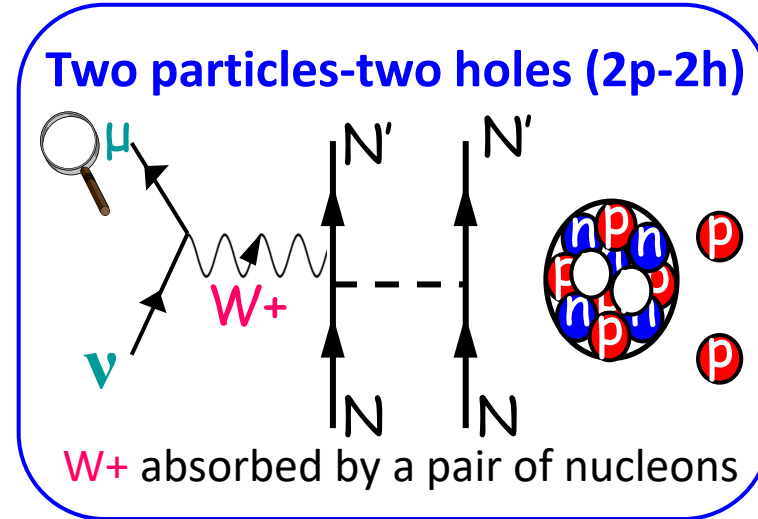
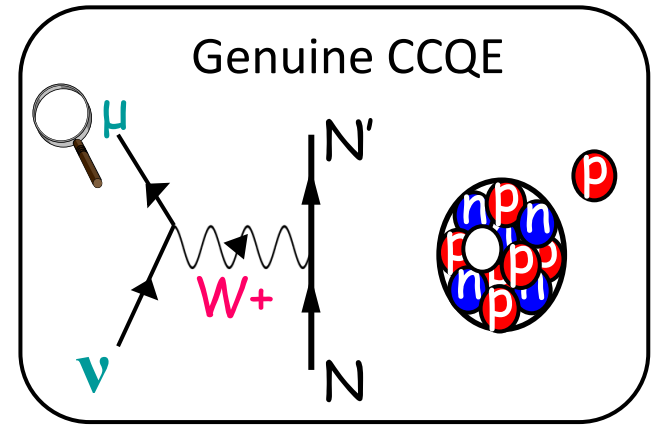


CCQE-like = Genuine CCQE + np-nh

M. Martini, M. Ericson, G. Chanfray, J. Marteau, Phys. Rev. C 80 065501 (2009)

Agreement with MiniBooNE without increasing M_A

➡ MiniBooNE measured CCQE-like, not genuine CCQE

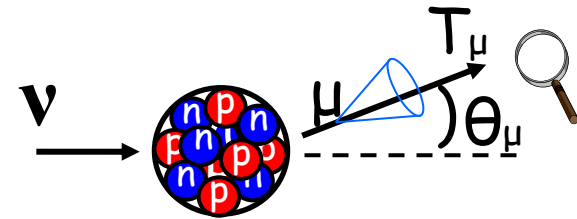
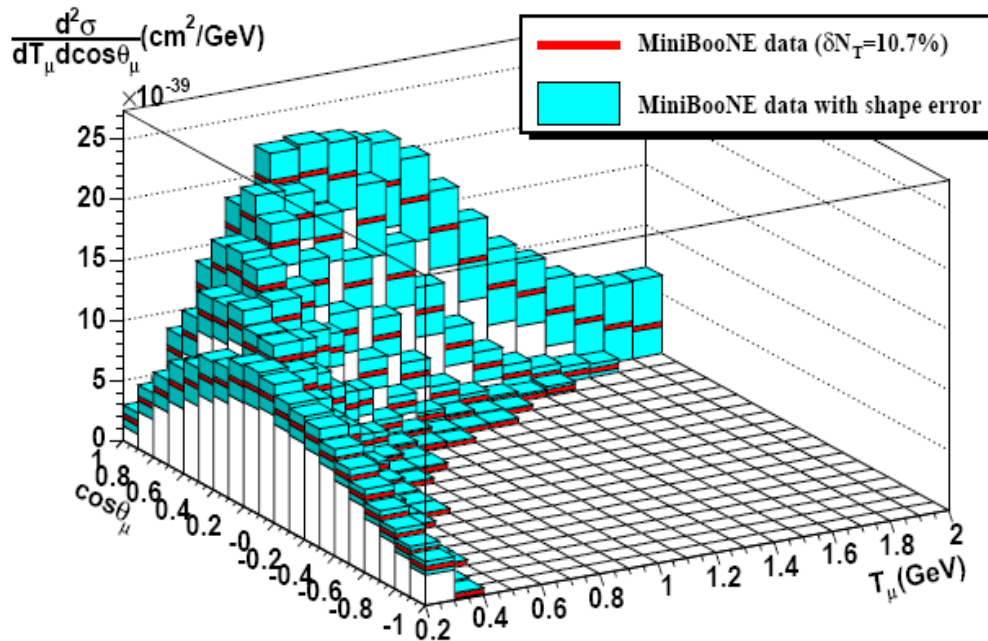


Flux-integrated double differential cross section

$$\left(\frac{d^2\sigma}{dT_l \cos\theta} \right)_i = \frac{\sum_j U_{ij}(d_j - b_j)}{\Phi \cdot T \cdot \epsilon_i \cdot (\Delta T_l, \Delta \cos\theta)_i} \quad (\text{see slide 9})$$

PHYSICAL REVIEW D **81**, 092005 (2010)

First measurement of the muon neutrino charged current quasielastic **double differential cross section**



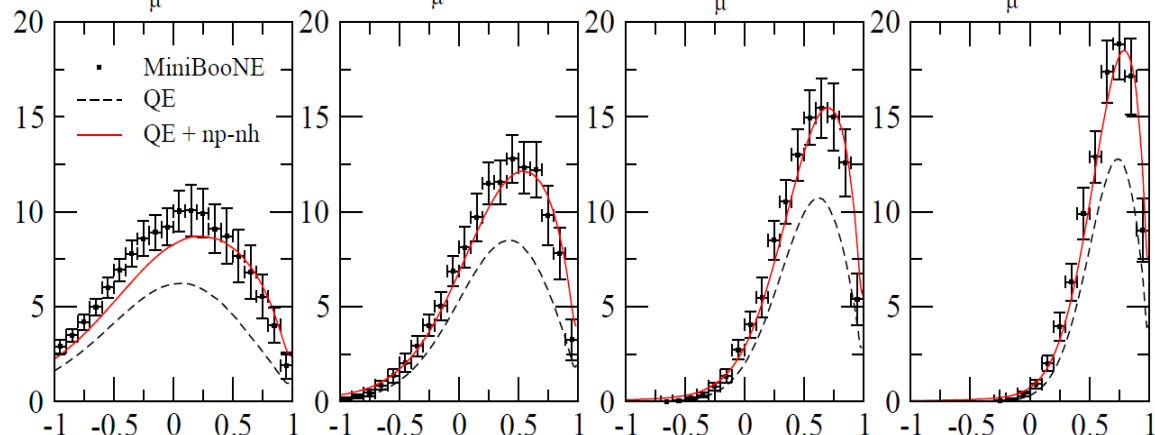
- Function of two measured variables
- Less model dependent than $\sigma(E_\nu)$: free from the neutrino energy reconstruction problem (see later)
- Flux dependent

Flux-integrated differential cross section is where theorists and experimentalists meet for ν interaction

MiniBooNE CCQE-like flux-integrated double differential cross section

$$\frac{d^2\sigma}{dT_l d\cos\theta} = \frac{1}{\int \Phi(E_\nu) dE_\nu} \int dE_\nu \left[\frac{d^2\sigma}{d\omega d\cos\theta} \right]_{\omega=E_\nu-E_l} \Phi(E_\nu)$$

0.2 < T_μ < 0.3 GeV 0.3 < T_μ < 0.4 GeV 0.4 < T_μ < 0.5 GeV 0.5 < T_μ < 0.6 GeV

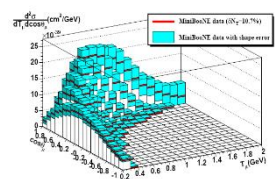


$\frac{d^2\sigma}{d\cos\theta dT_\mu} (10^{-39} \text{ cm}^2/\text{GeV})$

$\cos \theta$

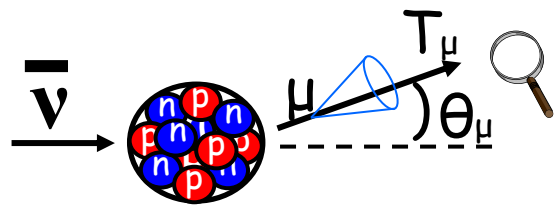
Martini, Ericson, Chanfray,
Phys. Rev. C 84 055502 (2011)

- Good agreement with data once multinucleon contributions are included
- Similar conclusions obtained by different theoretical calculations (see later)

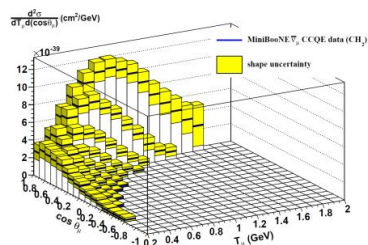


ν

MiniBooNE CCQE-like flux-integrated double differential cross section

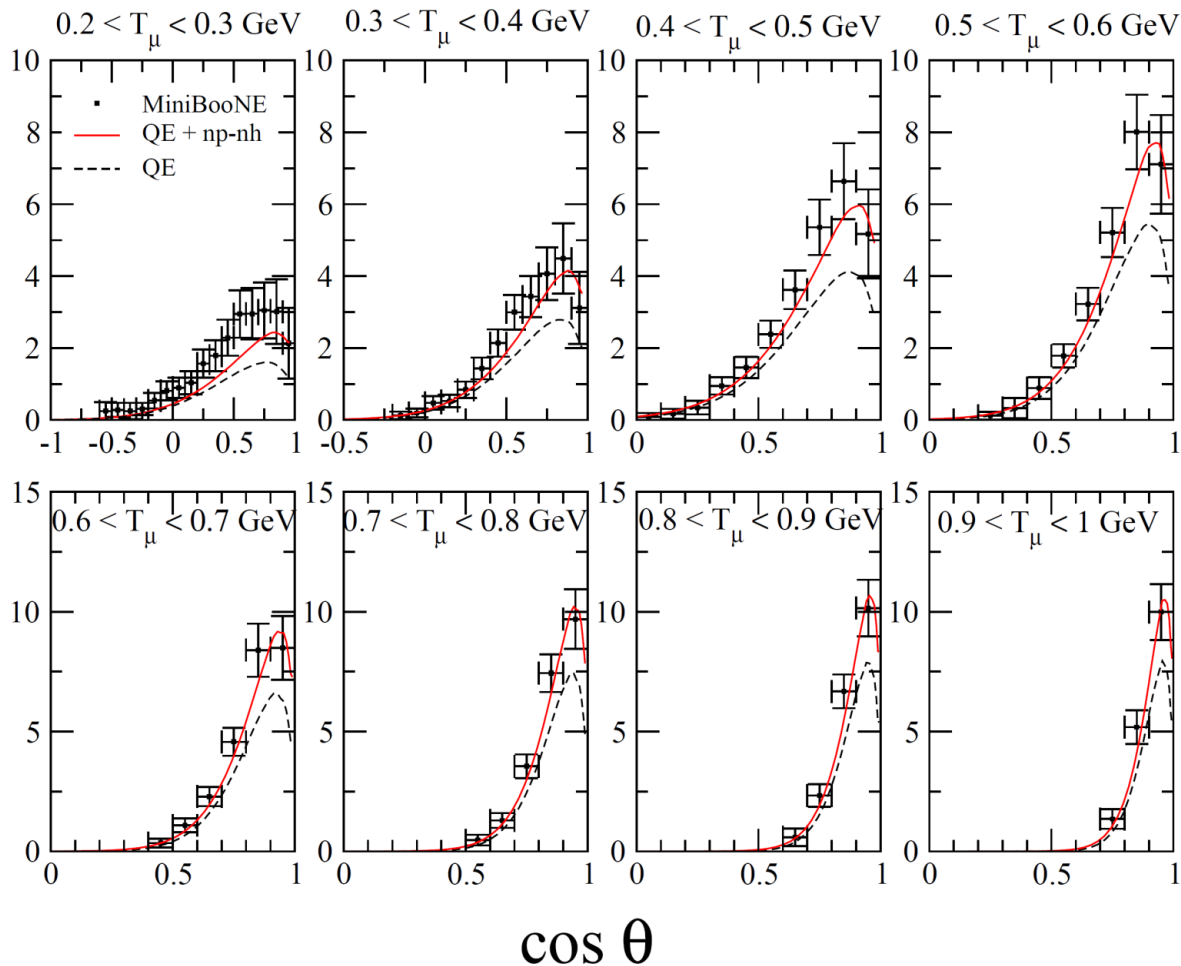


$\bar{\nu}$



MiniBooNE, *Phys. Rev. D* 88 032001 (2013)

$\frac{d^2 \sigma}{d \cos \theta_{\mu} d T_{\mu}} (10^{-39} \text{ cm}^2 / \text{GeV})$



Martini, Ericson, *Phys. Rev. C* 87 065501 (2013)

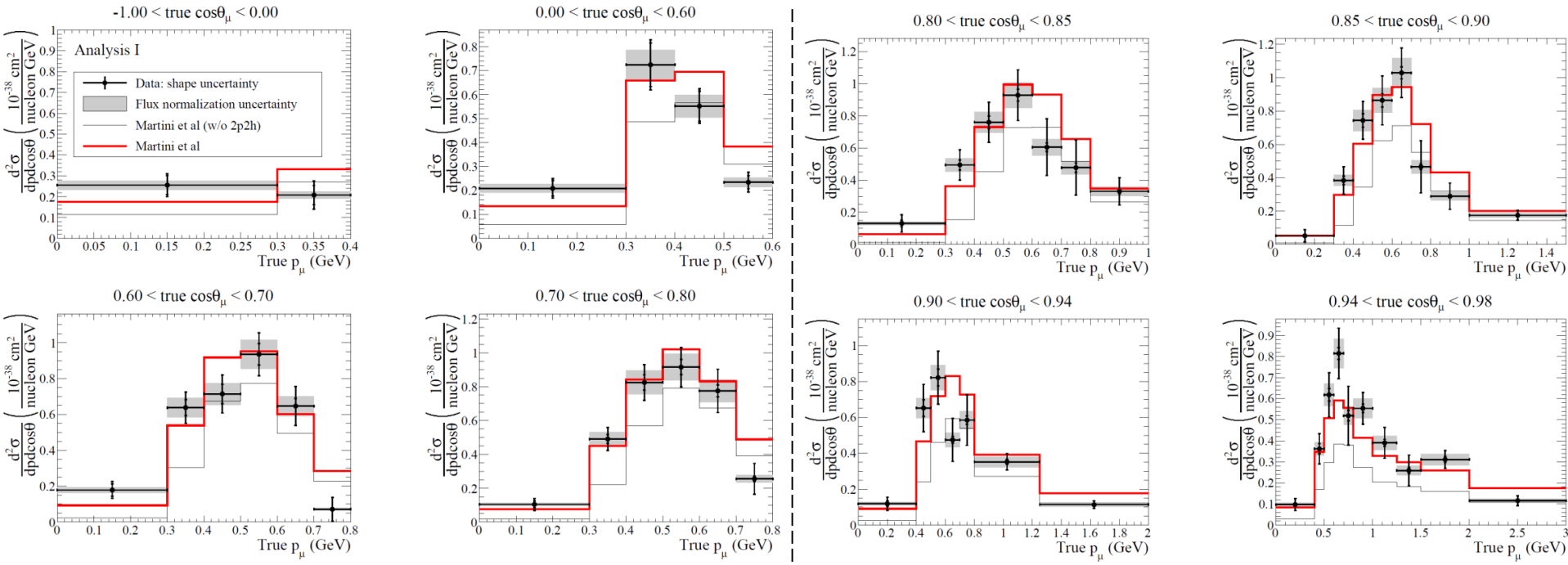
Similar conclusion also for the MiniBooNE CCQE-like antineutrino cross sections

The $CC0\pi$ measurement

After MiniBooNE, it has become more popular to present the data in terms of **final state particles**
 $CC0\pi = CCQE$ -like without subtraction of π absorption background ($CC0\pi \geq CCQE$ -like)

PHYSICAL REVIEW D **93**, 112012 (2016)

Measurement of double-differential muon neutrino charged-current interactions on C_8H_8 without pions in the final state using the T2K off-axis beam



— Including np - nh
 — Without np - nh

Better agreement including np - nh

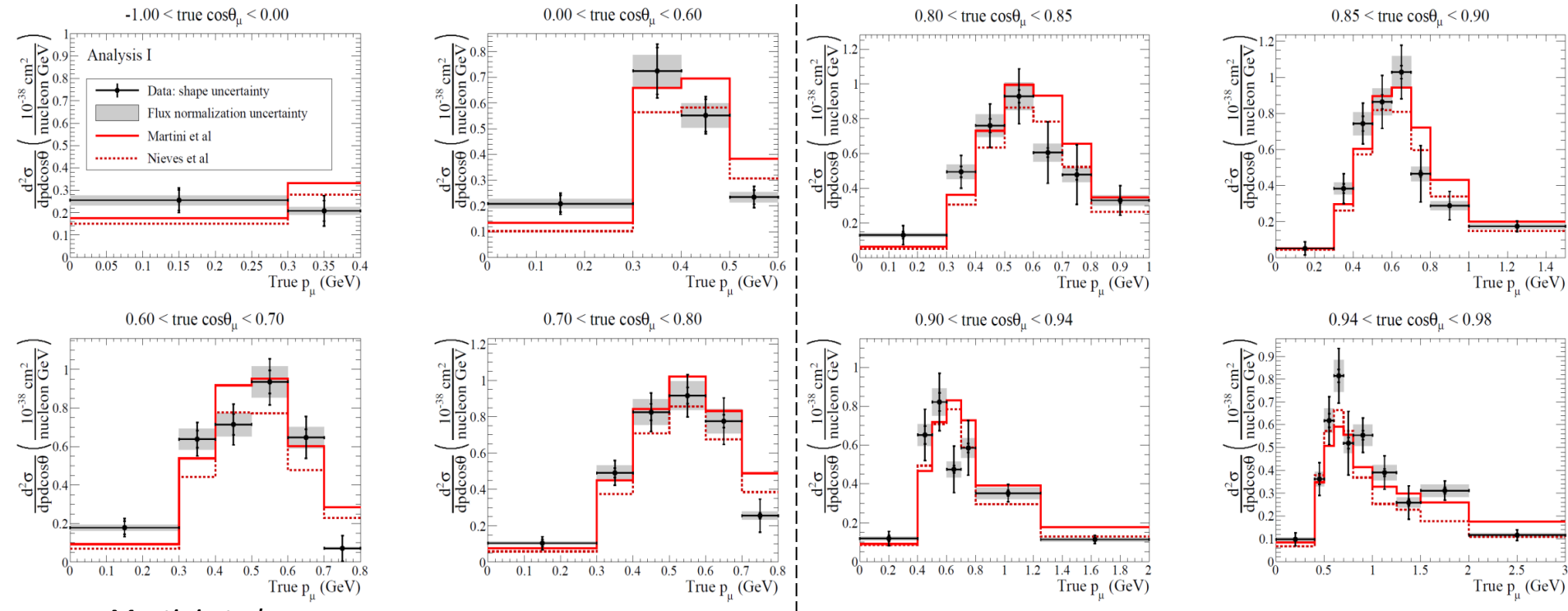
The $CC0\pi$ measurement

After MiniBooNE, it has become more popular to present the data in terms of final state particles

$CC0\pi = CCQE$ -like without subtraction of π absorption background

PHYSICAL REVIEW D **93**, 112012 (2016)

Measurement of double-differential muon neutrino charged-current interactions on C_8H_8 without pions in the final state using the T2K off-axis beam

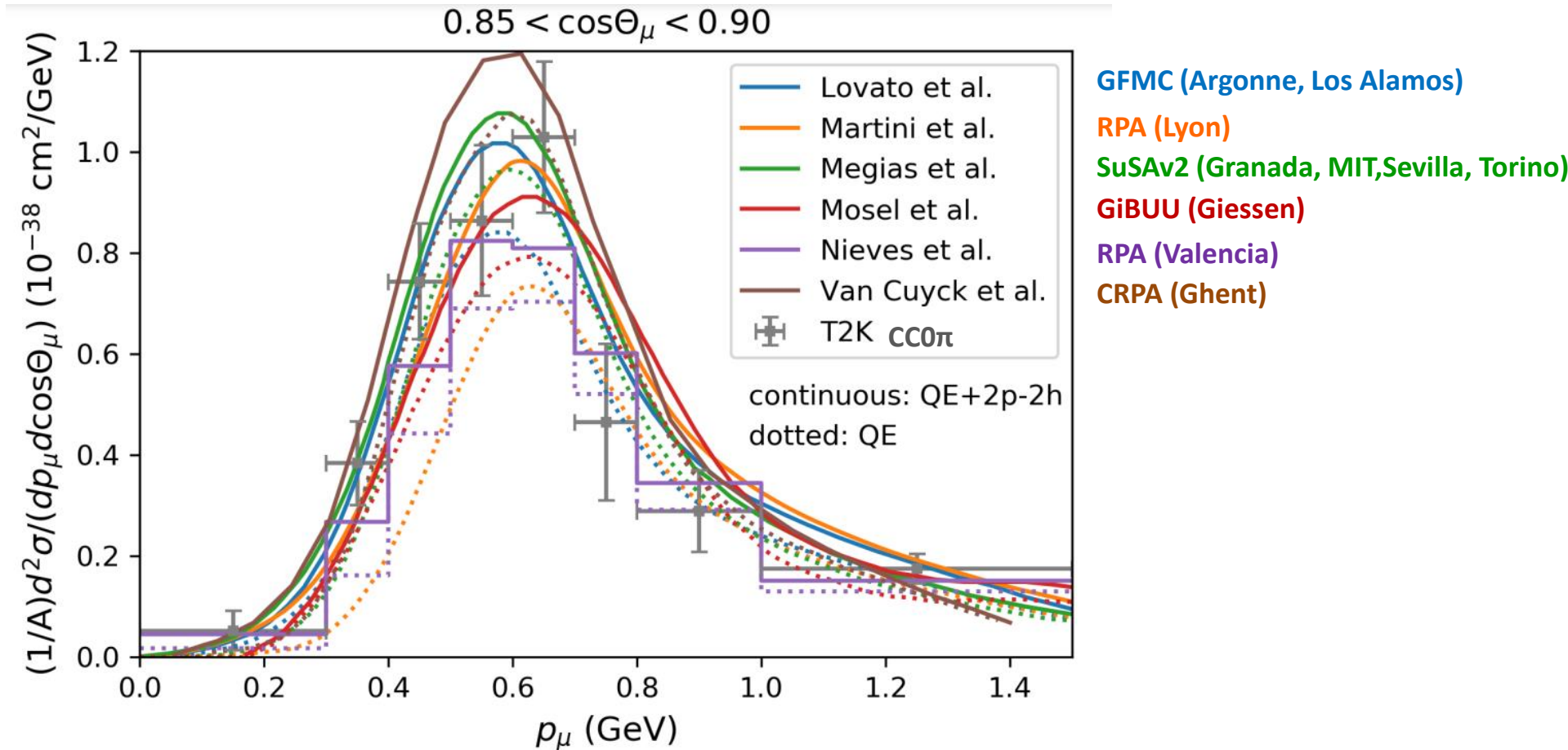


— Martini et al.
..... Nieves et al.

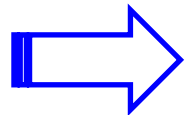
Differences between models' predictions

Comparison between different CCQE+2p-2h theoretical predictions

A. Branca et al. *Symmetry* 13 (2021) 9, 1625



Several theoretical calculations agree on the crucial role of 2p-2h to reproduce data but there are discrepancies between the different models' predictions

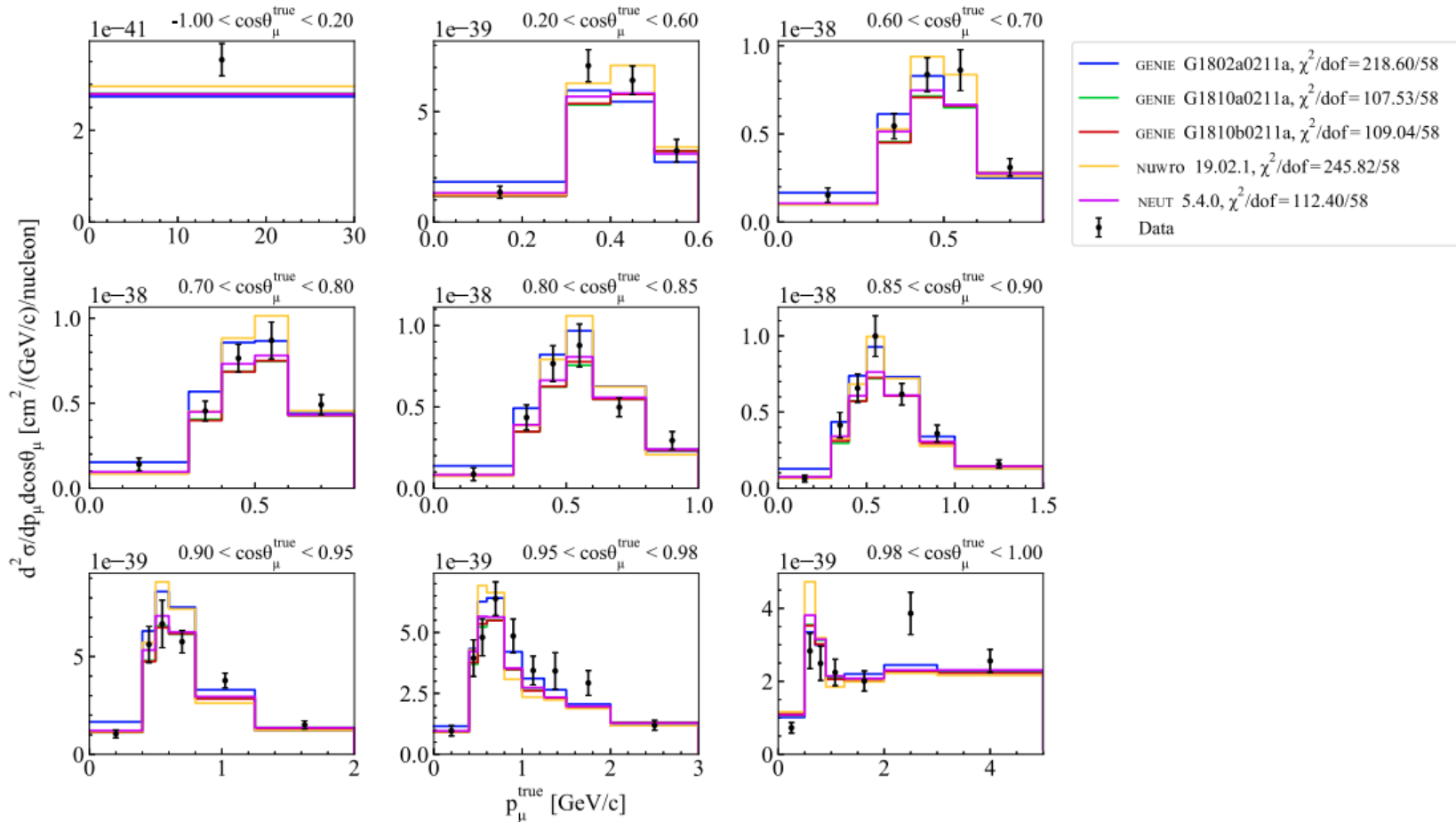


2p-2h are one of the most important source of the cross section uncertainties (systematic errors in oscillation experiments)

The T2K $\text{CC}0\pi$ data and the Monte Carlo predictions

M. BUIZZA AVANZINI *et al.*

PHYS. REV. D **105**, 092004 (2022)



Differences in the MC predictions (CCQE, 2p-2h and π absorption modeling)

p.s. The effort to implement different 2p-2h models in several Monte Carlo is still in progress

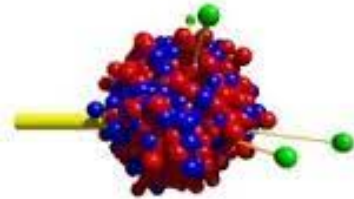
Monte Carlo Event Generators

Monte Carlo event generators connects theoretical models to experimental measurements

Main Event Generators for neutrino interactions:



GiBUU



NEUT



L. Alvarez-Ruso et al.,
EPJ Spec. Top. 230, 4449 (2021)

O. Buss et al.,
Phys.Rept. 512 1-124 (2012)

Y. Hayato and L. Pickering,
EPJ Spec. Top. 230, 4469 (2021)

T. Golan et al.,
NPB 229–232, 499 (2012)

PHYSICAL REVIEW D **105**, 092004 (2022)

Comparisons and challenges of modern neutrino-scattering experiments

M. Buizza Avanzini¹, M. Betancourt², D. Cherdack³, M. Del Tutto^{2,4}, S. Dytman⁵, A. P. Furmanski^{6,7},
S. Gardiner², Y. Hayato⁸, L. Koch⁹, K. Mahn¹⁰, A. Mastbaum¹¹, B. Messerly^{5,7}, C. Riccio^{12,13},
D. Ruterbories¹⁴, J. Sobczyk¹⁵, C. Wilkinson¹⁶ and C. Wret¹⁴

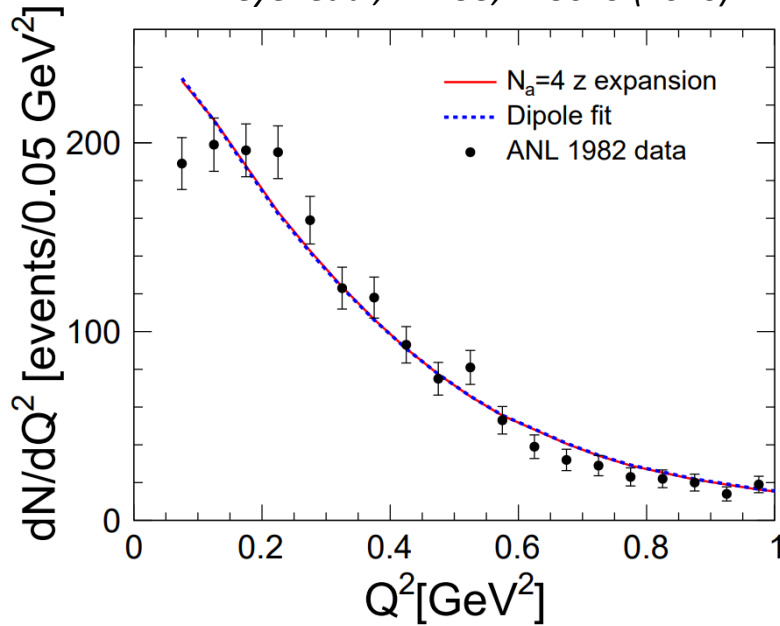
Main models implemented for the quasielastic and 2p-2h:

- Relativistic global and local Fermi Gas
- RPA
- Spectral Function
- SuperScaling (SuSAv2)

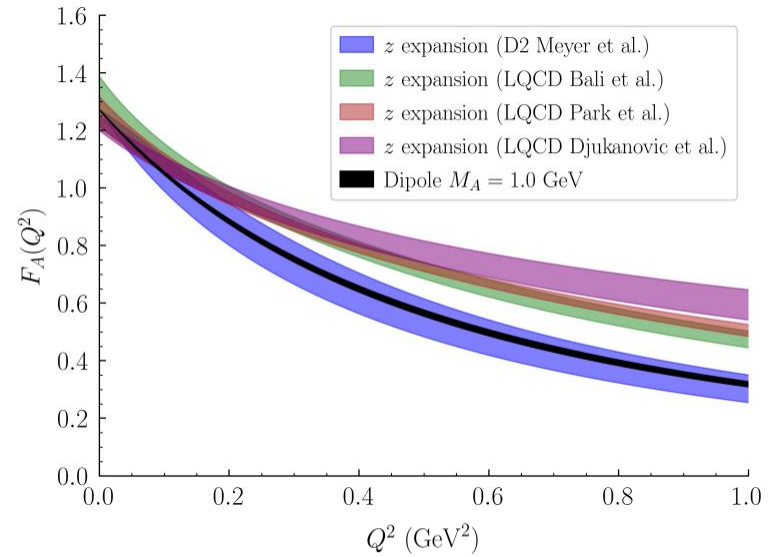
[For the illustration of the different models see for example the cross section lectures at the GIF school]

Axial Form factor and Lattice QCD predictions

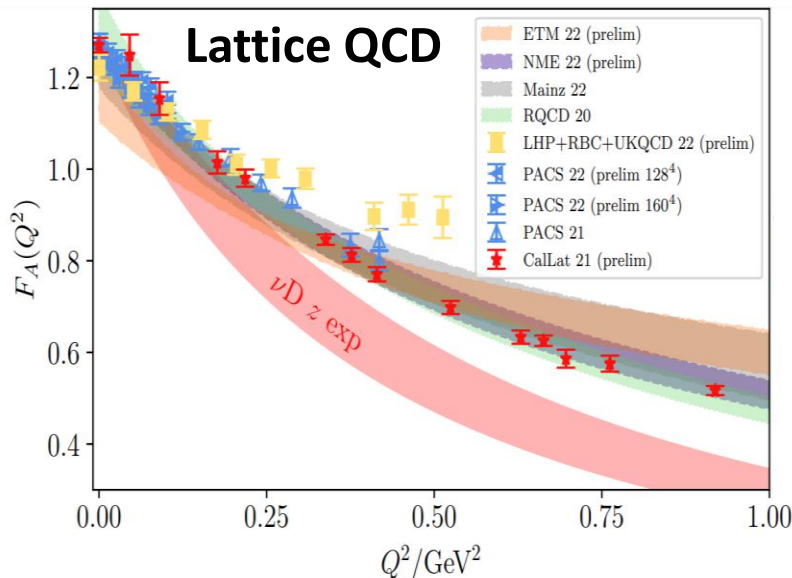
A. Meyer et al, PRD93, 113015 (2016)



D. Simons et al. 2210.02455



A. Meyer talk @ NUINT 2022; Ann.Rev.Nucl.Part.Sci. 72 (2022)

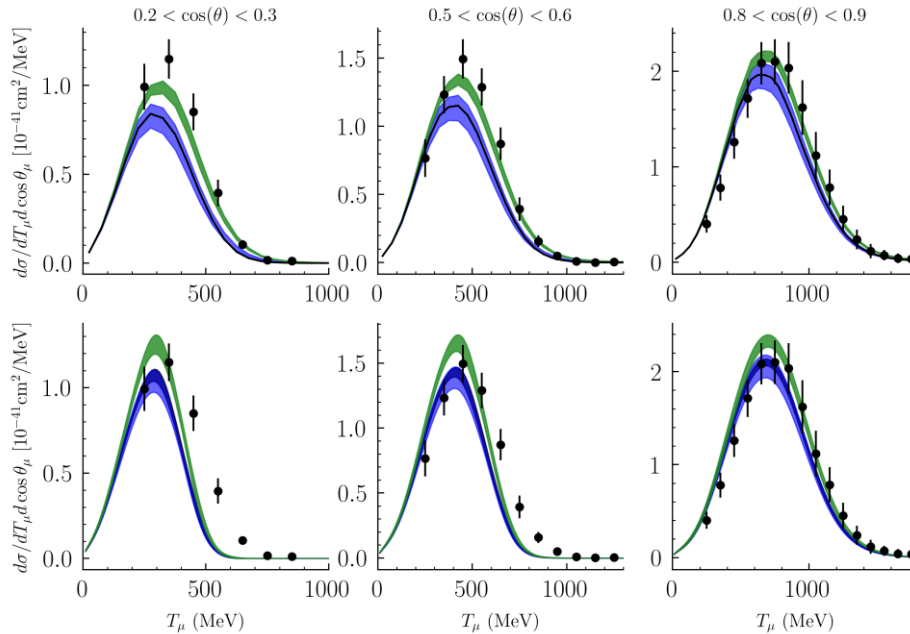


- Dipole parameterization underestimates uncertainties
- Meyer et al. z -expansion: similar to dipole parameterization but larger errors
- Lattice QCD calculations show evidence of slow Q^2 falloff
- LQCD: much larger normalization at $Q^2 > 0.3$ GeV²

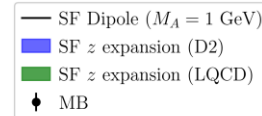
Impact of enhanced axial form factor from LQCD

D. Simons et al. 2210.02455

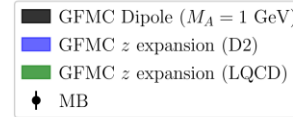
MiniBooNE



SF

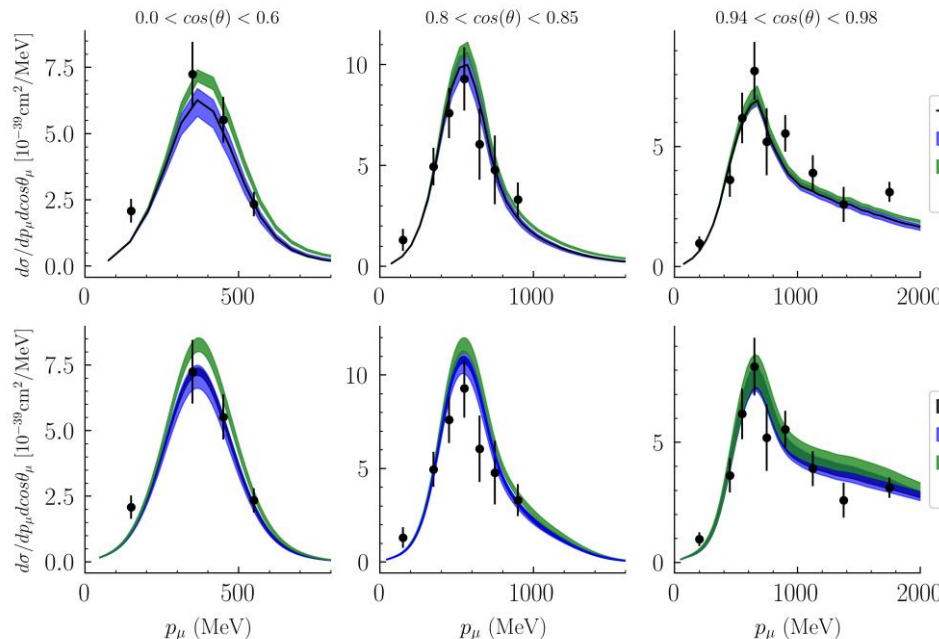


GFMC

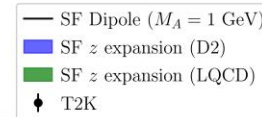


MiniBooNE:
 Universal 10-20% increase
 in normalization with LQCD

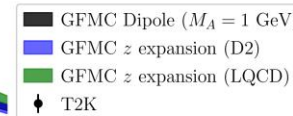
T2K



SF



GFMC



T2K:
 Results fairly independent of
 parameterization
 Mostly due to T2K's lower
 beam energy hence lower Q^2
 where form factors agree

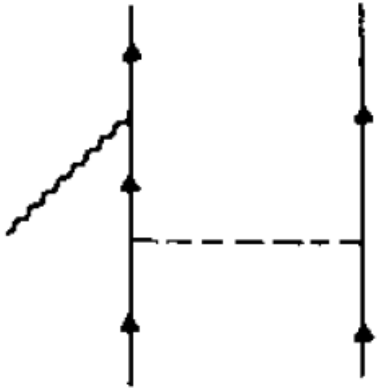
**Data have room for both 2p-2h and
 enhanced axial form factor for LQCD**

Some details on 2p-2h

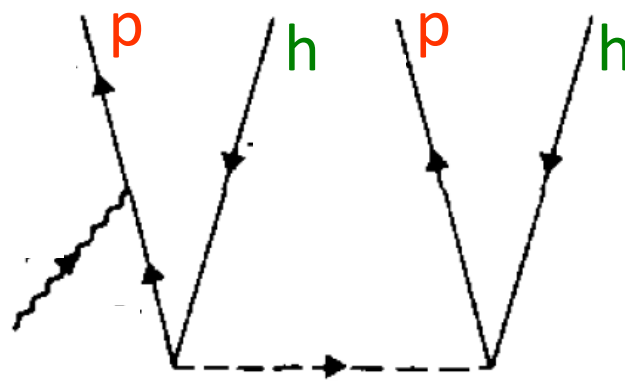
Two particle-two hole sector (2p-2h)

Three equivalent representations of the same process

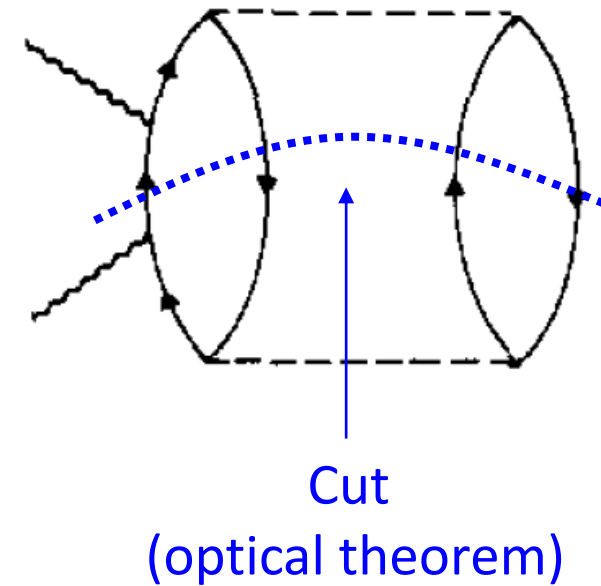
2 body current



2p-2h matrix element



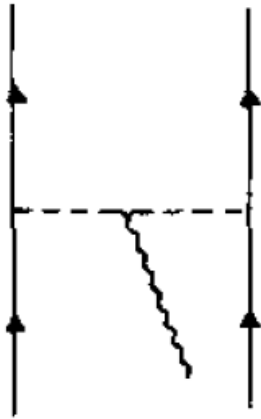
2p-2h response



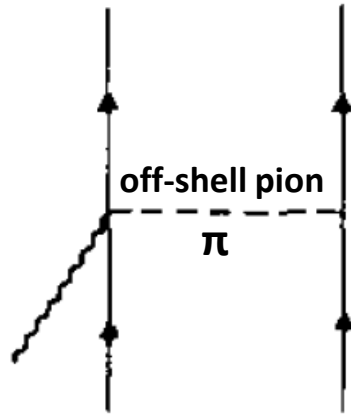
Final state: two particles-two holes

Diagrams for 2 body currents

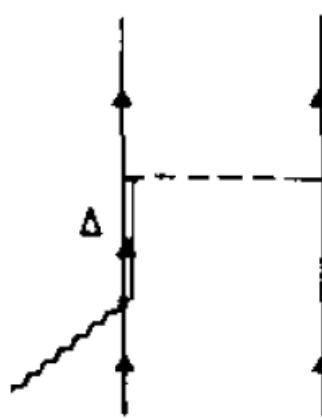
Meson Exchange Currents (MEC) J^{MEC}



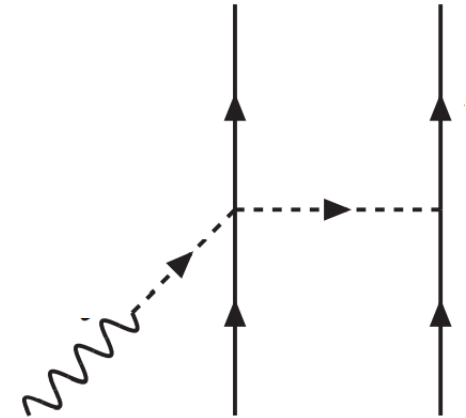
Pion in flight



Seagull or
Contact

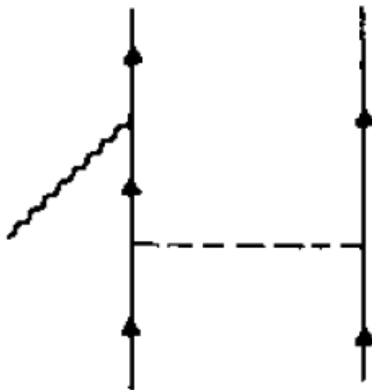


Delta



Pion pole
(purely axial)

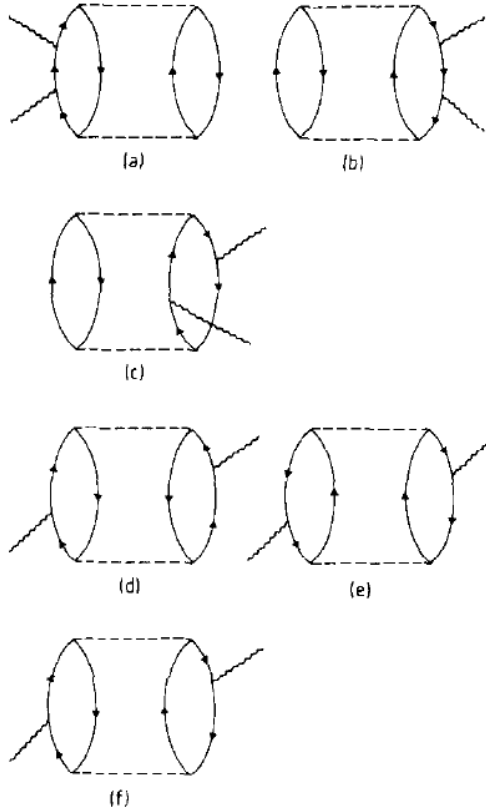
Nucleon-Nucleon Correlations (SRC) J^{corr}



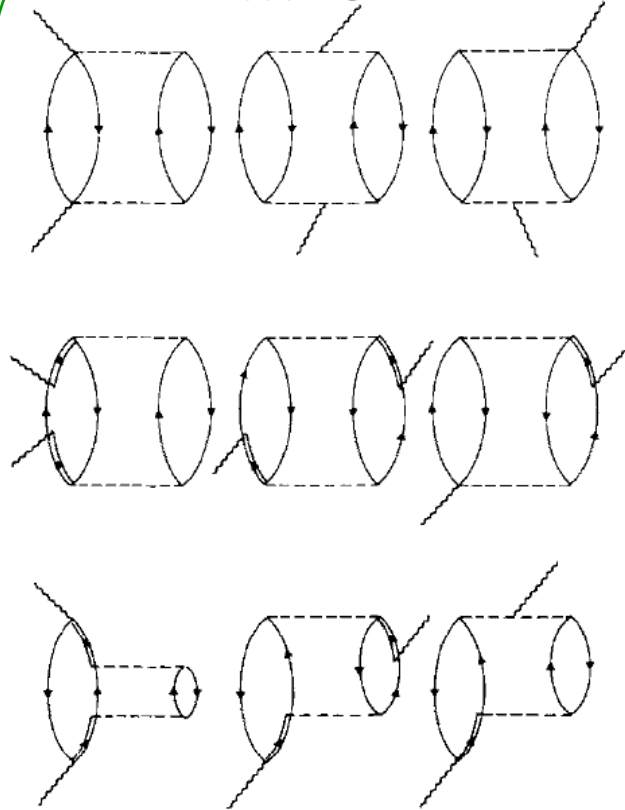
- An additional two-body current to be included in the framework of independent particle models for QE such as the Fermi Gas or Hartree-Fock.
- Absent in the approaches which start from the description of the nucleus in terms of correlated wave functions (such as CBF spectral function or GFMC) since the hadronic tensor of the one body current already includes this contribution.
- **There is a risk of a double counting of SRC in the Monte Carlo if different contributions to the neutrino cross sections are taken from different models.**

Some diagrams for 2p-2h responses

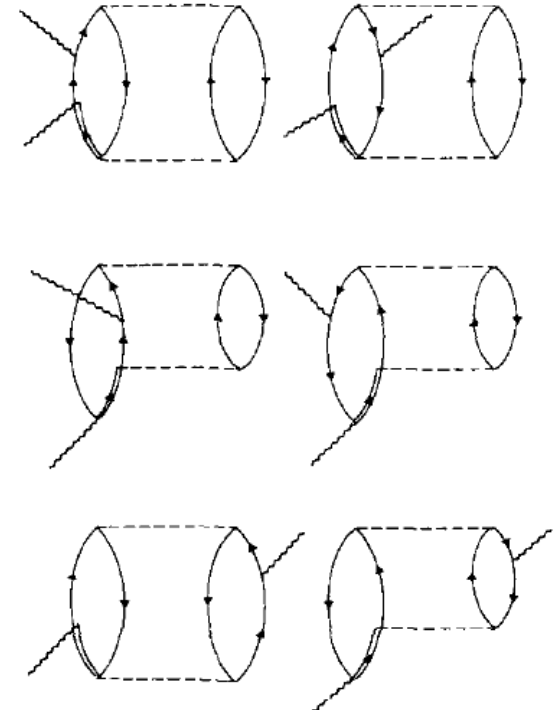
NN correlations



MEC



NN correlation-MEC interference



also called
1-body—2-body interference

Alberico, Ericson, Molinari, Ann. Phys. 154, 356 (1984)

Main difficulties in the np-nh sector

$$W^{\mu\nu}(\mathbf{q}, \omega) = W_{1p1h}^{\mu\nu}(\mathbf{q}, \omega) + W_{2p2h}^{\mu\nu}(\mathbf{q}, \omega) + \dots$$

$$W_{2p-2h}^{\mu\nu}(\mathbf{q}, \omega) = \frac{V}{(2\pi)^9} \int d^3p'_1 d^3p'_2 d^3h_1 d^3h_2 \frac{m_N^4}{E_1 E_2 E'_1 E'_2} \theta(p'_2 - k_F) \theta(p'_1 - k_F) \theta(k_F - h_1) \theta(k_F - h_2) \\ \underbrace{\langle 0 | J^\mu | \mathbf{h}_1 \mathbf{h}_2 \mathbf{p}'_1 \mathbf{p}'_2 \rangle \langle \mathbf{h}_1 \mathbf{h}_2 \mathbf{p}'_1 \mathbf{p}'_2 | J^\nu | 0 \rangle}_{\text{matrix elements}} \delta(E'_1 + E'_2 - E_1 - E_2 - \omega) \delta(\mathbf{p}'_1 + \mathbf{p}'_2 - \mathbf{h}_1 - \mathbf{h}_2 - \mathbf{q})$$

- 7-dimensional integrals $\int d^3h_1 d^3h_2 d\theta'_1$ of thousands of terms
- Huge number of diagrams and terms
- Divergences (angular distribution; NN correlations contributions)
- Calculations for all the kinematics compatible with the experimental neutrino flux

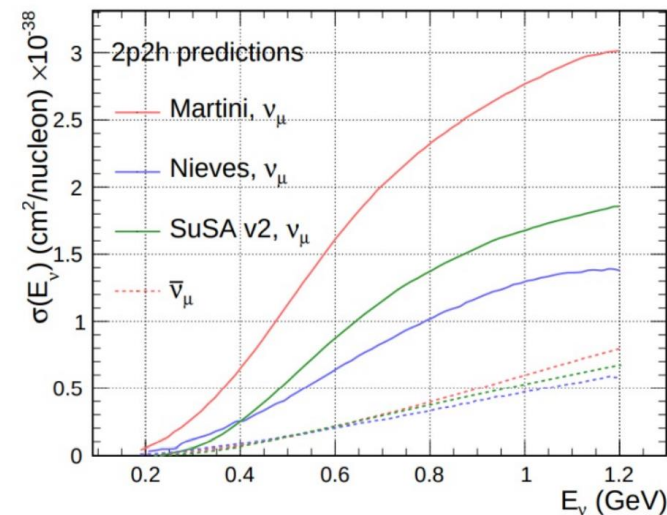
Computing very demanding

Hence different approximations by different groups:

- choice of subset of diagrams and terms;
- different prescriptions to regularize the divergences;
- reduce the dimension of the integrals
(7D --> 2D if non relativistic; 7D --> 1D if $h_1 = h_2 = 0$)

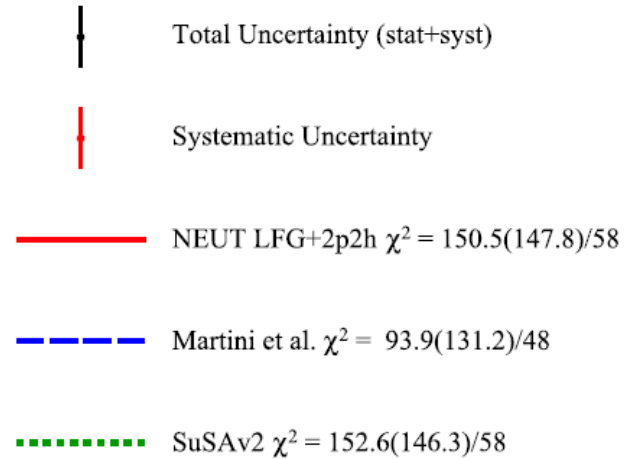
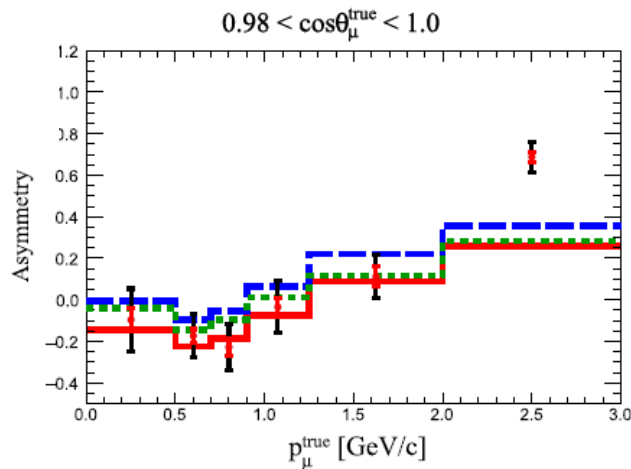
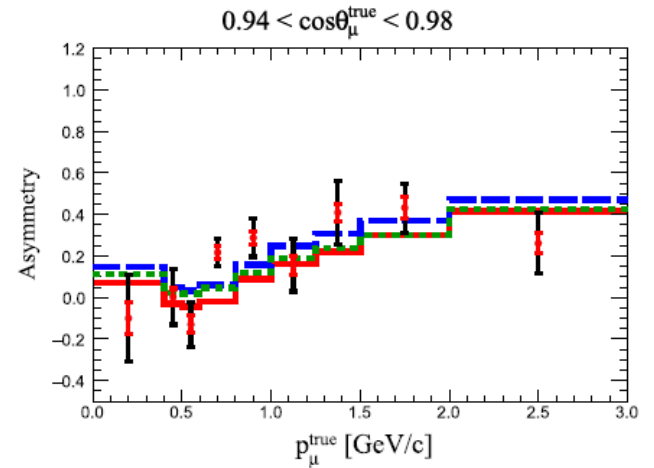
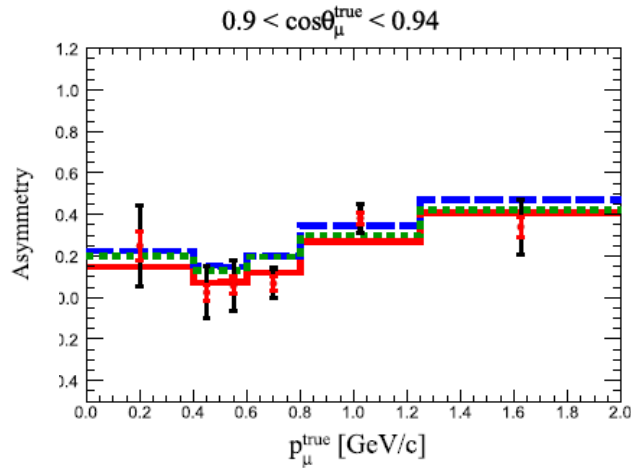
⇒ **Different final results by different groups**

- **The relative role of np-nh for neutrinos and antineutrinos is different in different approaches**



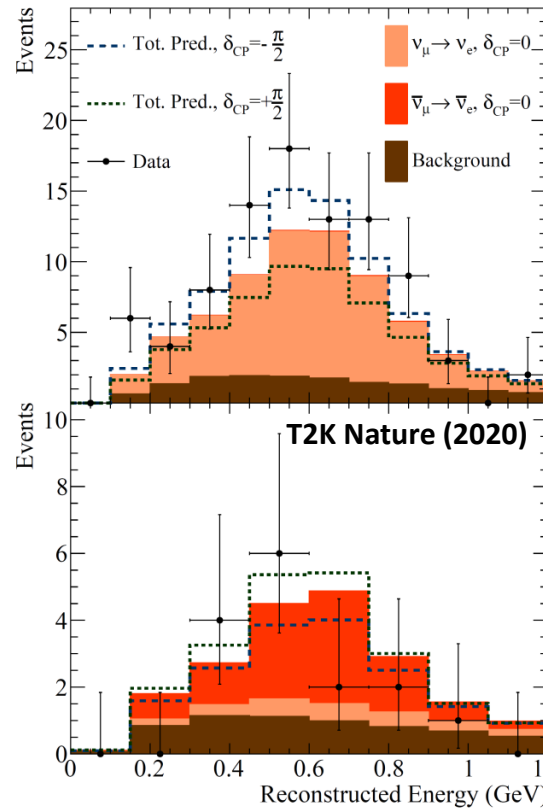
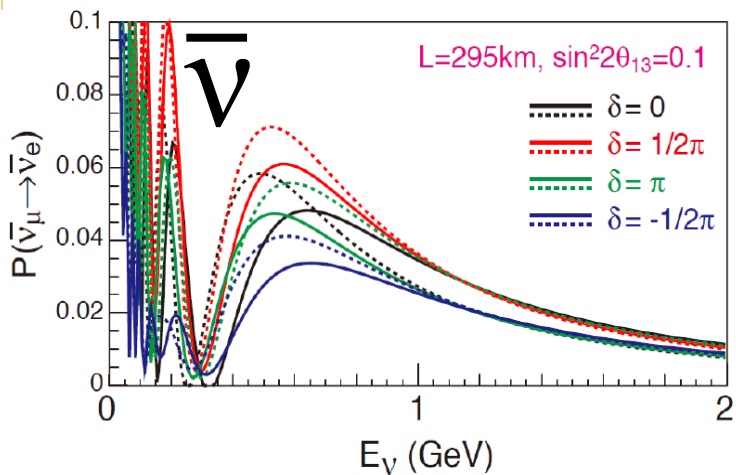
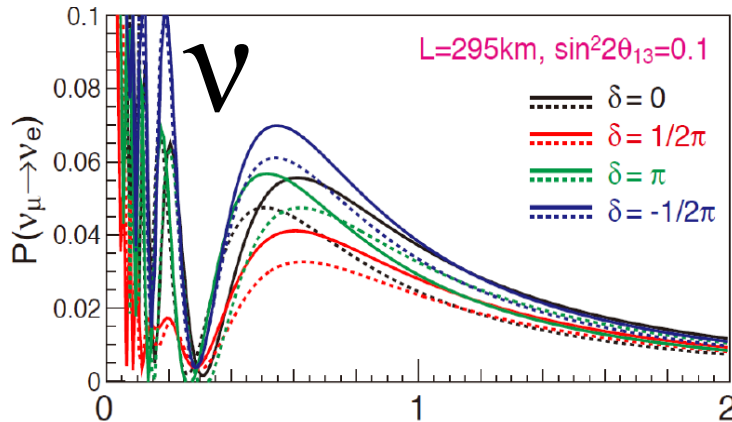
First combined measurement of the muon neutrino and antineutrino charged-current cross section without pions in the final state at T2K

$$\frac{\nu - \bar{\nu}}{\nu + \bar{\nu}}$$



What about ν vs $\bar{\nu}$ interaction? And ν_μ vs ν_e ?

$$P(\nu_\mu \rightarrow \nu_e) \stackrel{?}{\neq} P(\bar{\nu}_\mu \rightarrow \bar{\nu}_e)$$



$\nu_\mu \rightarrow \nu_e$

$\bar{\nu}_\mu \rightarrow \bar{\nu}_e$

A precise and simultaneous knowledge of the four cross sections is important in connection to the oscillation experiments aiming at the search for CP violation in the lepton sector (T2K, NOvA, Hyper-K, DUNE).

Non-trivial differences in the cross sections (see Appendix)

Neutrino energy reconstruction

Energy reconstruction in neutrino oscillation experiments

$$N_{\nu\beta}(\overline{E_\nu}) \sim \int \Phi_{\nu\alpha}(E_\nu) P_{\nu\alpha \rightarrow \nu\beta}(E_\nu, L, \{\Theta\}) \sigma_{\nu\beta}(E_\nu) \epsilon_{\text{det.}} d(E_\nu, \overline{E_\nu}) dE_\nu$$

Reconstructed ν energy
True ν energy

Number of detected events

ν flux	ν oscillation probability	ν cross section	Detector efficiency	Migration matrix
------------	-------------------------------	---------------------	---------------------	-------------------------

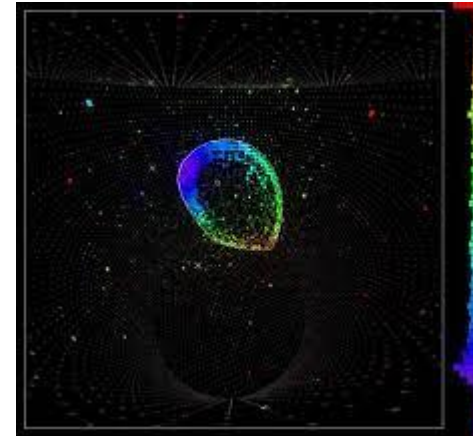
Two methods for ν energy reconstruction

Tracking detectors

- Use all the detected particles
- Calorimetric method

Cherenkov detectors

- Use only lepton (1 ring signal)
- Quasielastic-based method

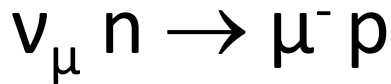
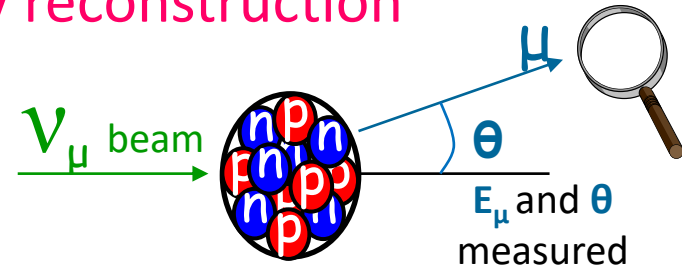


[For details see the cross section lectures at the GIF school]

Quasielastic-based neutrino energy reconstruction

Reconstructed neutrino energy

$$\overline{E}_\nu = \frac{m_p^2 - (m_n - E_b)^2 - m_\mu^2 + 2(m_n - E_b)E_\mu}{2(m_n - E_b - E_\mu + p_\mu \cos \theta_\mu)}$$

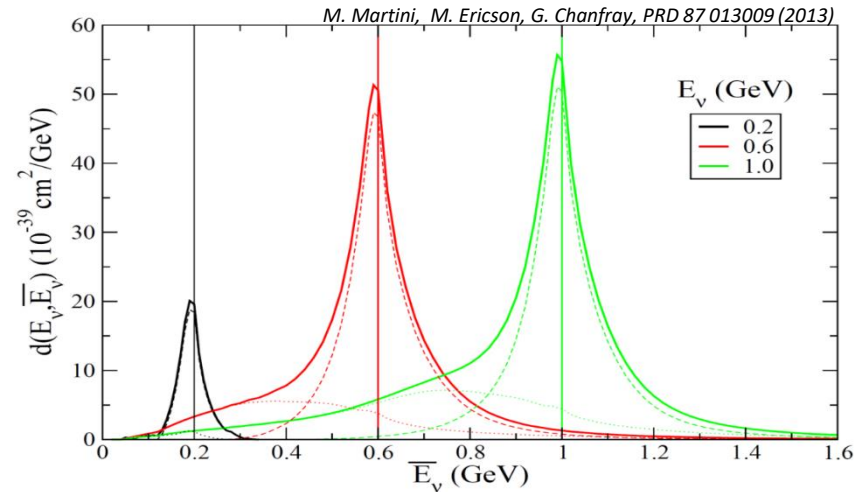


via two-body kinematics

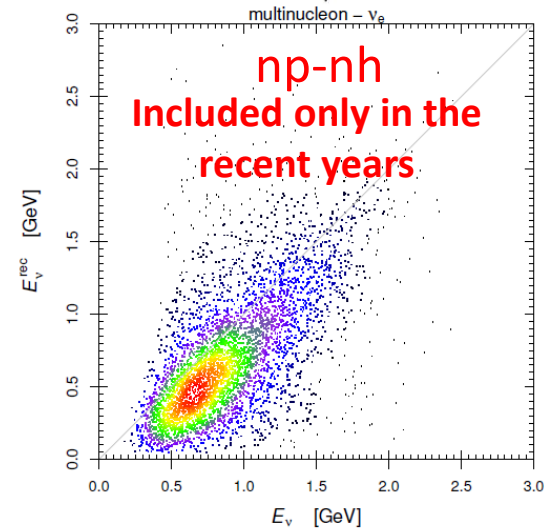
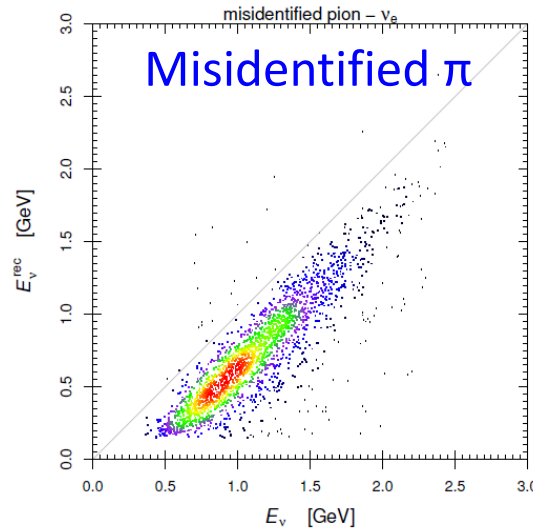
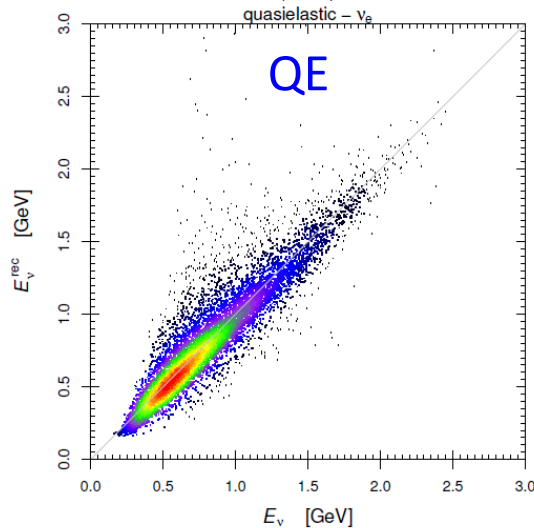
$\overline{E}_\nu = E_\nu$ exact only for CCQE with free nucleon

$$d(E_\nu, \overline{E}_\nu)$$

Migration matrix:
to take into account
nuclear effects

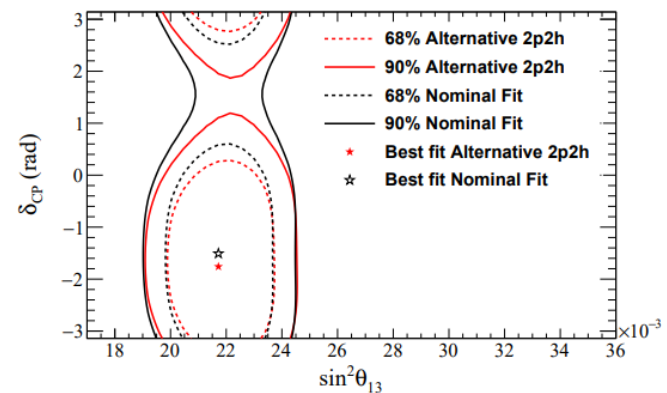
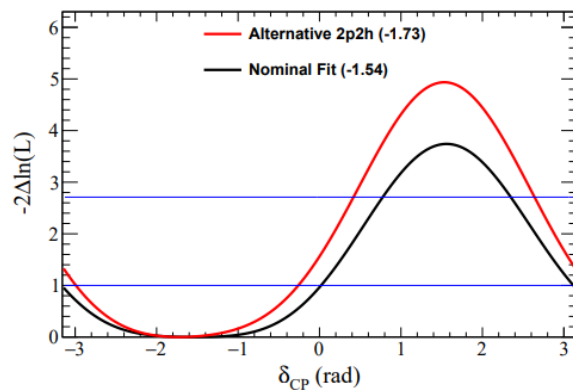
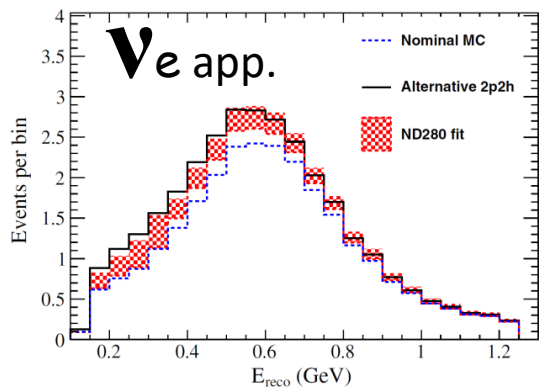
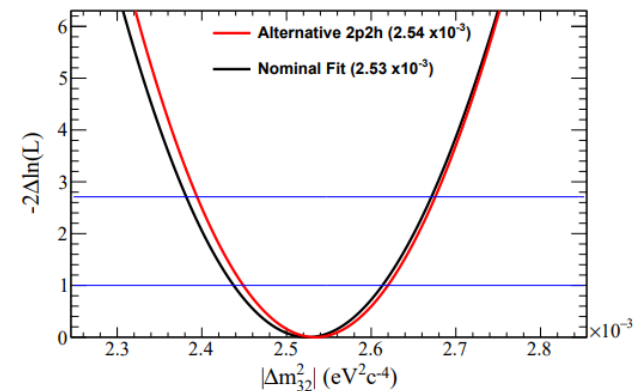
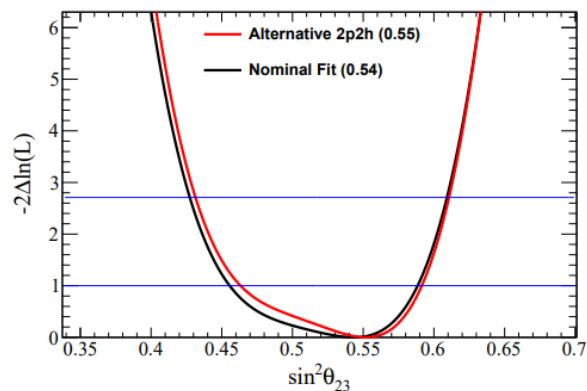
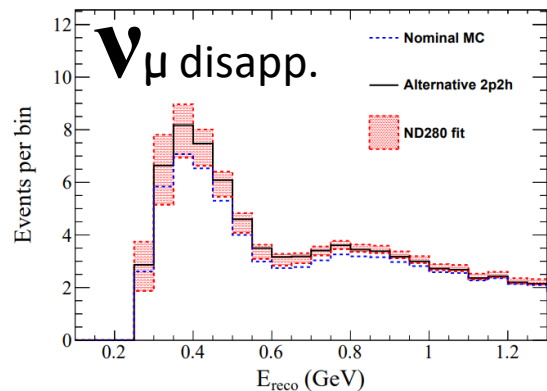


M. Ericson et al. PRD 93, 073008 (2016)



Impact of 2p-2h modeling on T2K oscillation analysis

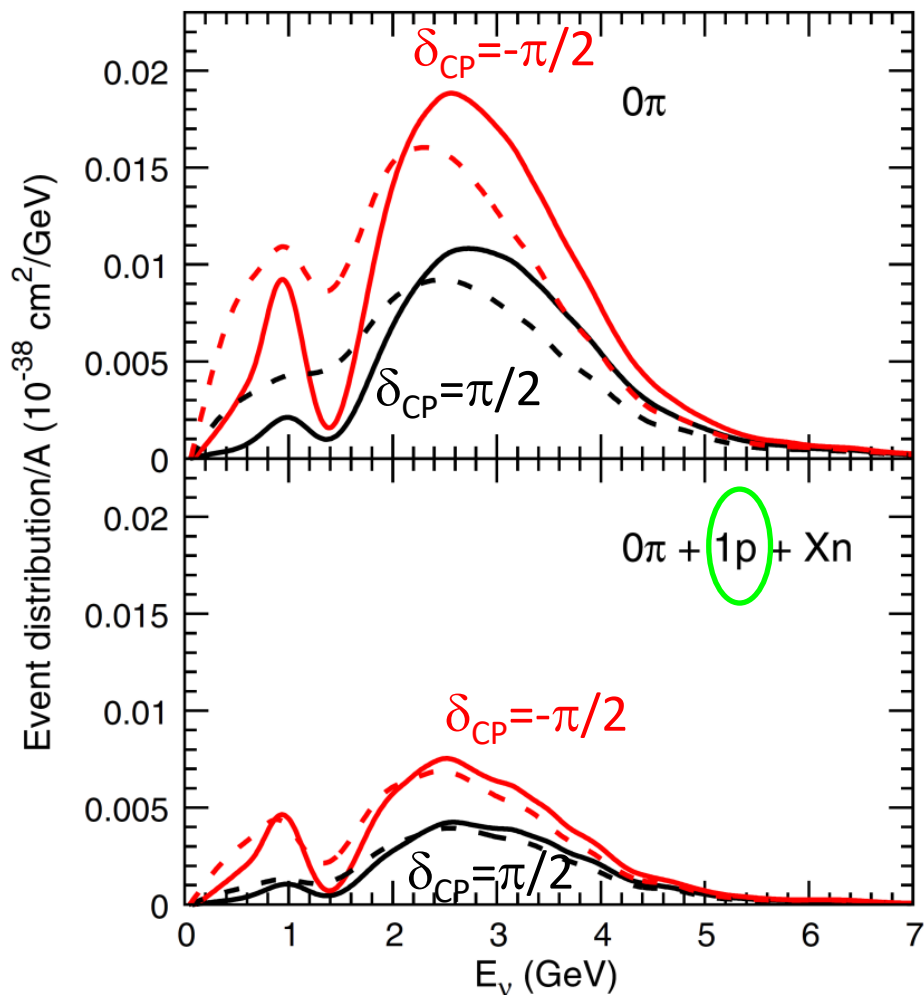
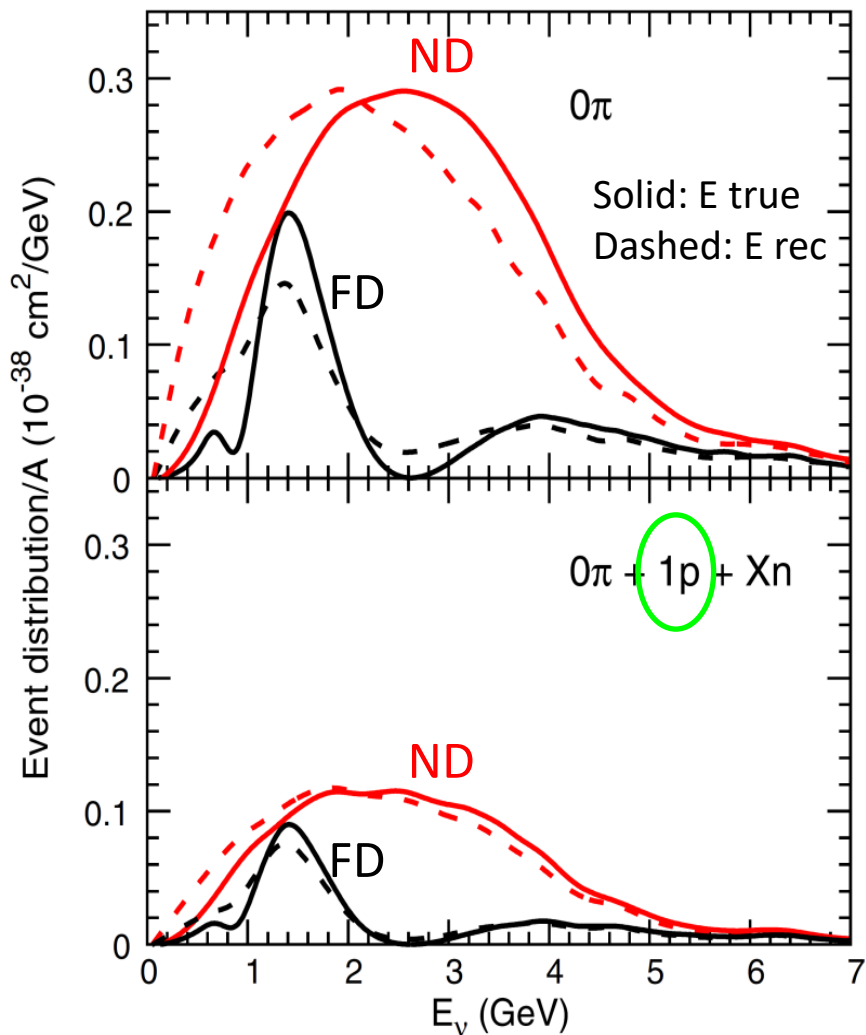
T2K Phys.Rev.D 96 (2017) 9, 092006



QE-based E_ν reconstruction using proton information

ν_μ disappearance in DUNE

ν_e appearance in DUNE

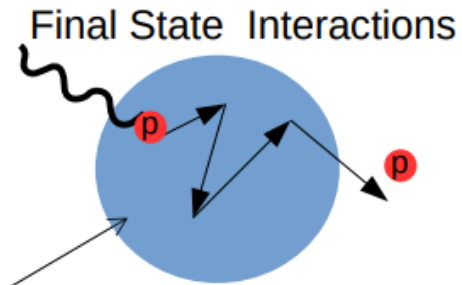


Major improvement in $0\pi + 1p + Xn$ sample, events down by only factor 3

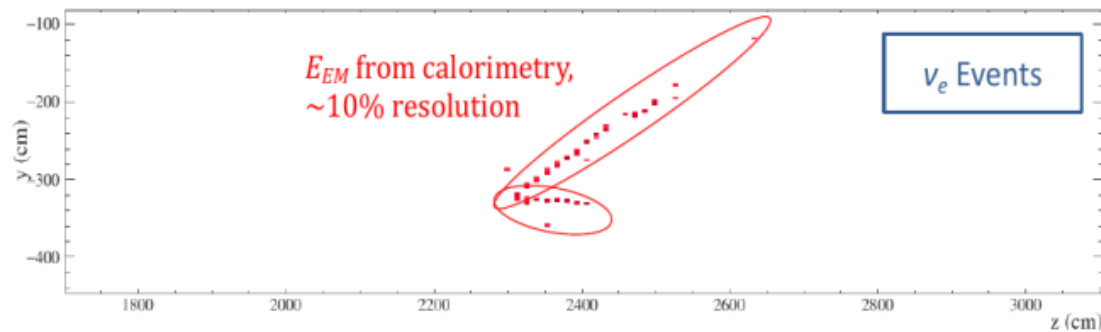
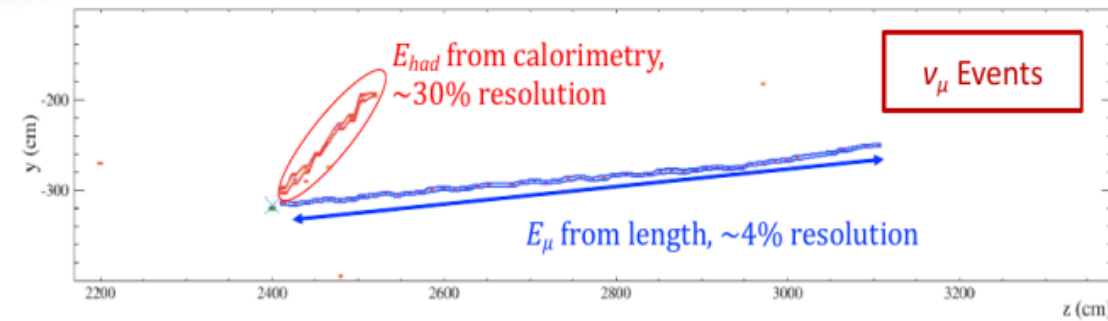
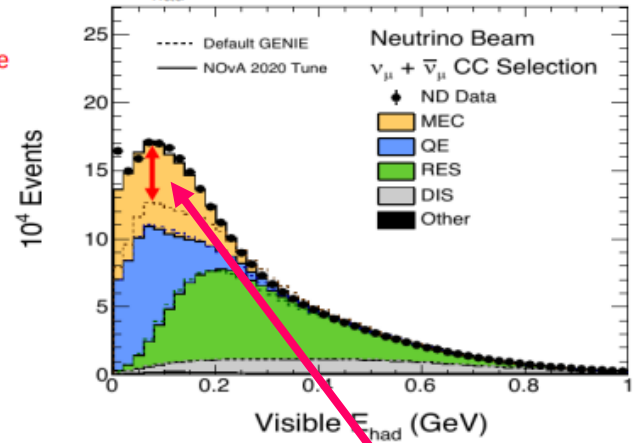
E_ν reconstruction NOvA

Calorimetric method

- E_ν reconstructed with hadronic deposits:
 - important difference $\nu - \bar{\nu}$: proton vs neutron (~undetected)
 - proton/pion energy smeared by Final State Interactions
- Different reconstruction and energy resolution for ν_μ and ν_e

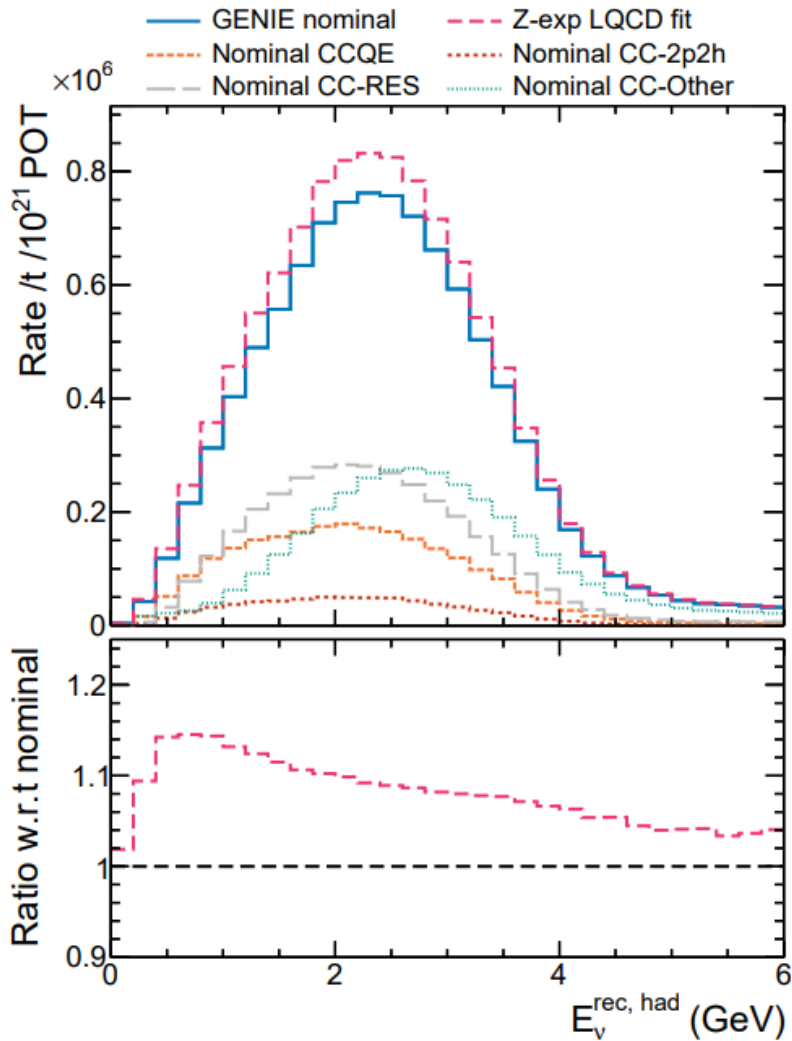


Important to tune model predictions for E_{had} NOvA Preliminary

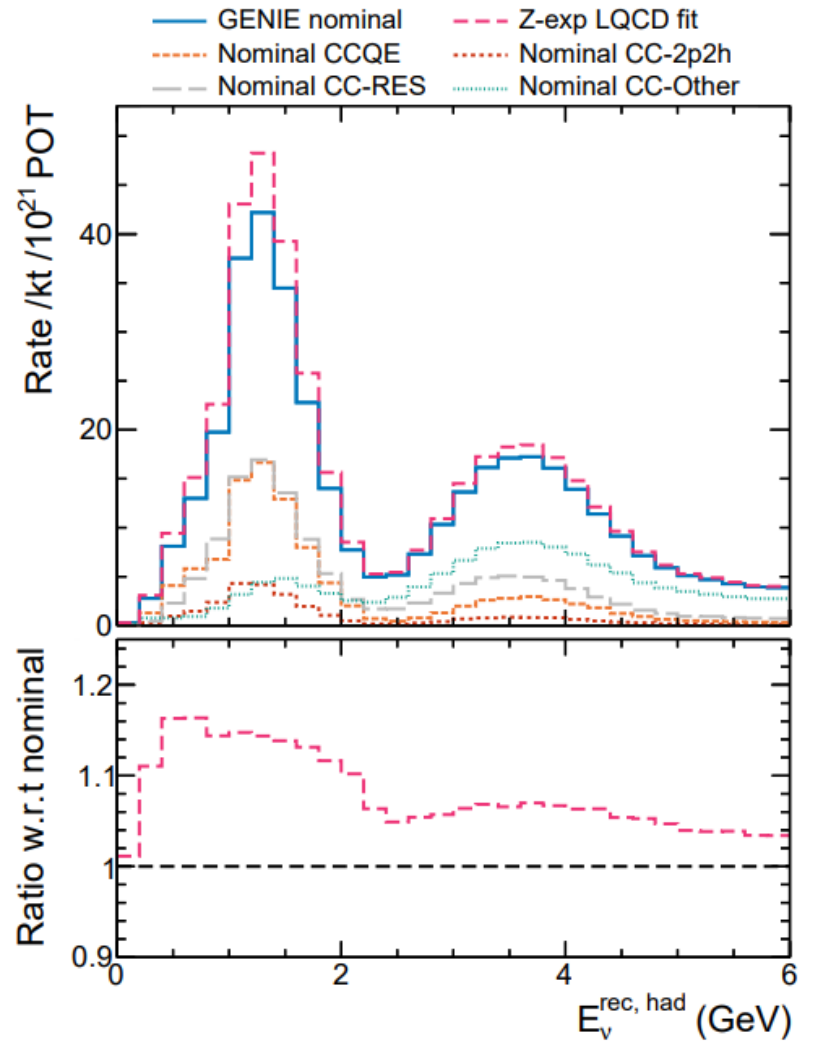


S. Bognesi @ GIF school 119

GENIE predictions of ν_μ - ^{40}Ar event rates at DUNE ND and FD



(a) ND



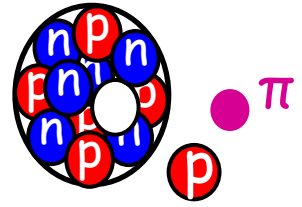
(b) FD

A. Meyer et al., *Ann.Rev.Nucl.Part.Sci.* 72 (2022)

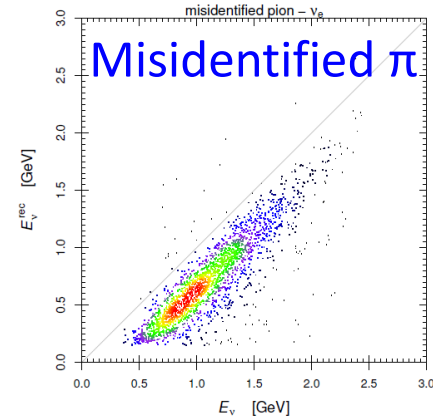
1π production

The one pion production channel

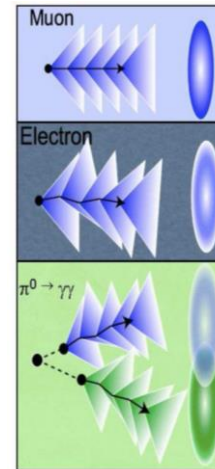
Important for several reasons:



- Misidentified π is part of the ν energy migration matrix in QE-based method



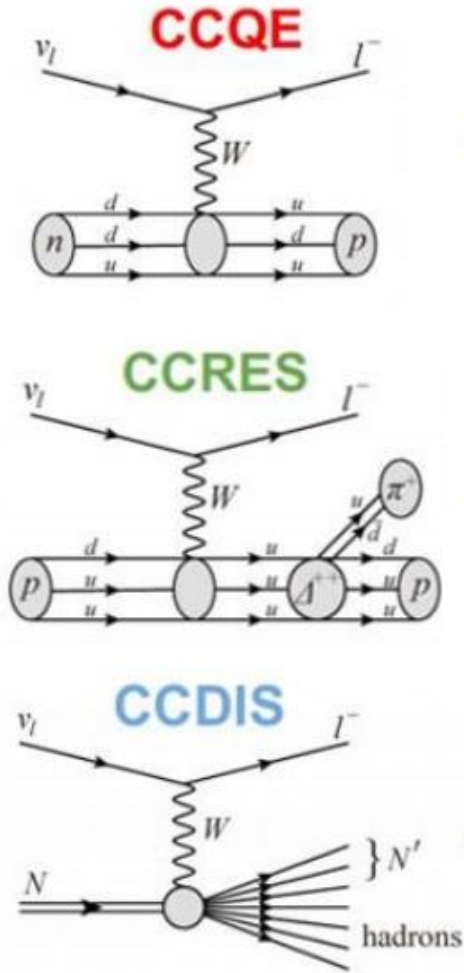
- In Cherenkov detectors NC1 π^0 can mimic electron-like signal in $\nu_\mu \rightarrow \nu_e$ oscillation search



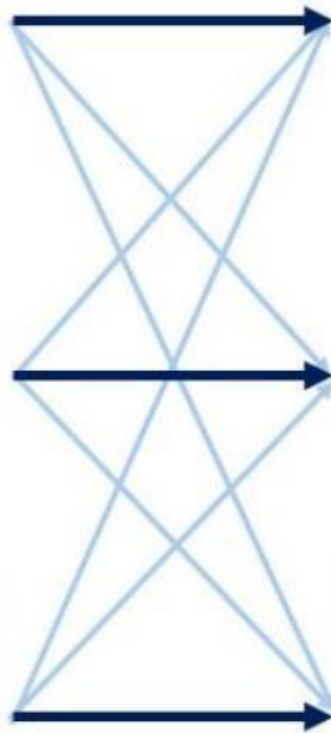
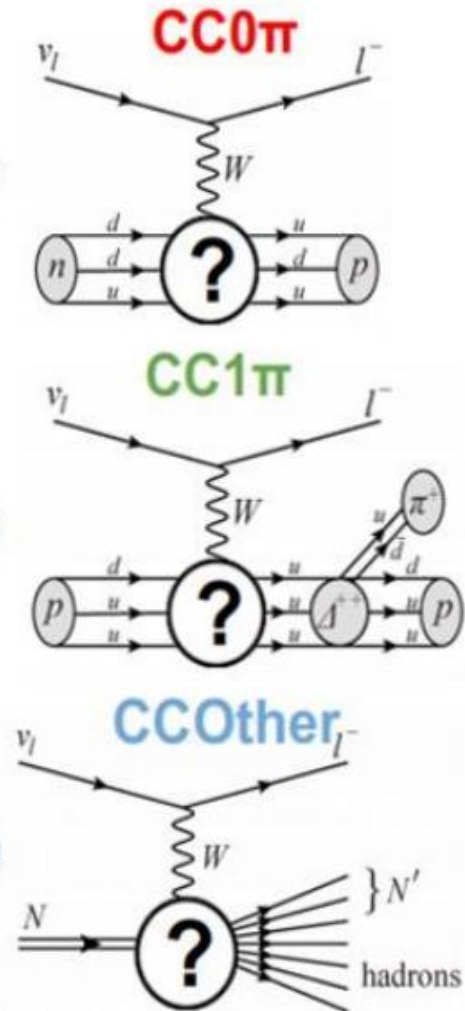
- There is an increasing interest on CC 2-ring signal (charged lepton and π) at SK
- It is one of the dominant channels in DUNE

Elementary vertices .vs. detection topologies

Elementary vertices
(nucleon level)



Detection topologies
(nucleus level)



Nuclear Effects
and Final State
Interactions

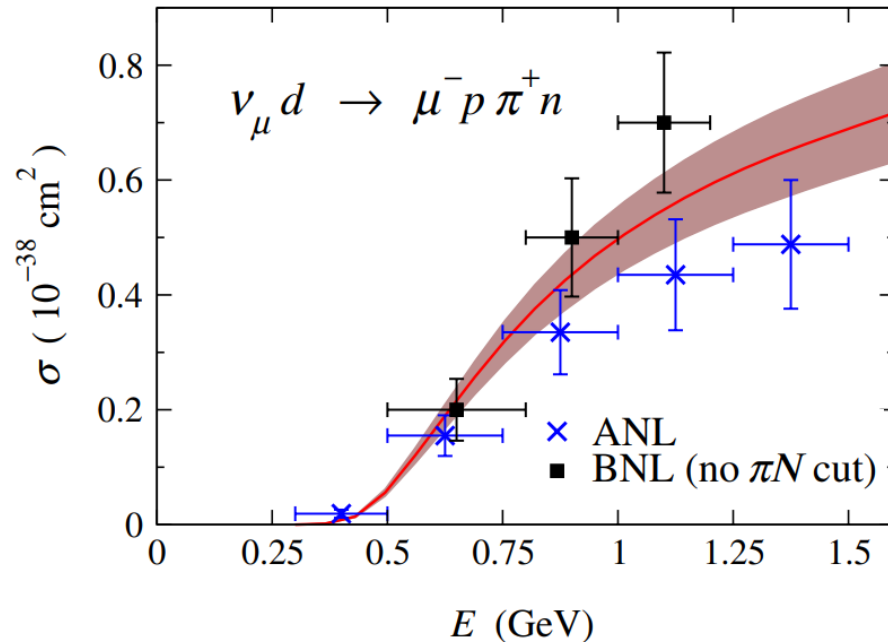
Figure from Dr. Stephen Dolan

Different interaction vertices can lead to the same final state due to nuclear effects and FSI

1π production in neutrino-deuteron scattering

- Discrepancies between “old” deuteron bubble-chamber data (Argonne ANL and Brookhaven BNL)
- Both ANL and BNL data suffer from a large flux-normalization error

E. Hernandez et al. Phys. Rev. D 87, 113009 (2013)



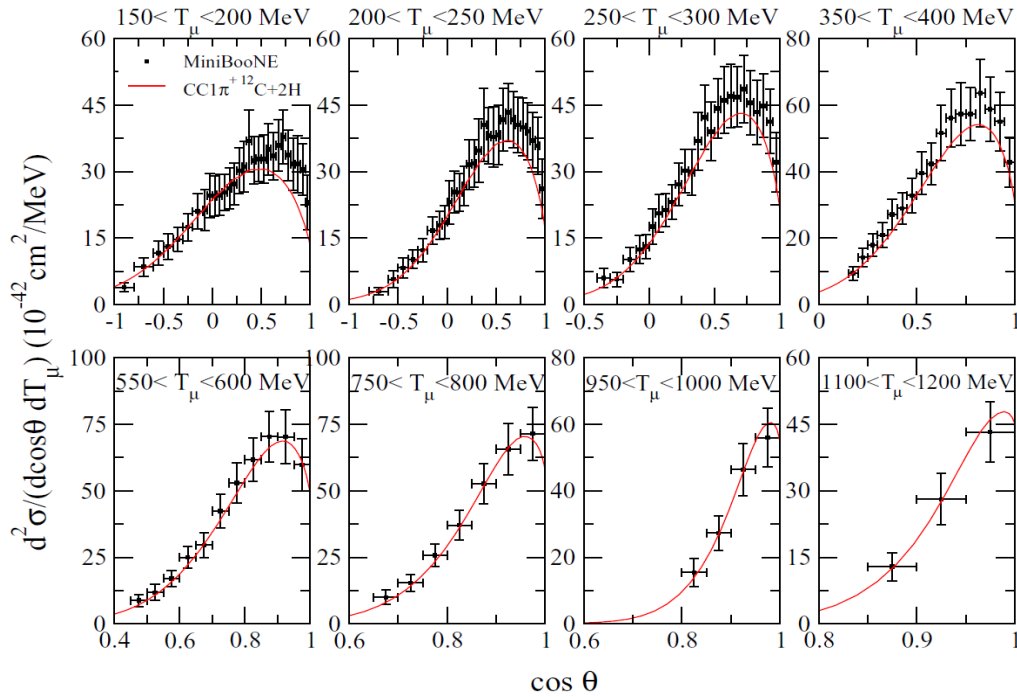
As for the CCQE, also for the 1π production there is a strong desire to repeat bubble-chamber experiments to better determine the axial form factors (in particular the C_5^A)

$$C_5^A(Q^2) = \frac{C_5^A(0)}{(1 + Q^2/M_{A\Delta}^2)^2}$$

CC1 π^+ flux-integrated differential cross sections on carbon

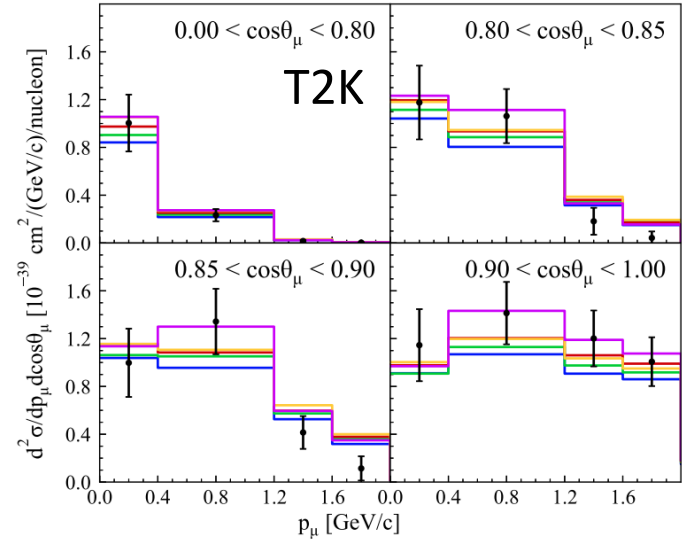
Results in terms of muon variables

MiniBooNE

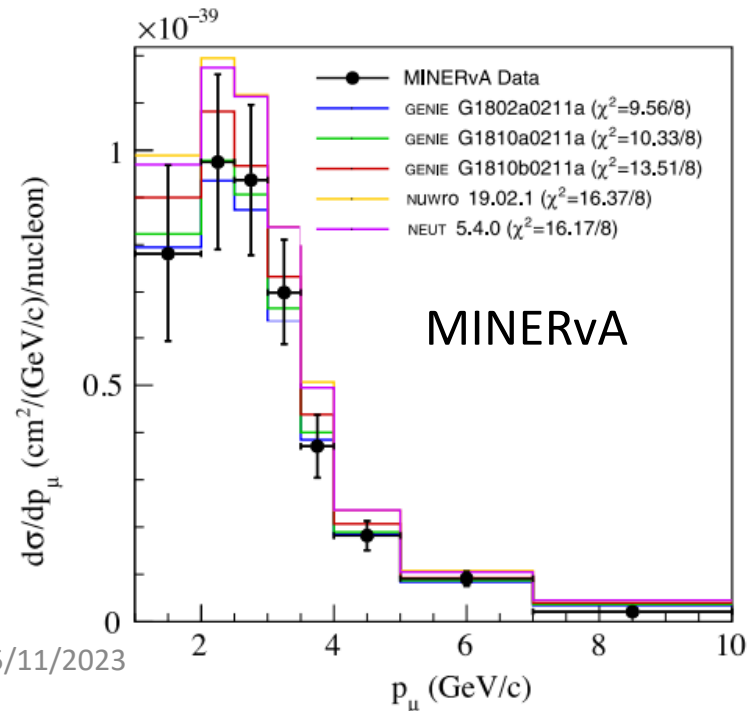


M. Martini, M. Ericson, *Phys. Rev. C* 90 025501 (2014)

Reasonable agreement between models and data, in particular at MiniBooNE and T2K energies



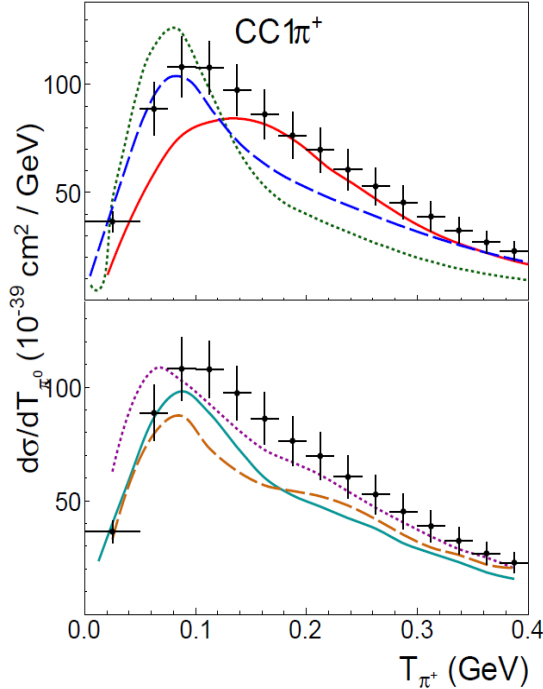
M. Buizza Avanzini et al. *PRD* 105, 092004 (2022)



CC1 π results in terms of pion variables

MiniBooNE

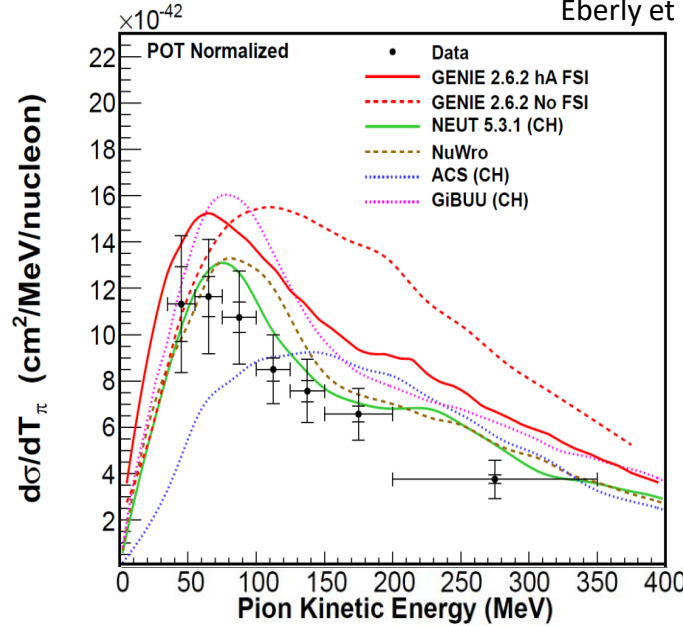
Rodrigues, AIP Conf. Proc. 1663 (2015)



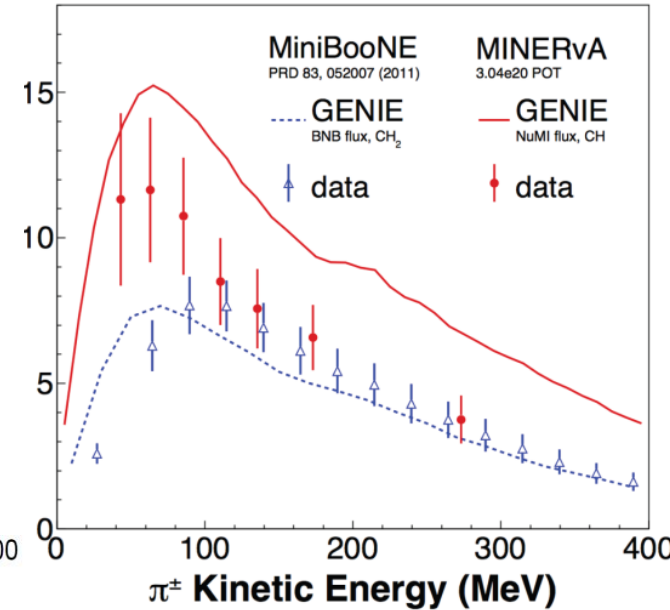
— Athar *et al.* - - - Nieves *et al.* - - - GiBUU — NuWro
 - - - GENIE — NEUT — + MB data

MINERvA

Eberly *et al.*, PRD 92 (2015)



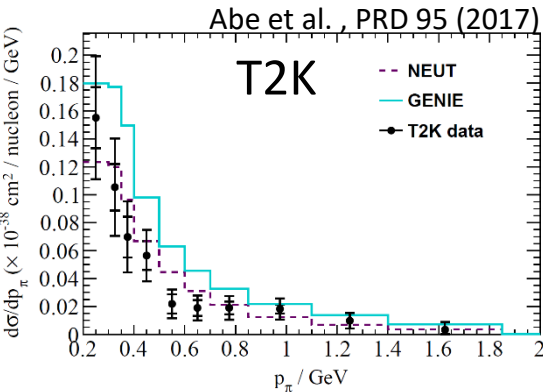
MiniBooNE - MINERvA



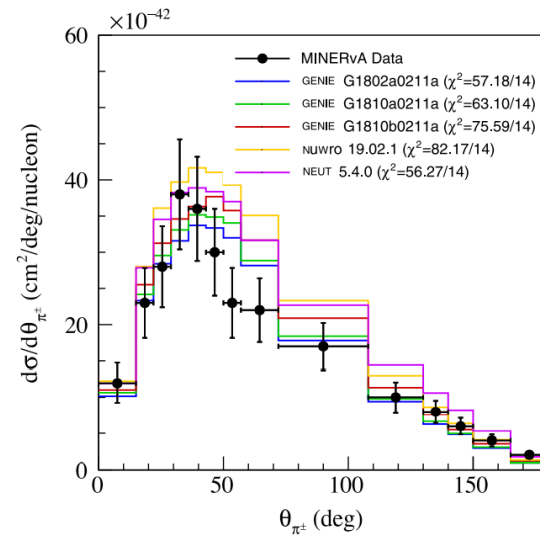
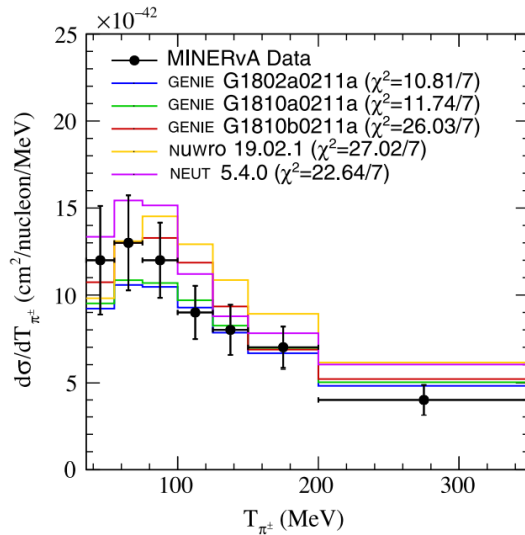
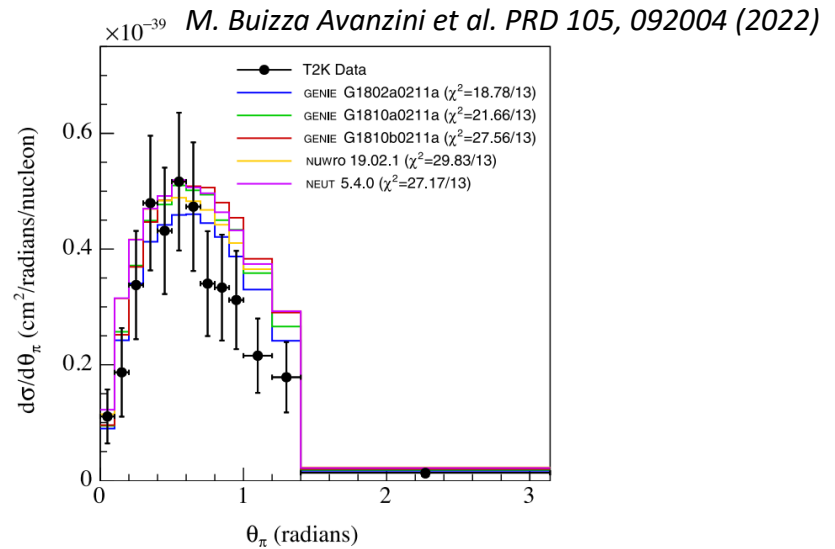
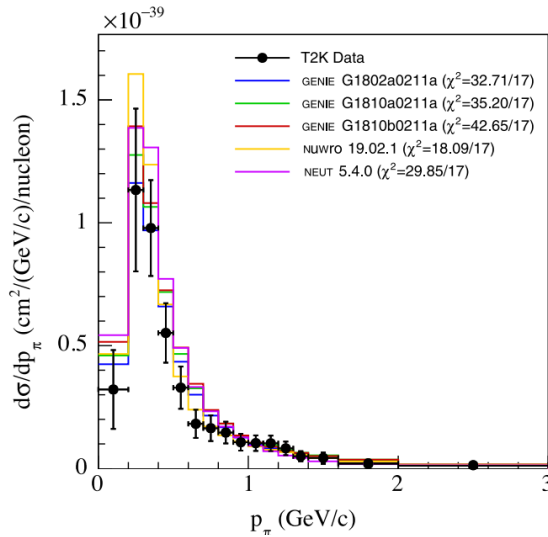
Historically many tensions

- models .vs. data ??
- models .vs. models??
- data .vs. data (through models)??

the 1 π puzzle



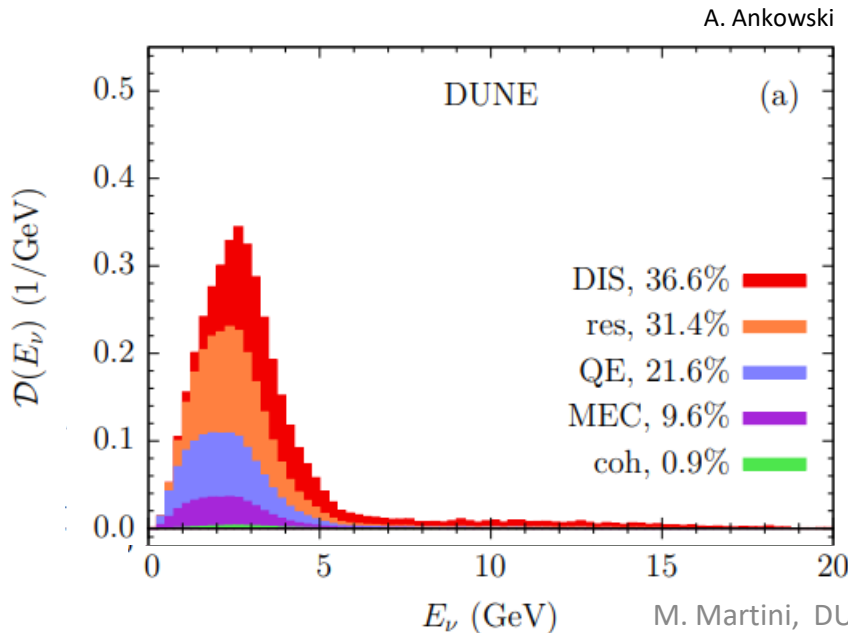
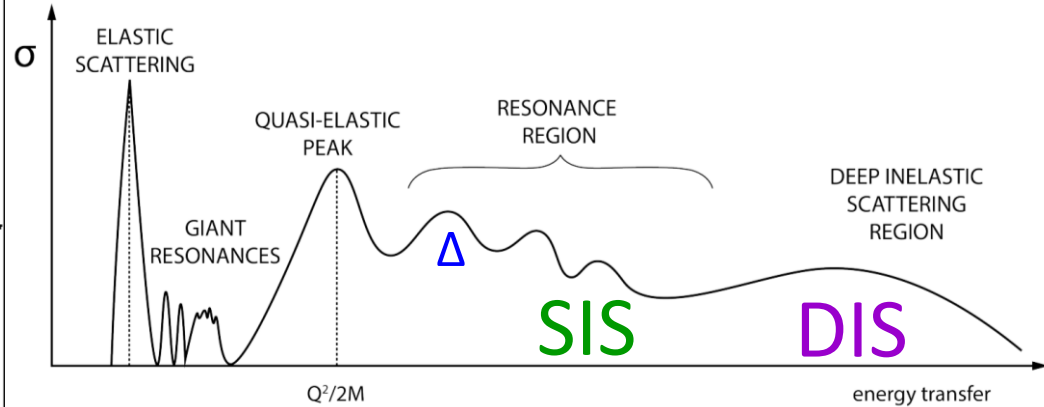
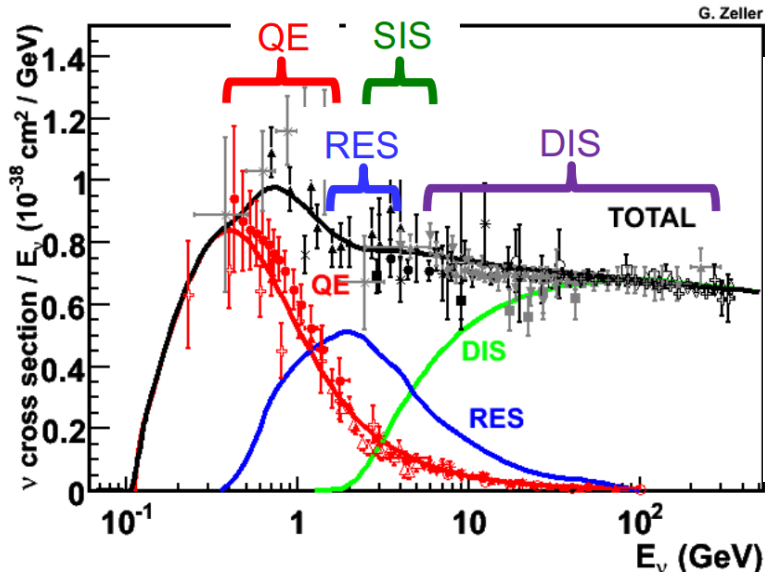
Pion puzzle – T2K and MINERvA data .vs. Monte Carlo (2022)



Tensions remain

- The generators used to extract the cross section is often the one with the best description of the data
- Experimental collaborations have more advanced analyses in progress (T2K Vargas and MINERvA McFarland @ NuInt22)
- These Monte Carlo results are based on Δ dominated models
- None of the common event generators include nuclear medium effects for the Δ

Beyond Δ resonance



- The complications of pion data analyses lay not only on the modeling of primary production and pion FSI but also on the fact that **all hadronic processes** related to shallow inelastic scattering (SIS) and DIS regions **must be modeled correctly**
- **SIS and DIS have been minimally studied both experimentally and theoretically with neutrino scattering**
- **A major challenge, important in particular for DUNE**

T. Katori, M. Martini, J.Phys.G 45 1, 013001 (2018)

L. Alvarez-Ruso et al. Prog. Part. Nucl. Phys. 100, 1–68 (2018)

M. Sajjad Athar, J. G. Morfín, J.Phys. G 48, 034001 (2021)

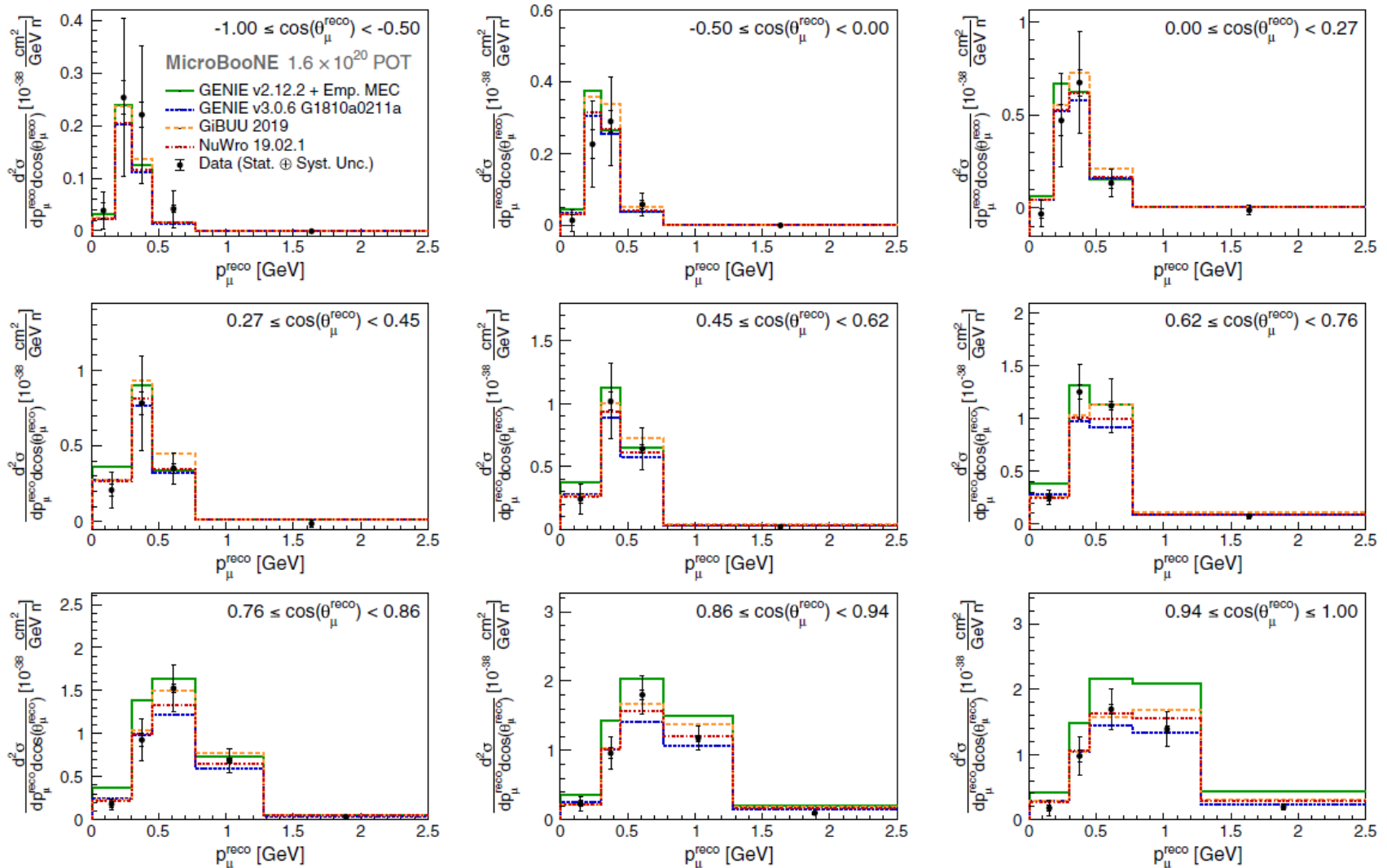
Recent cross sections results on Argon (MicroBooNE)

A) Inclusive measurements :
only the muon is detected

First MicroBooNE measurement on Argon: inclusive $d^2\sigma/dp_\mu d\cos\theta_\mu$

- CC Inclusive: only the charged lepton is detected. All reaction mechanisms contribute

PHYSICAL REVIEW LETTERS **123**, 131801 (2019)

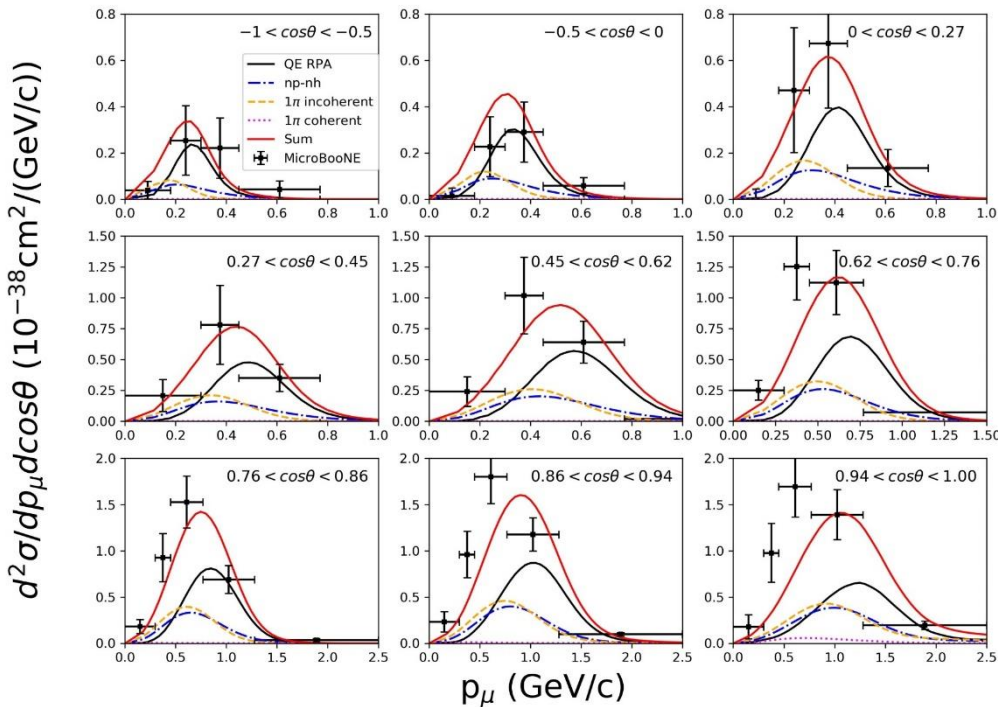


RPA and SuSAv2 calculations of MicroBooNE inclusive $d^2\sigma$ on argon

RPA

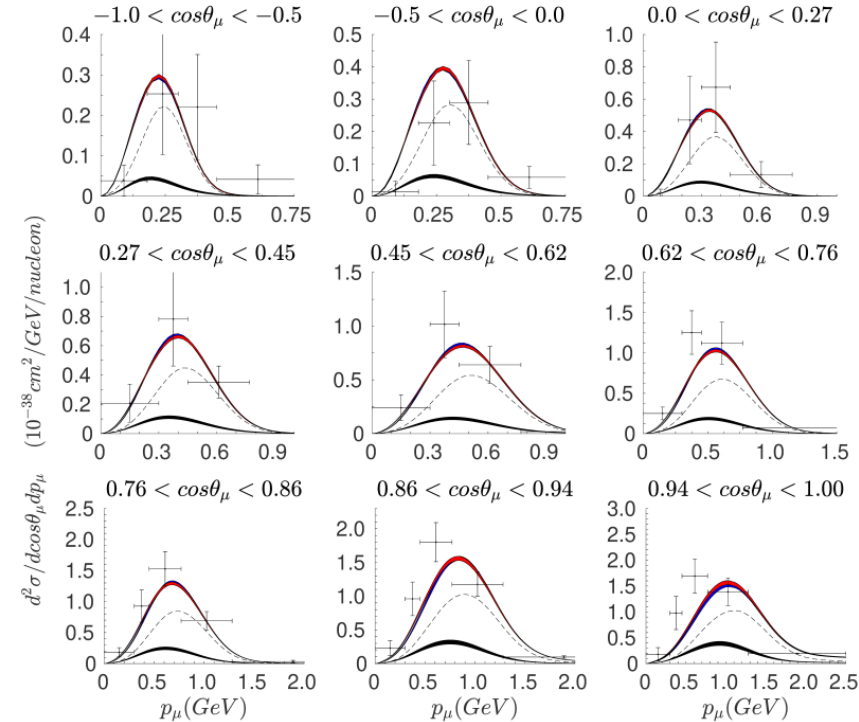
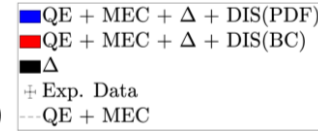
Total = QE + np-nh + 1π inc. + 1π coh.

M. Martini, M. Ericson, G. Chanfray, PRC 106 (2022)



SuSAv2

Gonzalez-Rosa et al. PRD 105 (2022)



Results also with SuSA
Barbaro et al. Universe 7 (2021)

- Reasonable overall **agreement**, though **not as good as in the ^{12}C T2K** inclusive case (see next slide)
- At backward angles the predictions of the different models are slightly shifted to lower values of p_μ , whereas the reverse occurs at forward angles

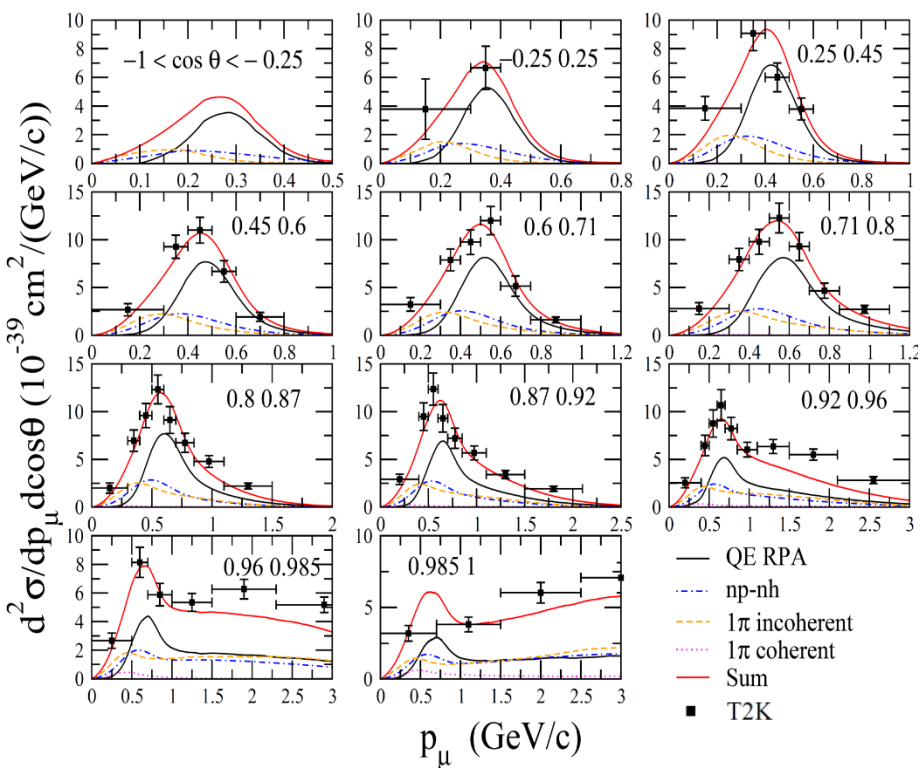
RPA and Monte Carlo calculations of T2K inclusive $d^2\sigma$ on carbon

PHYSICAL REVIEW D **98**, 012004 (2018)

Measurement of inclusive double-differential ν_μ charged-current cross section with improved acceptance in the T2K off-axis near detector

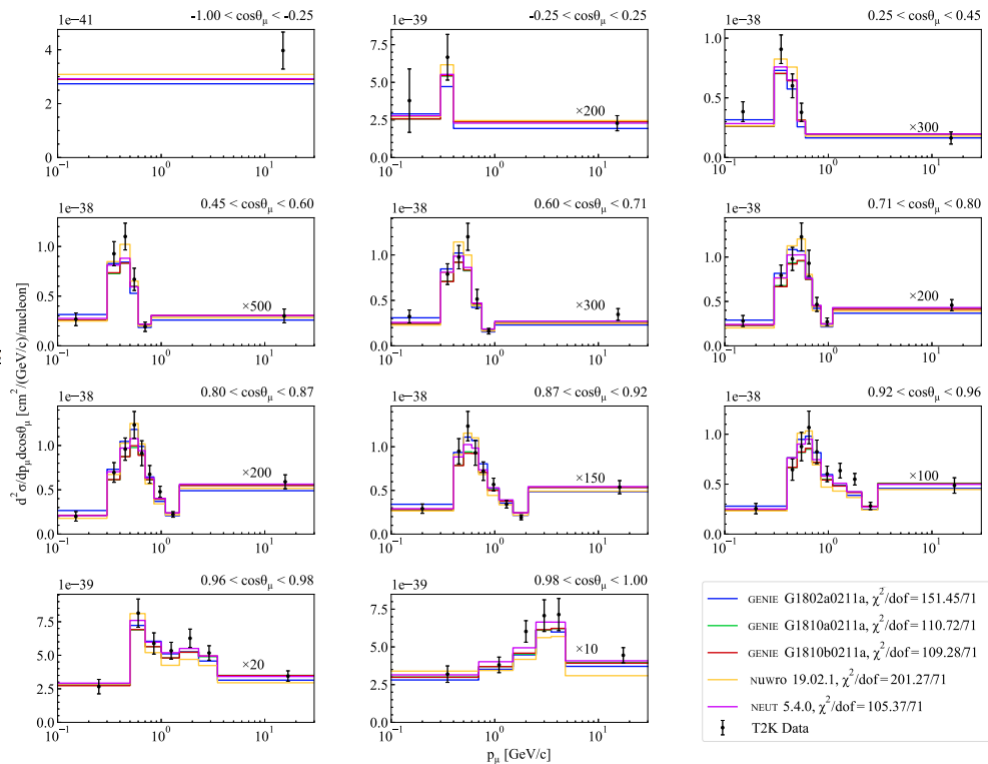
RPA

M. Martini, M. Ericson, G. Chanfray, PRC 106, 015503 (2022)



Monte Carlo

M. Buizza Avanzini et al. PRD 105, 092004 (2022)

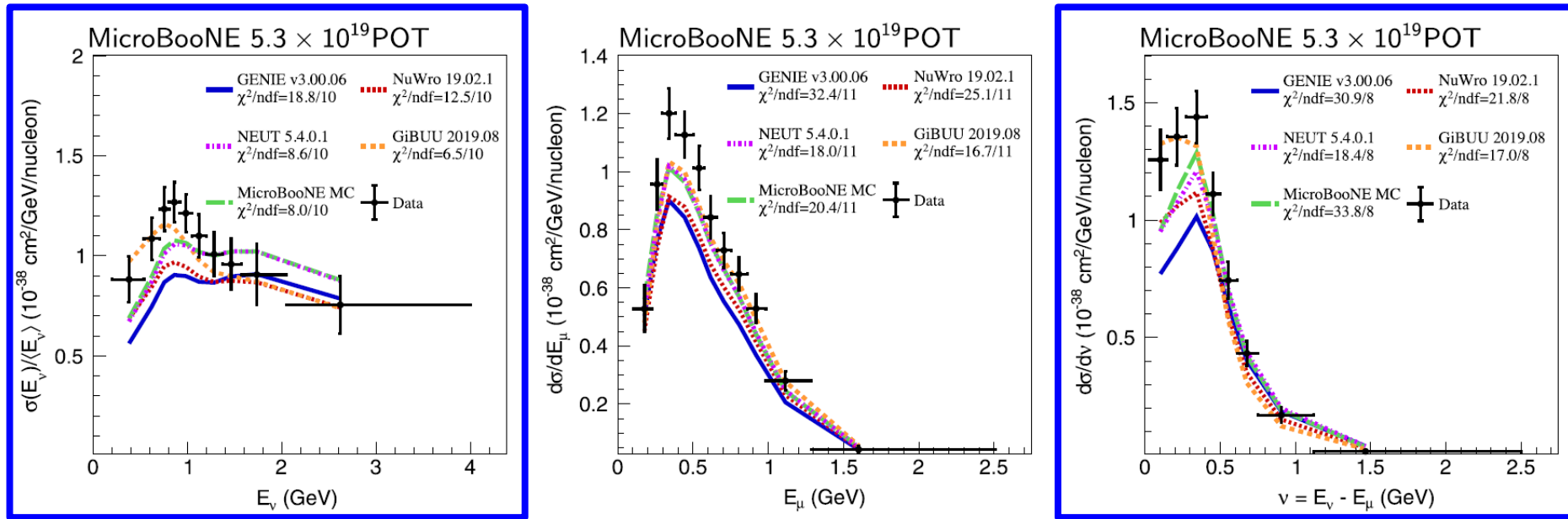


Remarkable agreement

Recent energy-dependent inclusive MicroBooNE cross sections on argon

PHYSICAL REVIEW LETTERS **128**, 151801 (2022)

First Measurement of Energy-Dependent Inclusive Muon Neutrino Charged-Current Cross Sections on Argon with the MicroBooNE Detector



Results presented for the first time as a function of true neutrino energy E_ν and transferred energy (ν or ω)

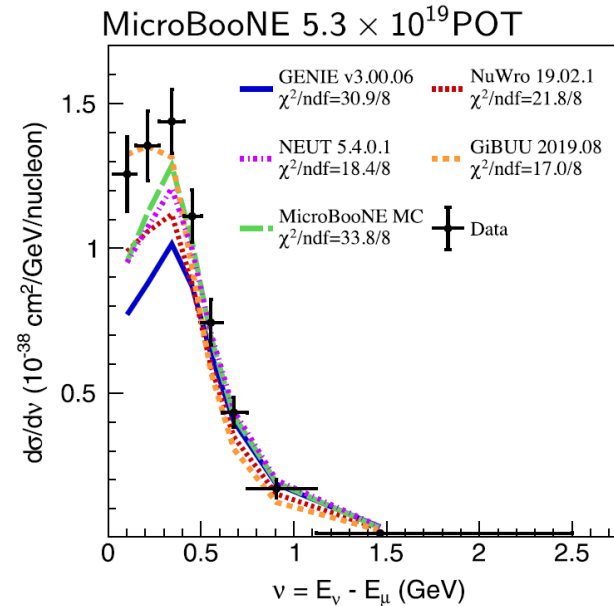
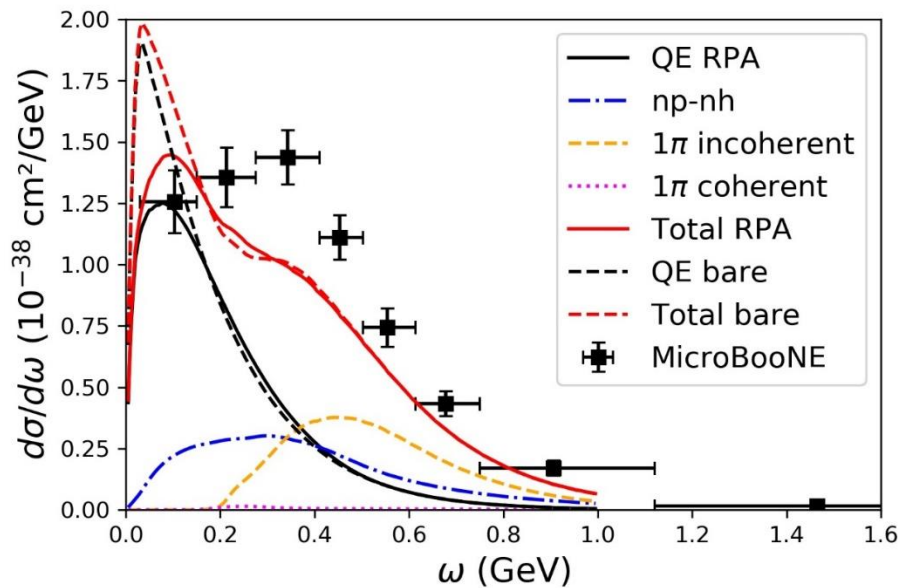
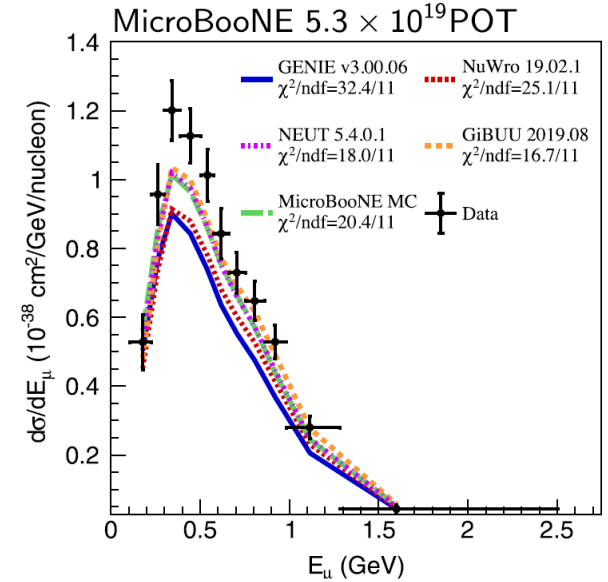
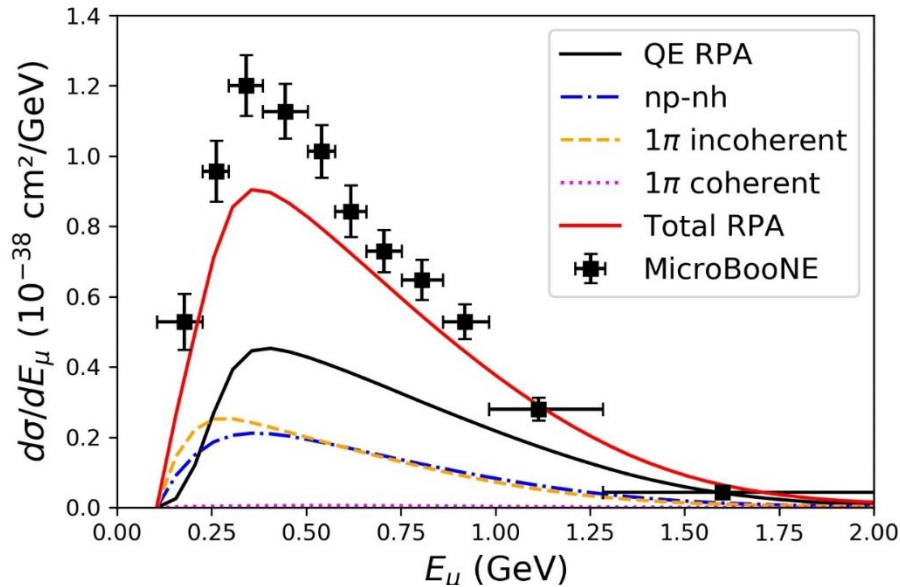
This has been made possible by a **new procedure, based on the comparison between the data and the Monte Carlo predictions constrained on the lepton kinematics**, allowing the mapping between the true E_ν and ω on one hand, and the reconstructed neutrino energy E_ν^{rec} and hadronic energy $E_{\text{had}}^{\text{rec}}$ on the other hand

- Model dependence ?

MicroBooNE flux-averaged inclusive $d\sigma/dE_\mu$ and $d\sigma/d\omega$ on argon

M. Martini, M. Ericson, G. Chanfray, Phys. Rev. C 106, 015503 (2022)

PRL 128, 151801 (2022)



In principle $d\sigma/d\omega$ allows a better separation of the different channels

Detector effects: unfolding measures and smearing theoretical models

Measured observables are always convoluted with detector effects. Up to now neutrino cross sections (MiniBooNE, T2K, MINERvA,...) data have been presented after a deconvolution of these effects. Such measurements are usually called “**unfolded**”. Unfolded measurements can be easily compared with models

$$\left(\frac{d\sigma}{dx}\right)_j = \sum_i \frac{U_{ji}(N_i - B_i)}{\Phi T \epsilon_j (\Delta x)_j}$$

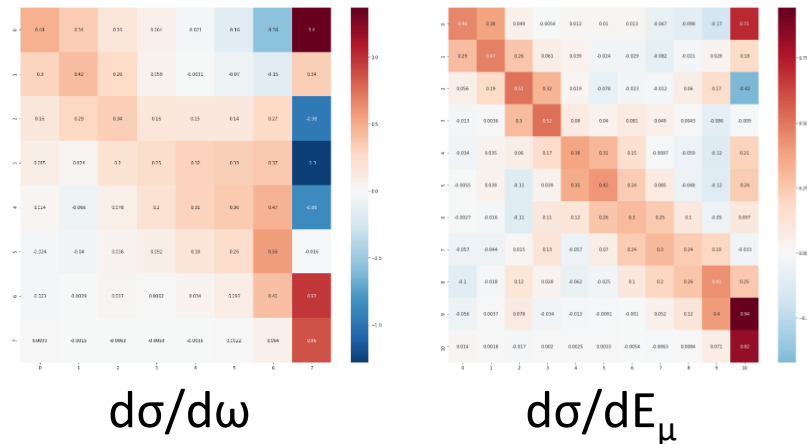
(see slide 9)

In the case of MicroBooNE the bias introduced in unfolding is captured in an **additional smearing matrix** that should be applied to every theoretical prediction.

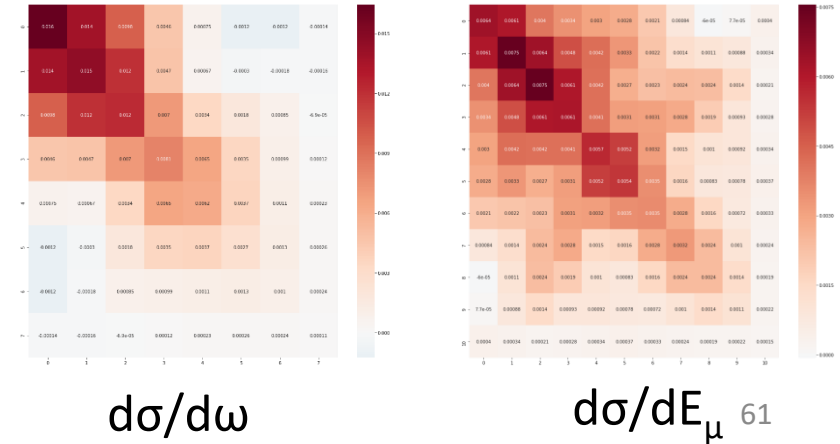
$$\sigma_{smearred} = M_{add_smr} \times \sigma_{model}$$

For quantitative analysis additional smearing and covariant matrices are hence shared by MicroBooNE

Additional Smearing Matrices

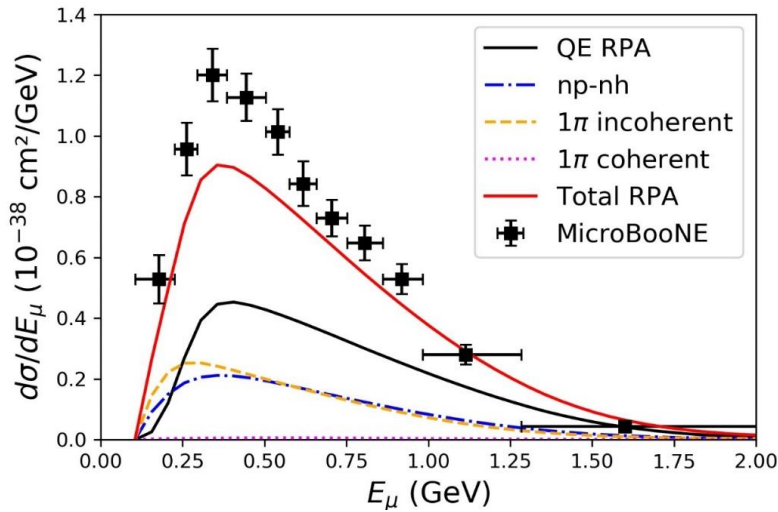


Covariant Matrices

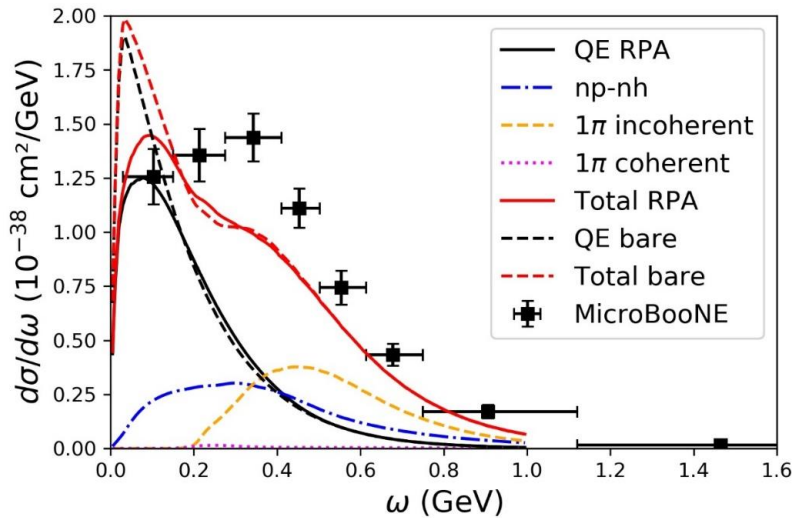
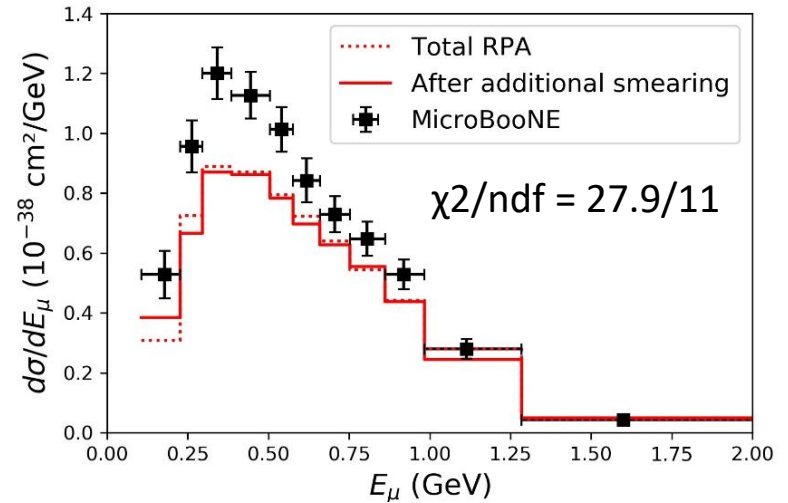


Theoretical results before and after the additional smearing

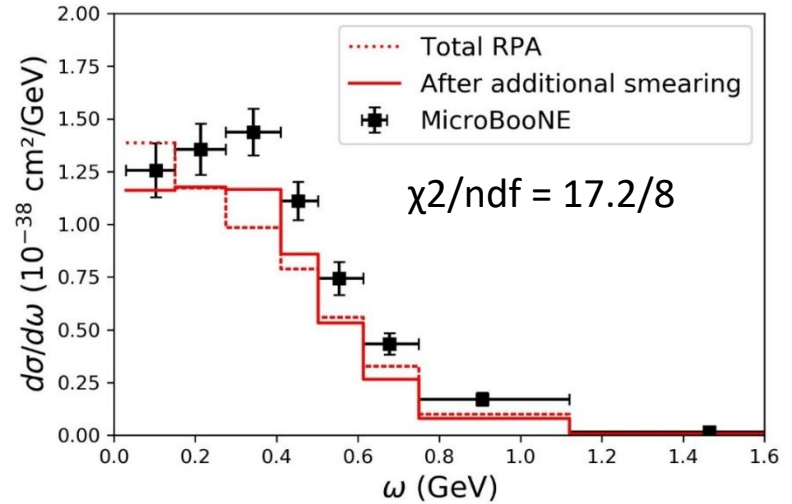
M. Martini, M. Ericson, G. Chanfray, Phys. Rev. C 106, 015503 (2022)



$d\sigma/dE_\mu$



$d\sigma/d\omega$



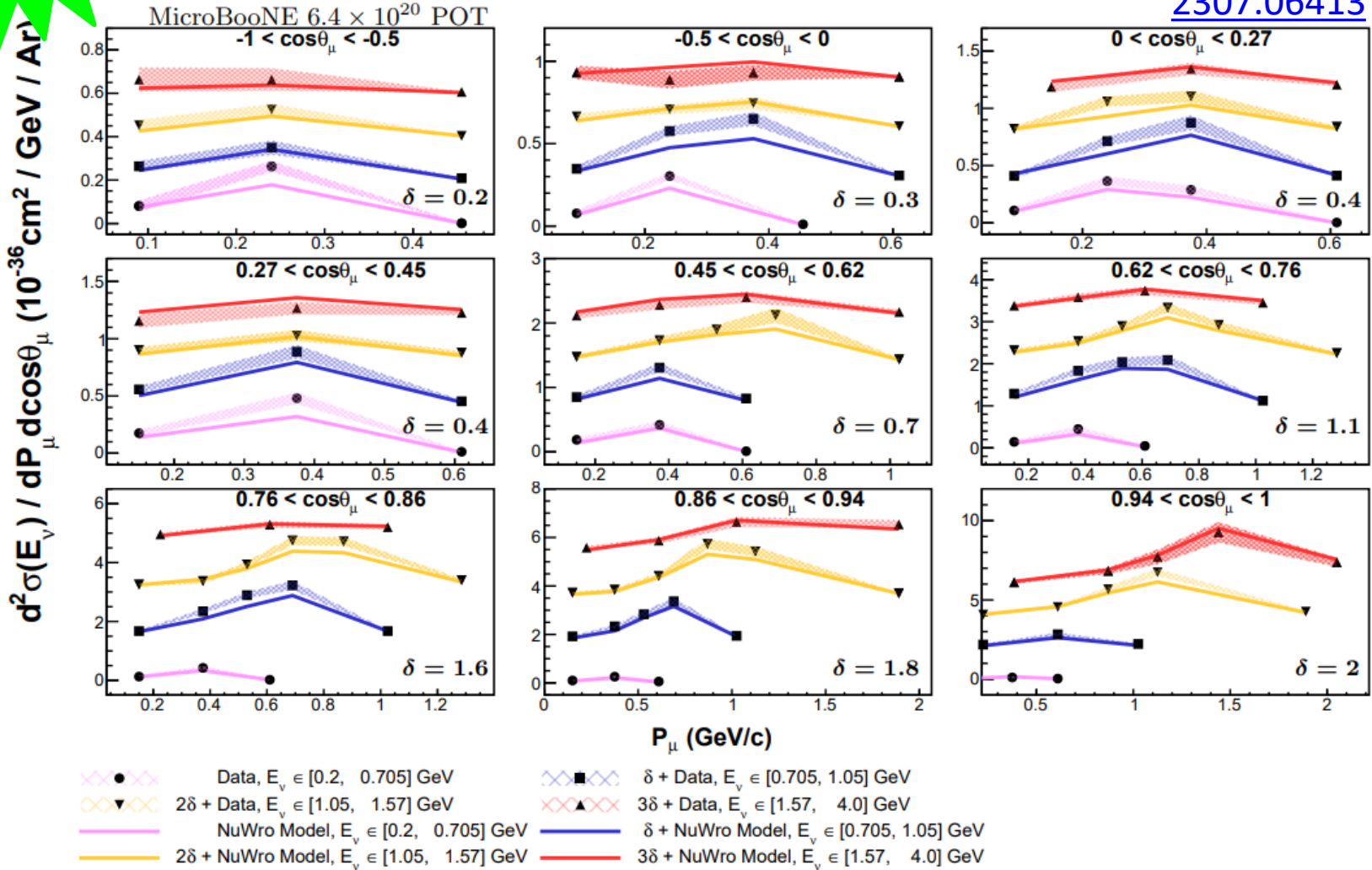
- The impact of the smearing is larger for $d\sigma/d\omega$ than for the $d\sigma/dE_\mu$
- The smearing produces a redistribution of the strength which is more important when the cross section is peaked, such as in the quasielastic channel



MicroBooNE triple-differential CC inclusive cross section

Results for 4 different E_ν slices

2307.06413

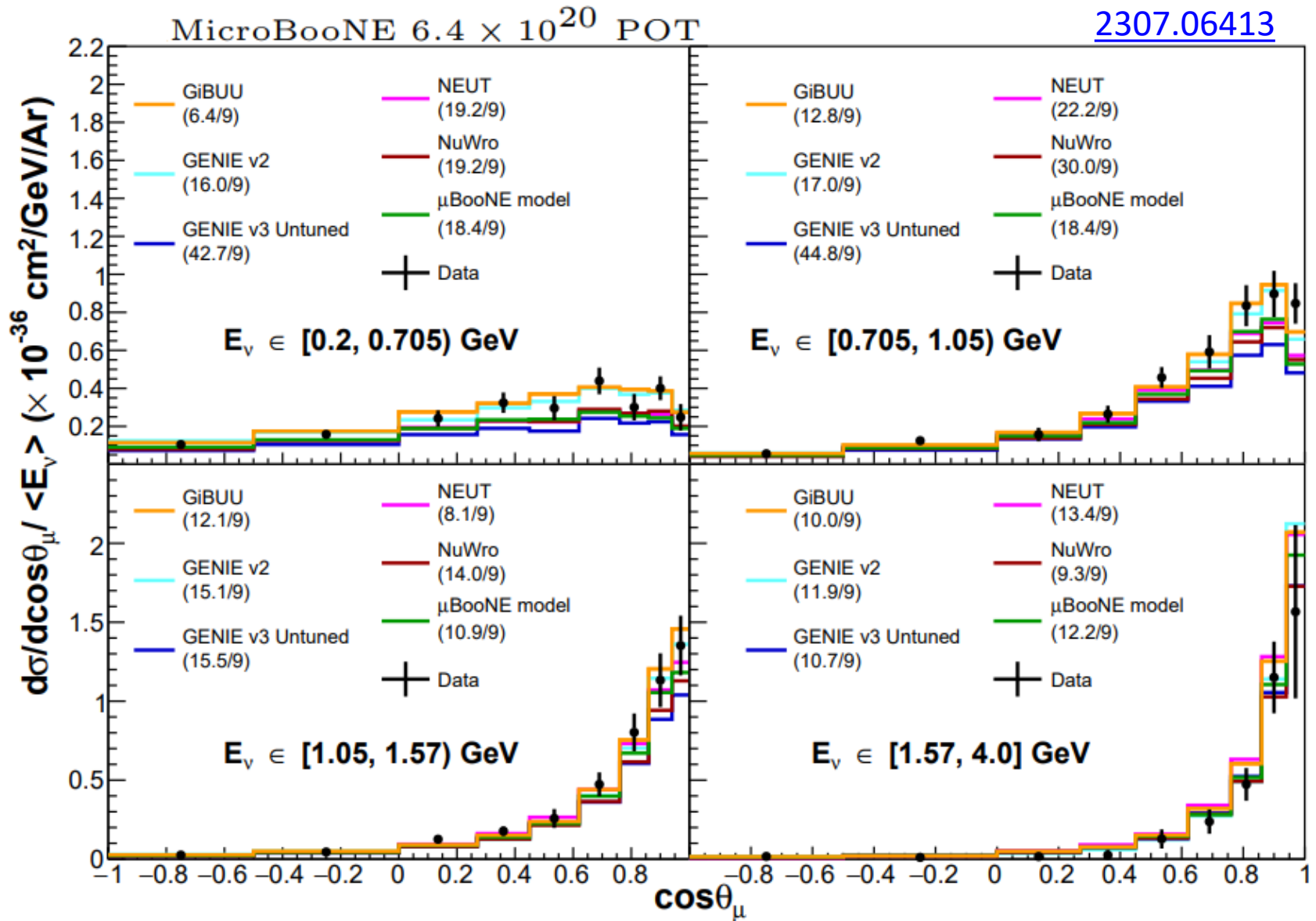


First time that this kind of results are available for neutrino cross sections

- No flux dependence!
- Model dependence ?

MicroBooNE double-differential CC inclusive cross section

After integrating over the muon momentum



Recent cross sections results on Argon (MicroBooNE)

B) Semi-inclusive processes:
muon + proton(s) are detected

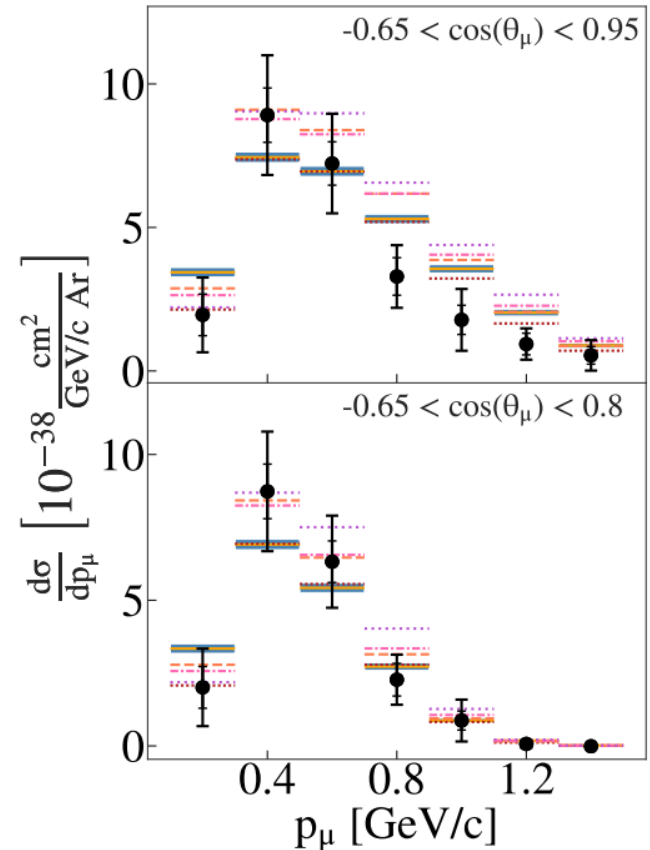
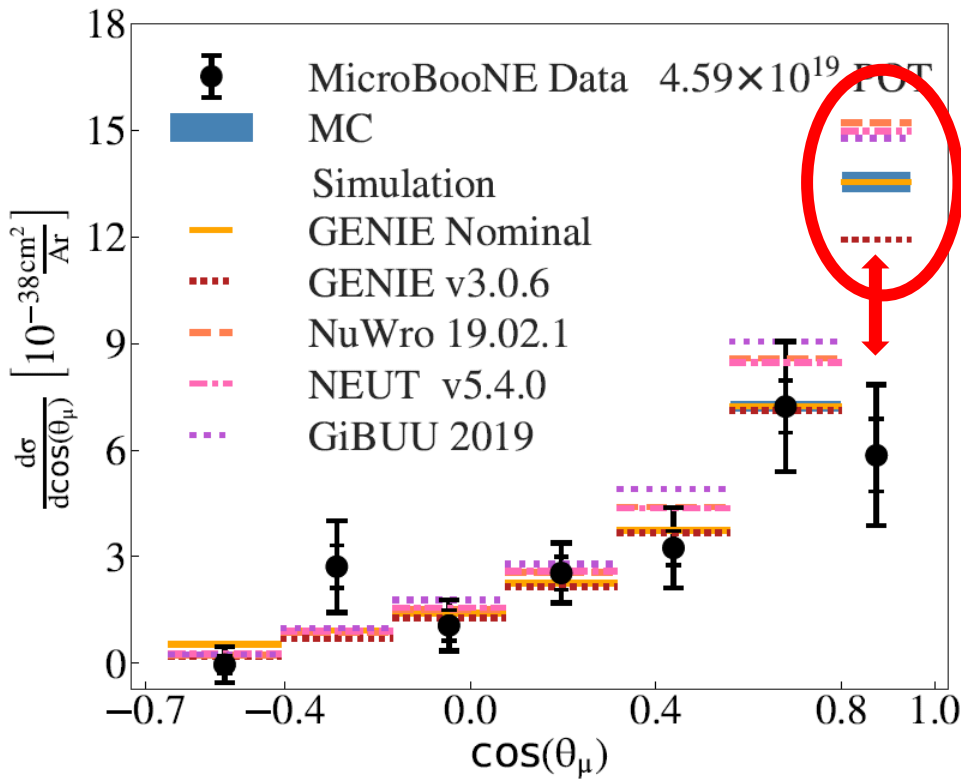
MicroBooNE semi-inclusive CC0 π 1p on argon

PHYSICAL REVIEW LETTERS 125, 201803 (2020)

First Measurement of Differential Charged Current Quasielasticlike ν_μ -Argon Scattering Cross Sections with the MicroBooNE Detector

?! CCQE-like with another meaning than in the past

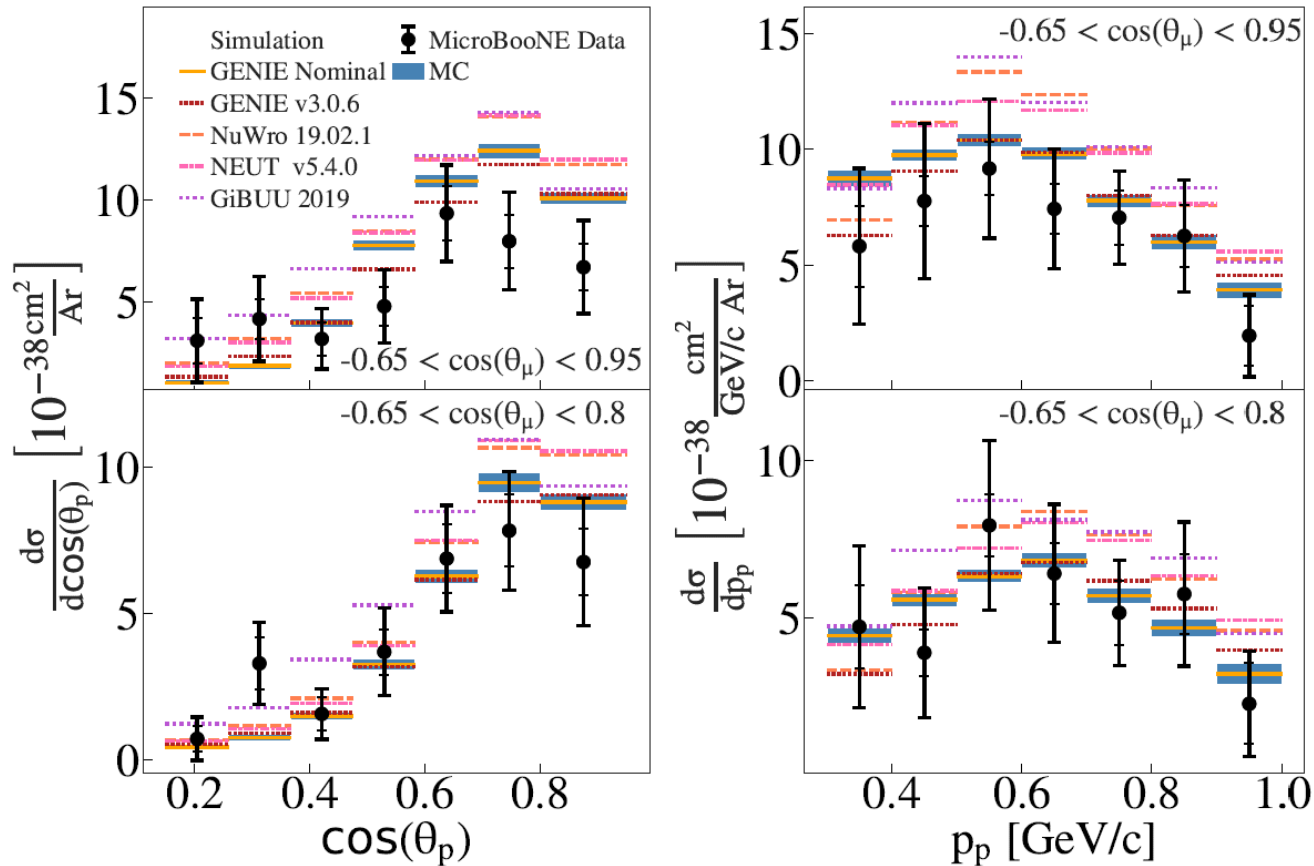
Results versus muon variables



Overestimation of Monte Carlo predictions in the muon forward direction

MicroBooNE semi-inclusive CC0 π 1p on argon versus proton variables

MicroBooNE PRL 125(2020)

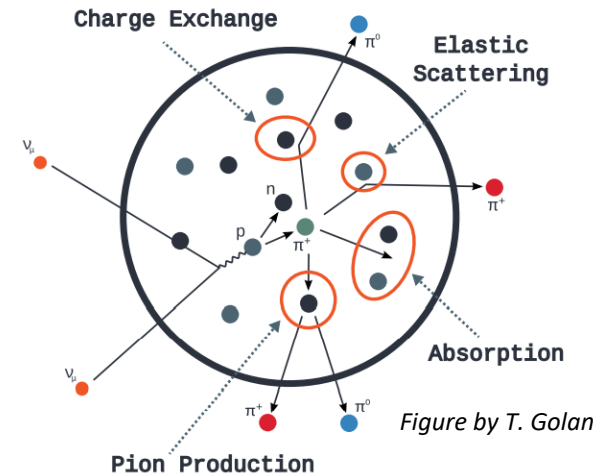
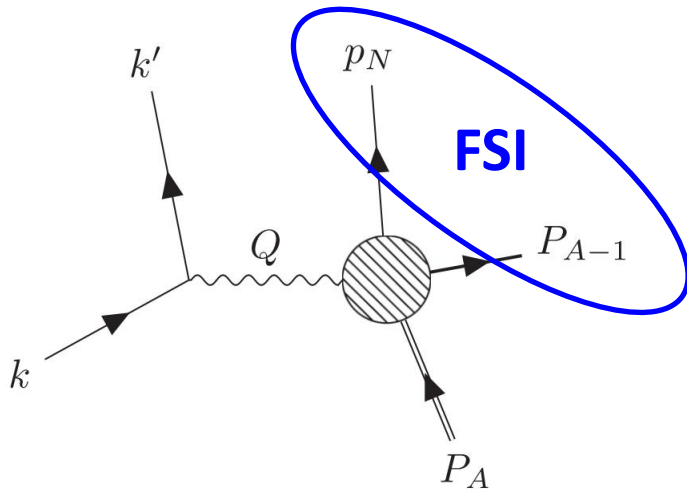


- Poor Monte Carlo – data agreement
- Spread of Monte Carlo predictions

How good are the current approximations (use “inclusive” models, factorization,...) of the Monte Carlos for the semi-inclusive processes?

Final State Interactions

FSI between the knocked-out particle(s) and the residual nucleus



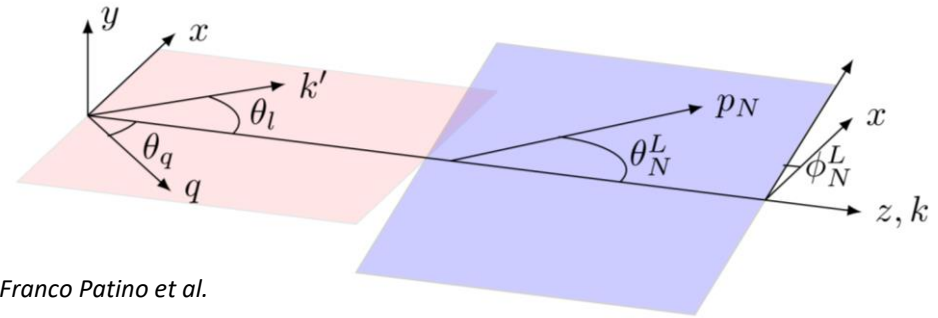
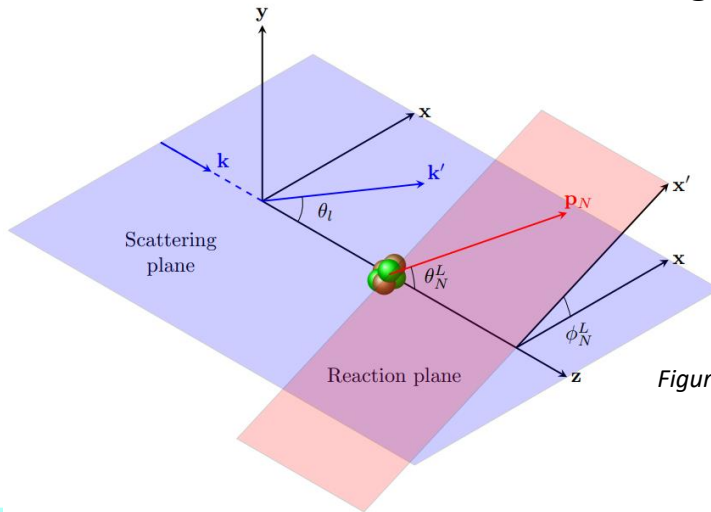
- Monte Carlo event generators include different models of intra-nuclear cascades: particles are assumed to be classical and move along a straight line
- FSI between the knocked-out nucleon and the residual nucleus can be microscopically treated using different approaches: Optical Potential, RMF, Energy-Dependent RMF

The inclusion of FSI effects is extremely important for the description of semi-inclusive data

[Some recent references: *R. Gonzalez-Jimenez et al., PRC 101, 015503 (2020)* ; *J. Isaacson et al., PRC 103 015502 (2021)*; *A. Nikolakopoulos et al. PRC 105, 054603 (2022)*; *A. Ershova et al., PRD 106 032009 (2022)*]

The semi-inclusive neutrino cross section

There is an increasing interest on semi-inclusive cross sections



Figures by J. M. Franco Patino et al.

M. B. Barbaro talk @NUFACT 2021

$$\begin{aligned} \mathcal{F}_\chi^2 &= L_{\mu\nu} W^{\mu\nu} \\ &= V_{CC} R^{CC} + 2V_{CL} R^{CL} + V_{LL} R^{LL} + V_T R^T + V_{TT} R^{TT} + V_{TC} R^{TC} + V_{TL} R^{TL} + \chi (V_T R^T + V_{TC} R^{TC} + V_{TL} R^{TL}) \end{aligned}$$

The $(\nu_\mu, \mu p)$ cross section is decomposed in **10 independent response functions** of **5 variables** $(\omega, q, \mathbf{p}_N)$.

More complex structure than in the **inclusive** (ν_μ, μ) case: **5 new responses**, which vanish after integration over the final nucleon variables

$$R^{TT,TC,TL,TC',TL'} \propto \cos(\phi), \cos(2\phi) \quad \phi \text{ outgoing nucleon azimuthal angle}$$

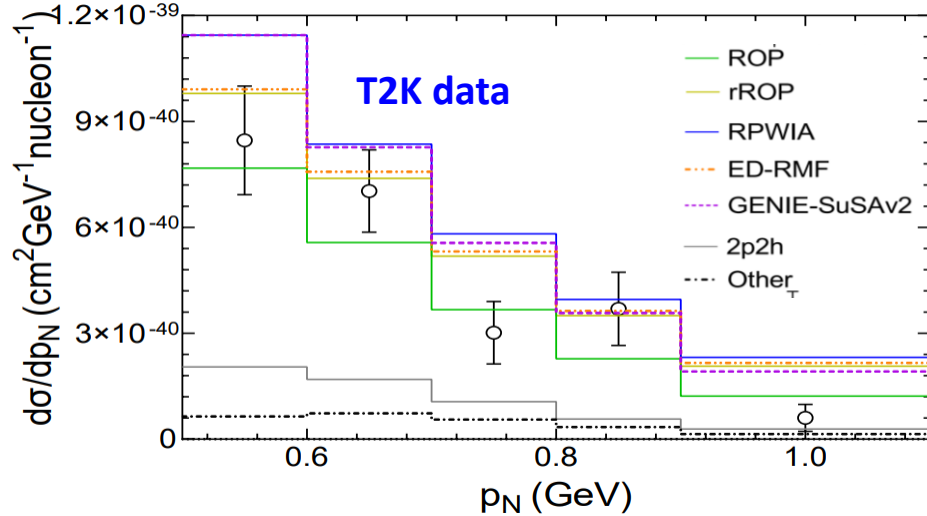
Semi-inclusive \rightarrow Inclusive (but not viceversa!)

Theoretical situation:

- few models and papers for genuine CCQE [J. M. Franco Patino et al, PRC 102 (2020); PRD 104 (2021), PRD 106 (2022), 2304.01916; A. V. Butkevich PRC 105 (2022)]
- one (incomplete due to the absence of Δ -MEC) model for 2p-2h [T. Van Cuyck et al. PRC 94 (2016); PRC 95 (2017)]

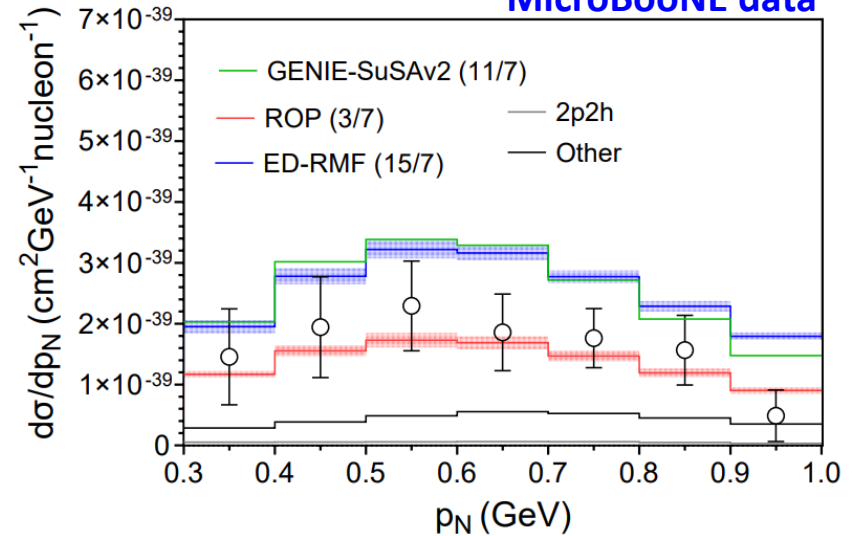
Semi-inclusive CC0 π 1p cross section: role of proton FSI

$0.8 < \cos(\theta_l) < 1.0$; $0.3 < \cos(\theta_N^L) < 0.8$



$-0.65 < \cos(\theta_l) < 0.95$

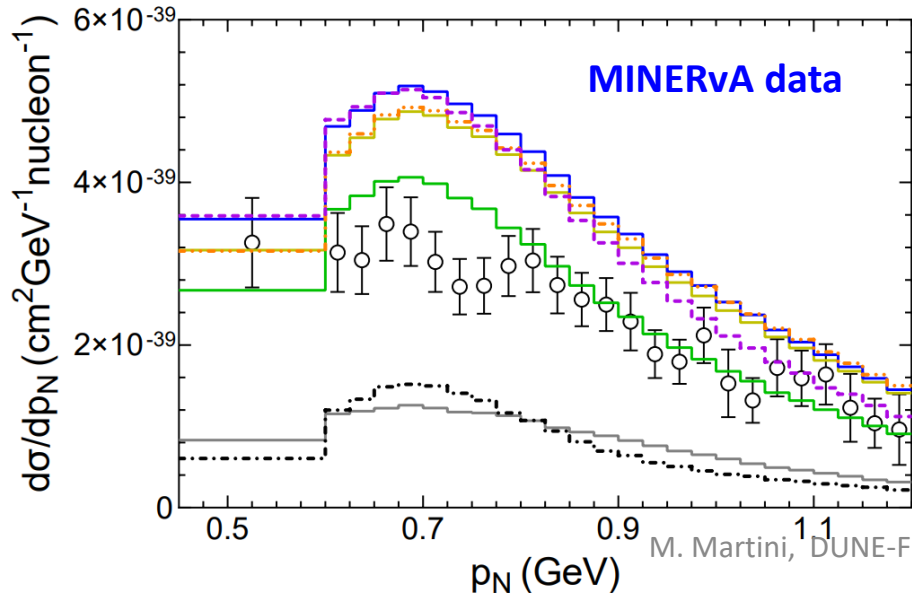
MicroBooNE data



RPWIA: no FSI

GENIE-SuSAv2: include FSI but from inclusive model (factorization)

ED-RMF, rROP, ROP: different theoretical approaches for FSI



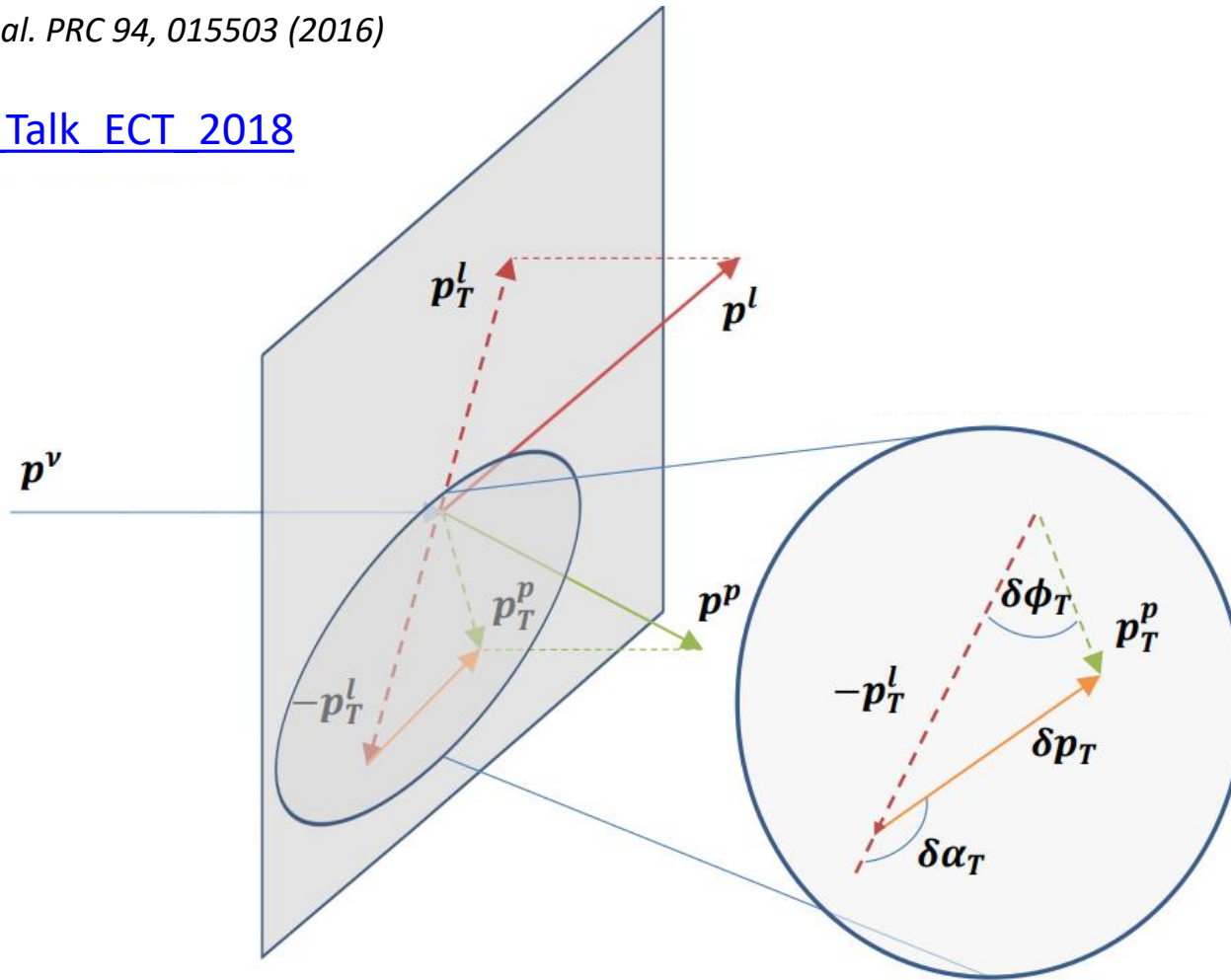
J. M. Franco Patino et al, PRD 106 (2022); 2304.01916

- FSI improve the agreement with data with respect to the RPWIA (no FSI) prediction
- Large differences between different FSI models

Single Transverse Kinematic Imbalance (STKI) variables (STV)

X. -G. Lu et al. PRC 94, 015503 (2016)

[S Dolan Talk ECT 2018](#)



Scattering on a free nucleon at rest: $\vec{p}_T^p = -\vec{p}_T^l$

$\delta p_T = 0$; $\delta \phi_T = 0 \longrightarrow$ peaked distributions

$\delta \alpha_T$ undefined \longrightarrow flat distribution

Deviations (imbalance) from these behaviors “measure” nuclear effects

Several recent MicroBooNE studies using Kinematic Imbalance Variables



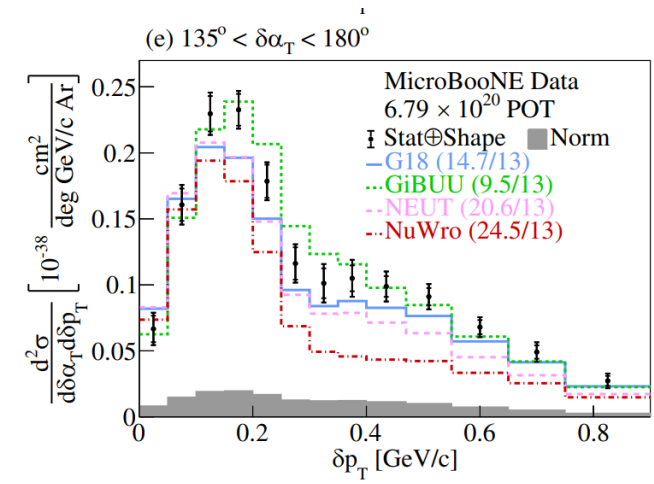
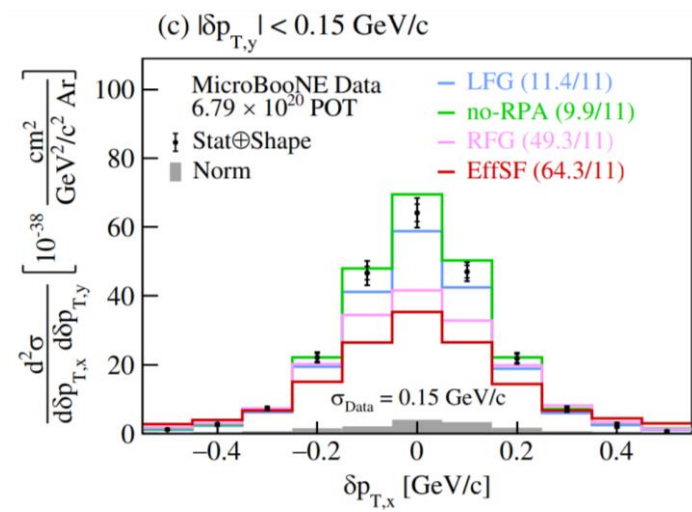
2D results for the first time on any neutrino target

PHYSICAL REVIEW LETTERS **131**, 101802 (2023)

First Double-Differential Measurement of Kinematic Imbalance in Neutrino Interactions with the MicroBooNE Detector

PHYSICAL REVIEW D **108**, 053002 (2023)

Multidifferential cross section measurements of ν_μ -argon quasielasticlike reactions with the MicroBooNE detector



[2310.06082](#)

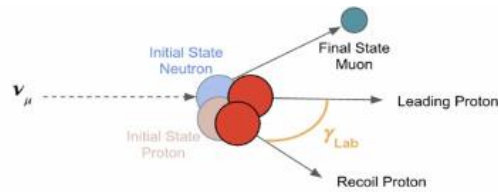
Measurement of nuclear effects in neutrino-argon interactions using generalized kinematic imbalance variables with the MicroBooNE detector

“These measurements allow us to demonstrate that the treatment of CCQE interactions in GENIEv2 is inadequate to describe data. Further, they reveal tensions with more modern generator predictions particularly in regions of phase space where FSI are important.”

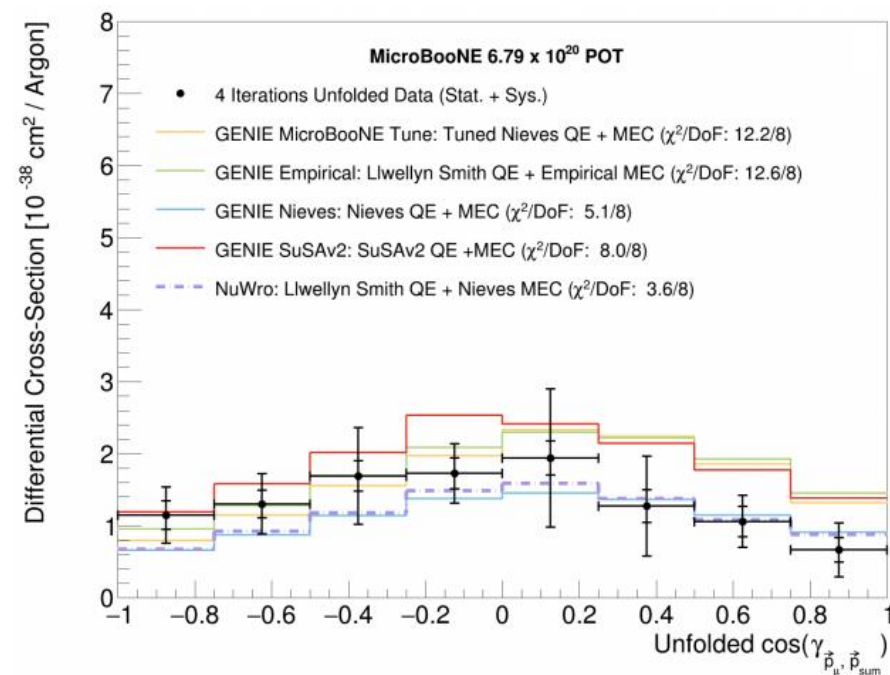
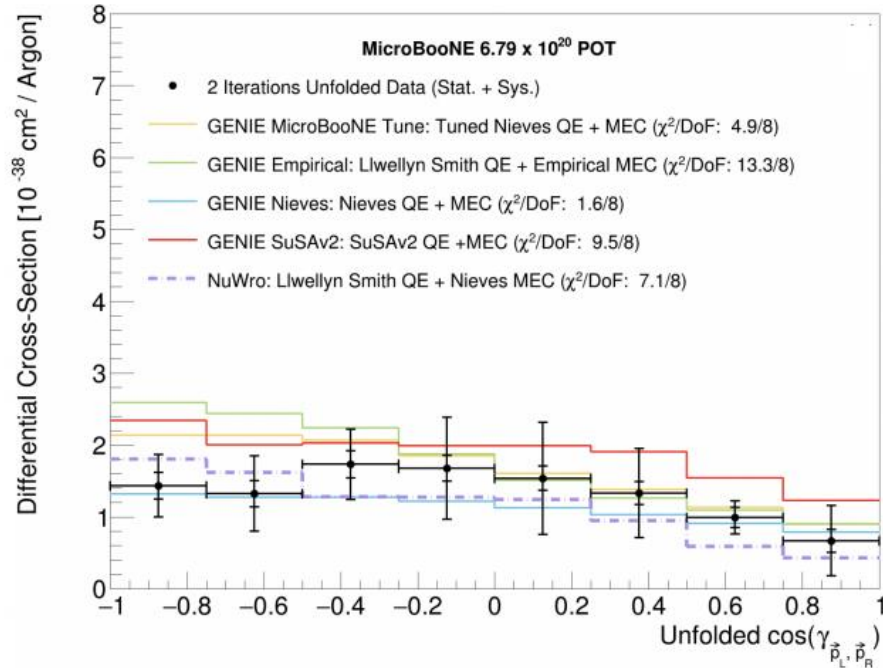
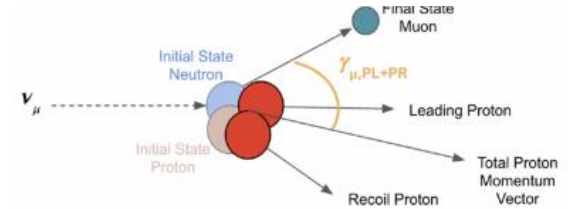
This is not a surprise since the generators implement “inclusive” microscopic models and “classical” cascade for FSI

MicroBooNE semi-inclusive $CC0\pi2p$ on argon

First Measurement of Differential Cross Sections for Muon Neutrino Charged Current Interactions on Argon with a Two-proton Final State in the MicroBooNE Detector



[2211.03734](#)



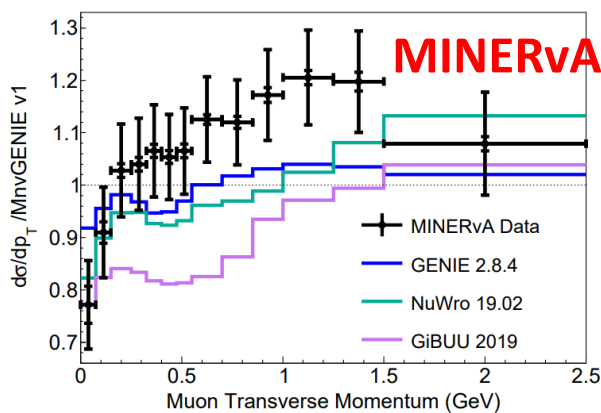
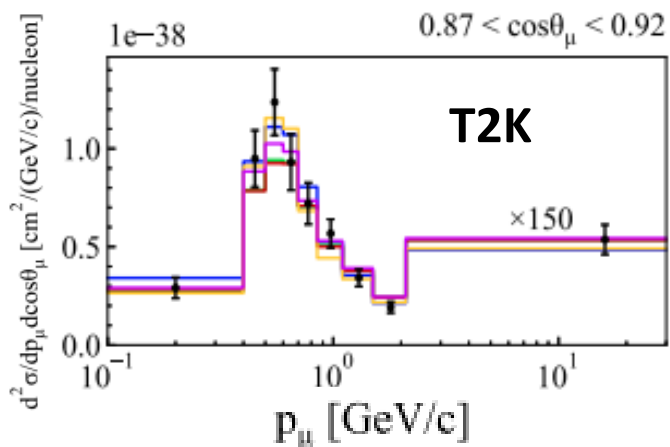
- Spread of Monte Carlo predictions
- How good are the current approximations of the MC for the semi-inclusive processes?

Complete semi-inclusive fully microscopic calculations of 2p-2h are not yet available

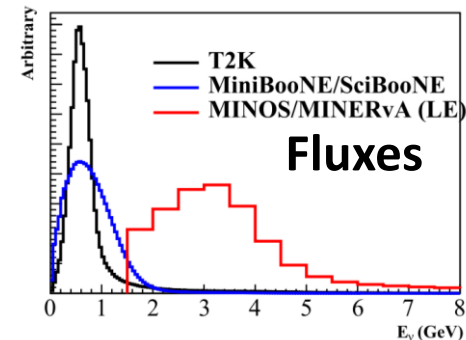
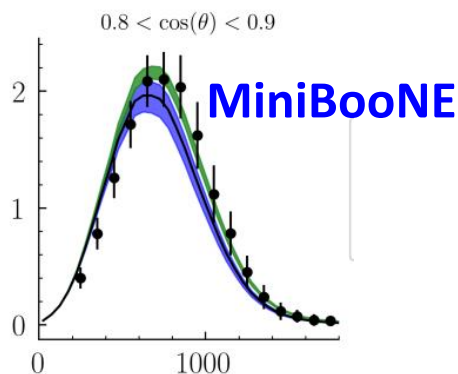
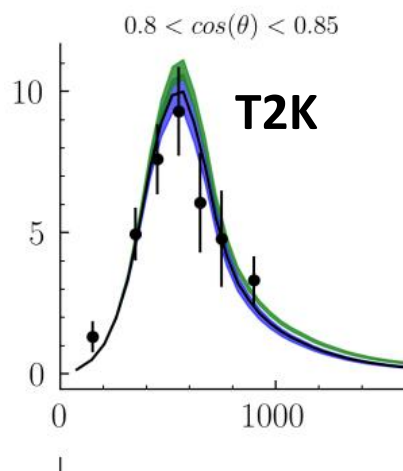
General considerations

1) The spread of the models increases with the neutrino energy

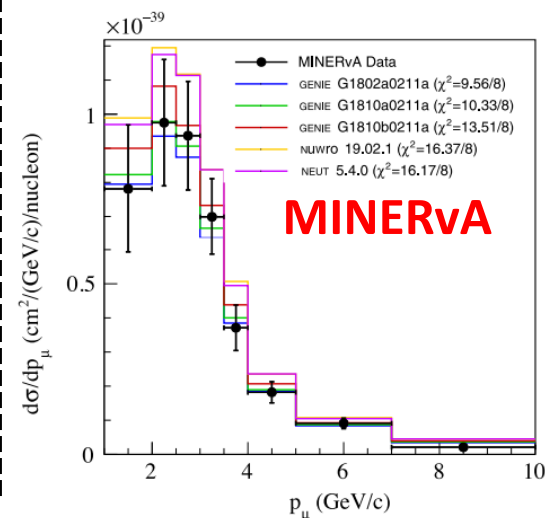
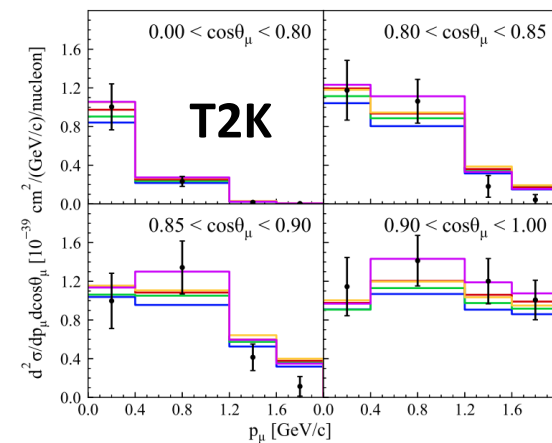
CC Inclusive



CC0 π

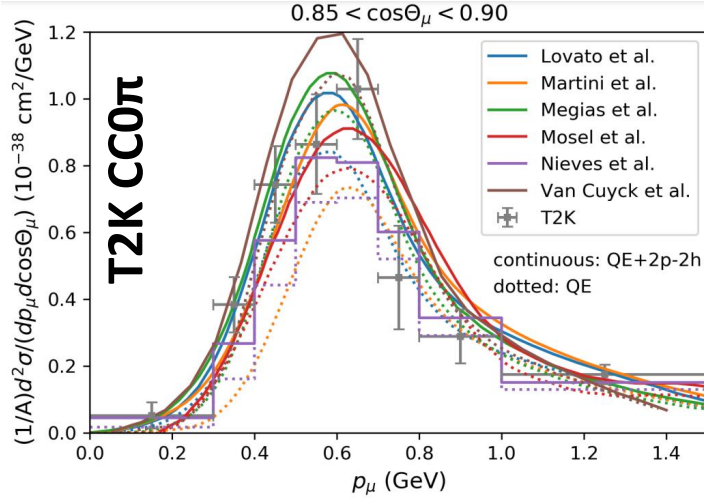


CC1 π

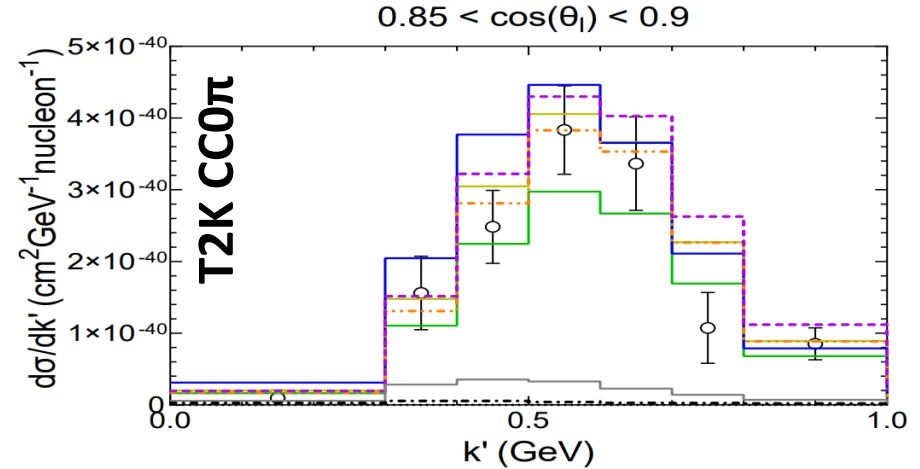


2) The spread of the models is larger in semi-inclusive processes

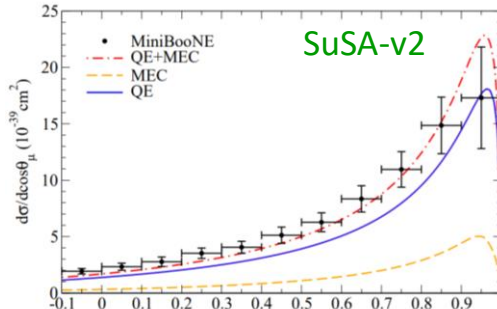
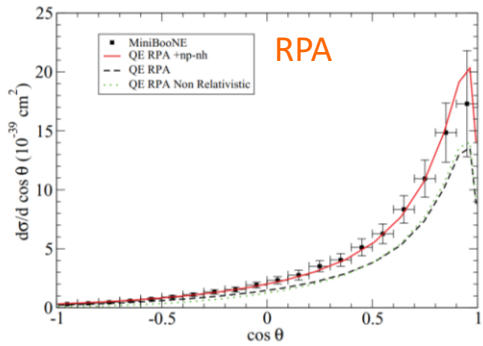
“Inclusive”



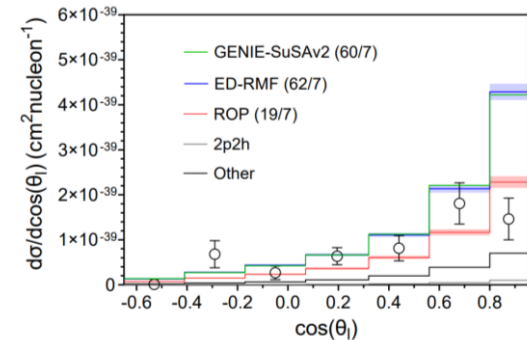
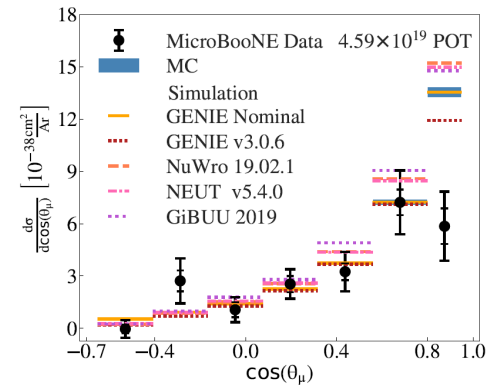
Semi-inclusive



MiniBooNE “CCQE-like”

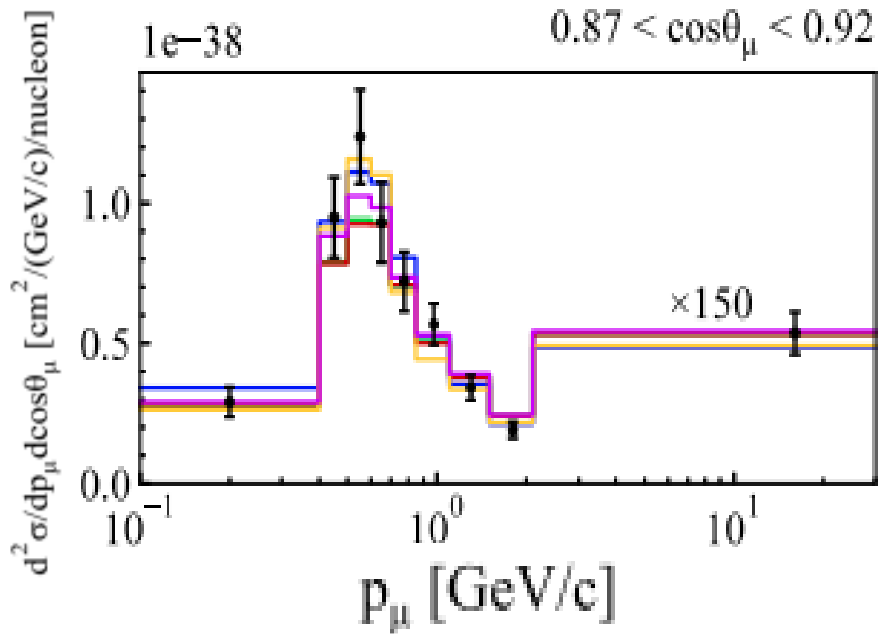


MicroBooNE CC0 π 1p

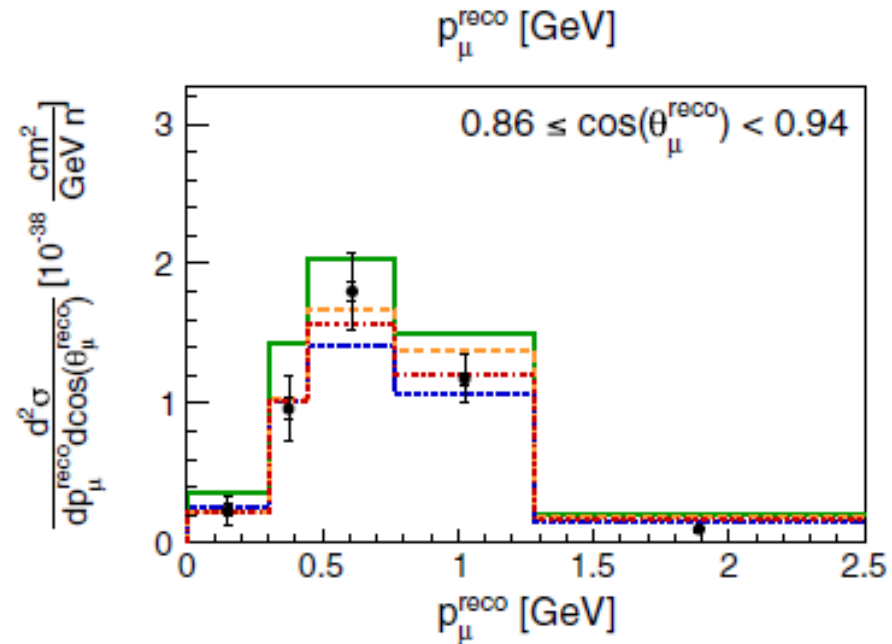


3) The spread of the models is larger for Argon than for Carbon

T2K Carbon



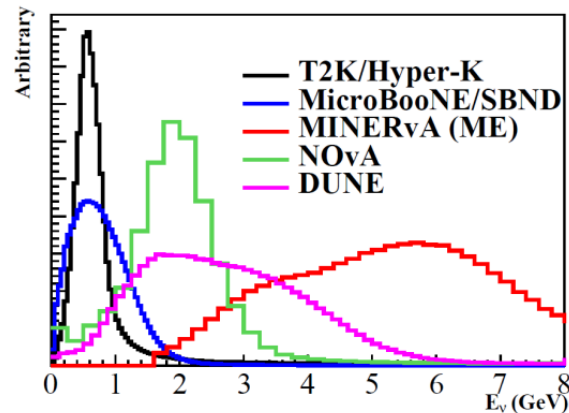
CC Inclusive



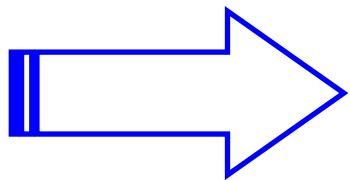
General comments

- 1) The spread of the models increases with the neutrino energy
- 2) The spread of the models is larger in semi-inclusive processes
- 3) The spread of the models is larger for Argon than for Carbon

This is not surprising since in the last 15 years the neutrino community focused on Carbon, on “inclusive” measurements as a function of the leptonic variables (Cherenkov detectors) and on “low” neutrino energy (MiniBooNE and T2K)



DUNE will be at larger energies, will use Argon detectors, will exploit semi-inclusive measurements as a function of leptonic and hadronic variables

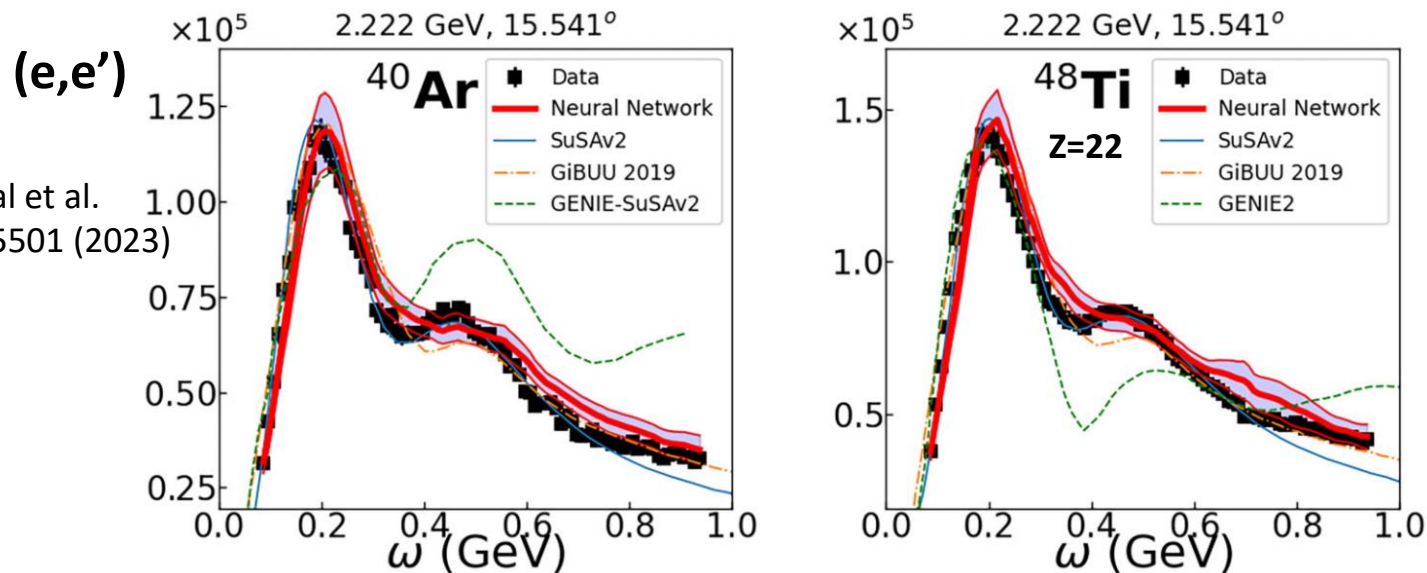


Many studies are needed!

Further elements for discussion

- Any model pretending to describe neutrino cross sections should first be validated by comparing its predictions with electron scattering data.

Many data exists for N=Z nuclei (^{12}C , ^{16}O , ^{40}Ca). Not so much for ^{40}Ar ($Z=18$, $N=22$).



- Many microscopic models have been initially developed for N=Z nuclei.
 - how good are their generalizations to asymmetric nuclei?
 - how reliable are in the Monte Carlo the approximations to obtain Argon predictions starting from microscopic models for Carbon?
- For the moment fully microscopic models for semi-inclusive processes are scarce and not yet implemented in Monte Carlo
 - what we learn by comparing semi-inclusive measurement as a function of hadronic variables with Monte Carlo predictions based on inclusive models?

Neutrino cross sections: summary of status and perspectives

A) Cross sections in terms of muon variables (CC inclusive, CC0 π)

- **Significant progress in the last 15 years**
- Many experimental and theoretical results
- Still we have to tackle currently existing degeneracies:
 1. between cross sections and flux uncertainties
 2. between nucleon uncertainties and nuclear effects
 3. between different nuclear models and approximations

B) Cross sections in terms of hadronic variables (CC1 π , CC0 π 1p, CC0 π Np, CCOther)

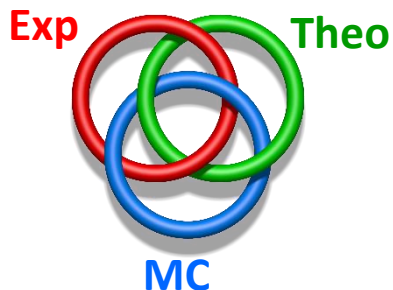
We are only at the beginning!

- Few experimental and theoretical results
- The one pion puzzle is still there
- SIS and DIS have been minimally studied
- Theoretical models and Monte Carlo implementation of semi-inclusive processes are needed

The DUNE and Fermilab SBN programs based on liquid argon detectors open new important and exciting perspectives on neutrino cross section measurements!

This is what is already happening in the case of MicroBooNE

It is important to establish the priorities in relation to the neutrino oscillation program



Close collaboration between theorists, experimentalists and generator developers is crucial

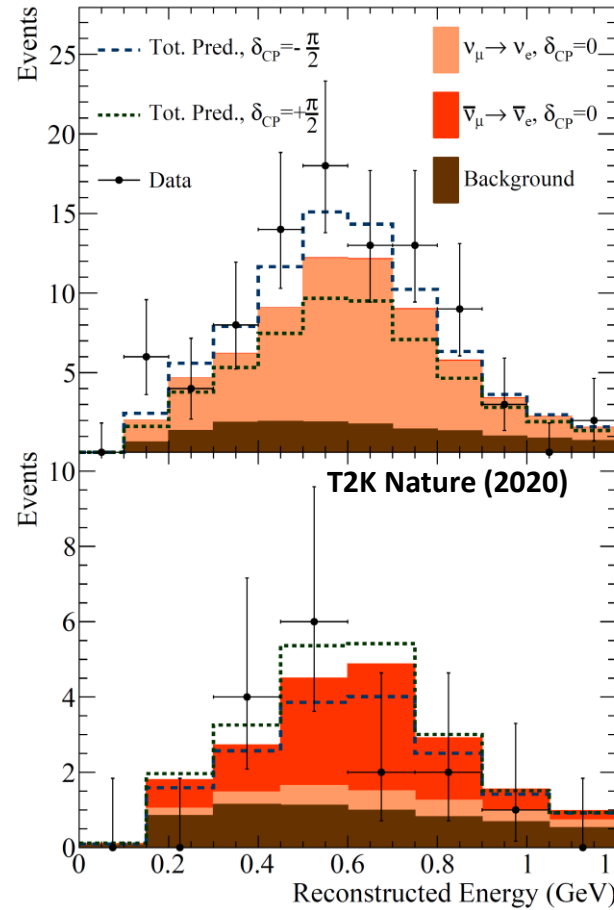
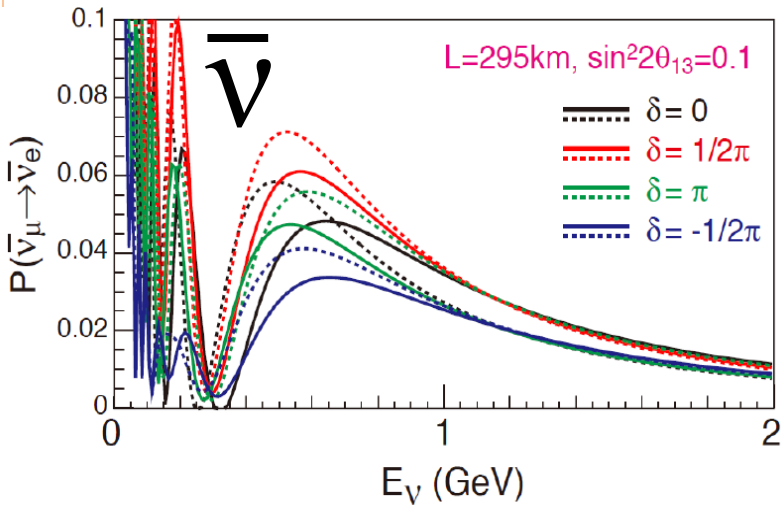
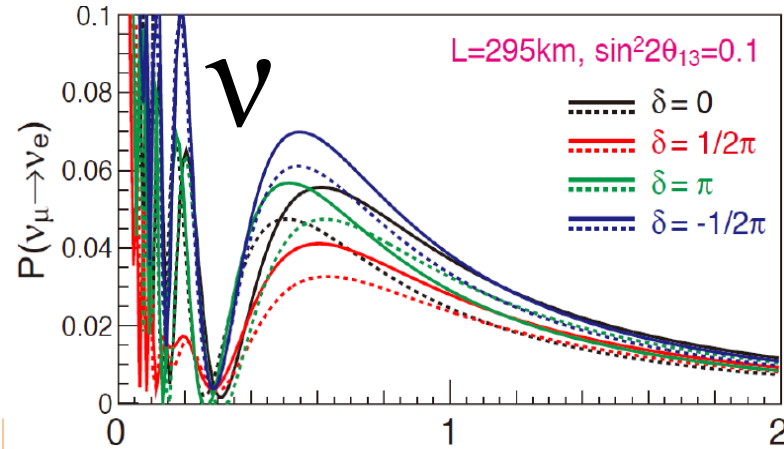
For the moment the community (at least theorists and generator developers) is not so large

APPENDIX

ν .vs. $\bar{\nu}$ and ν_{μ} .vs. ν_e

ν oscillation and CP violation

$$P(\nu_\mu \rightarrow \nu_e) \stackrel{?}{\neq} P(\bar{\nu}_\mu \rightarrow \bar{\nu}_e) \iff \delta_{\text{CP}}$$



$\nu_\mu \rightarrow \nu_e$

$\bar{\nu}_\mu \rightarrow \bar{\nu}_e$

A precise and simultaneous knowledge of the four cross sections is important in connection to the oscillation experiments aiming at the search for CP violation in the lepton sector.

Neutrino vs Antineutrino interactions

The ν and anti ν cross sections differ by the sign of the V-A interference term

$$\frac{d^2\sigma}{d\cos\theta d\omega} = \frac{G_F^2 \cos^2\theta_c |\mathbf{k}'| E_l' \cos^2\frac{\theta}{2}}{\pi} \left[\frac{(\mathbf{q}^2 - \omega^2)^2}{\mathbf{q}^4} G_E^2 R_\tau(\mathbf{q}, \omega) + \frac{\omega^2}{\mathbf{q}^2} G_A^2 R_{\sigma\tau(L)}(\mathbf{q}, \omega) \right. \\ \left. + 2 \left(\tan^2\frac{\theta}{2} + \frac{\mathbf{q}^2 - \omega^2}{2\mathbf{q}^2} \right) \left(G_M^2 \frac{\mathbf{q}^2}{4M_N^2} + G_A^2 \right) R_{\sigma\tau(T)}(\mathbf{q}, \omega) \pm 2 \frac{E_\nu + E_l'}{M_N} \tan^2\frac{\theta}{2} G_A G_M R_{\sigma\tau(T)}(\mathbf{q}, \omega) \right]$$

Vector-Axial interference

$$\begin{cases} + & (\nu) \\ - & (\bar{\nu}) \end{cases}$$

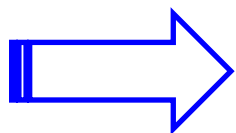
Vector-Axial interference:

basic asymmetry from weak interaction theory

different sign in the Leptonic tensor

$$L_{\mu\nu} = k_\mu k'_\nu + k_\nu k'_\mu - g_{\mu\nu} k \cdot k' \mp i\varepsilon_{\mu\nu\alpha\beta} k^\alpha k'^\beta$$

ν
 $\bar{\nu}$

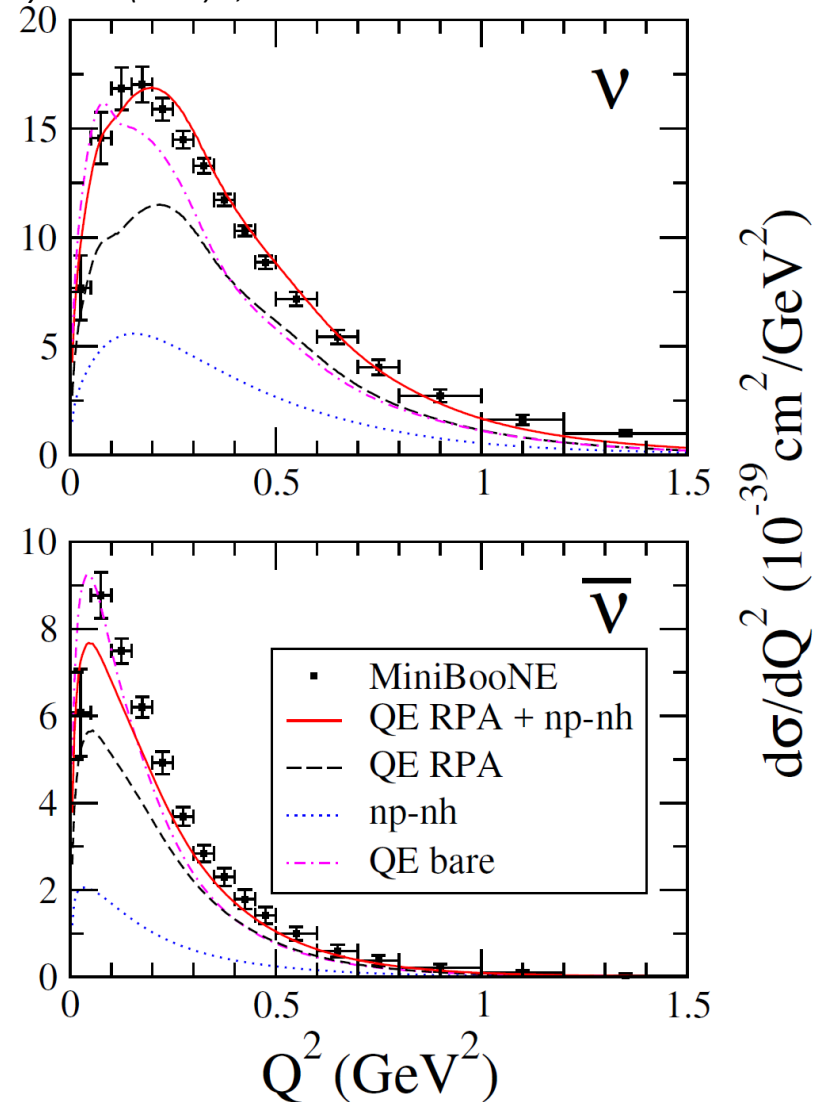
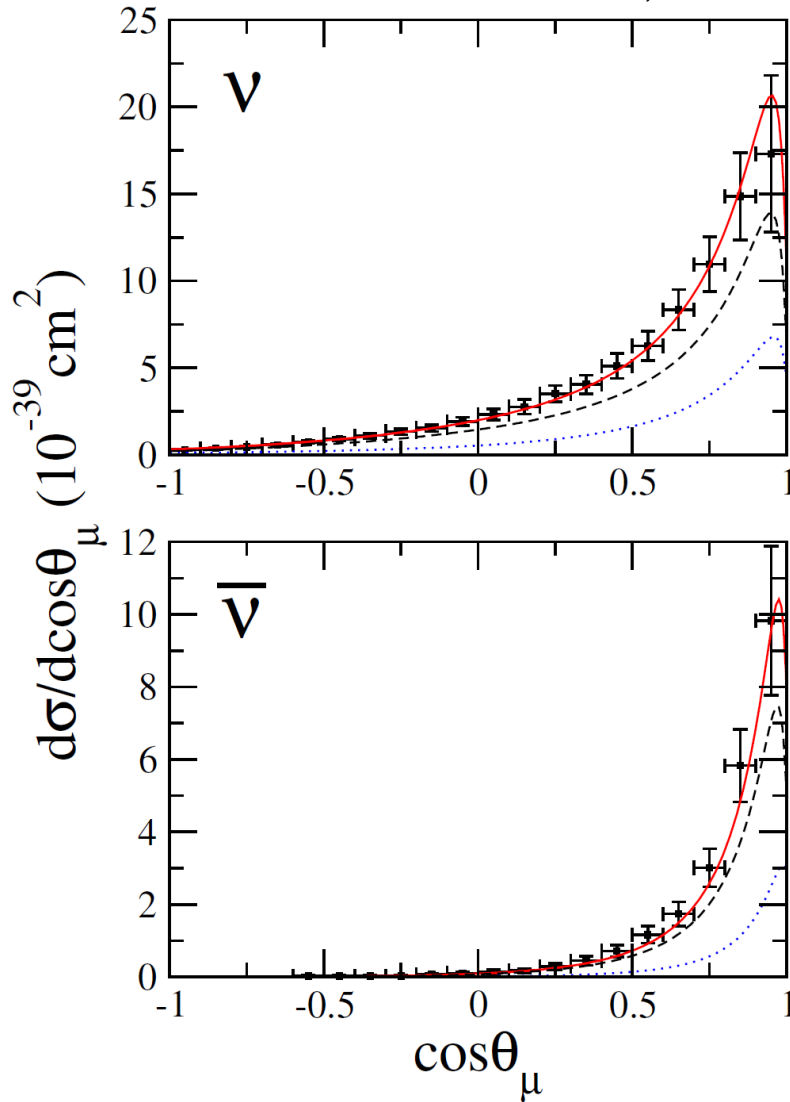


Even neglecting nuclear effects, the absolute value and the kinematic behavior of neutrino and antineutrino cross sections are different

$d\sigma/d\cos\theta$

Q^2 distribution

T. Katori, M. Martini, *J.Phys.G* 45 (2018) 1, 013001



- Antineutrino cross section falls more rapidly than the neutrino one
- Antineutrino Q^2 distribution peaks at smaller Q^2 values than the neutrino one

Neutrino vs Antineutrino interactions and nuclear effects

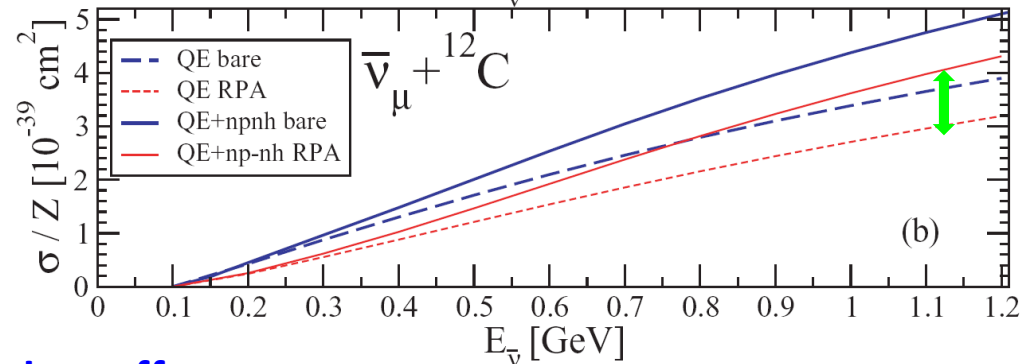
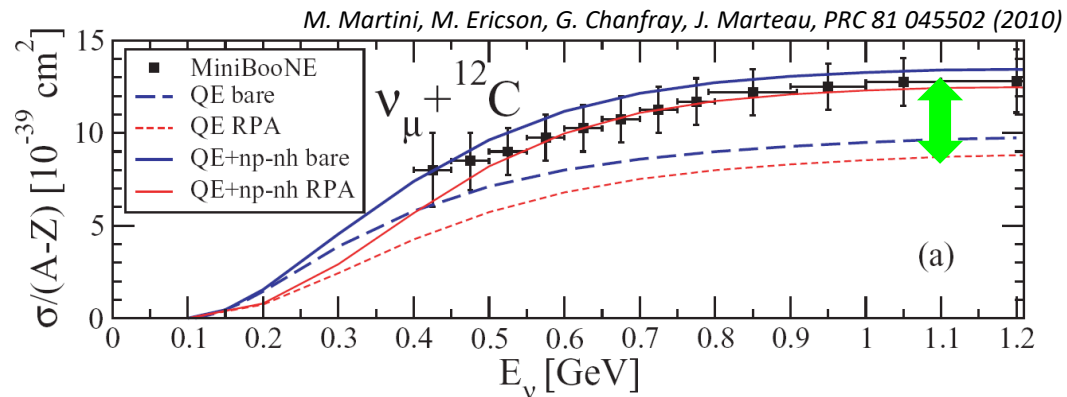
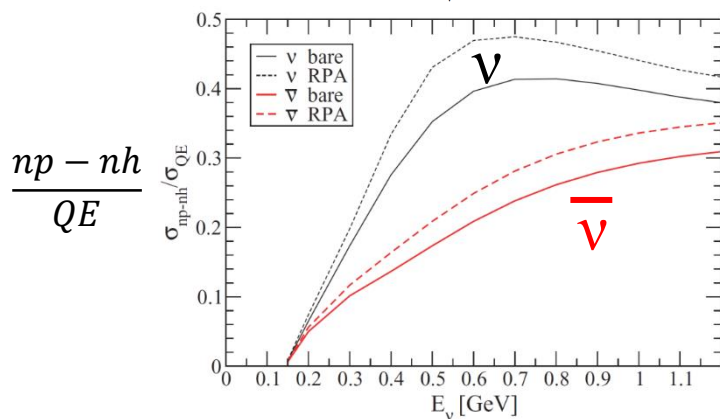
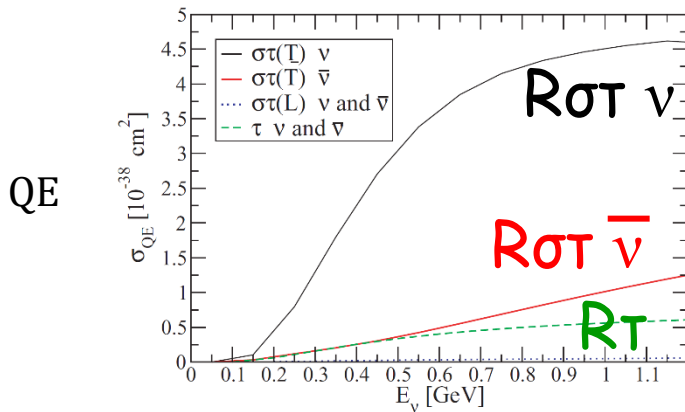
$$\frac{d^2\sigma}{d\cos\theta d\omega} = \frac{G_F^2 \cos^2\theta_c}{\pi} |\mathbf{k}'| E_l' \cos^2\frac{\theta}{2} \left[\frac{(\mathbf{q}^2 - \omega^2)^2}{\mathbf{q}^4} G_E^2 R_\tau(\mathbf{q}, \omega) + \frac{\omega^2}{\mathbf{q}^2} G_A^2 R_{\sigma\tau(L)}(\mathbf{q}, \omega) \right. \\ \left. + 2 \left(\tan^2\frac{\theta}{2} + \frac{\mathbf{q}^2 - \omega^2}{2\mathbf{q}^2} \right) \left(G_M^2 \frac{\mathbf{q}^2}{4M_N^2} + G_A^2 \right) R_{\sigma\tau(T)}(\mathbf{q}, \omega) \pm 2 \frac{E_\nu + E_l'}{M_N} \tan^2\frac{\theta}{2} G_A G_M R_{\sigma\tau(T)}(\mathbf{q}, \omega) \right]$$

Vector-Axial interference

The ν and anti ν interactions differ by the sign of the V-A interference term

→ the relative weight of the different nuclear responses is different for neutrinos and antineutrinos

→ the relative role of np-nh contributions is different for neutrinos and antineutrinos



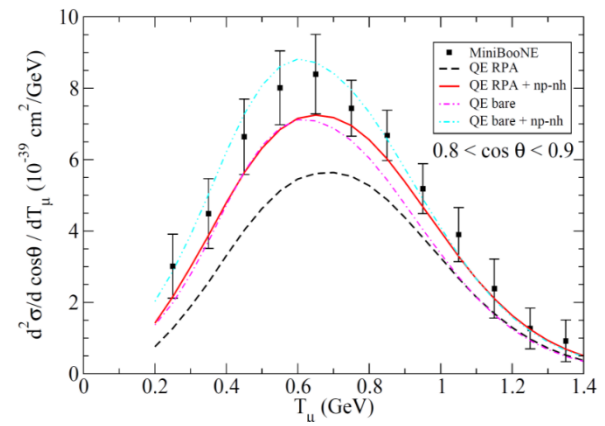
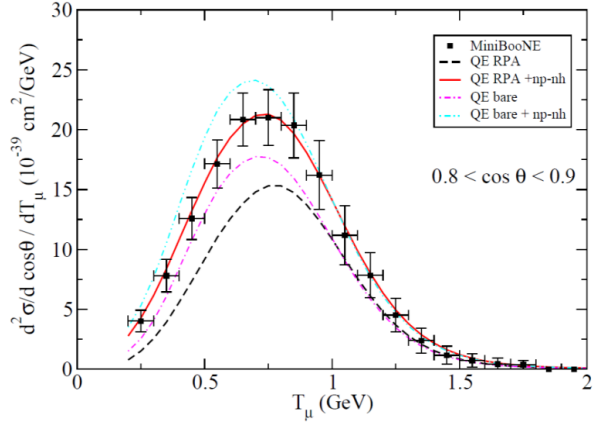
**Nuclear effects generate an asymmetry
unrelated to CP violation**

The relative role of np-nh for neutrinos and antineutrinos is different in different approaches



Lyon RPA
Martini et al.

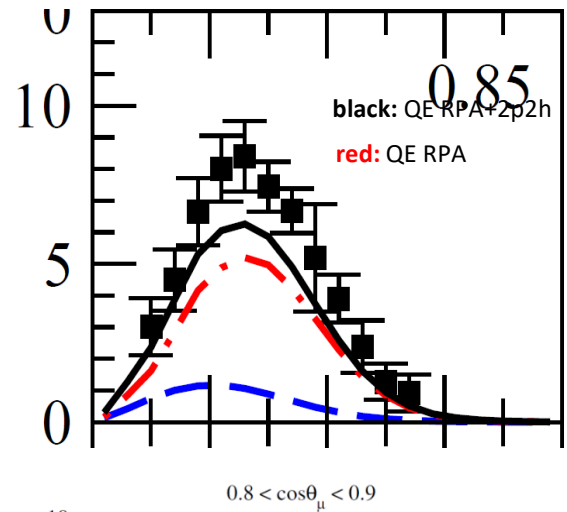
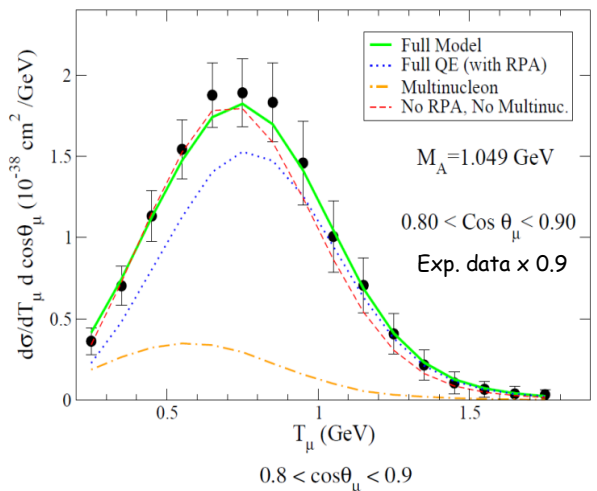
PRC 84 (2011)



PRC 87 (2013)

Valencia RPA
Nieves et al.

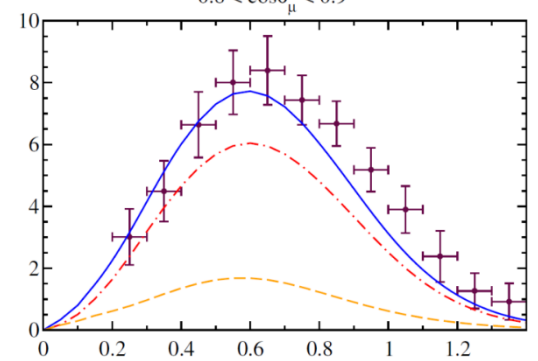
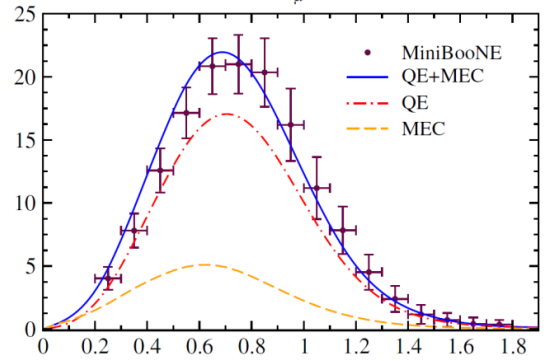
PLB 707 (2012)



PLB 721 (2013)

SuSAv2

PRD 94 (2016)



PRD 94 (2016)

Difference of ν and $\bar{\nu}$ cross sections and the VA interference term

$$d\sigma \sim d\sigma_L + d\sigma_T \pm d\sigma_{VA}$$

$$d\sigma_\nu - d\sigma_{\bar{\nu}} \overset{?}{\leftrightarrow} 2d\sigma_{VA}$$

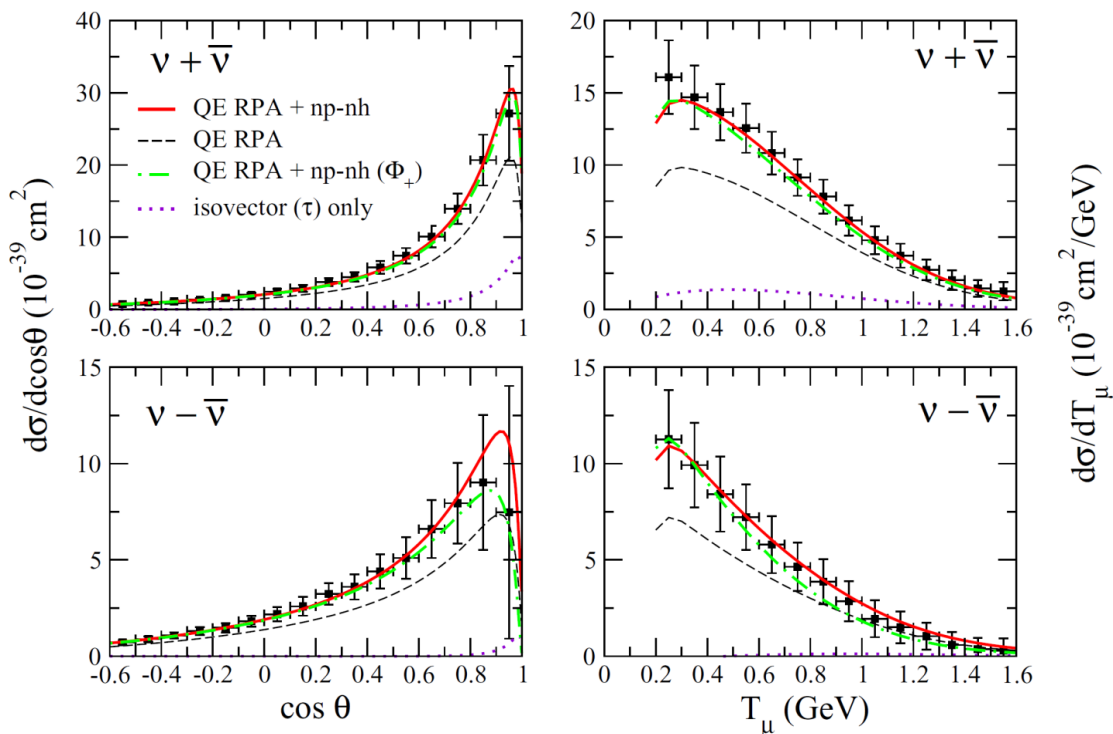
Difference gives only the VA term for identical ν and $\bar{\nu}$ flux

Problem: flux dependence of $d\sigma$ $\frac{d^2\sigma}{dE_\mu d\cos\theta} = \int dE_\nu \left[\frac{d^2\sigma}{d\omega d\cos\theta} \right]_{\omega=E_\nu-E_\mu} \Phi(E_\nu)$

We introduce the **mean flux** $\Phi_+ = 1/2[\Phi_\nu + \Phi_{\bar{\nu}}]$

We calculate the sum and the difference using **real** and **mean** MiniBooNE fluxes results

M. Ericson, M. Martini Phys. Rev. C 91 035501 (2015)



The mean flux contribution is dominant



The VA interference term is experimentally accessible in MBdata

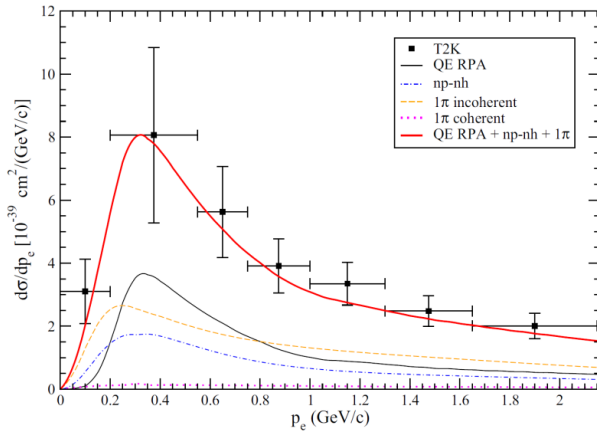


Need for the multinucleon component in the VA interference

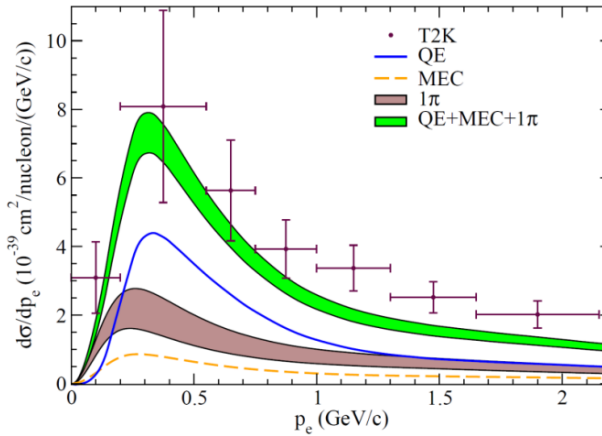
ν_e cross sections

- There are few published results on ν_e cross sections. This is essentially due the relatively small component of ν_e fluxes with respect to the ν_μ ones hence to small statistics.
- The ν_e experimental published results essentially concern inclusive cross sections
T2K flux-integrated ν_e CC inclusive differential cross sections on carbon

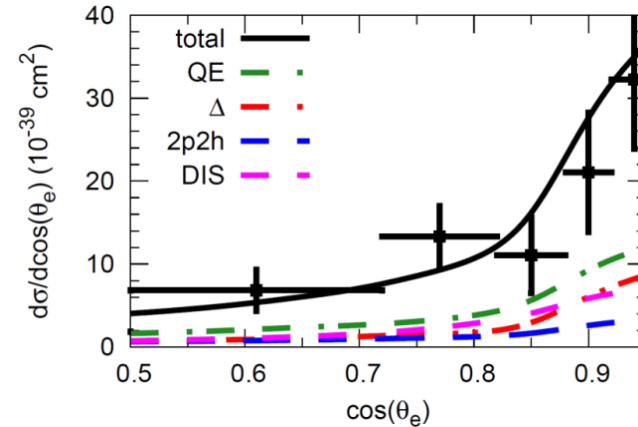
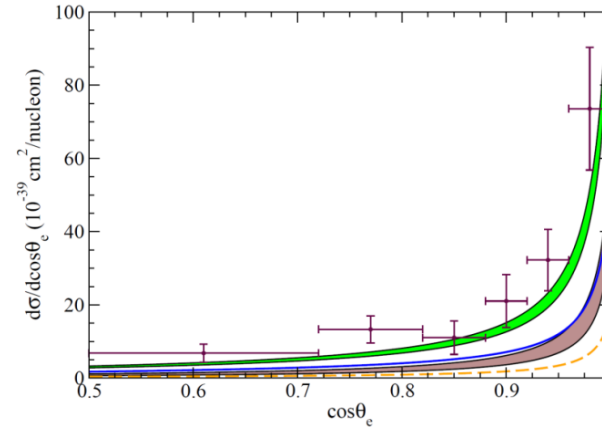
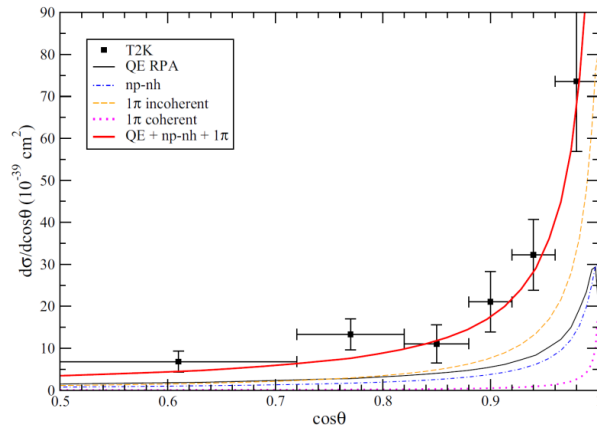
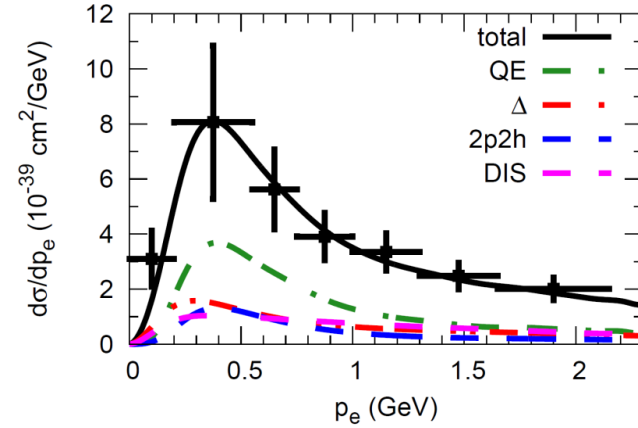
Martini et al., PRC 94 (2016)



Megias et al., PRD 94 (2016)

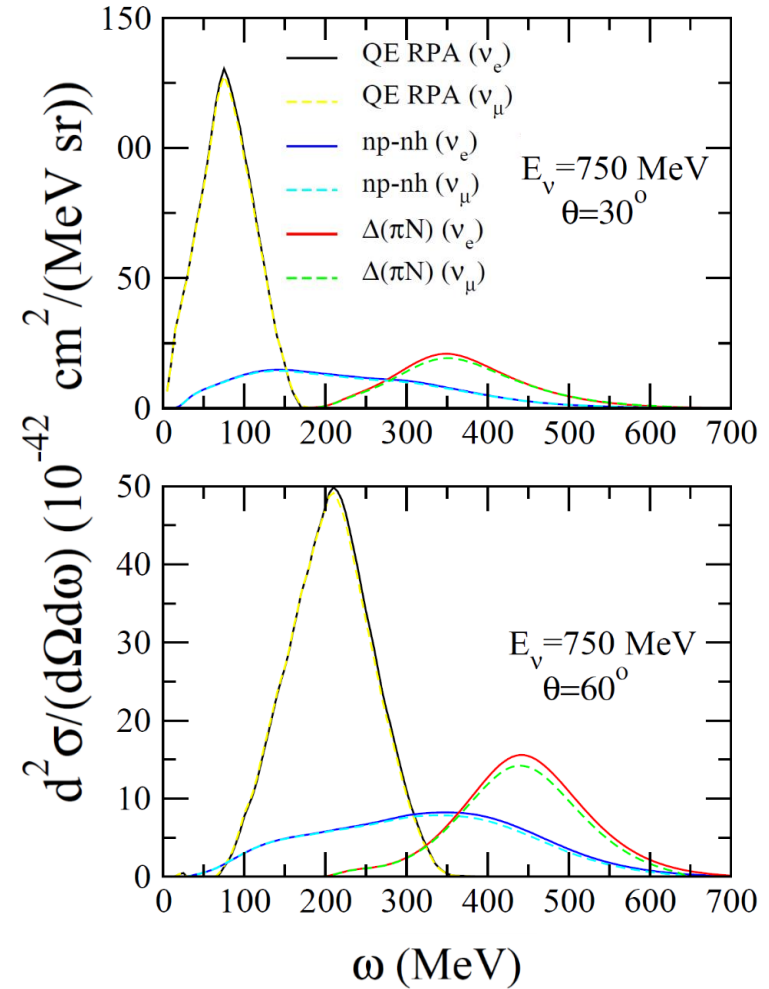
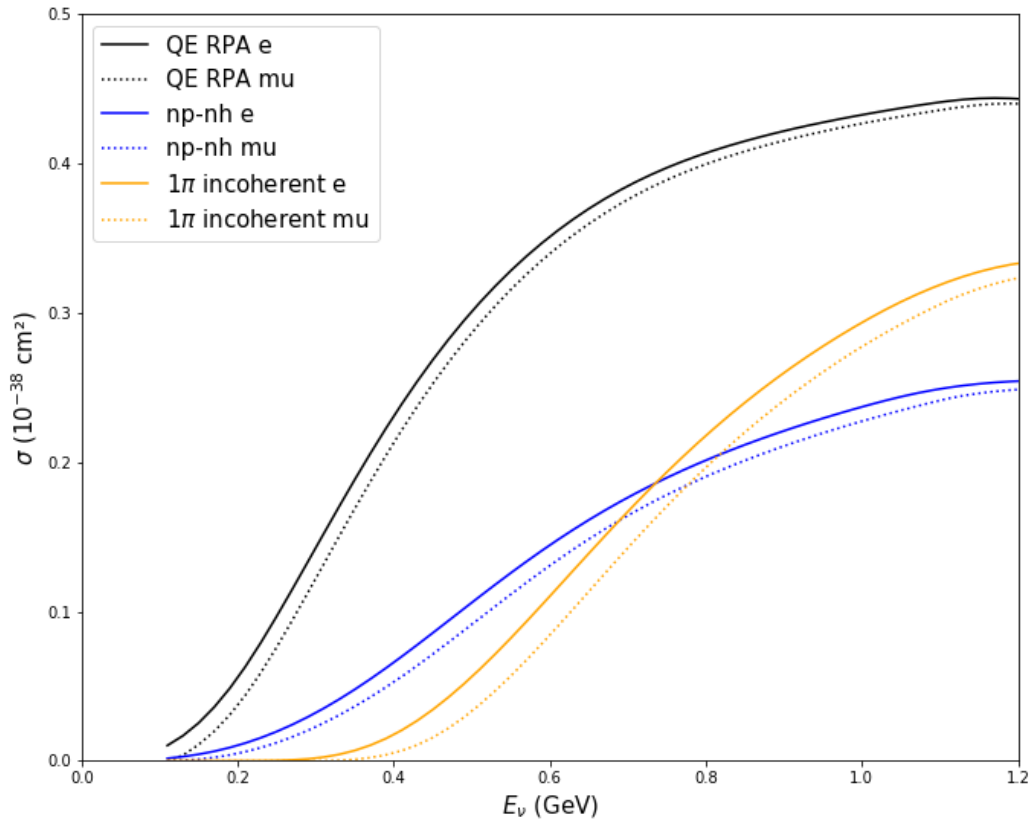


Gallmeister et al. PRC 94(2016)



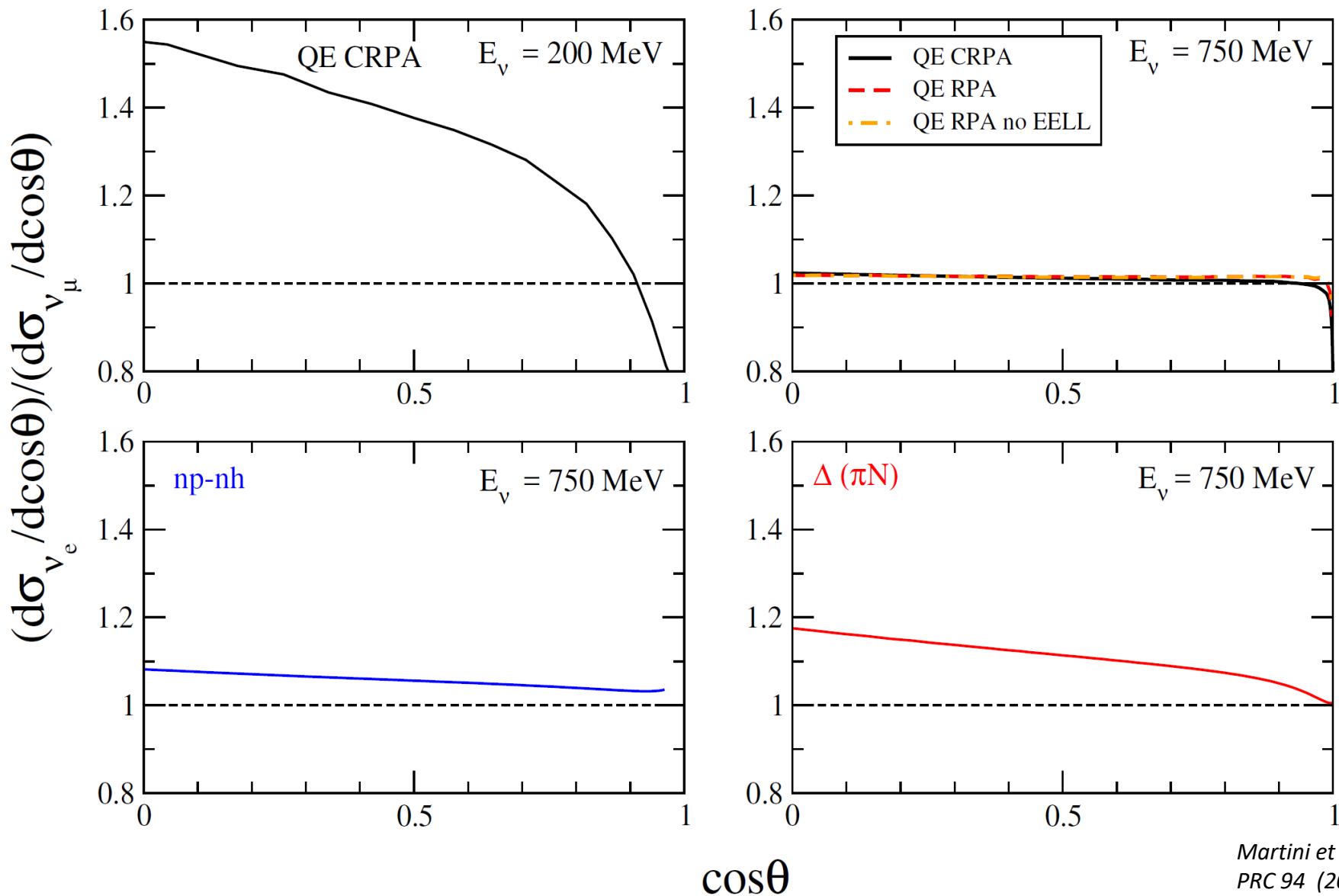
- Theoretical results agree with data
- Similarity of the theoretical results for the inclusive $d\sigma$

ν_e and ν_μ total and double differential cross sections



Due to the different kinematic limits, the ν_e cross sections are expected to be larger than the ν_μ ones

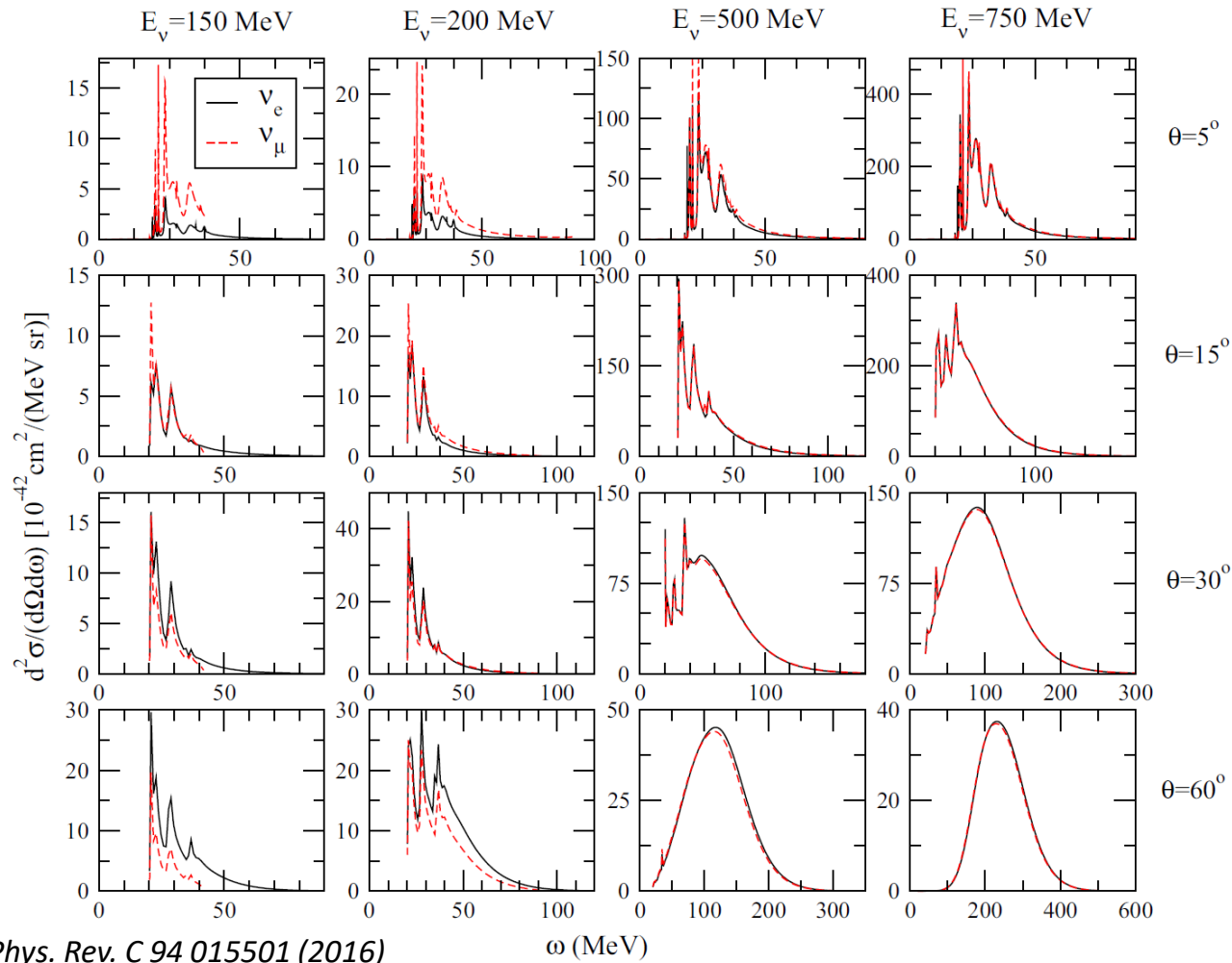
Ratio v_e/v_μ for $d\sigma/d\cos\theta$ in different channels



Martini et al.,
PRC 94 (2016)

Due to the different kinematic limits, the ν_e cross sections are expected to be larger than the ν_μ ones. However for forward scattering angles this hierarchy is opposite in the QE channel.

A theoretical study (HF+CRPA Ghent) of the ν_μ and ν_e $d^2\sigma$



M. Martini et al., Phys. Rev. C 94 015501 (2016)

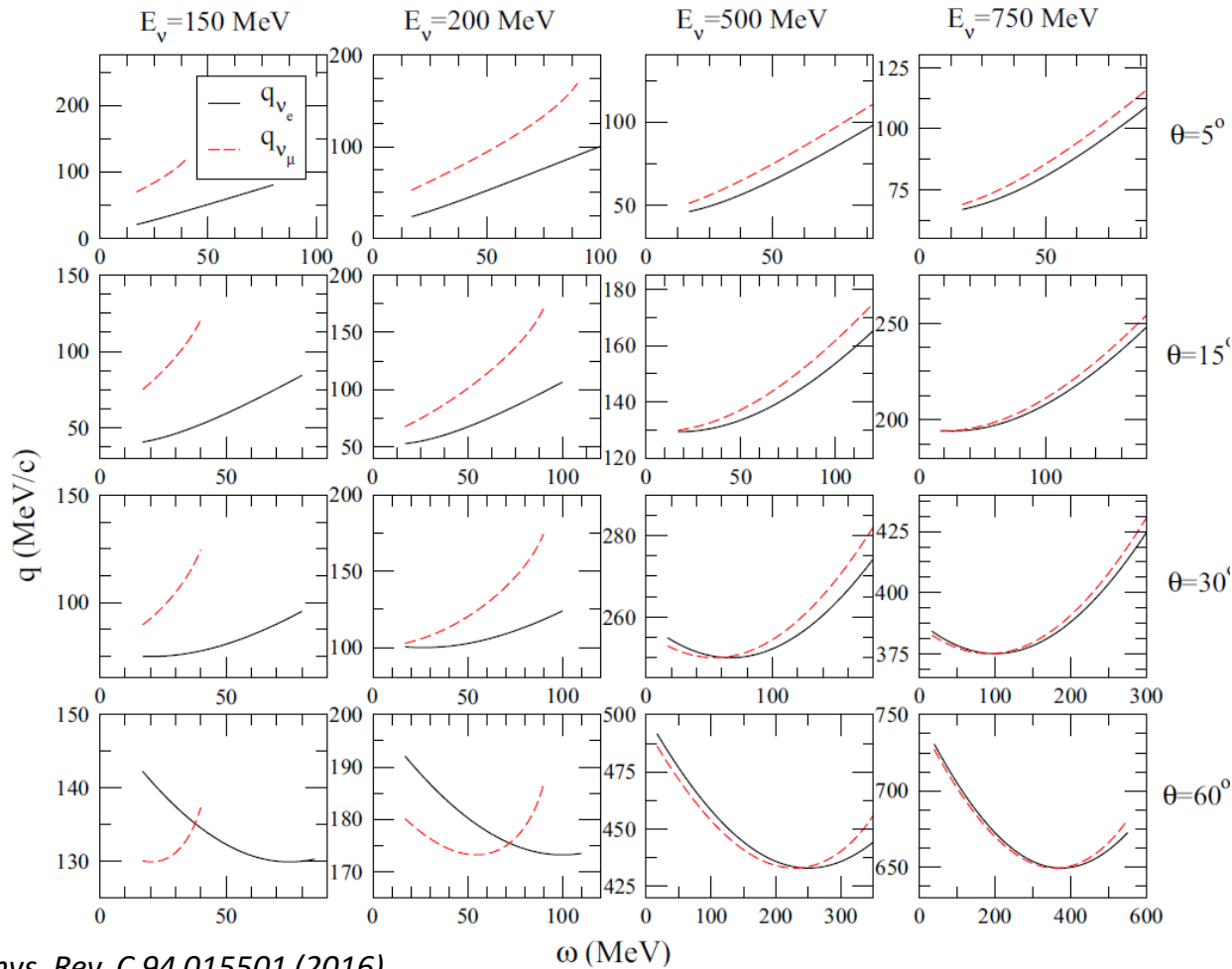
Due to the different kinematic limits, the ν_e cross sections are expected to be larger than the ν_μ ones. However for forward scattering angles this hierarchy is opposite.

The only difference between ν_μ and ν_e cross sections is the mass of the outgoing lepton.

But the mass affects the three momentum transfer which enters into the kinematics as well as the dynamics of the nuclear model

Momentum transfer q versus transferred energy ω for ν_μ and ν_e $d^2\sigma$

Kinematical conditions of the previous slide



M. Martini et al., Phys. Rev. C 94 015501 (2016)

$$q^2 = E_\nu^2 + p_l^2 - 2E_\nu p_l \cos \theta$$

$$p_l^2 = E_l^2 - m_l^2 = (E_\nu - \omega)^2 - m_l^2$$

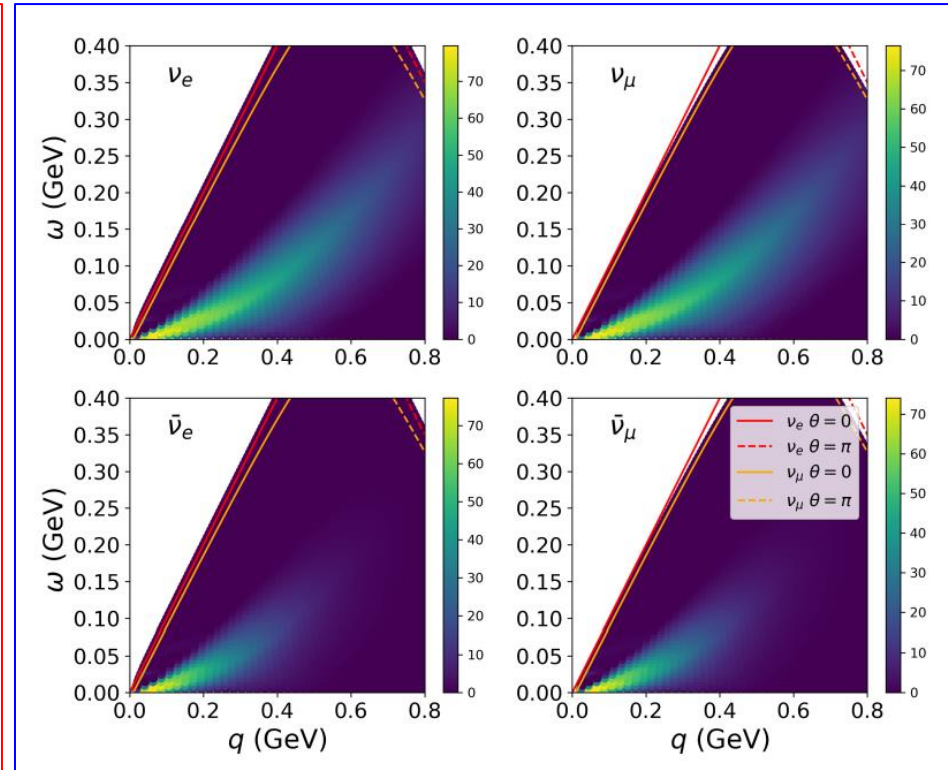
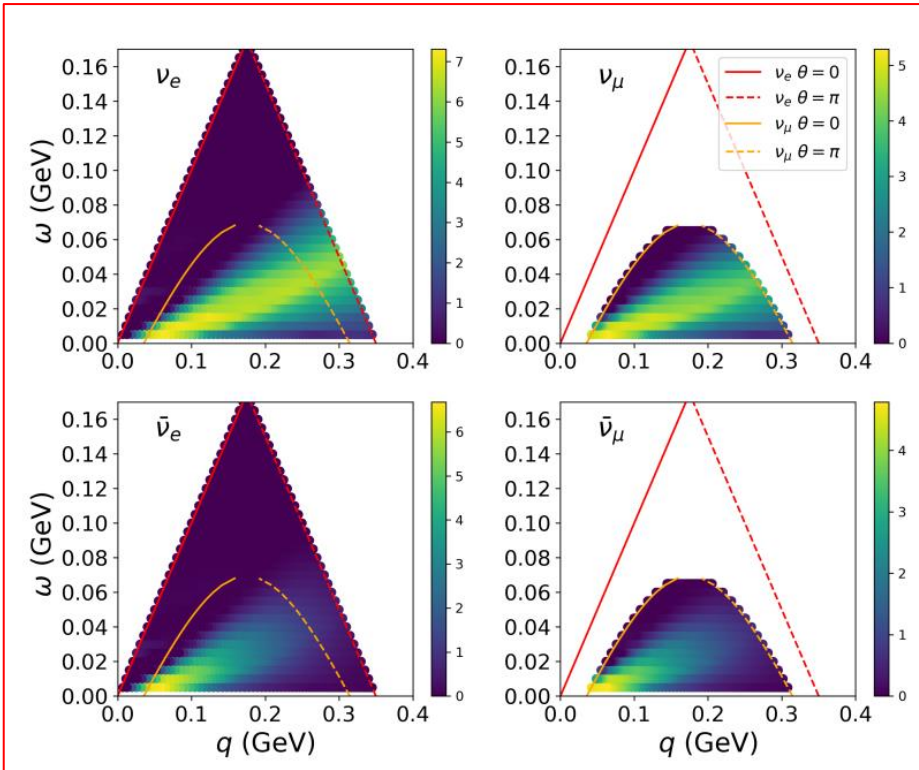
The only difference between ν_μ and ν_e cross sections is the mass of the outgoing lepton. But the mass affects the three-momentum transfer which enters into the kinematics as well as the dynamics of the nuclear model

Projection of ν_μ and ν_e $d^2\sigma$ on (q, ω) plane

Martini, Ericson, Chanfray [2310.06388](#)

Ev = 175 MeV

Ev = 575 MeV



For neutrino and antineutrino scattering the $\theta = 0$ muon and electron lines explore in the (q, ω) plane two different regions, the muon one corresponding to larger quasielastic cross sections

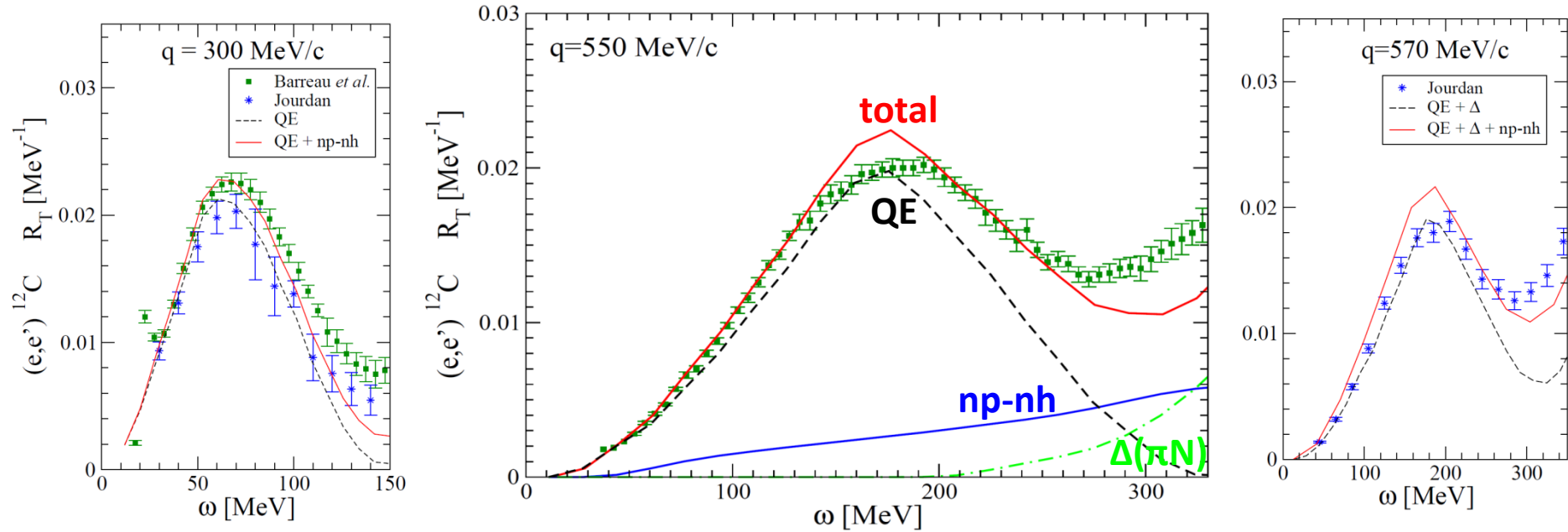
By increasing the neutrino energies the difference between the muon and electron $\theta = 0$ lines decreases and the two curves explore more and more similar region in the (q, ω) plane

Testing the
responses in other
processes

Electron scattering

$$\frac{d^2\sigma}{d\theta d\omega} = \sigma_M \left\{ \frac{(\omega^2 - q^2)^2}{q^4} R_L(\omega, q) + \left[\tan^2\left(\frac{\theta}{2}\right) - \frac{\omega^2 - q^2}{2q^2} \right] R_T(\omega, q) \right\}$$

M. Martini, J.Phys.Conf.Ser. 408 (2013) 012041

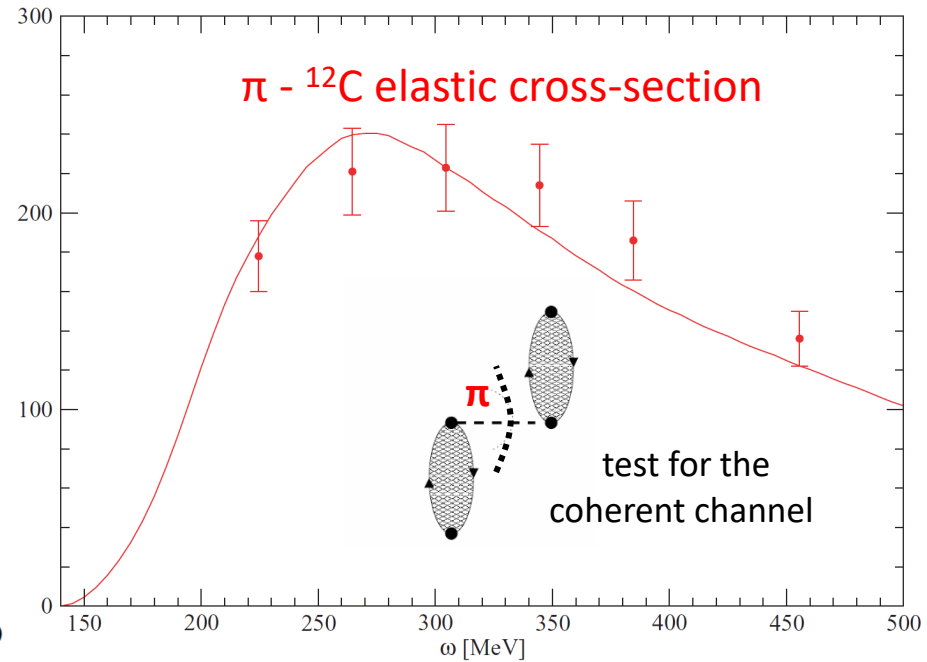
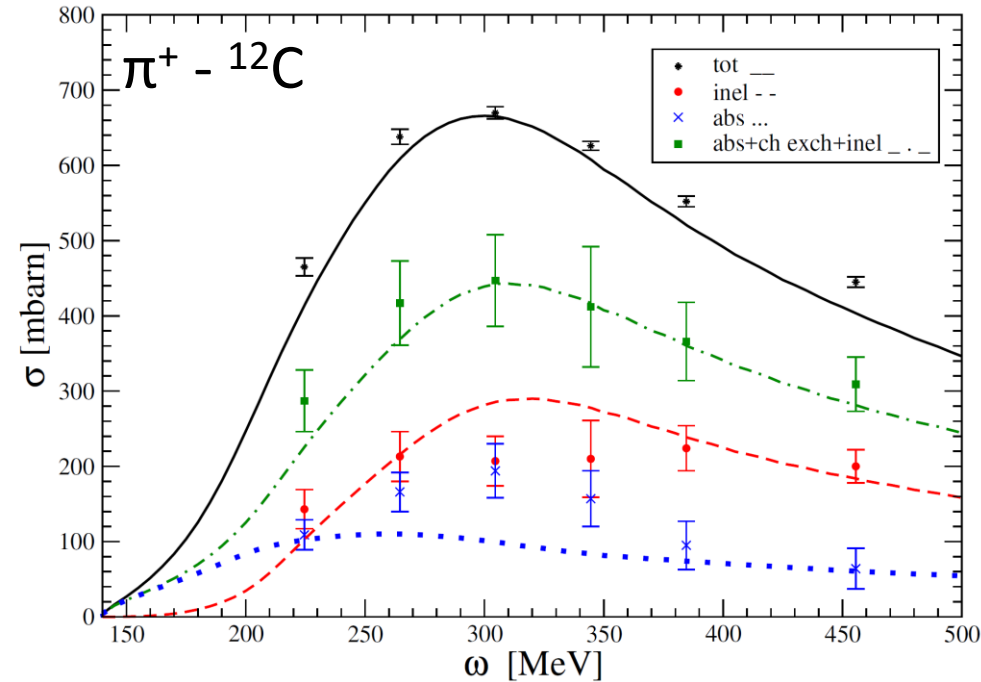


Pion scattering

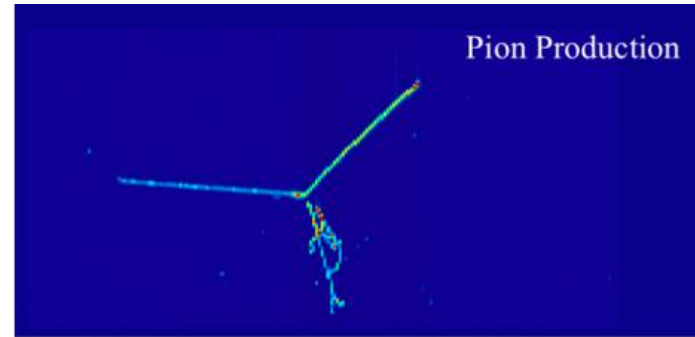
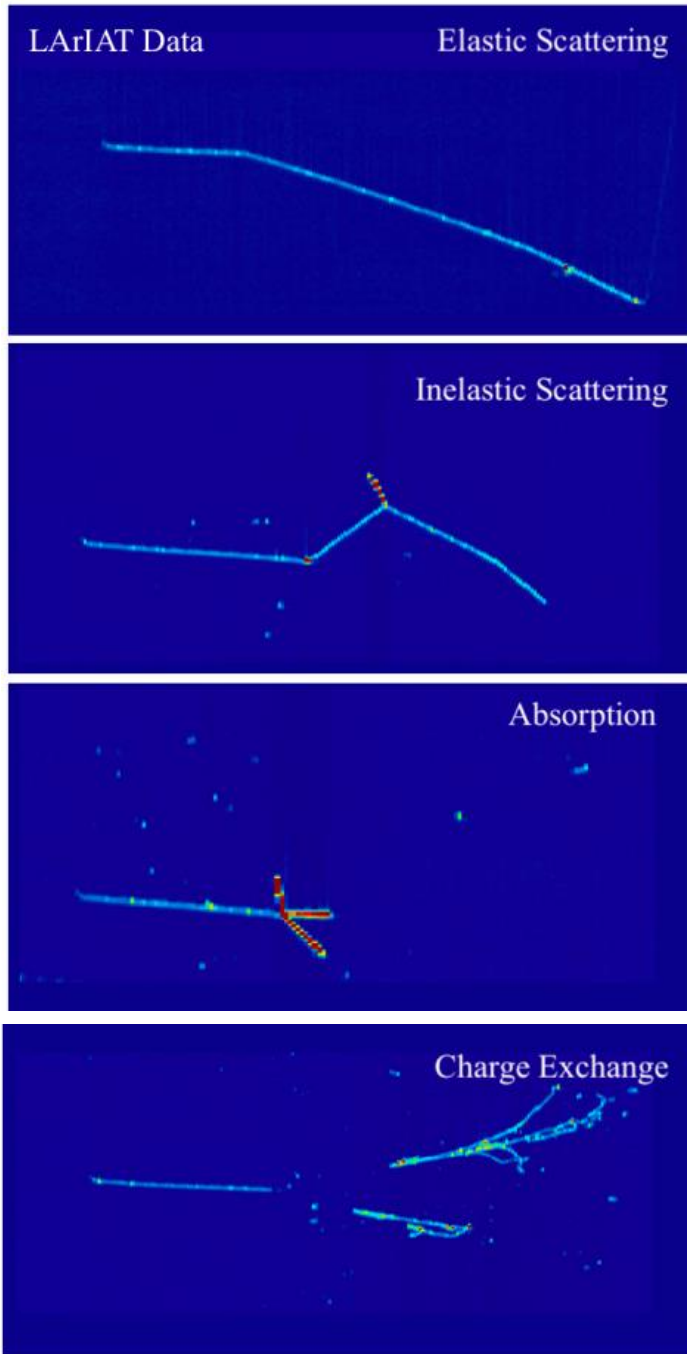
$$\sigma^{tot}(\omega) = \left(\frac{g_r}{2M_N} \right)^2 \pi q_\pi R_L(\omega, q_\pi)$$

$$q_\pi^2 = \omega^2 - m_\pi^2$$

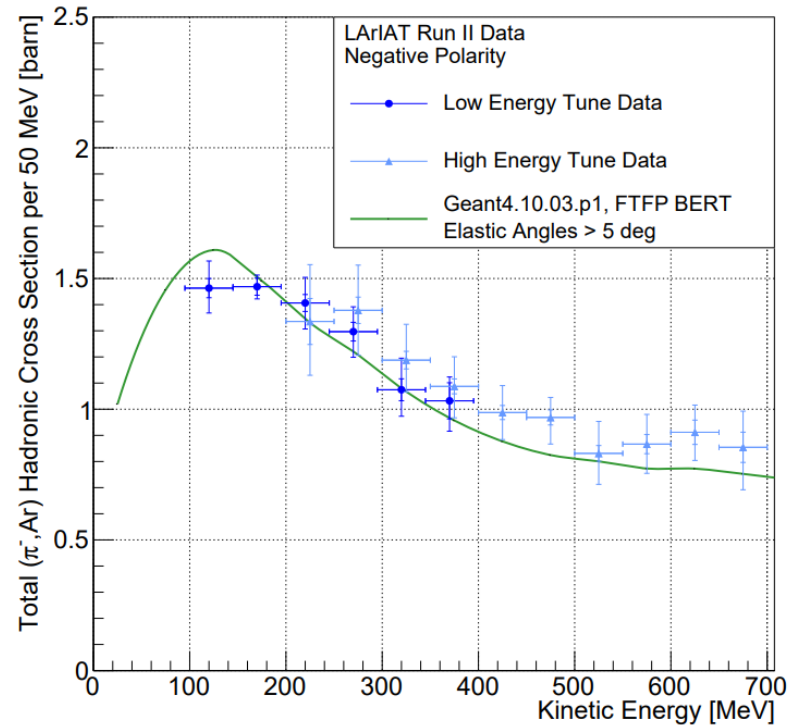
M. Martini, M. Ericson, G. Chanfray, J. Marteau, PRC 80 065501 (2009)



π -Ar cross section: LArIAT experiment



Phys.Rev.D 106 (2022) 5, 052009



SPARES

Standard Model of electroweak interaction

Electroweak interaction Lagrangian

$$\mathcal{L}_{\text{int}} = -e J_{\text{EM}}^\mu A_\mu - \frac{g}{2\sqrt{2}} \left(J_{\text{CC}}^\mu W_\mu^\dagger + \text{h. c.} \right) - \frac{g}{2 \cos \theta_W} J_{\text{NC}}^\mu Z_\mu$$

Feynman Rules

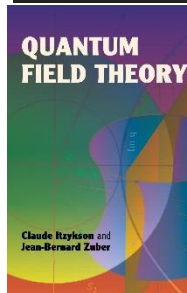
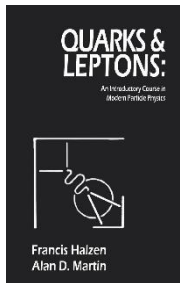
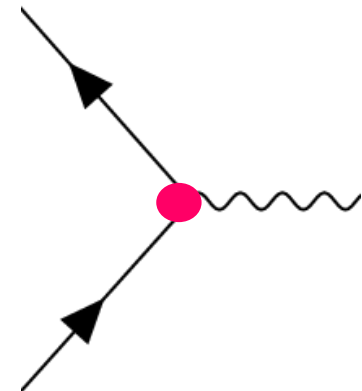
Gauge Bosons Propagators

- Photon (γ) $\frac{i}{q^2} (-g^{\mu\nu})$
- Massive vector bosons (W,Z) $\frac{i}{q^2 - M_V^2} \left(-g^{\mu\nu} + \frac{q^\mu q^\nu}{M_V^2} \right) \xrightarrow{|q^2| \ll M_V^2} \frac{i g^{\mu\nu}}{M_V^2}$

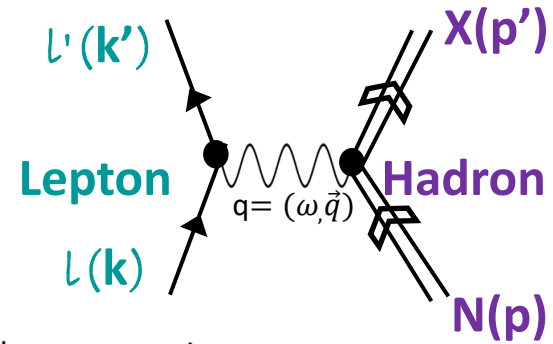


Fermion Vertices

- Electromagnetic $-ieQ_f \gamma_\mu$
 - $Q_{e^-} = -1, Q_{up} = 2/3, \dots$
- Weak (W exchange) $-i \frac{g}{\sqrt{2}} c \gamma_\mu \frac{1 - \gamma^5}{2}$
 - $c = 1$ for leptons
 - $c =$ Cabibbo-mixing matrix element for quarks



Electroweak transition matrix elements



Electromagnetic transition $\ell^- N \rightarrow \ell^- X$

$$-i\mathcal{M} = -(\underbrace{ie^2}_{\text{e.m. lepton current}}) \bar{u}(k') \gamma_\mu u(k) \frac{-ig^{\mu\nu}}{q^2} \langle X(p'_f) | \underbrace{J_\nu(0)}_{\text{hadronic current (Vector)}} | N(p) \rangle$$

Charged current transition $\nu N \rightarrow \ell^- X$

$$-i\mathcal{M} = \left(\frac{-ig}{2\sqrt{2}} \right)^2 \cos \theta_C \underbrace{\bar{u}(k') \gamma_\mu (1 - \gamma^5) u(k)}_{\text{weak lepton current}} \frac{ig^{\mu\nu}}{M_W^2} \langle X(p'_f) | \underbrace{J_\nu(0)}_{\text{hadronic current (Vector-Axial)}} | N(p) \rangle$$

θ_C

Cabibbo angle

$$\frac{g^2}{8M_W^2} = \frac{G_F}{\sqrt{2}}$$

Fermi coupling constant

The single nucleon electroweak current

Electromagnetic current - Electron scattering

$$J_{s's}^\mu(\mathbf{p}', \mathbf{p}) = \bar{u}_{s'}(\mathbf{p}') \left[F_1(Q^2) \gamma^\mu + F_2(Q^2) i \sigma^{\mu\nu} \frac{q_\nu}{2m_N} \right] u_s(\mathbf{p})$$

$$Q^2 = -q^2 \quad \sigma^{\mu\nu} = \frac{i}{2} [\gamma^\mu, \gamma^\nu]$$

Weak current – CC neutrino scattering

$$J^\mu = V^\mu - A^\mu \quad \text{Vector – Axial}$$

$$\text{Vector } V_{s's}^\mu(\mathbf{p}', \mathbf{p}) = \bar{u}_{s'}(\mathbf{p}') \left[2F_1^V \gamma^\mu + 2F_2^V i \sigma^{\mu\nu} \frac{q_\nu}{2m_N} \right] u_s(\mathbf{p})$$

$$\text{Conserved Vector Current (CVC) } q_\alpha V^\alpha = 0 \text{ and isospin symmetry } \Rightarrow F_i^V = F_i^p - F_i^n$$

$$\text{Axial } A_{s's}^\mu(\mathbf{p}', \mathbf{p}) = \bar{u}_{s'}(\mathbf{p}') \left[G_A \gamma^\mu \gamma_5 + G_P \frac{q^\mu}{2m_N} \gamma_5 \right] u_s(\mathbf{p})$$

$$\text{Partially Conserved Axial Current (PCAC) and pion-pole dominance } \Rightarrow G_P = \frac{4m_N^2}{m_\pi^2 + Q^2} G_A$$

$$q_\alpha A^\alpha = i(m_u + m_d) \bar{q}_u \gamma_5 q_d \rightarrow 0$$

Some two-body currents

Electromagnetic

- Seagull or contact:

$$j_s^\mu(\mathbf{p}'_1, \mathbf{p}'_2, \mathbf{p}_1, \mathbf{p}_2) = \frac{f^2}{m_\pi^2} i\epsilon_{3ab} \bar{u}(\mathbf{p}'_1) \tau_a \gamma_5 \not{K}_1 u(\mathbf{p}_1) \frac{F_1^V}{K_1^2 - m_\pi^2} \bar{u}(\mathbf{p}'_2) \tau_b \gamma_5 \gamma^\mu u(\mathbf{p}_2) + (1 \leftrightarrow 2) .$$

- Pion-in-flight:

$$j_p^\mu(\mathbf{p}'_1, \mathbf{p}'_2, \mathbf{p}_1, \mathbf{p}_2) = \frac{f^2}{m_\pi^2} i\epsilon_{3ab} \frac{F_\pi (K_1 - K_2)^\mu}{(K_1^2 - m_\pi^2)(K_2^2 - m_\pi^2)} \bar{u}(\mathbf{p}'_1) \tau_a \gamma_5 \not{K}_1 u(\mathbf{p}_1) \bar{u}(\mathbf{p}'_2) \tau_b \gamma_5 \not{K}_2 u(\mathbf{p}_2) .$$

- Correlation:

$$j_{\text{cor}}^\mu(\mathbf{p}'_1, \mathbf{p}'_2, \mathbf{p}_1, \mathbf{p}_2) = \frac{f^2}{m_\pi^2} \bar{u}(\mathbf{p}'_1) \tau_a \gamma_5 \not{K}_1 u(\mathbf{p}_1) \frac{1}{K_1^2 - m_\pi^2} \bar{u}(\mathbf{p}'_2) [\tau_a \gamma_5 \not{K}_1 S_F(P_2 + Q) \Gamma^\mu(Q) + \Gamma^\mu(Q) S_F(P'_2 - Q) \tau_a \gamma_5 \not{K}_1] u(\mathbf{p}_2) + (1 \leftrightarrow 2) .$$

Amaro et al. Phys.Rev.C 82 044601 (2010)

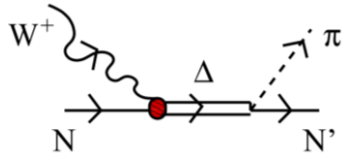
Weak

- CC Seagull

$$j_s^\mu(\mathbf{p}'_1, \mathbf{p}'_2, \mathbf{h}_1, \mathbf{h}_2) = (\tau_0 \otimes \tau_{+1} - \tau_{+1} \otimes \tau_0) \frac{f}{m_\pi} \frac{1}{\sqrt{2} f_\pi} \bar{u}(\mathbf{p}'_1) \gamma_5 \not{K}_1 u(\mathbf{h}_1) \frac{\bar{u}(\mathbf{p}'_2) [g_A F_1^V(Q^2) \gamma_5 \gamma^\mu + F_\rho(K_2^2) \gamma^\mu] u(\mathbf{h}_2)}{K_1^2 - m_\pi^2} - (1 \leftrightarrow 2)$$

Ruiz-Simo et al. Phys.Rev.D 90 033012 (2014); J.Phys.G 44 065105 (2017)

The 1π production via $\Delta(1232)$ resonance excitation and decay



At energies of our interest, it is the dominant mechanism of the reaction

$$WN \rightarrow N'\pi$$

E. Hernandez et al. Phys. Rev. D 76, 033005 (2007)

$$W^+n \rightarrow \Delta^+ \quad \text{Hadron matrix element} \quad \langle \Delta^+; p_\Delta = p + q | j_{cc+}^\mu(0) | n; p \rangle = \bar{u}_\alpha(\vec{p}_\Delta) \Gamma^{\alpha\mu}(p, q) u(\vec{p}) \cos \theta_C$$

Electroweak vertex

$$\Gamma^{\alpha\mu}(p, q) = \left[\frac{C_3^V}{M} (g^{\alpha\mu} \not{q} - q^\alpha \gamma^\mu) + \frac{C_4^V}{M^2} (g^{\alpha\mu} q \cdot p_\Delta - q^\alpha p_\Delta^\mu) + \frac{C_5^V}{M^2} (g^{\alpha\mu} q \cdot p - q^\alpha p^\mu) + C_6^V g^{\mu\alpha} \right] \gamma_5$$

$$+ \left[\frac{C_3^A}{M} (g^{\alpha\mu} \not{q} - q^\alpha \gamma^\mu) + \frac{C_4^A}{M^2} (g^{\alpha\mu} q \cdot p_\Delta - q^\alpha p_\Delta^\mu) + C_5^A g^{\alpha\mu} + \frac{C_6^A}{M^2} q^\mu q^\alpha \right], \quad p_\Delta = p + q$$

Vector form factors

$C_{3,4,5,6}^V$ can be extracted from single-pion electro-production data

Axial form factors

$$C_{3,4,5,6}^A \quad C_5^A(Q^2) = \frac{C_5^A(0)}{(1 + Q^2/M_{A\Delta}^2)^2} \quad C_6^A \underset{\text{PCAC}}{=} M^2/(m_\pi^2 + Q^2) \cdot C_5^A \quad C_4^A \underset{\text{Adler}}{=} -1/4 \cdot C_5^A \quad C_3^A \text{ Small, usually neglected}$$

Δ propagator

$$G^{\mu\nu}(p_\Delta) = \frac{P^{\mu\nu}(p_\Delta)}{p_\Delta^2 - M_\Delta^2 + iM_\Delta\Gamma_\Delta}$$

Spin 3/2 projection operator

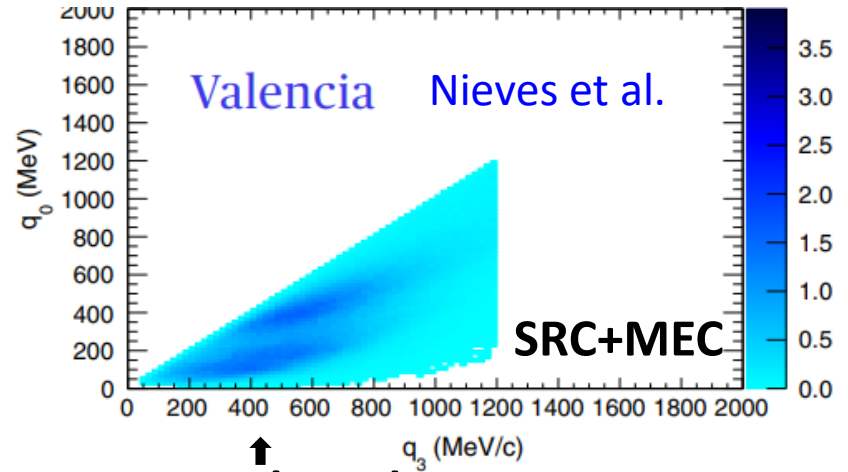
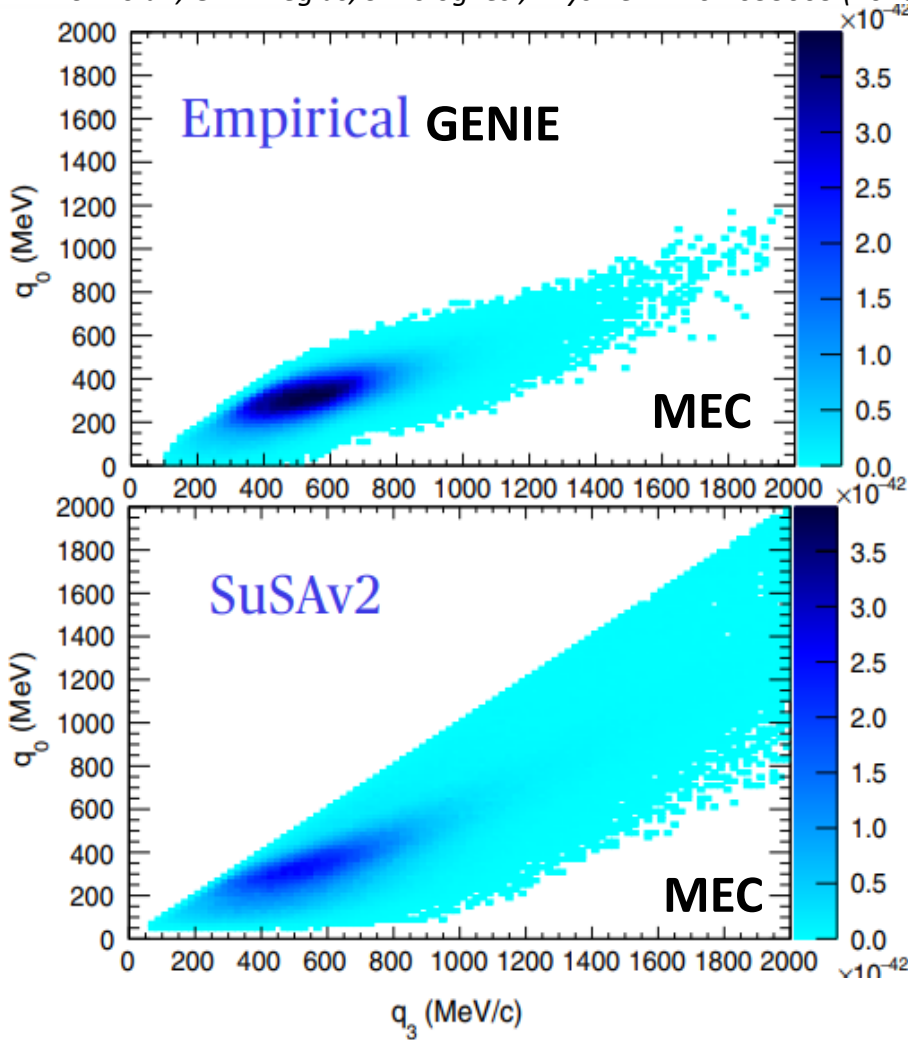
$$P^{\mu\nu}(p_\Delta) = -(\not{p}_\Delta + M_\Delta) \left[g^{\mu\nu} - \frac{1}{3} \gamma^\mu \gamma^\nu - \frac{2}{3} \frac{p_\Delta^\mu p_\Delta^\nu}{M_\Delta^2} + \frac{1}{3} \frac{p_\Delta^\mu \gamma^\nu - p_\Delta^\nu \gamma^\mu}{M_\Delta} \right]$$

$N\Delta\pi$ coupling

$$\mathcal{L}_{\pi N\Delta} = \frac{f^*}{m_\pi} \bar{\Psi}_\mu \vec{T}^\dagger (\partial^\mu \vec{\phi}) \Psi + \text{h.c.}$$

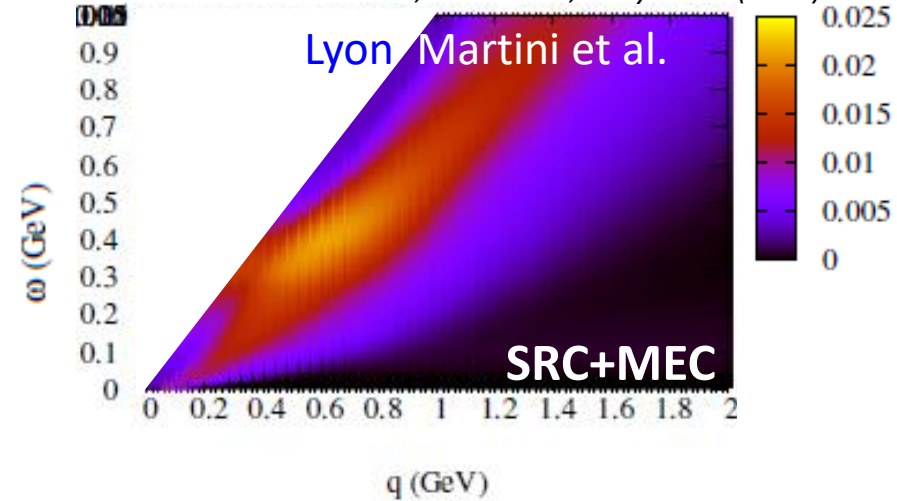
Example of different results for 2p-2h in the (q,ω) or (q_0,q_3) plane

S. Dolan, G.D. Megias, S. Bolognesi, *Phys.Rev.D* 101 033003 (2020)



RPA-based

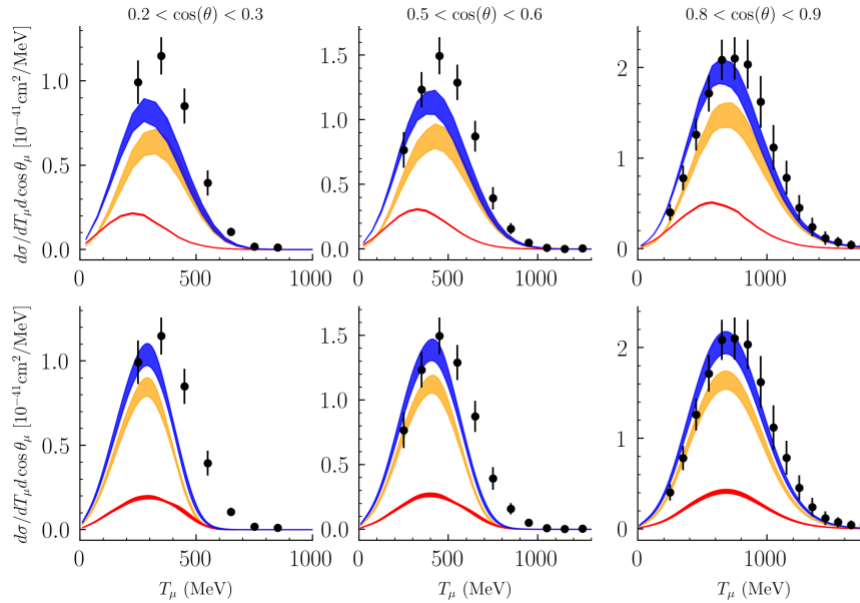
T. Katori, M. Martini, *J.Phys.G* 45 (2018)



N.B. A one-to one correspondence between different exclusive channel's contributions can be misleading [e.g. NN SRC contributions are part of the 2p-2h channel in RPA-based approaches while they are included in QE in SuSA.]

Example of different results in recent Spectral Function and Green's Function Monte Carlo (ab-initio) calculations

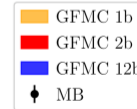
MiniBoONE



SF



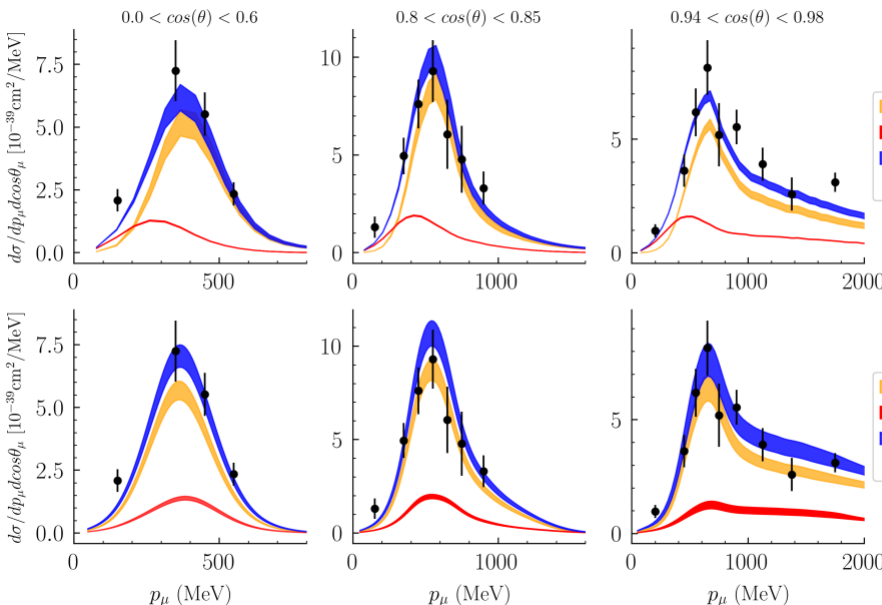
GFMC



D. Simons et al. 2210.02455

N. Steinberg talk @ NUINT 2022

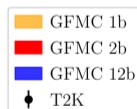
T2K



SF



GFMC

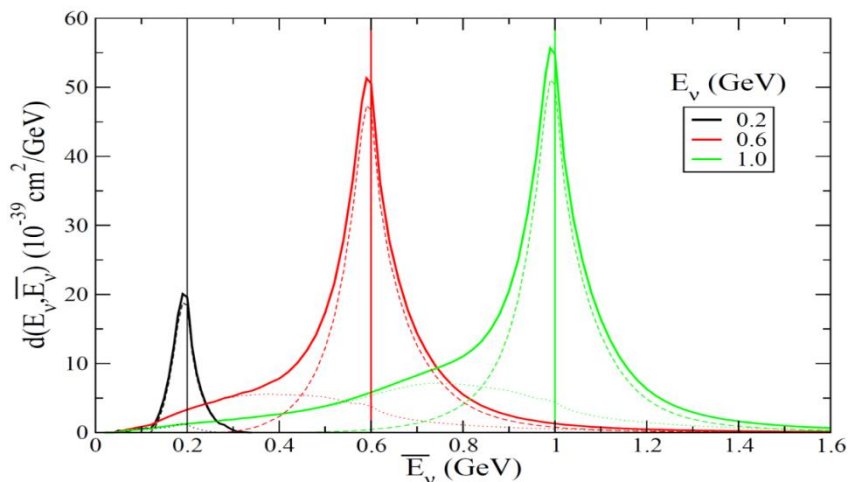


SF and GFMC 2-body contributions shifted because of different

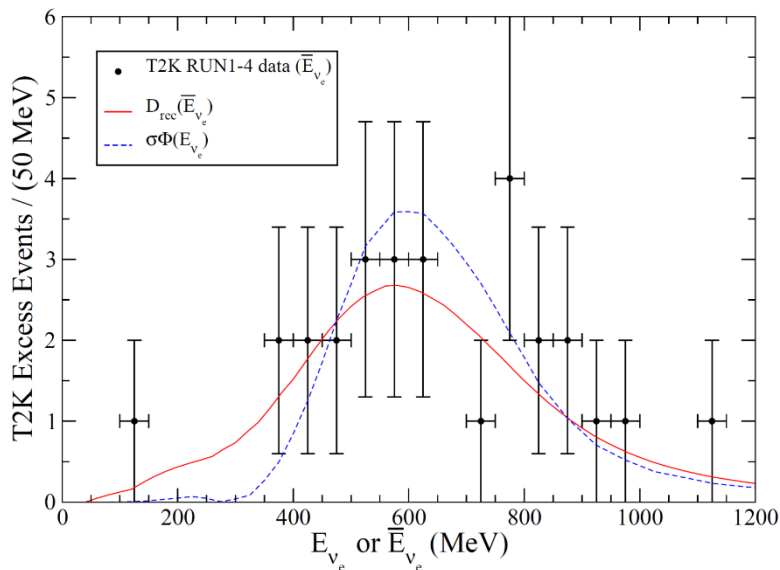
1 body – 2 body interference effects

QE-based neutrino energy reconstruction and neutrino oscillations

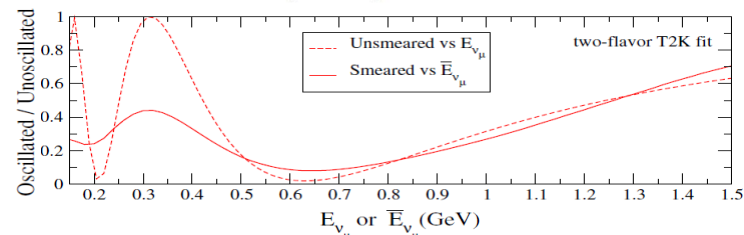
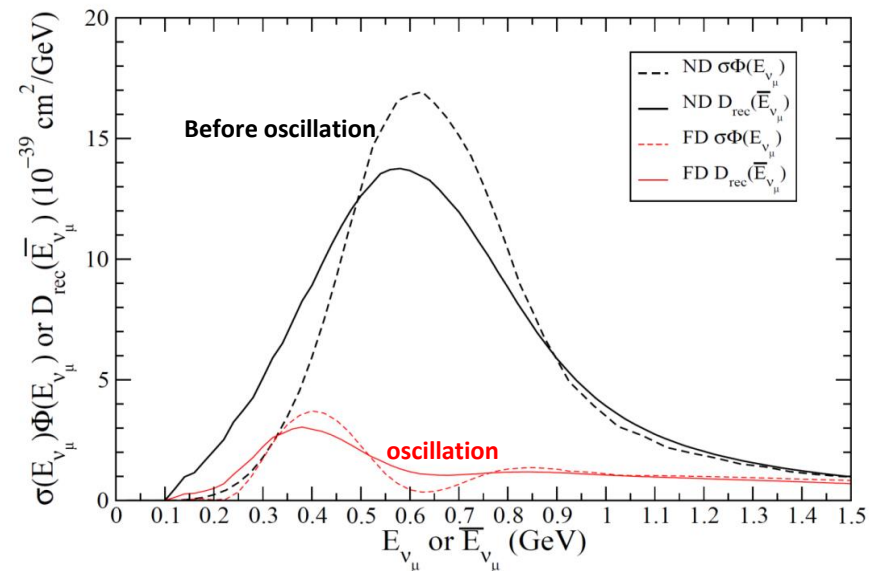
ν_e energy migration matrix



ν_e appearance T2K



ν_{μ} disappearance T2K

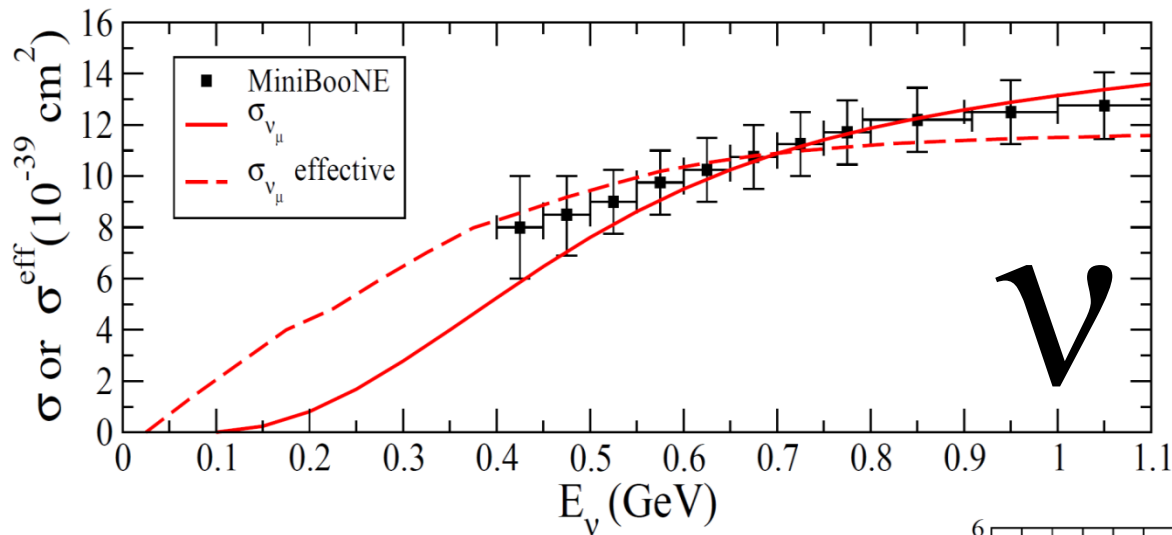


M. Martini, M. Ericson, G. Chanfray
Phys. Rev. D 85 093012 (2012); *Phys. Rev. D* 87 013009 (2013)

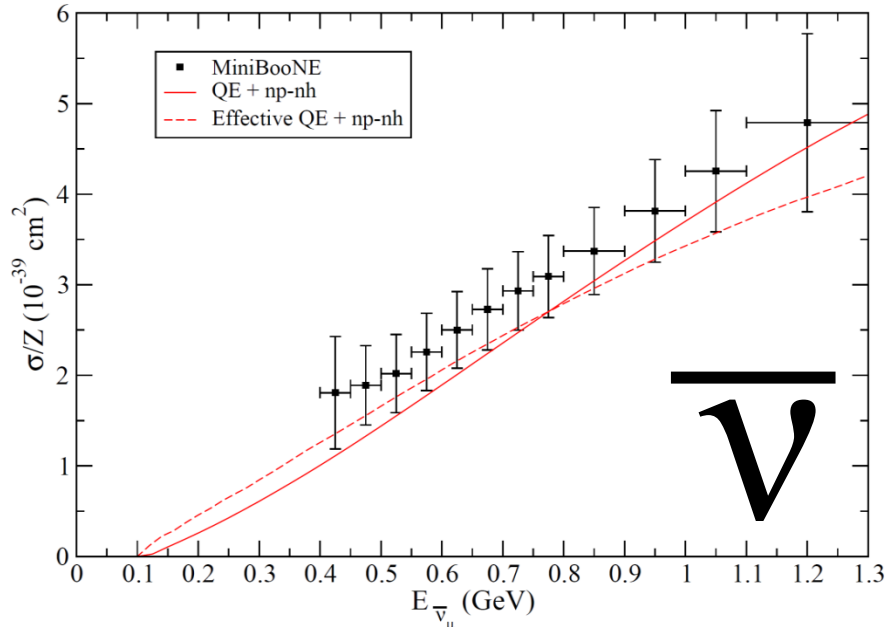
Similar results in:
 Nieves et al. *PRD* 85 113008 (2012);
 Lalakulich et al. *PRC* 86 054606 (2012)

Neutrino energy reconstruction and neutrino oscillation analysis are affected by np-nh

CCQE-like cross sections as a function of real (continuous line) and reconstructed (dashed line) neutrino energy



M. Martini, M. Ericson, G. Chanfray, *Phys. Rev. D* 87 013009 (2013)



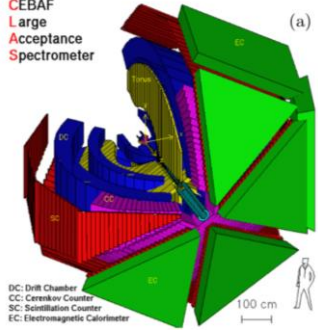
Martini, Ericson, *Phys. Rev. C* 87 065501 (2013)

Electron-beam energy reconstruction for ν oscillation measurements

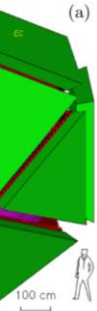
$e4\nu$



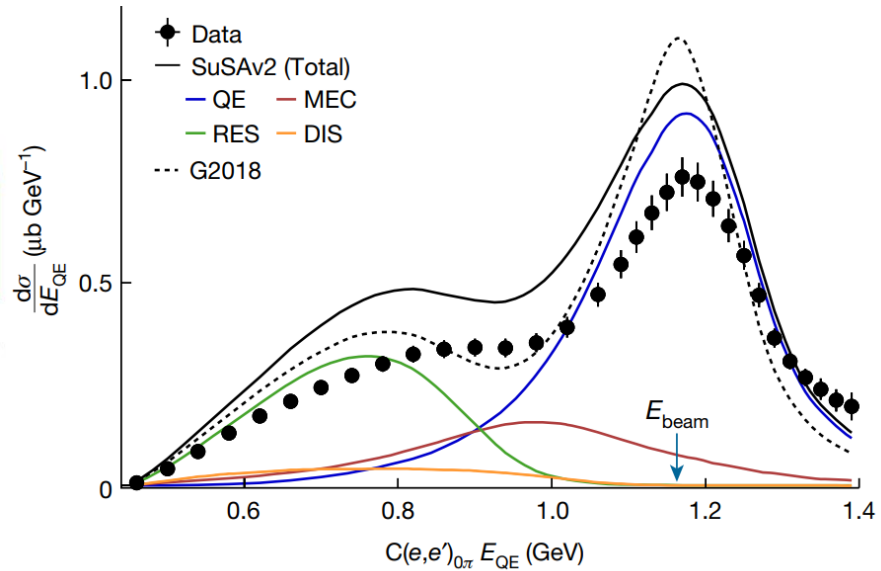
CEBAF
Large
Acceptance
Spectrometer



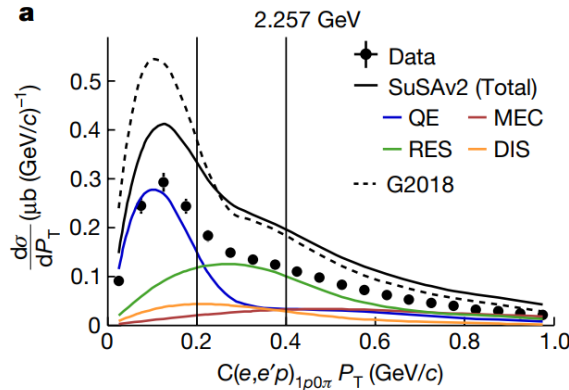
DC: Drift Chamber
CC: Cerenkov Counter
SC: Scintillation Counter
EC: Electromagnetic Calorimeter



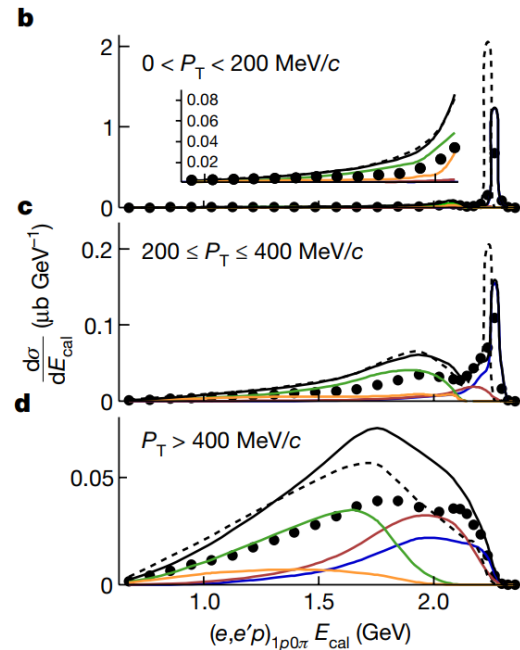
Nature 599 (2021) 7886, 565-570



QE-based
(e, e')



$$\mathbf{P}_T = \mathbf{P}_T^{e'} + \mathbf{P}_T^p$$



Calorimetric
-based
($e, e'p$)

Semi-inclusive cross section: impact of different initial state modeling

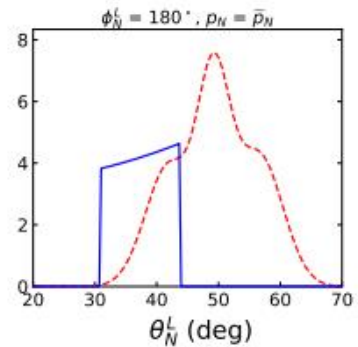
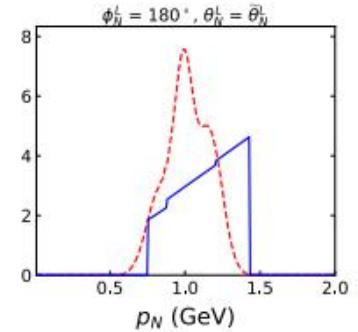
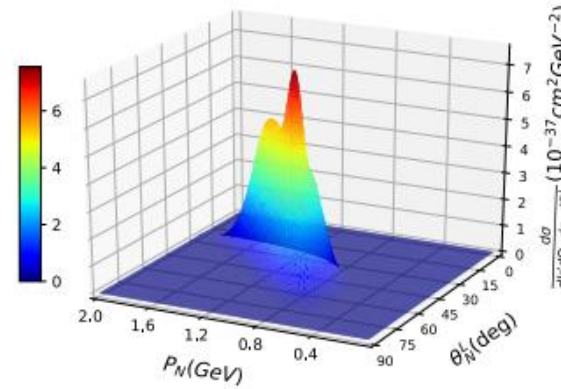
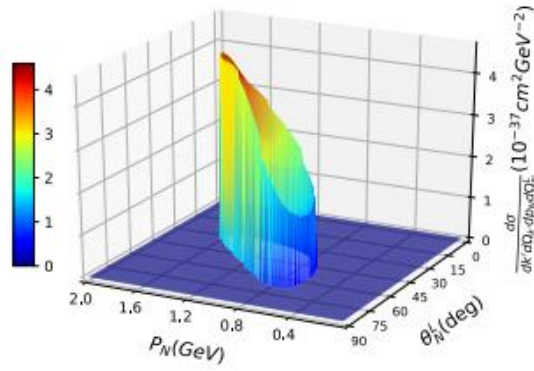
M. Barbaro
talk @IPSA
2022

6-differential semi-inclusive cross section ($\nu_\mu, \mu p$) nucleon knock-out

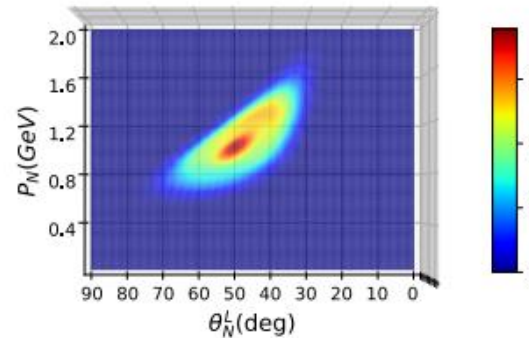
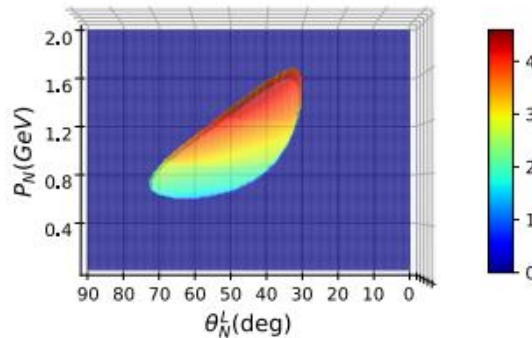
$${}^{40}\text{Ar}(\nu_\mu, \mu^- p){}^{39}\text{Cl} \quad \text{DUNE flux} \quad k' = 1.5 \text{ GeV}, \theta_\mu = 30^\circ, \phi_N^L = \pi$$

Relativistic Fermi Gas

Independent Particle Shell Model



--- IPSM
— RFG



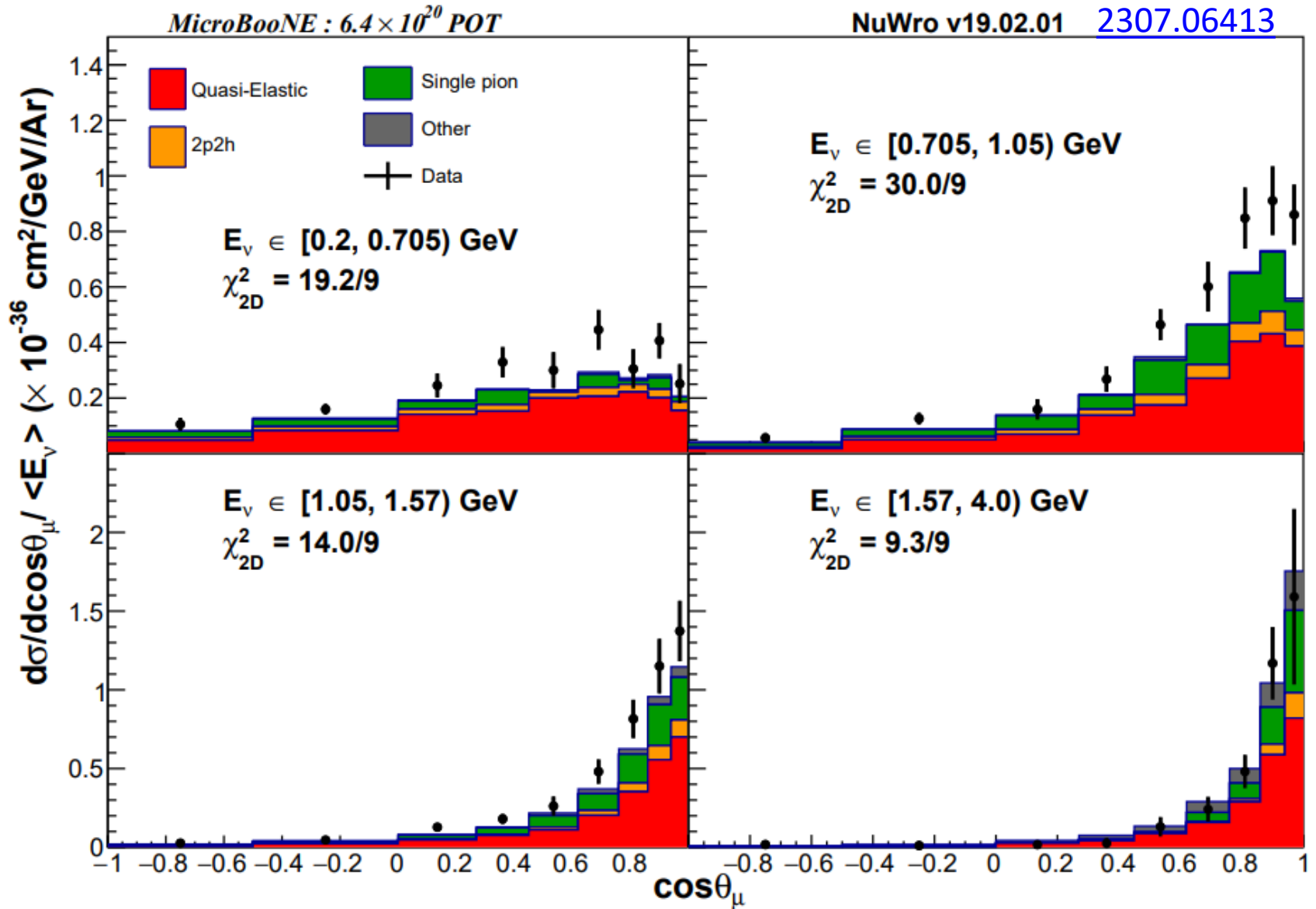
J.M. Franco-Patiño *et al.*, PRC 102, 064626 (2020)

Relativistic Plane Wave Impulse Approximation (no FSI included)

Striking differences in the cross section due to initial state physics described by different spectral functions.
The precise knowledge of the SF is crucial for a reliable modelling of semi-inclusive reactions.

MicroBooNE double-differential CC inclusive cross section

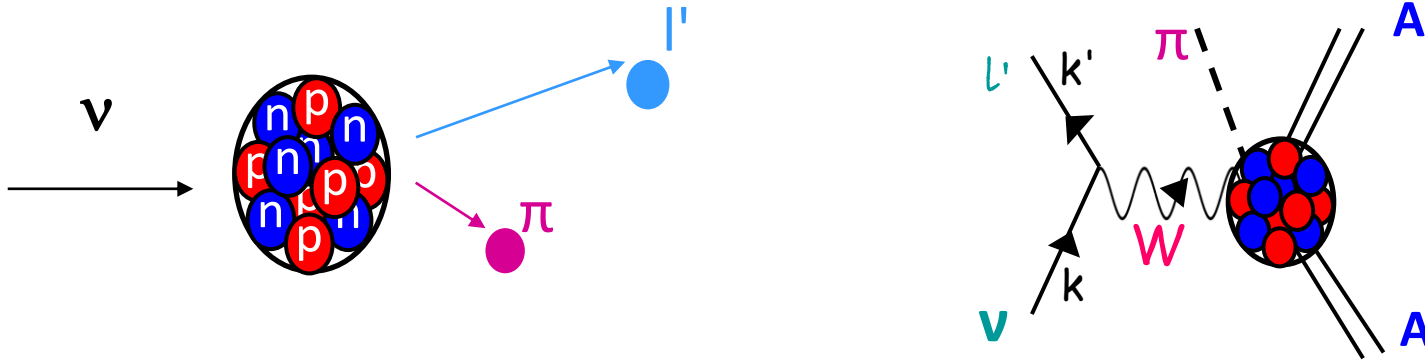
NuWro estimation of interaction channels breakdown



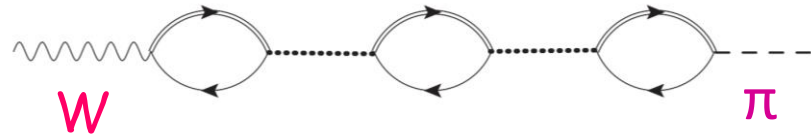
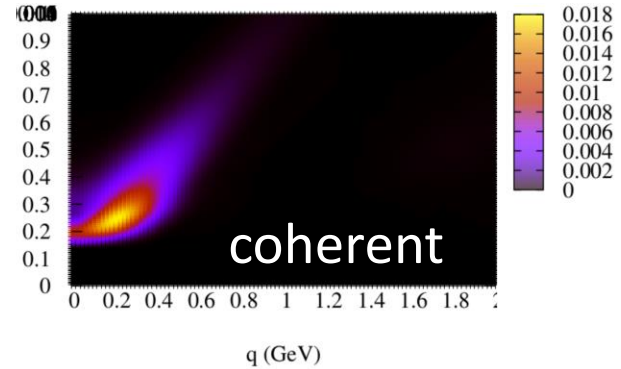
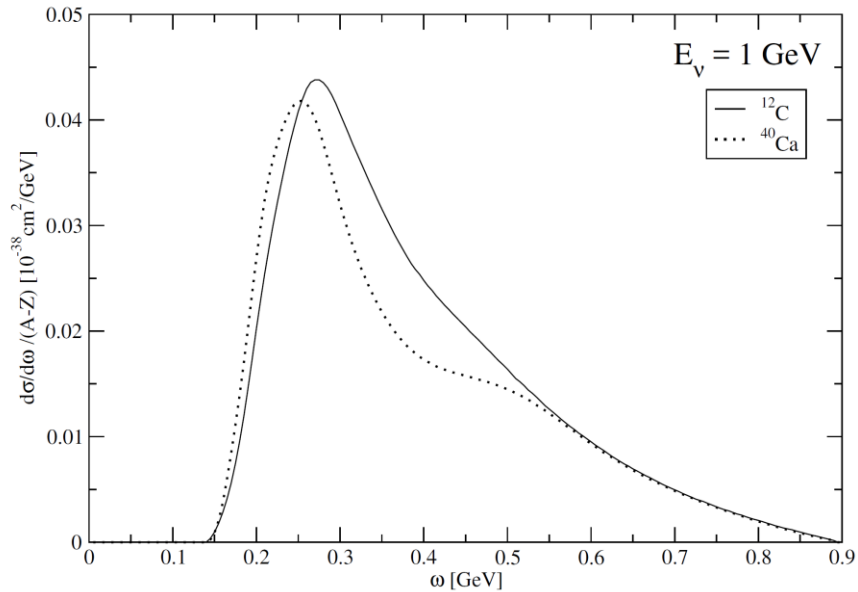
The coherent 1π production

Production of 1 pion with the nucleus remaining in its ground state

Relatively rare interaction channel, but can mimic oscillation signals



M. Martini, M. Ericson, G. Chanfray, J. Marteau, PRC 80 065501 (2009)



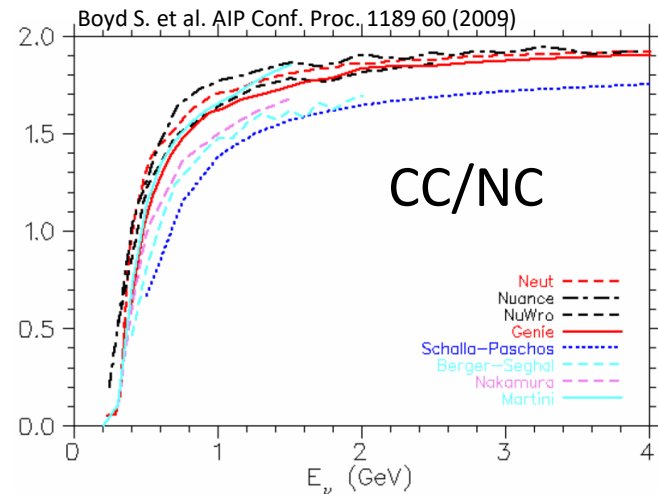
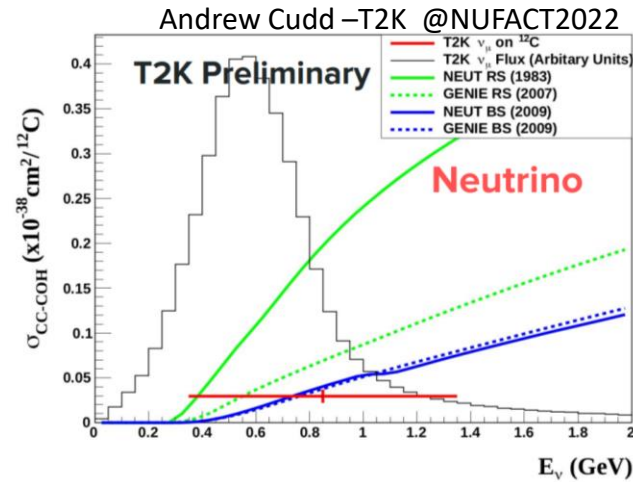
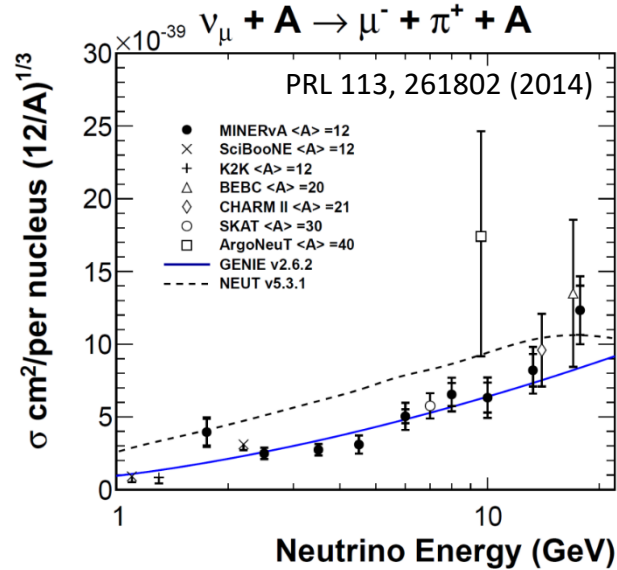
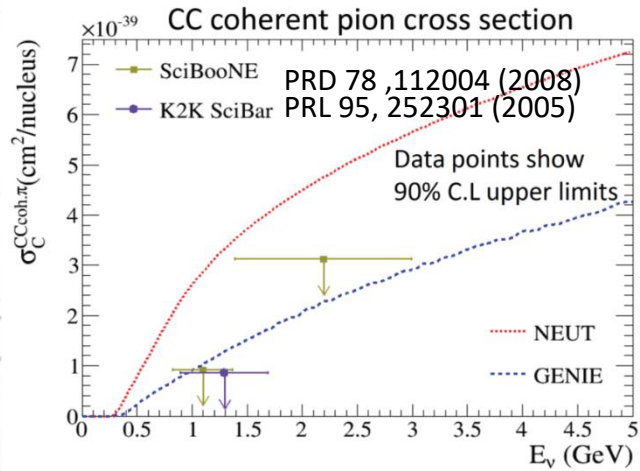
Cross sections reshaped by nuclear collective effects

Coherent 1π production experimental results

K2K and SciBooNE did not observe coherent π^+ production at neutrino energies $\sim 1\text{GeV}$

MINERvA and ArgoNeut see evidence for CC coherent pion production

Preliminary T2K cross section measurement: coherent π^+ production at neutrino energies $\sim 1\text{GeV}$



Coherent puzzle at $E_\nu \sim 1\text{ GeV}$

Theoretical models:

$$\frac{\pi^+ \text{ coh. CC}}{\pi^0 \text{ coh. NC}} = 1.5 \sim 2$$

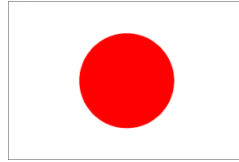
SciBooNE:

$$\frac{\pi^+ \text{ coh. CC}}{\pi^0 \text{ coh. NC}} = 0.14^{+0.30}_{-0.28}$$

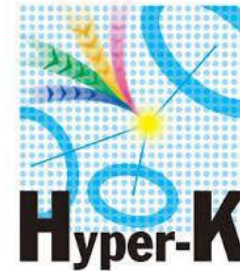
Kurimoto et al, PRD 81 (2010)

Nuclear targets of present and future LBL oscillation experiments

Present



Future



Carbon: T2K(ND) and NOvA

Oxygen (water): T2K (SuperK) and Hyper-K

Argon: DUNE

In the last 15 years many cross sections measurements and theoretical studies have been performed for Carbon (^{12}C). Less for Oxygen (^{16}O) and Argon (^{40}Ar)

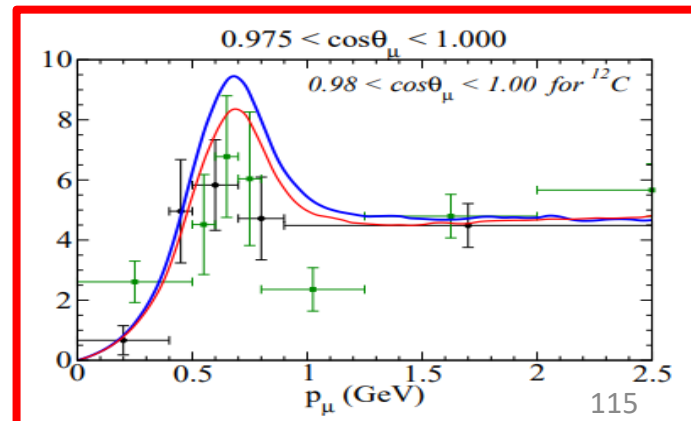
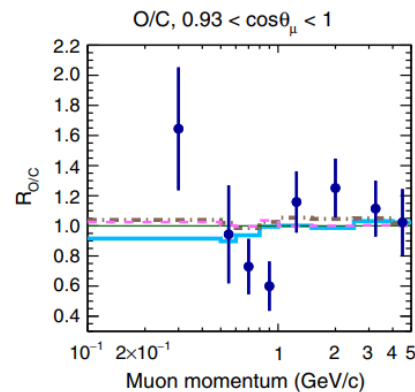
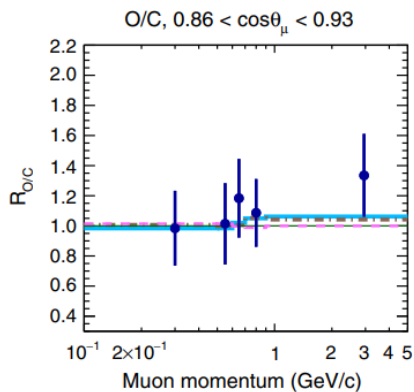
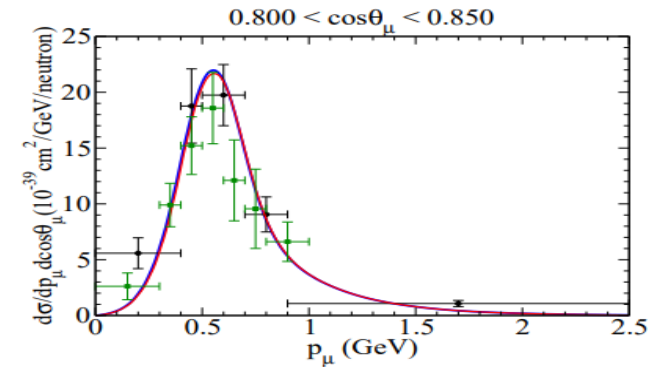
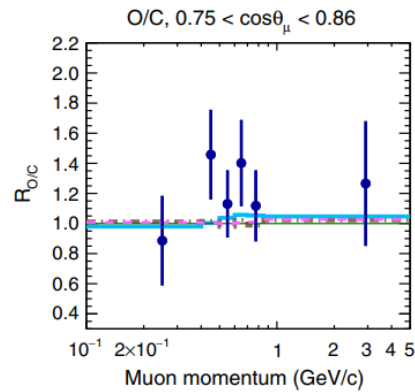
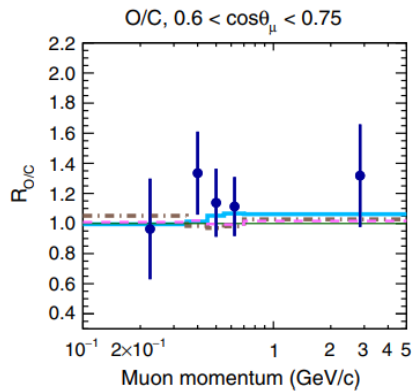
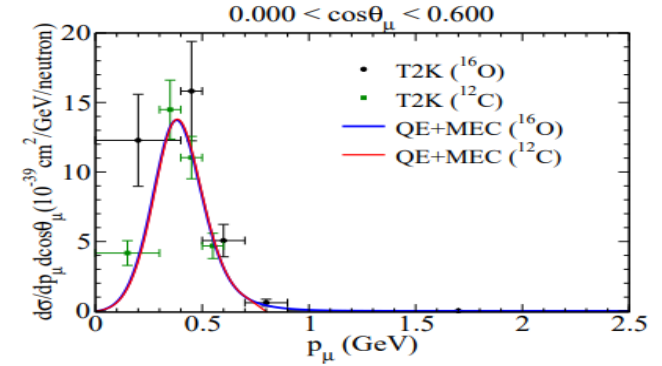
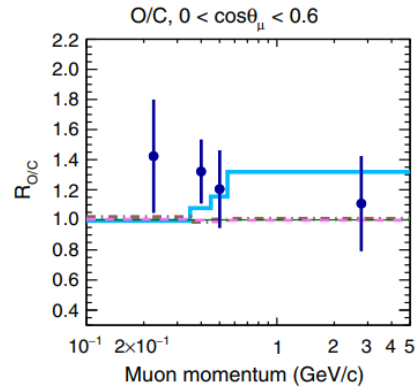
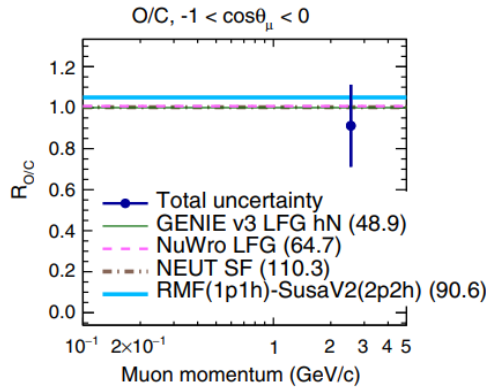
T2K CC0 π d² σ cross sections on oxygen and carbon

Ratio ¹⁶O/¹²C per nucleon

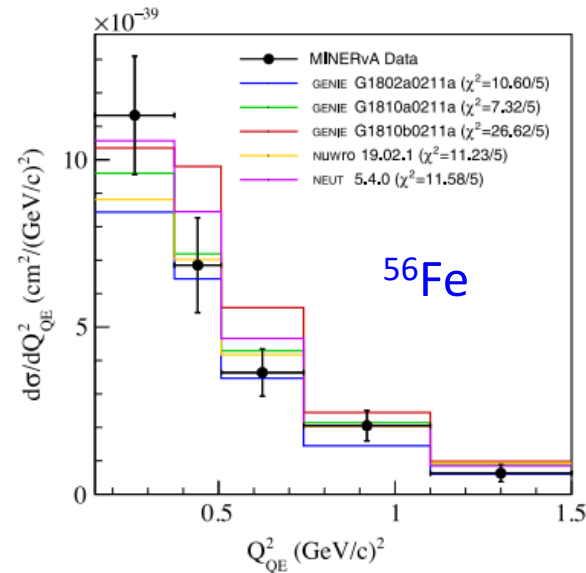
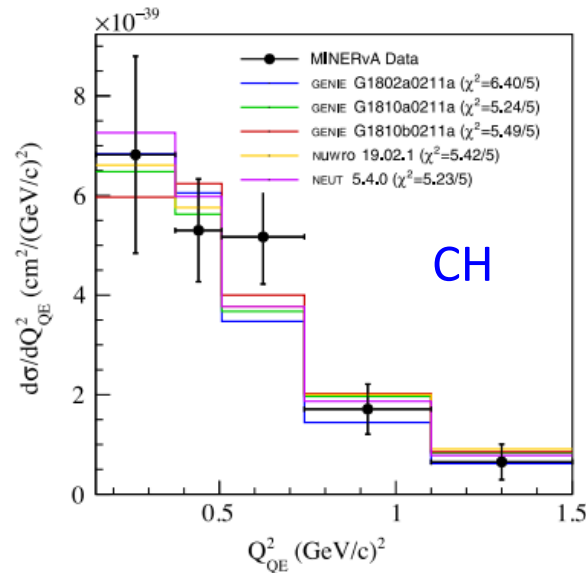
T2K PRD 101 (2020)

SuSAv2+MEC

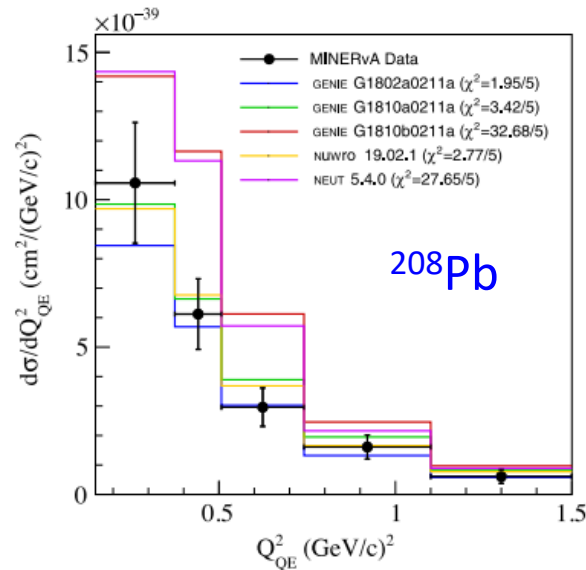
Megias et al., JPG46 (2019)



MINERvA CC0 π 1p(at least) Q²distributions for carbon, iron, lead



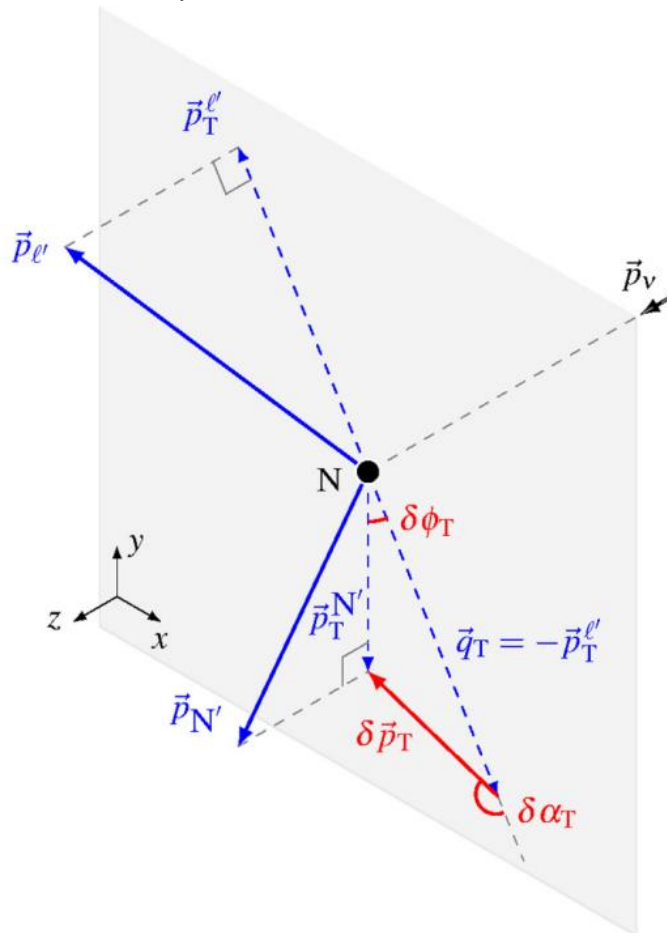
M. Buizza Avanzini et al. PRD 105, 092004 (2022)



- The spread of distributions predicted by generators increases from carbon to lead
- Most significant deviations are at low Q² where nuclear effects are more important

Measurement of nuclear effects in neutrino interactions with minimal dependence on neutrino energy

X.-G. Lu,^{1,*} L. Pickering,² S. Dolan,¹ G. Barr,¹ D. Coplowe,¹ Y. Uchida,² D. Wark,^{1,3} M. O. Wascko,² A. Weber,^{1,3} and T. Yuan⁴



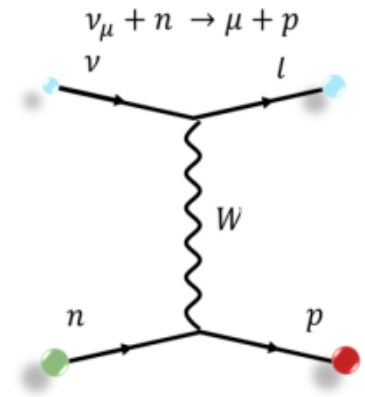
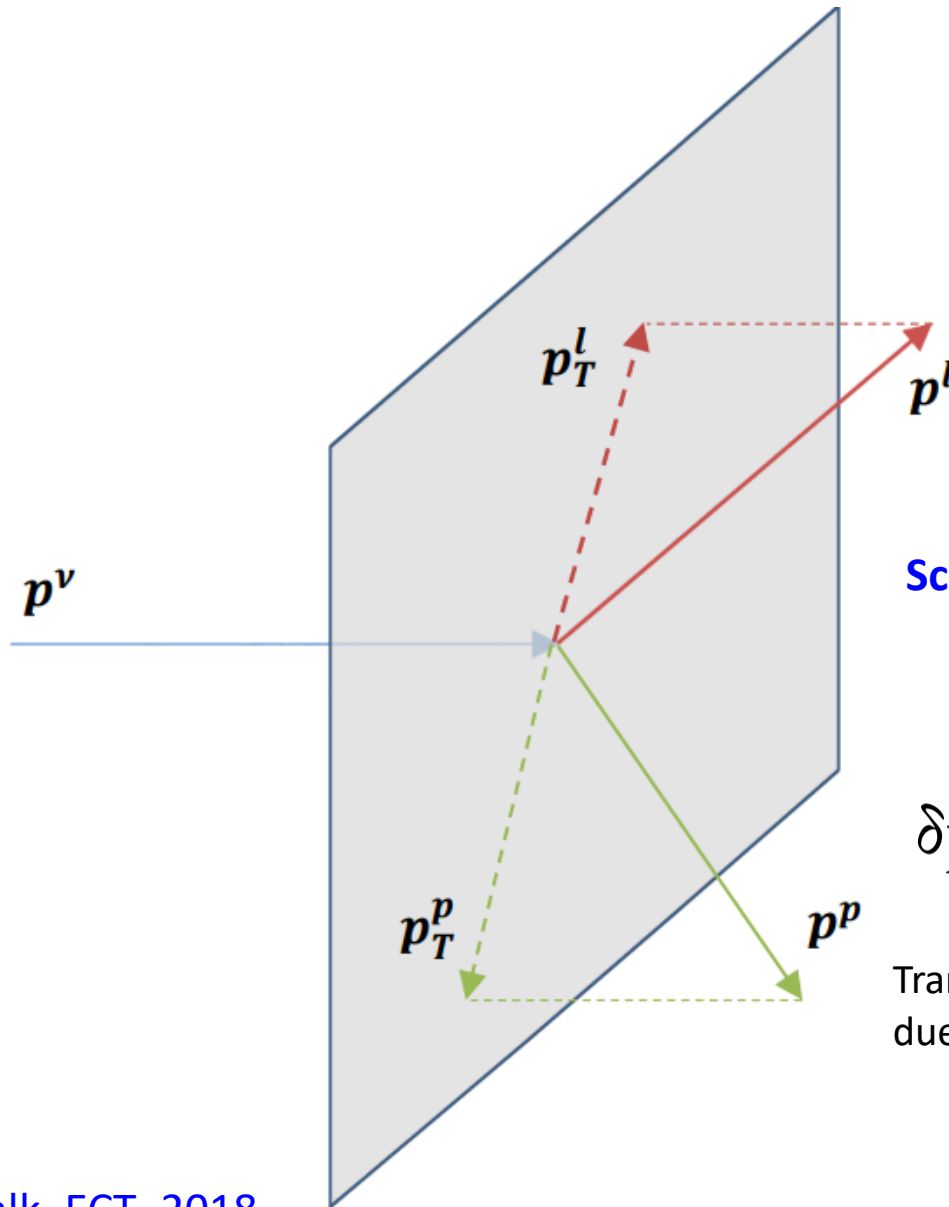
Single Transverse Variables (STV)

$$\delta \vec{p}_T \equiv \vec{p}_T^{\ell'} + \vec{p}_T^{N'}$$

$$\delta \alpha_T \equiv \arccos \frac{-\vec{p}_T^{\ell'} \cdot \delta \vec{p}_T}{p_T^{\ell'} \delta p_T}$$

$$\delta \phi_T \equiv \arccos \frac{-\vec{p}_T^{\ell'} \cdot \vec{p}_T^{N'}}{p_T^{\ell'} p_T^{N'}}$$

Single Transverse Kinematic Variables



No nuclear Effects

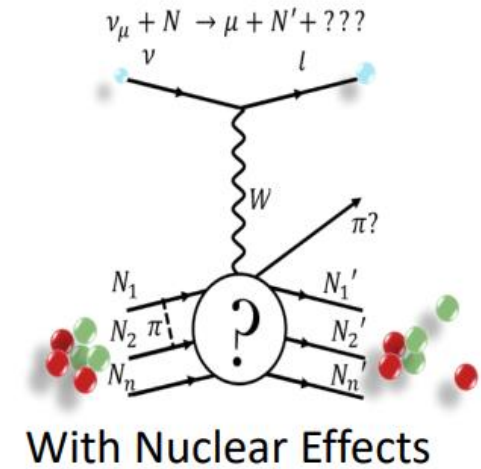
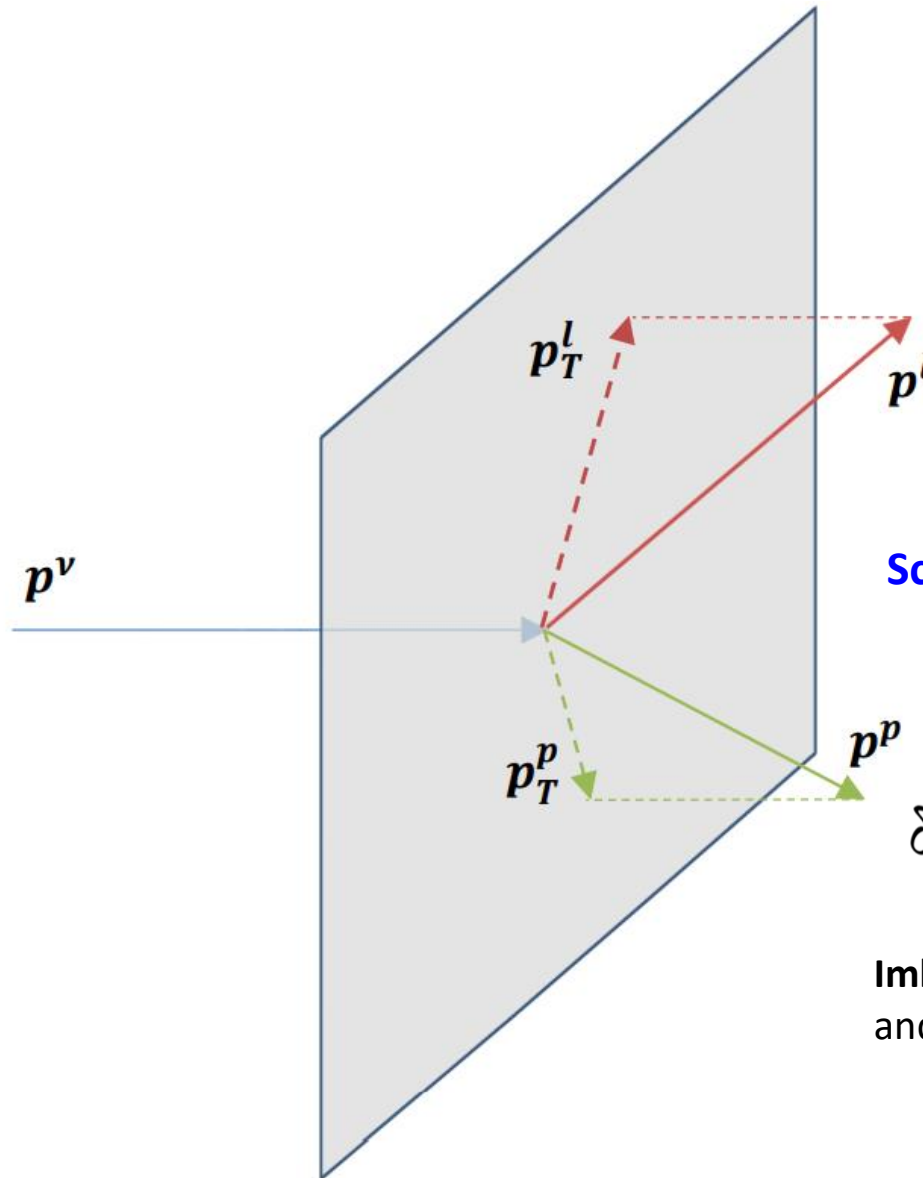
Scattering on a free nucleon at rest

$$\mathbf{p}_T^l = -\mathbf{p}_T^p$$

$$\delta p_T = |\mathbf{p}_T^l + \mathbf{p}_T^p| = 0$$

Transverse projections equal and opposite due to momentum conservation

Single Transverse Kinematic imbalance (STKI)



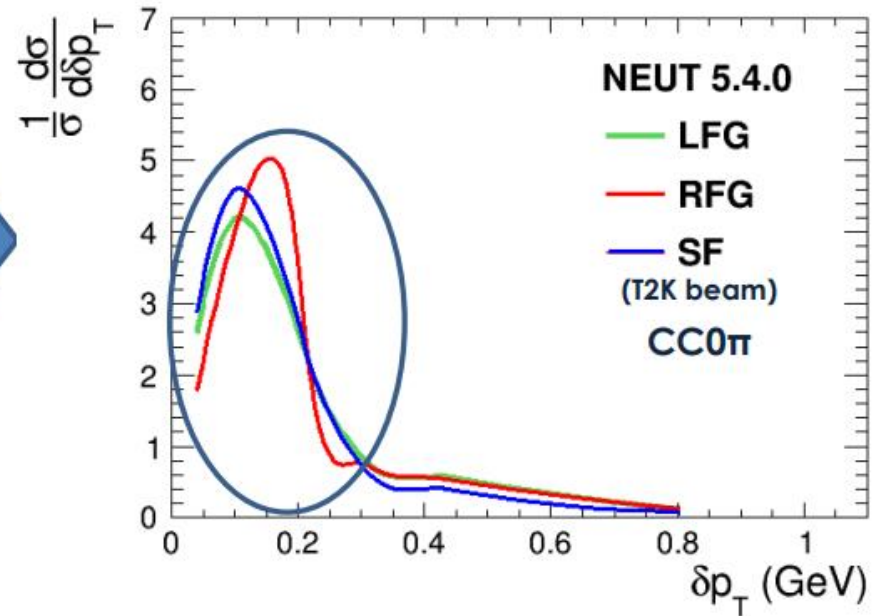
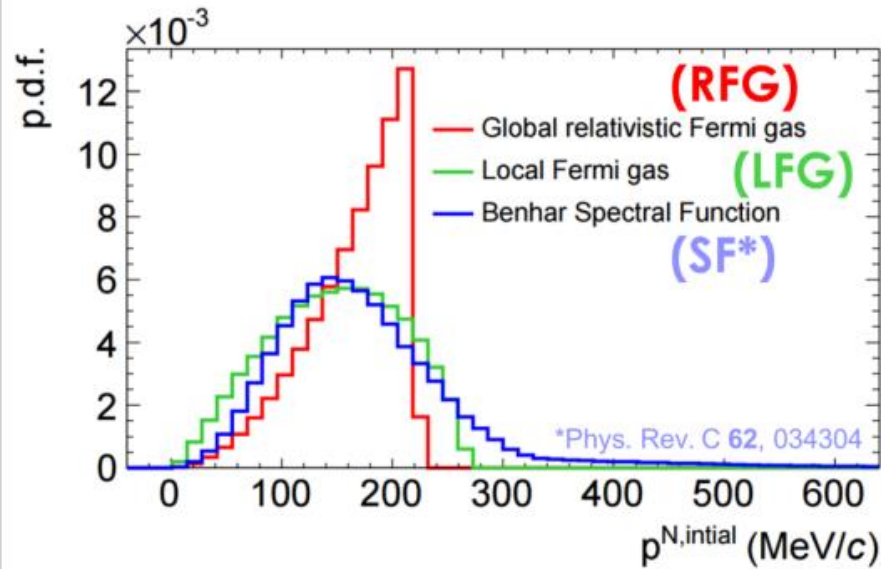
Scattering on nucleus

$$\mathbf{p}_T^l \neq -\mathbf{p}_T^p$$

$$\delta p_T = |\mathbf{p}_T^\mu + \mathbf{p}_T^p| > 0$$

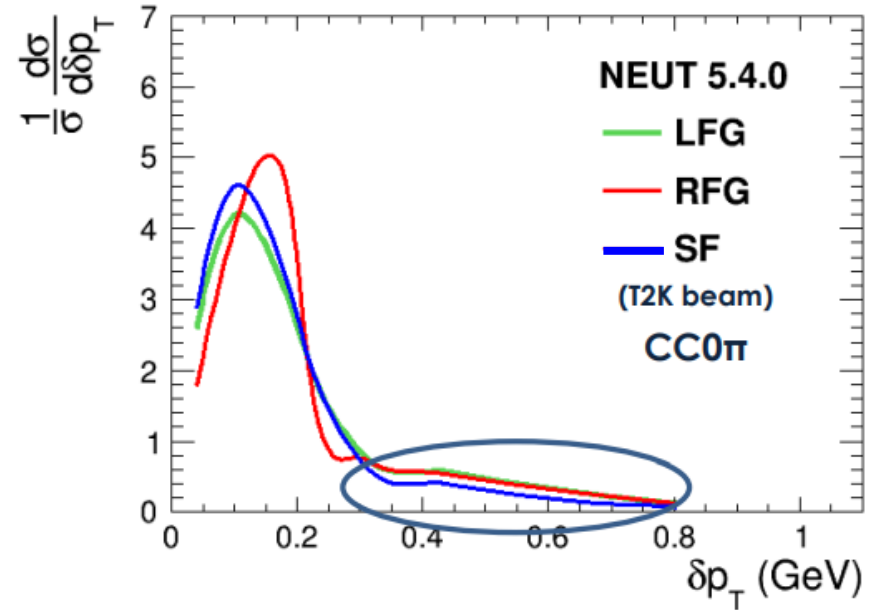
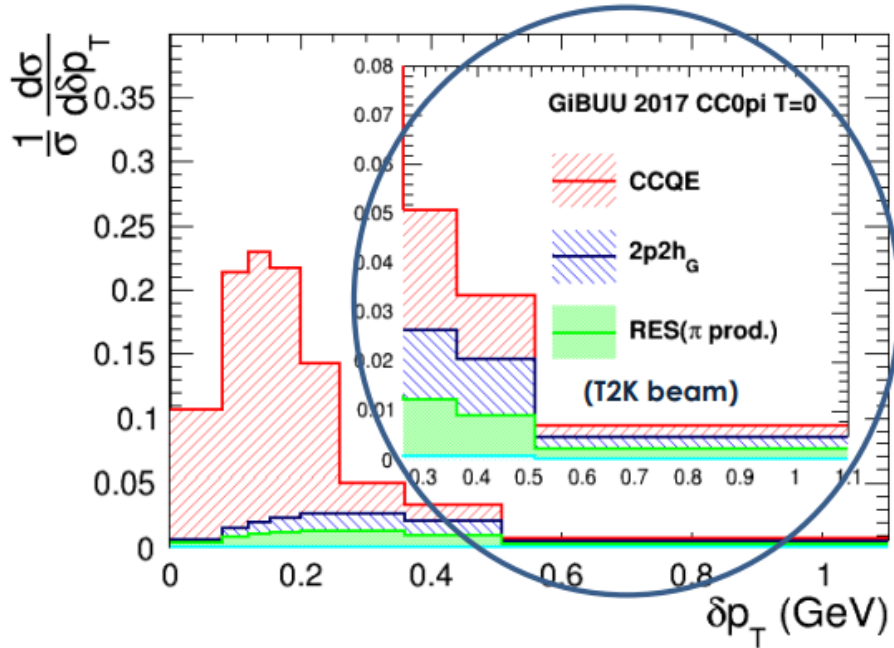
Imbalance due to initial nucleon motion and other nuclear effects

STV model discrimination - δp_T



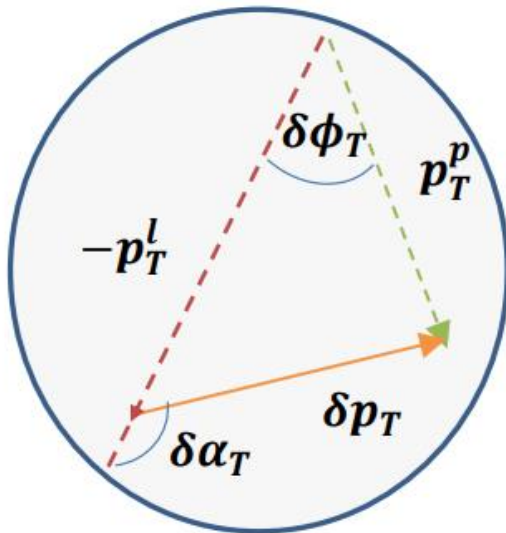
- In the absence of other nuclear effects, δp_T is the transverse projection of the Fermi motion.
- Since this motion is isotropic, $\delta p_T \rightarrow$ Fermi motion

STV model discrimination - δp_T

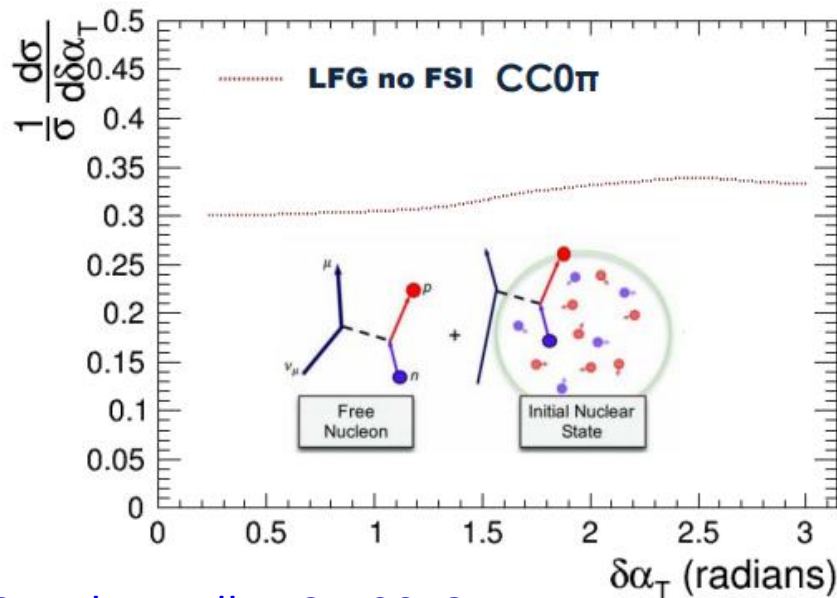


- In the absence of other nuclear effects, δp_T is the transverse projection of the Fermi motion.
- Since this motion is isotropic, $\delta p_T \rightarrow$ Fermi motion
- Cross section beyond the Fermi momentum must come from physics beyond RFG \rightarrow 2p2h, FSI, SRCs ...

STV model discrimination - $\delta\alpha_T$

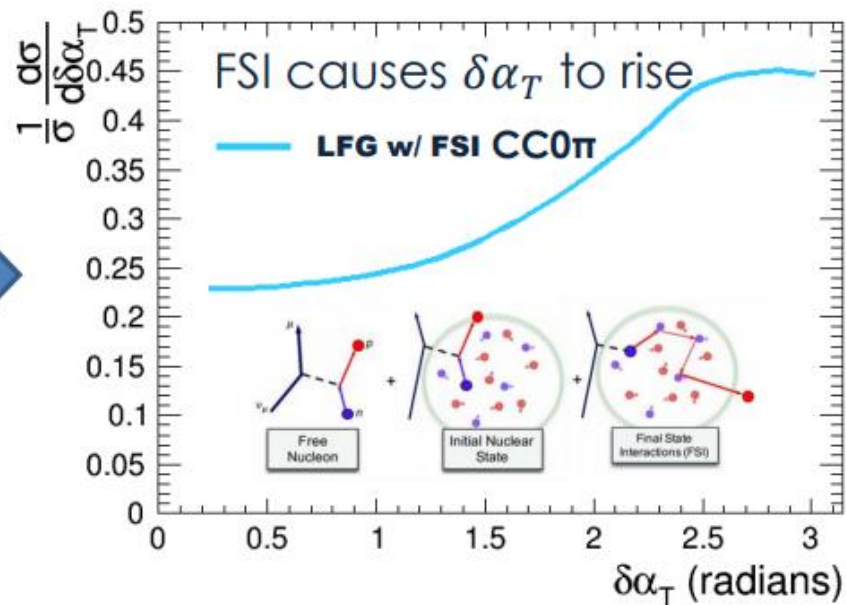
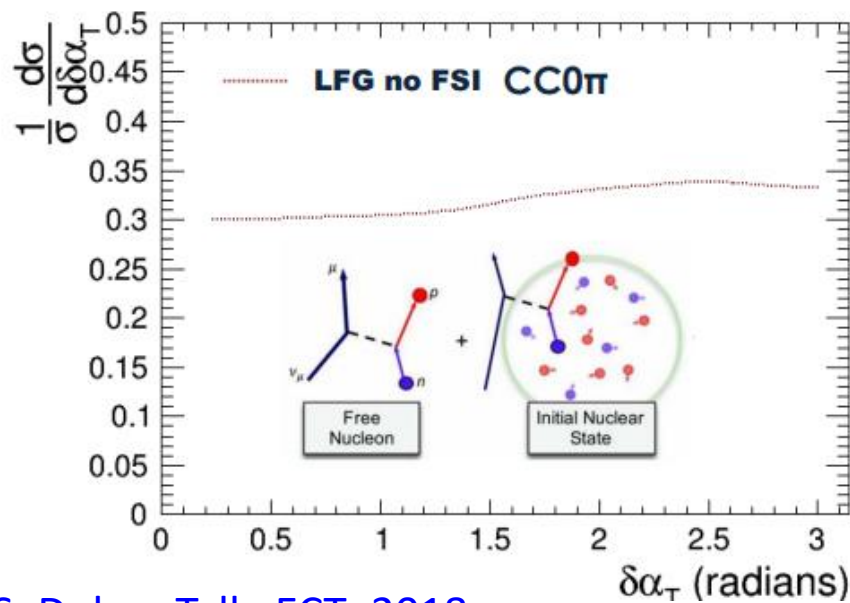
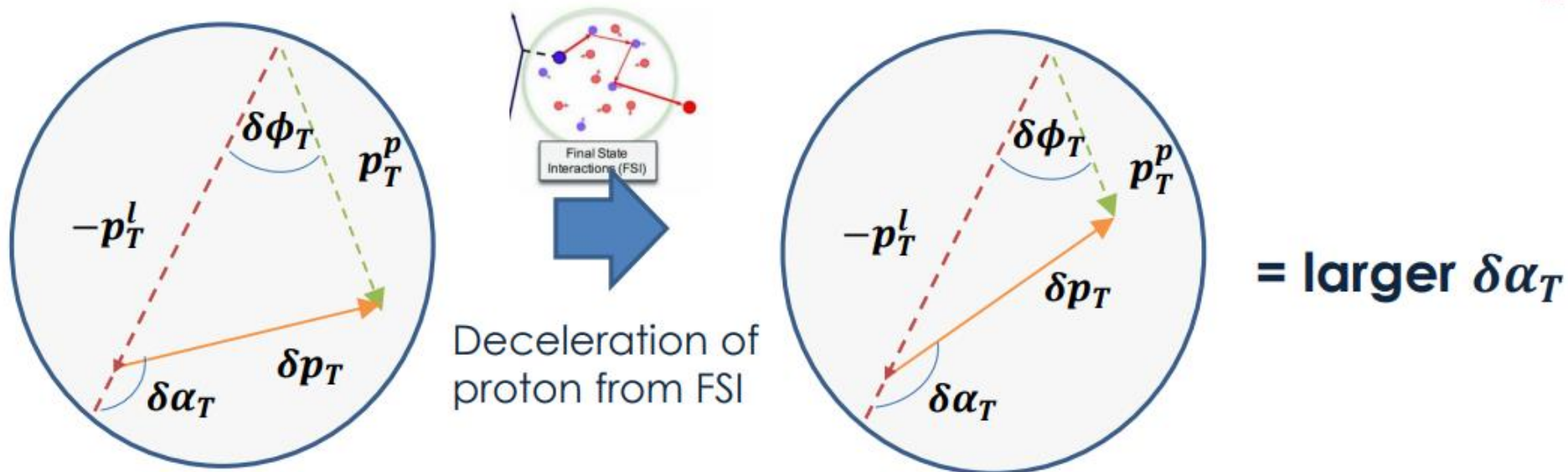


Consider imbalance from only Fermi motion

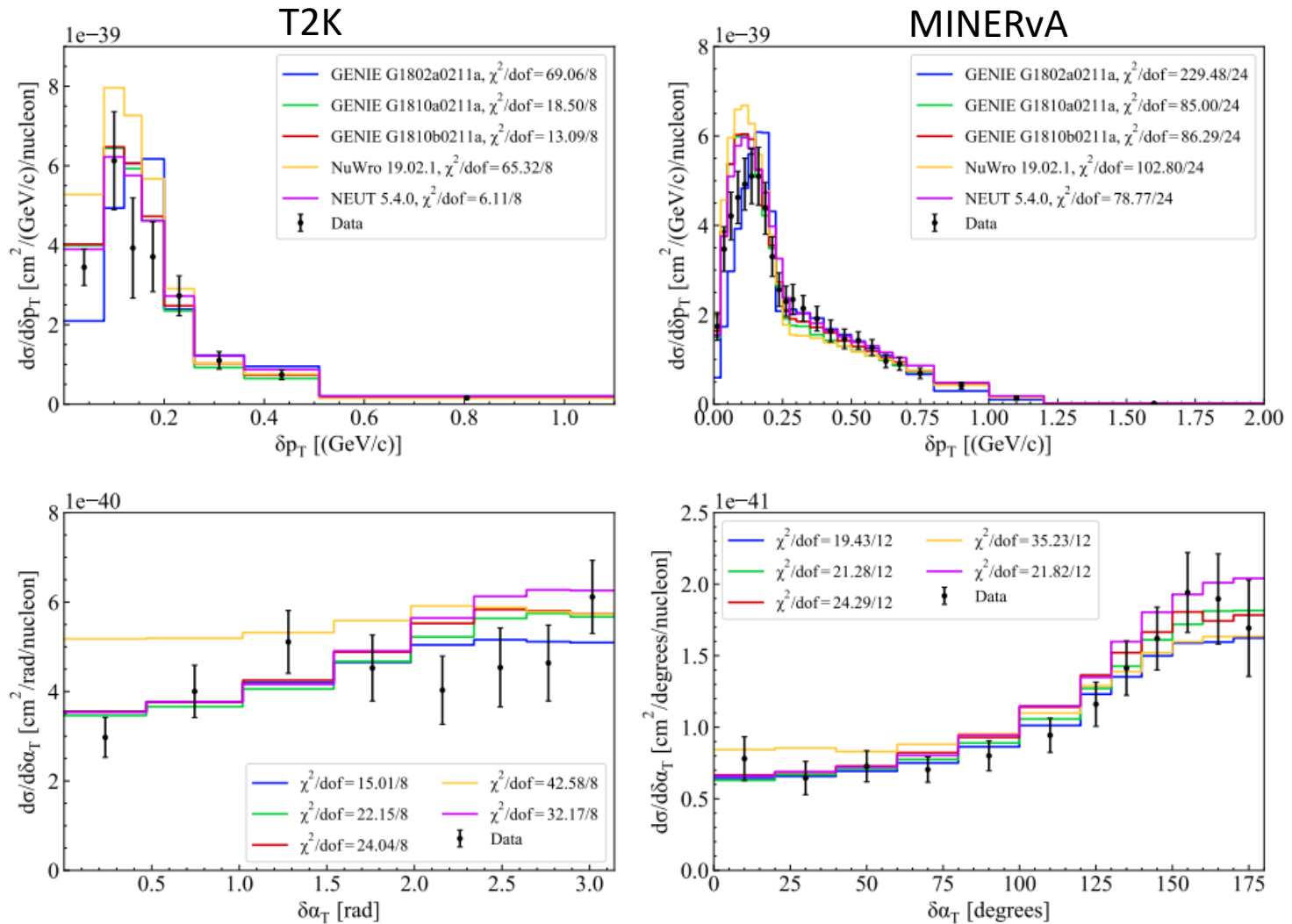


Fermi motion is isotropic so no preferred $\delta\alpha_T$ direction

STV model discrimination - $\delta\alpha_T$



Semi-inclusive $CC0\pi$ $d\sigma$ on carbon versus STKI Variables: Monte Carlo predictions



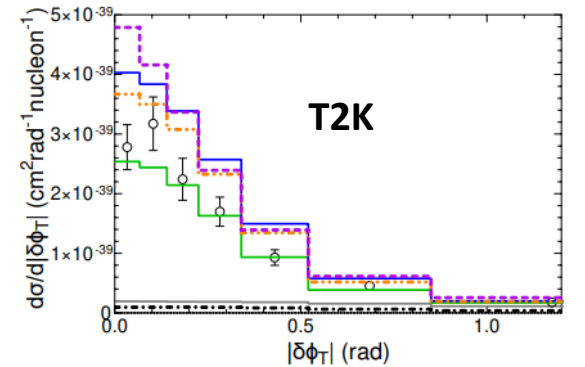
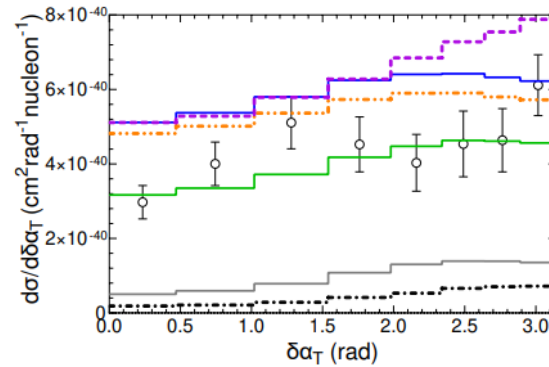
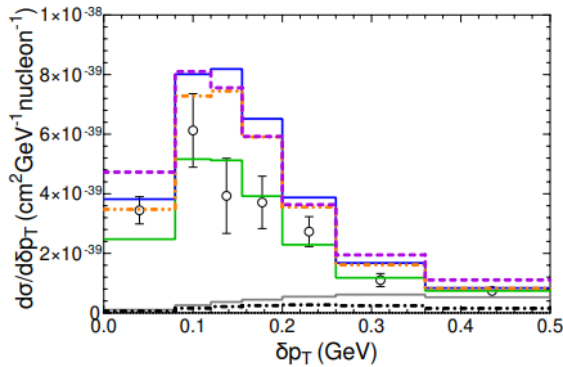
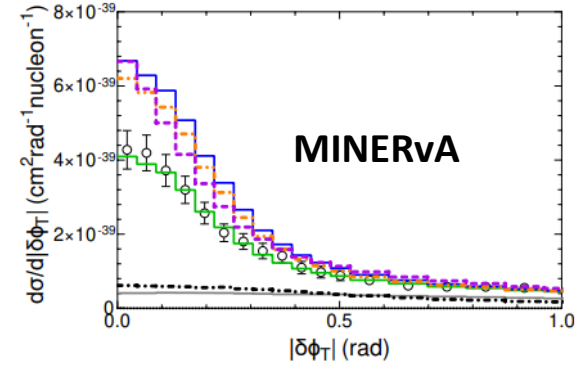
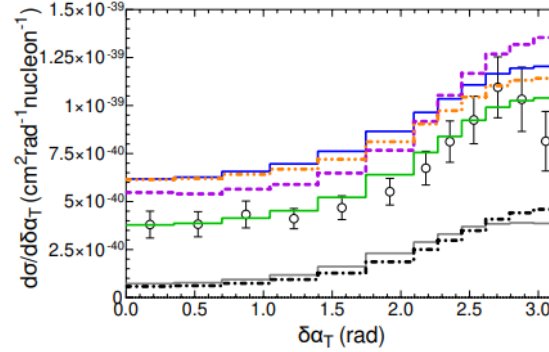
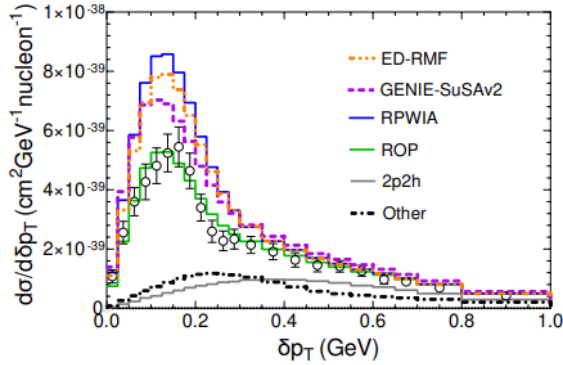
M. Buizza Avanzini et al. PRD 105, 092004 (2022)

None of the generators correctly reproduces all the data in the STKI variables without tuning

This is not a surprise since these generators implement “inclusive” microscopic models 124

Semi-inclusive CC0 π $d\sigma$ on carbon versus STKI Variables: discrimination of FSI microscopic modeling

J. M. Franco Patino et al, PRD 106 (2022)



RPWIA: no FSI

GENIE-SuSAv2: include FSI but from inclusive model (factorization)

ED-RMF, rROP, ROP: different theoretical approaches for FSI

- FSI improve the agreement with data respect to the RPWIA prediction
- STKI Variables helps to discriminate between different FSI models: data seem to prefer **ROP**
- 2p2h (from an inclusive-based model) give non-negligible contribution